Synthesis of Aromatic Aza-heterocycles and Exploration of their Chemical Characteristics

A Thesis Submitted

to

Sikkim University

In Partial Fulfilment of the Requirement for the

Degree of Doctor of Philosophy

By

Susanta Mandal

Department of Chemistry

School of Physical Science

July, 2022

6 माइल, सामदुर, तादोंग - 737102
गंगटोक, सिक्किम, भारत
फोन-03592-251212, 251415, 251656
टेलीफैक्स - 251067
वेबसाइट - www.cus.ac.in

6th Mile, Samdur, Tadong-737102
Gangtok, Sikkim, India
Ph. 03592-251212, 251415, 251656
Telefax : 251067
Website : www.cus.ac.in

सिक्किम विश्वविद्यालय
SIKKIM UNIVERSITY
(भारत के संसद के अधिनियम द्वारा वर्ष 2007 में स्थापित और नैक (एनएएसी) द्वारा वर्ष 2015 में प्रत्यायित केंद्रीय विश्वविद्यालय)
(A central university established by an Act of Parliament of India in 2007 and accredited by NAAC in 2015)

DECLARATION

I, **Susanta Mandal**, hereby declare that the thesis titled **"Synthesis of Aromatic Aza-heterocycles and Exploration of their Chemical Characteristics"** submitted by me for the award of the degree of **Doctor of Philosophy** to the Department of Chemistry, Sikkim University, represents my ideas in my own words and where others' ideas or words have been included, I have adequately cited and referenced the original sources. I declare that I have properly and accurately acknowledged all sources used in the production of this thesis.

I also declare that I have adhered to all principles of academic honesty and integrity and have not misrepresented or fabricated or falsified any idea/data/fact/source in my submission. This thesis has not been submitted for any other degree to any other university or institute.

Susanta Mandal.

Susanta Mandal

Reg. No. 15/Ph.D/CMS/02)

Place: Gangtok.

Date: 27. 07. 2022.

We recommend that, the thesis be placed before the examiners for evaluation.

Dr. Biswajit Gopal Roy

Signature of the Supervisor
Department of Chemistry
Sikkim University

Dr.Biswajit Gopal Roy
Assistant Professor
Department of Chemistry
Sikkim University

Prof. Sanjay Dahal

Signature of the Head
Department of Chemistry
Sikkim University

अध्यक्ष
Head
रसायन विज्ञान विभाग
Department of Chemistry
सिक्किम विश्वविद्यालय
Sikkim University

6 माइल, सामदुर, तादोंग - 737102
गंगटोक, सिक्किम, भारत
फोन-03592-251212, 251415, 251656
टेलीफैक्स - 251067
वेबसाइट - www.cus.ac.in

6th Mile, Samdur, Tadong-737102
Gangtok, Sikkim, India
Ph. 03592-251212, 251415, 251656
Telefax : 251067
Website : www.cus.ac.in

सिक्किम विश्वविद्यालय
SIKKIM UNIVERSITY
(भारत के संसद के अधिनियम द्वारा वर्ष 2007 में स्थापित और नैक (एनएएसी) द्वारा वर्ष 2015 में प्रत्यायित केंद्रीय विश्वविद्यालय)
(A central university established by an Act of Parliament of India in 2007 and accredited by NAAC in 2015)

CERTIFICATE

This is to certify that the thesis titled **"Synthesis of Aromatic Aza-heterocycles and Exploration of their Chemical Characteristics"** is being submitted by **Mr. Susanta Mandal** (Reg. No.15/Ph.D/CMS/02) to the Department of Chemistry, Sikkim University, for the award of the degree of **Doctor of Philosophy**. This thesis is a record of bonafide research work carried out by him under my guidance and supervision. In my opinion, the thesis has reached the standards fulfilling the requirements of the regulations related to the degree.

The results contained in this thesis have not been submitted to any other university or institute for the award of any degree or diploma.

Dr. Biswajit Gopal Roy
Assistant Professor
Department of Chemistry
School of Physical Sciences
Sikkim University

Place: Gangtok.
Date: 25.07.2022.

Dr.Biswajit Gopal Roy
Assistant Professor
Department of Chemistry
Sikkim University

6 माइल, सामदुर, तादोंग - 737102
गंगटोक, सिक्किम, भारत
फोन-03592-251212, 251415, 251656
टेलीफैक्स - 251067
वेबसाइट - www.cus.ac.in

6th Mile, Samdur, Tadong-737102
Gangtok, Sikkim, India
Ph. 03592-251212, 251415, 251656
Telefax : 251067
Website : www.cus.ac.in

सिक्किम विश्वविद्यालय
SIKKIM UNIVERSITY

(भारत के संसद के अधिनियम द्वारा वर्ष 2007 में स्थापित और नैक (एनएएसी) द्वारा वर्ष 2015 में प्रत्यायित केंद्रीय विश्वविद्यालय)
(A central university established by an Act of Parliament of India in 2007 and accredited by NAAC in 2015)

Date — 25.07.22

CERTIFICATE FOR PLAGIARISM CHECK

This is to certify that plagiarism check has been carried out for the following Ph.D thesis with the help of URKUND software and the result is 0% similarity, which is within the permissible limit (below 10% tolerance rate) as per the norm of Sikkim University.

"Synthesis of Aromatic Aza-heterocycles and Exploration of their Chemical Characteristics"

Submitted by **Mr. Susanta Mandal** under the supervision of
Dr. Biswajit Gopal Roy, Assistant Professor, Department of Chemistry,
School of Physical Sciences, Sikkim University.

Susanta Mandal

Susanta Mandal
Signature of the candidate

Dr. Biswajit Gopal Roy
Assistant Professor
Department of Chemistry
School of Physical Sciences
Sikkim University

Dr.Biswajit Gopal Roy
Assistant Professor
Department of Chemistry
Sikkim University

25/7/2022

Dr. Shri Ram
Librarian
Sikkim University

Acknowledgement

Foremost, I would like to express my sincere gratitude to my supervisor Dr. Biswajit Gopal Roy, for the continuous support and guidance throughout my project. His expertise, understanding, generous guidance and support made it possible for me to work on this topic.

I am grateful to Sikkim University and Dr. Sanjay Dahal, HOD, Department of Chemistry for permitting me to utilize all the necessary facilities of the institution. I would like to thank the entire faculty members of the Department of Chemistry for their kind co-operation, help and encouragement.

Besides my supervisor, I would also like to acknowledge my indebtedness and render my warmest thanks to my friends-Samuzal, Karan, Joneswar, Nandagopal, Ankit, Ambika Didi, Kimron and many others for their advice, support and friendship that have been invaluable throughout all the stages of my work.

I would also like to thank Mr. Binod Chettri and Mr. Sovan Dutta laboratory staff for helping me by providing all the necessary support during the course of my research.

Last but not the least; I would like to thank my family for the moral and spiritual support throughout.

Table of Contents

List of Abbreviations		i-ii
List of Figures, Tables and Schemes		iii-vi
Preface		vii-viii
List of Publications		ix
Aim of the Thesis		x
CHAPTER 1	**EFFICIENT IRON CATALYZED LIGAND-FREE ACCESS TO ACRIDINES**	
1.1	Introduction	1-3
1.2	Literature review	4-9
1.3	Limitations of previous methods	10-11
1.3	Synthetic scheme	12
1.4	Results and discussions	13-24
1.5	Conclusions	25
1.6	Experimental Section	26-27
1.7	Spectral data of newly formed compounds	28-36
CHAPTER 2	**VISIBLE LIGHT MEDIATED SYNTHESIS OF QUINOLIN-2(*1H*)-ONES FROM QUINOLINE *N*- OXIDES**	
2.1	Introduction	68-70
2.2	A brief introduction of visible-light photocatalysis	70-73

2.3	Literature Review	74-78
2.4	Limitations of previous methods	79
2.5	Current synthetic scheme	80
2.6	Results and discussions	81-89
2.7	Conclusions	90
2.8	Experimental section	91-92
2.9	Spectral data of the newly synthesized compounds	93-102

CHAPTER 3 VISIBLE LIGHT MEDIATED DEOXYGENATION OF HETERO-ARYL *N*-OXIDES

3.1	Introduction	137-138
3.2	Literature Review	139-144
3.3	Synthetic scheme	145
3.4	Results and discussion	146-151
3.5	Conclusions	152
3.6	Experimental section	153
3.7	Spectral data of the compounds	154-161

List of Abbreviations

ACN	Acetonitrile
TFA	Trifluoroacetic acid
NaOH	Sodium hydroxide
EtOAc	Ethylacetate
DCM	Dichloromethane
DMSO	Dimethyl sulfoxide
DCE	Dichloroethane
DMA	Dimethyl acetamide
THF	Tetrahydrofuran
DIPA	Di-isopropyl amine
$Na_2S_2O_8$	Sodiumperoxodisulphate
SET	Single electron transfer
PET	Photo induced electron transfer
LED	Light emitting diode
OLED	Organic light emitting diode
CPY	Cytochrome
HAT	Hydrogen atom transfer
MW	Microwave
MCR	Multicomponent reaction
NMR	Nuclear magnetic resonance
FTIR	Fourier transformed infrared spectroscopy

UV	Ultraviolet
TLC	Thin layer chromatography
BDE	Bond dissociation energy
TEMPO	(2, 2, 6, 6-Tetramethylpiperidin-1-yl)oxyl
RB	Round bottom flask
PC	Photocatalyst
DMF	Dimethylformamide
Ir-PC	Iridium photocatalyst
Ru-PC	Ruthenium photocatalyst
DIPEA	*N*, *N*-Diisopropyethylamine
Ac_2O	Acetic anhydride
FDA	Food and Drug Administration
HIV	Human immunodeficiency virus
HPLC	High Performance Liquid Chromatography
PTSA	*p*-Toluenesulfonic acid
TCE	Tricholoroethylene

List of figures, tables and schemes:

		Page No.
Fig. 1.1	Natural products and bioactive molecules of acridines.	2
Fig. 1.2	Bond forming strategies applied so far for synthesis of acridines.	2
Fig. 1.3	Isolated product profile of oxidative dehydrogenation of **1** after 40 min of MW heating with respect to $FeCl_3$ concentration.	16
Fig. 1.4	Substrate scope for the formation of acridines.	19
Fig. 1.5	Analysis of product profile with respect to reaction time in conventional reflux with 1 equiv. of $FeCl_3$ in methanol using HPLC.	21
Fig. 1.6	Plausible mechanism for $FeCl_3$ catalyzed oxidative dehydrogenation to acridines.	22
Fig. 2.1	Natural products and bioactive drugs containing a quinoline-2(*1H*)-one moiety.	68
Fig. 2.2	Schematic representation of photoinduced electron transfer process.	72
Fig. 2.3	Mechanistic pathways of photocatalysis (A) photoredox catalysis pathway (B) energy transfer pathway.	73
Fig. 2.4	Photocatalysts used for the optimization of reaction.	83
Fig. 2.5	Substrate scope for the formation of 2-quinolones.	84
Fig. 2.6	Concentration dependent change in rate of the reaction.	86

Fig. 2.7	Computed Gibbs free energy profile for photocatalytic synthesis of quinolin-2(1H)-one.	87
Fig. 2.8	Proposed mechanism for visible light photoredox catalytic synthesis of quinolin-2(*1H*)-ones.	88
Fig. 3.1	Substrate scope for the deoxygenation of aza-aromatic *N*-oxides.	148
Fig. 3.2	Deoxygenation of substituted pyridine *N*-oxides.	149
Fig. 3.3	Proposed mechanism for organo-photocatalytic deoxygenation of heteroaromatic *N*-oxides.	151
Table.1.1	Optimization table for the synthesis of acridines.	14
Table. 2.1	Optimization table for the synthesis of quinoline-2(*1H*)-ones from quinoline *N*-oxides.	82
Table. 3.1	Evaluation of reaction conditions for the deoxygenation of *N*-aryl *N*-oxides.	147
Scheme. 1.1	Bernthsen acridine synthesis via condensation reaction.	4
Scheme. 1.2	Rh-catalyzed synthesis of unsymmetrical acridines.	5
Scheme. 1.3	A facile synthesis of acridines via Pd-catalyzed coupling reactions.	5
Scheme. 1.4	Synthesis of acridines by Pd-catalyzed C=C bond formation and C-N cross-coupling.	6
Scheme. 1.5	A Pd-catalyzed synthetic route to acridines.	6
Scheme. 1.6	Synthesis of acridines through [4+2] annulation reaction.	7
Scheme. 1.7	An excess to acridines through nitrogen-iodine exchange reaction.	7
Scheme. 1.8	A Pd-catalysed one-pot synthesis of acridines.	8

Scheme. 1.9	A Cu-catalyzed synthetic route to acridines through cascade relay reactions.	8
Scheme. 1.10	Rh-catalyzed synthesis of asymmetric acridines.	9
Scheme. 1.11	Rh(III)-catalyzed synthesis of acridine derivatives.	9
Scheme. 1.12	Schematic representation for the synthesis of acridines.	12
Scheme. 2.1	A synthetic route to 2-quinolines via Pd-catalyzed C-H activation.	74
Scheme. 2.2	Ruthenium-catalyzed synthesis of 2-quinolones.	75
Scheme. 2.3	A palladium-catalysed synthetic route to quinoline-2(1H)-ones via an intramolecular amidation reaction.	75
Scheme. 2.4	A one-pot copper catalyzed synthesis of isoquinolin-1(2H)-ones.	76
Scheme. 2.5	An efficient Pd-catalyzed route to isoquinolin-1(2H)-ones.	76
Scheme. 2.6	A fast and aqueous synthesis of quinoline-2(*1H*)-ones under milder conditions.	77
Scheme. 2.7	Palladium-catalyzed synthesis of Quinoline-2(*1H*)-ones.	77
Scheme. 2.8	A general synthesis of hydroxyazines from azine *N*-oxides.	78
Scheme. 2.9	A facile synthesis of *N*-methoxyquinolin-2(1H)-ones from *N*-methoxyquinoline-1-ium.	78
Scheme. 2.10	Schematic representation for the synthesis of quinoline-2(*1H*)-ones from quinoline *N*-oxides.	80
Scheme. 3.1	Metal-free deoxygenation of aza-aromatic *N*-oxides.	139

Scheme. 3.2	Molybdenum-catalyzed deoxygenation of heteroaromatic *N*-oxides.	140
Scheme. 3.3	Cu-catalyzed deoxygenation of *N*-heterocyclic *N*-oxides.	140
Scheme. 3.4	Deoxygenation of aza-heterocycle *N*-oxides using gold-hybrid carbon nano tube.	141
Scheme. 3.5	Catalytic deoxygenation of pyridine *N*-oxides using rhodium POP pincer complex.	142
Scheme. 3.6	Visible-light photocatalyzed deoxygenation of aza-heterocycle *N*-oxides.	142
Scheme. 3.7	A metal-free approach to deoxygenation of pyridine *N*-oxides.	143
Scheme. 3.8	Catalyst-free *N*-deoxygenation by Hantzsch ester as reducing agent.	144
Scheme. 3.9	A chemo-selective deoxygenation of *N*-heterocyclic *N*-oxides.	144
Scheme. 3.10	Schematic representation for the deoxygenation of aza-aromatic *N*-oxides.	145
Scheme. 3.11	Stepwise synthesis of 8-tolyl substituted quinoline.	150

PREFACE

Synthesis of nitrogen containing heterocyclic compounds is one of the most important areas of organic chemistry due to their ubiquity in biologically important natural products and enormous importance in medicinal chemistry. According to the recent FDA data over 60% of the approved antibiotics, antivirals, antimalarials and anticancer drugs contain *N*-based heterocyclic subunits and this trend remain unchanged in broad spectrum of drug classes. Apart from the biological activities these azaheterocycles are frequently used as reagents, ligands in the formation of metal complexes and value-added organic materials like, conducting polymers, organophoto catalysts and ion sensors. They also play a significant role in our daily lives as dyes, flavoring agents, sensitizers, agrochemicals, herbicides etc.

Their biological and industrial usefulness have attracted considerable attention from synthetic chemists and with time many methods have been developed for their synthesis. Most of the earlier synthetic methods are focused on accomplishing the desired product with very little concern for the mild reaction condition, eco-friendliness and sustainability. However, developing more efficient, milder and ecofriendly synthetic methods remain a quest for sustainable synthesis. Therefore, in last two decades the environmental concern and economic implications have made scientist more interested in developing hassle-free, more efficient and environment-friendly synthetic route; that encourage the use of ecofriendly, inexpensive, catalytic methods which is highly atom-economic and produce no hazardous byproducts. Though in recent times significant progress has been made for the synthesis of various azaheterocycles through discovery of comparatively milder and efficient catalytic methods, use of expensive heavy metal catalyst, commercially unavailable starting

materials, harsh reaction condition and generation of hazardous byproducts still remains as a serious concern.

Keeping that in mind, in this thesis we endeavored to develop efficient and greener synthetic methods for synthesis of some industrially important class of azaheterocycles. The methods described here are efficient, mild and operationally simple and often use commercially available inexpensive starting materials and ecofriendly reagents to get access to some commercially important azaheterocycles with very high atom-economy, thus provides much better alternatives to all previous synthetic methods. The thesis is divided in three different chapters. The first chapter discuss about green atom and step-economic synthesis of acridines starting from inexpensive and commercially available starting materials. The second chapter describes reagent-free ambient-temperature photocatalytic synthesis of 2-quinolones starting from easily synthesizable pyridine *N*-oxides using acridinium ion based photocatalyst. The third chapter deals with the deoxygenation of aza-aromatic *N*-oxides using di-isopropyl amine as hydrating agent under visible light irradiation at room temperature.

List of Publications:

1. **Mandal, S**.; Chhetri, K.; Bhuyan, S.; Roy, B. G. Efficient Iron Catalyzed Ligand-Free Access to Acridines and Acridinium Ions. *Green Chem.* **2020**.
2. **Mandal, S.**; Bhuyan, S.; Jana, S.; Hossain, J.; Chhetri, K.; Roy, B. G. Efficient Visible Light Mediated Synthesis of Quinolin-2(1H)-Ones from Quinoline N-Oxides. *Green Chem.*, **2021**, *23*, 5049–5055.
3. Chhetri, K.; Bhuyan, S.; **Mandal, S.;** Chhetri, S.; Lepcha, P. T.; Lepcha, S. W.; Basumatary, J.; Roy, B. G. Efficient Metal-Free Visible Light Photocatalytic Aromatization of Azaheterocyles. *Current Research in Green and Sustainable Chemistry* **2021**, *4*, 100135.
4. Subba, S.; Saha, S.; **Mandal, S**. A Diastereoselective Synthetic Approach towards the Synthesis of Berkeleylactone F and Its 4-Epi-Derivative. *SynOpen* **2020**, *04* (04), 66–70.
5. Bhuyan, S.; Das, D.; Chakraborty, A.; **Mandal, S.;** Dhanabal, K.; Roy, B. G. A Carbohydrate-Based Synthetic Approach to Diverse Structurally and Stereochemically Complex Chiral Polyheterocycles. *Chem. – Asian J.* **2021**, *16* (24), 4108–4121.
6. Bhuyan, S.; **Mandal, S.;** Jana, S.; Chhetri, K.; Roy, B. G. Efficient Greener Visible Light Catalyzed Debenzylation of Benzyl Ethers and Esters: A Gateway to Wider Exploitation of Stable Benzyl Protecting Group. *Asian J. Org. Chem.* **2022**.
7. Pradhan, A.; Bhuyan, S.; Chhetri, K.; **Mandal, S.;** Bhattacharyya, A. Saponins from Albizia Procera Extract: Surfactant Activity and Preliminary Analysis. *Colloids Surf. Physicochem. Eng. Asp.* **2022**, *643*, 128778.

Aim of the Thesis:

The primary aim of this thesis was to extend the use of cheaper and eco-friendly catalysts in organic synthesis. The use of $FeCl_3$ can be considered as a better alternative to low sustainable palladium catalysts for the oxidative aromatization of six membered rings. In our first approach for the synthesis of aza-aromatic heterocycles the presence of $FeCl_3$ was investigated as an alternative of heavy transition metal and to our delight $FeCl_3$ proved to be a very successful catalyst for such aromatization to produce 1,8 dimethoxy acridines in presence of alcohols.

In second approach the use of organo-photo catalysts was investigated for the synthesis of 2-quinolone systems under visible light irradiation. Acridinium based photocatalysts can absorb energy in blue light region and can promote the isomerization of quinoline *N*-oxides to quinoline-2(*1H*)-ones. This methodology also provides a reagent free alternative, which reduced the hazardous byproducts.

The last chapter of our work focus on the importance of organo-photo catalyst for the deoxygenation of *N*-heterocyclic *N*-oxides. The conventional deoxygenation methods either require harsh reaction conditions or heavy metal photocatalysts which are not suitable for the substrates with labile functional groups. Due to the milder reaction conditions this strategy tolerates labile functional groups, which is the main advantage of this methodology.

Chapter-1 Efficient iron catalyzed ligand-free access to acridines

1.1 Introduction.

Acridines are a class of heteroaromatic compounds which are structurally related to anthracenes where the aromatic C-H at 10 position is replaced by a Nitrogen. Since the initial isolation of acridine in 1870 from coal tar, this class of compounds attracted considerable scientific attention due to gradual realization of their scientific and industrial utility. The first synthesis was carried out by Bernthsen in 1884,[1] where it was synthesized through condensation of diphenylamine with benzoic acid using zinc chloride and high temperatures. Initial commercial significance of acridine as organic dye and later gradual exploration of industrial significance of many of their derivatives made this class of compounds cynosure of the synthetic community. The biological importance and other commercial significances encouraged the development of many more new methodologies, which ultimately resulted in synthesis of more analogues/derivatives leading to exploration of more interesting properties. Till date acridines have been found to show very broad range of research and industrial utility in medicinal chemistry[2–4], chemosensor,[5,6] organic dye,[7,8] photo catalysis[9] and in photovoltaic cell as hole transport materials.[10,11] Acridine have demonstrated important antibacterial,[12] antiviral activity,[13] including activity against cancer due to their ability to intercalate into DNA and disrupt unwanted cellular processes. It shows significant biological activities towards parasites,[14] fungus, Alzheimer's disease[15] and HIV/AIDS.[16,17] Many of the acridine derivatives are available in natural products and also being used as the FDA approved drugs[18–22] (some representative examples are shown in Fig. 1.1). Besides its ubiquitous presence in pharmaceutical and natural products, acridines have also found their application as value added materials as many of their derivatives and polymers displayed promising potential in the field of organic

semiconductor materials.[23] Acridine complex with iridium have also been used as light emitting materials for application in OLEDs.[24]

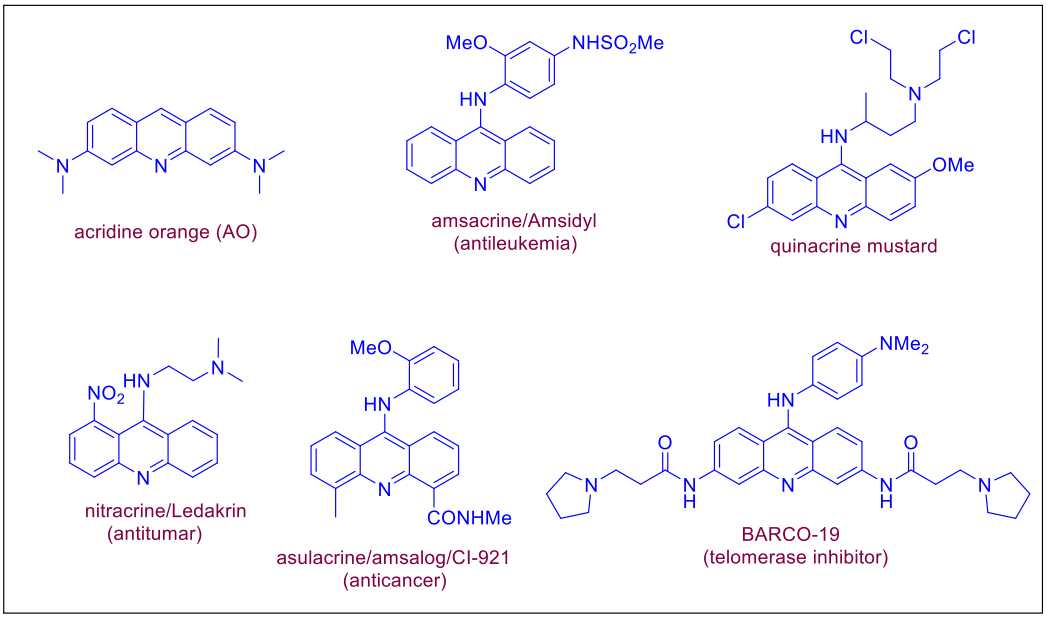

Fig. 1.1 Natural products and bioactive molecules of acridines.

Due to their enormous industrial importance since the first synthesis by Bernthsen many synthetic methods have been reported. All these reported synthetic methods mainly deal with construction of a new 6-membered ring through formation of any one or two bonds on appropriately substituted functional groups in the pre-functionalized aromatic

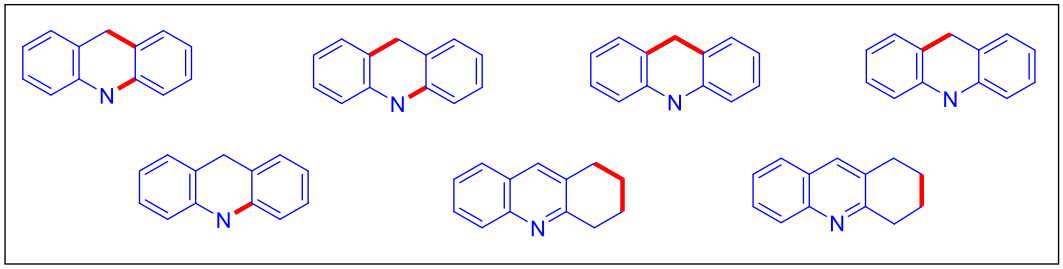

Fig. 1.2 Bond forming strategies applied so far for synthesis of acridines.

systems (Fig. 1.2). In most cases, these suitably substituted aromatic precursors are not commercially available and their synthesis itself are often difficult, require multiple steps and extra resources. Moreover, many of these syntheses require high temperature, which limits their functional group tolerance and consequently reduce generality and

versatility of the reaction. Some recent approaches as discussed in the literature review have tried to employ comparatively milder reaction conditions. However, all these syntheses also started with pre-functionalized aromatic system and required heavy metal-ligand complexes as catalyst or highly reactive precursors for synthesis of acridines. To overcome these challenges, we were interested in synthesizing acridine from commercially available starting materials by employing more efficient, tolerant, ecofriendly and atom-economic approach. To provide a correct perspective and motivation behind the current work, some of the recent methodology for the synthesis of acridines have been discussed below.

1.2 Literature Review.

In this segment we have reviewed some of the interesting synthesis of acridine reported by various groups using different strategies and starting materials.

Bernthsen first synthesized acridine in 1884[1] by the condensation reaction between diphenyl amine and benzoic acid using $ZnCl_2$ as the catalyst at 220 ^oC. To explore the substrate scope, they have used number of other aliphatic and aromatic carboxylic acids for condensation with diphenyl amine to obtain different 9-alkyl/aryl acridines. In this initial synthesis they have only demonstrated the preparation of different 9-alkyl/aryl substituted acridines. Moreover, the reaction requires considerably high temperature to give low yield and hence constrained by reduced efficiency and low substrate scopes. However, this early synthetic success has inspired scientist around the world to come up with numerous intriguing methods for synthesis of diverse acridine derivatives. Some of the very prominent recent approaches have been discussed below.

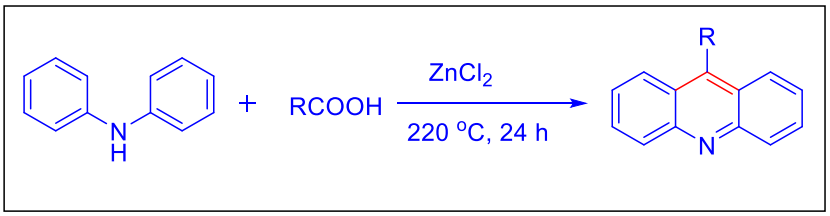

Scheme: 1.1 Bernthsen acridine synthesis via condensation reaction.

In 2013, Jonathan A. Ellman[25] group have reported a Rh-catalyzed synthesis of acridine through a [3+3] annulation process using aromatic azides and imines as the starting materials. The synthesis of imines by the condensation reactions from aromatic aldehydes in presence of benzylamines increased one extra step in this methodology. The authors proposed a two steps cascade mechanism where in the first step ortho amination occurred through C-H activation by Rh-catalyzed and in the second step

intramolecular electrophilic substitution and aromatization took place to generate acridines. The authors also tested a variety of additives and found that Ac_2O as additive gives highest yield (77%) at 110 °C.

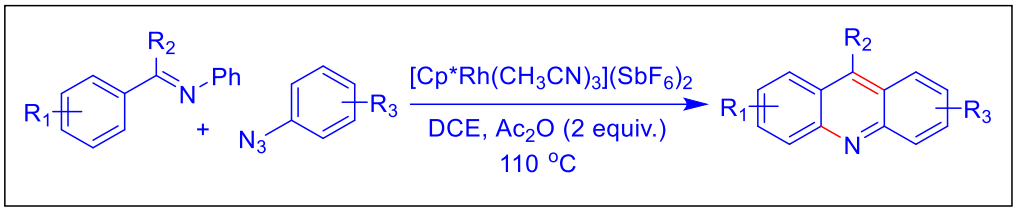

Scheme: 1.2 Rh-catalyzed synthesis of unsymmetrical acridines.

Ming-Hua Xu group[26] in the year 2015, reported an efficient and facile method for the synthesis of acridines from substituted anilines and 2-Br benzaldehydes through tandem coupling reaction using palladium-ligand complex as the catalyst in presence of K_2CO_3 as a base. With this methodology they have synthesized a variety of acridine derivatives in moderate to excellent yields by changing the substituents in aldehydes and anilines. They found that $AlCl_3$ is needed as Lewis acid for cyclization in case of neutral or electron-deficient anilines. However, this methodology uses expensive heavy metal catalyst $Pd_2(dba)_2$ and biphosphate ligand dppf at 80 °C for the desired coupling.

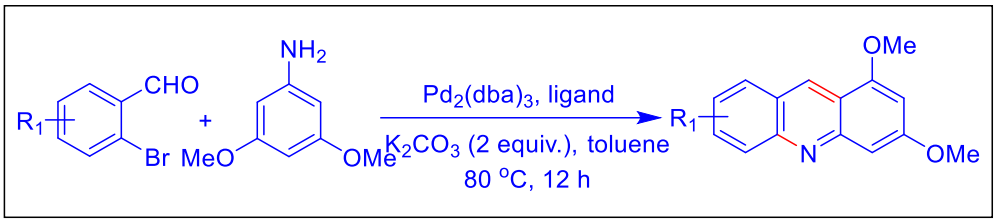

Scheme: 1.3 A facile synthesis of acridines via Pd-catalyzed coupling reactions.

A facile Pd-catalyzed synthesis of acridines has been reported by Jianbo Wang *et. al.*[27] from 1,2 dihalobenzenes and *N*-tosylhydrazones in dioxane solvent at 110 °C. The authors have proposed a two-step mechanism consisting of simultaneous C=C bond formation followed by C-N bond formation through intramolecular cross-coupling

reaction in presence of palladium complex catalyst. They have tested a series of ligands to find Ru-Phos to give the highest yield in presence of LiO^{t}Bu base at 110 ^{o}C. The use of expensive heavy metal complex as the catalyst and high equivalent of base reduces the substrate scope and sustainability of the reaction.

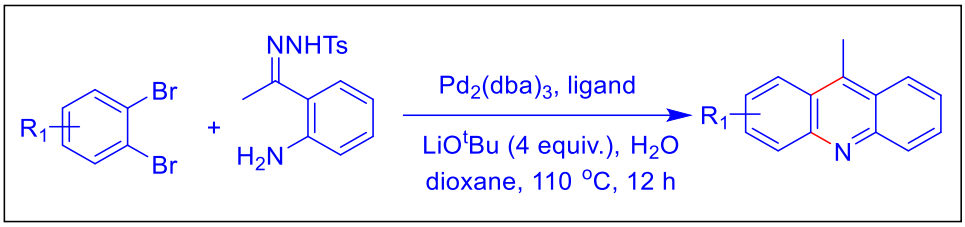

Scheme: 1.4 Synthesis of acridines by Pd-catalyzed C=C bond formation and C-N cross-coupling.

Stephen L. Buchwald group[28] in the year 2010, developed a methodology for the synthesis of six membered aza-aromatic heterocycles from suitably substituted diphenylamine precursor in presence of $Pd_2(dba)_3$ catalyst at 100 ^{o}C for 24 h. In this methodology the precursors have been prepared by the reactions between 2-Cl anilines and 2-Br styrenes through Pd-catalyzed condensation reaction. Synthesis of these suitably substituted precursors requires several steps, which add to the energy and resources, moreover use of heavy metal catalysts and basic condition create significant environmental hazard.

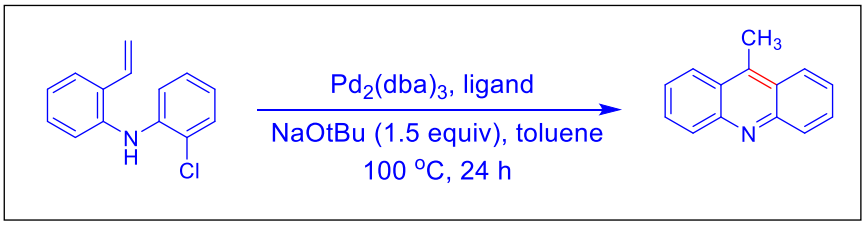

Scheme: 1.5 A Pd-catalyzed synthetic route to acridines.

In 2010, Larock et. al.,[29] reported the synthesis of acridine derivatives through a [4+2] annulation reactions using 2-aminoaryl ketones and o-(trimethylsilyl)aryl triflates at 65 ^{o}C in acetonitrile solvent. In this methodology they have used highly activated o-(trimethylsilyl)aryl triflate for the synthesis of aryne intermediates in presence of CsF, which participate in annulation reaction to form acridines.

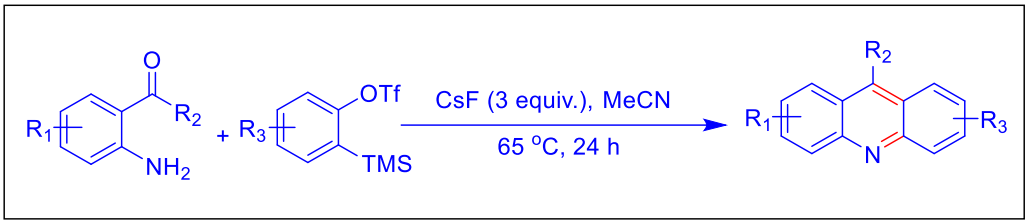

Scheme: 1.6 Synthesis of acridines through [4+2] annulation reaction.

A copper-catalyzed synthetic route for the synthesis of acridines has been developed by X. Jiang group[30] through a nitrogen-iodine exchange reaction between activated diaryliodonium salts and excess sodium azide. In this methodology they used stoichiometric amount of triphenylphosphine to reduce the amount of sodium azide. They have not observed the desired acridine product when $Fe(acac)_2$ or $Pd(OAc)_2$ was used as catalyst instead of CuTc. However, high reaction temperature, very long reaction time and requirement of activated systems are required for the synthesis of desired acridine.

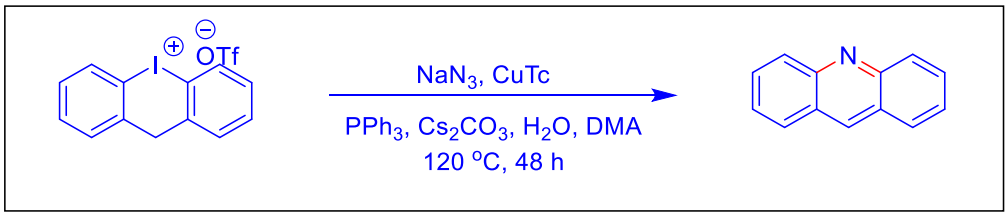

Scheme 1.7 An excess to acridines through nitrogen-iodine exchange reaction.

In 2013, Gui-Rong Qu and co-workers[31], reported a Pd-catalysed one-pot synthesis of asymmetric acridines via an amination/cyclization/aromatization process using toluene as the solvent. During the optimization process they observed that $Pd(OAc)_2$/X-Phos catalyst system is capable to produce excellent yield only when they used K_2CO_3 as additive in stoichiometric amount, whereas the other bases such as *t*-BuOK, Cs_2CO_3, K_3PO_4 and Na_2CO_3 resulted only trace amount of product under same reaction conditions.

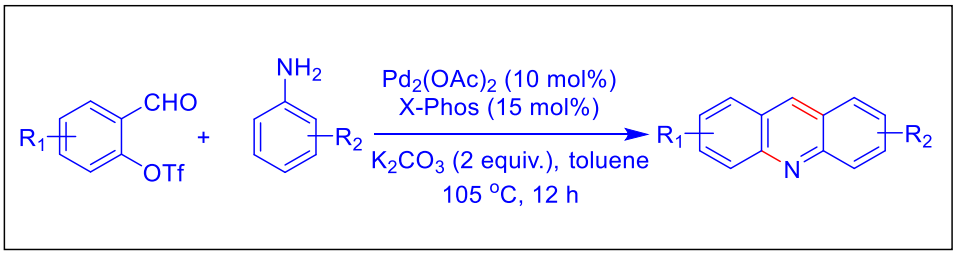

Scheme 1.8 A Pd-catalysed one-pot synthesis of acridines.

Another Cu-catalyzed synthetic route has been developed for the synthesis of acridines by G. Zhang group[32] through an intermolecular coupling/intramolecular annulation reaction. After screening different Cu(II) catalysts they found that $Cu(OTf)_2$ as a catalyst led to the highest yield at 100 °C. The authors also tested a number of additives like pyridine, L-proline, triphenylphosphine or 1,10-phenanthroline to improve the reaction yield but no noticeable improvement was observed under same reaction conditions.

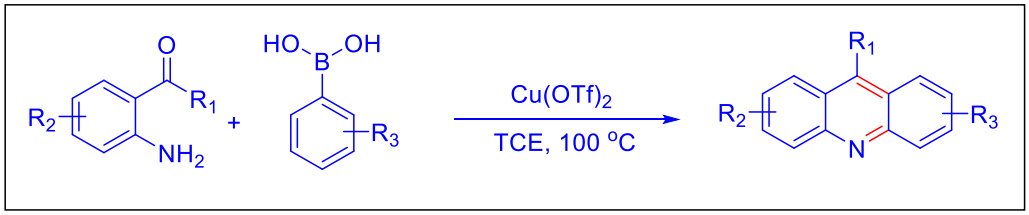

Scheme 1.9 A Cu-catalyzed synthetic route to acridines through cascade relay reactions.

J. Shen *et. al.*,[33] developed a methodology for the synthesis of acridines using aldehydes and azides as starting materials in presence of Rh-catalyst at 120 ^{o}C. Using $[RhCp^{*}Cl_2]_2$ as catalyst, their initial attempt to generate the product was failed and later the use of glycine as directing group resulted only 23% yield of the product. After that switching glycine to different amines such as aniline, amino acids and benzyl amine they found that only benzyl amine produced the satisfactory yield (63%), which suggests that the presence of benzyl amine as transient directing group (TDG) is essential for the *ortho*-amination of benzaldehydes through C-H activation.

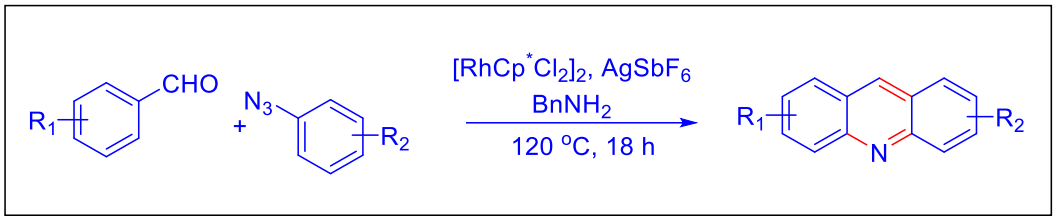

Scheme 1.10 Rh-catalyzed synthesis of asymmetric acridines.

R. Samanta *et. al.*,[34] reported a synthetic route to acridine derivatives through an amination/annulation strategy using Rh-catalyst at 110 ^{o}C. In this methodology, they have proposed an amination followed by intramolecular annulation mechanism for the formation of acridine derivatives. After screening different Rh-metal catalysts and additives they found that $[Cp^{*}RhCl_2]_2$ was the best one for this methodology in presence of NaOAc as additive in DCE as the solvent.

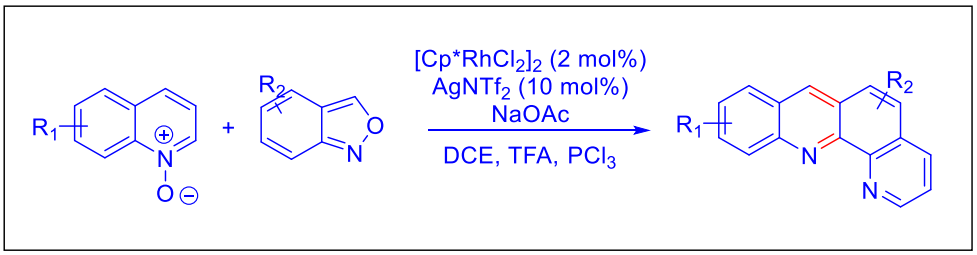

Scheme 1.11 Rh(III)-catalyzed synthesis of acridine derivatives.

1.3 Limitations of all previous methods:

As evident from the literature, from its initial synthesis by Brenthsen in 1884 till date, all the reported syntheses have mainly dealt with construction of a new 6-membered ring through formation of any one or two bonds on suitably pre-functionalized aromatic system. In most cases, the suitably substituted aromatic precursors used in these methods are not commercially available, often difficult to prepare, require multiple steps and hence demand extra time and resource, also create significant environmental hazards. Moreover, these reported methods either require high temperature and expensive heavy metal-ligand complex catalyst or highly reactive substrates for synthesis of acridines, which limit their substrate scope and functional group tolerance. These current challenges motivated us to develop an efficient, eco-friendly method for the synthesis of acridine from commercially available inexpensive starting materials. As described below, to make our synthesis efficient, inexpensive and atom-economical we have used an efficient and popular multicomponent reaction, Hantzsch synthesis, which deals in synthesis of varieties of hexahydroacridine 1,8-dione starting material from commercially available cyclohexyl-1,3-dione, aldehydes and ammonium acetate. The capability of generating multigram scale pure hexahydroacridine 1,8-dione as solid in a single-step and its structural similarity with desired acridine prompted us to take it as the starting material for our oxidative dehydrogenation approach. Though there were multiple reports for oxidative dehydrogenation of core dihydropyridine to yield tetrahydroacridine-1,8-diones using several oxidizing agents,[35–37] we have not found any report regarding further dehydrogenation of two peripheral cyclohexene to get access to acridines. Stahl group[38–40] and others[41–43] have expended some effort in developing palladium complex catalyzed dehydrogenation of cyclohexanones and cyclohexenones to get access to phenol but no such methodology has been utilized for

synthesis of acridines. Moreover, a toxic heavy metal and ligand-free approach can be a more desirable solution to this problem. Keeping that in mind we have developed a direct one-pot synthesis of acridine as described below.

1.4 Current Synthetic Scheme

Herein, we have presented an environmentally friendly $FeCl_3$ catalyzed stepwise and one-pot method for the synthesis of substituted acridines directly from easily available 1,3-cyclohexadiones, aldehydes and ammonium acetate.

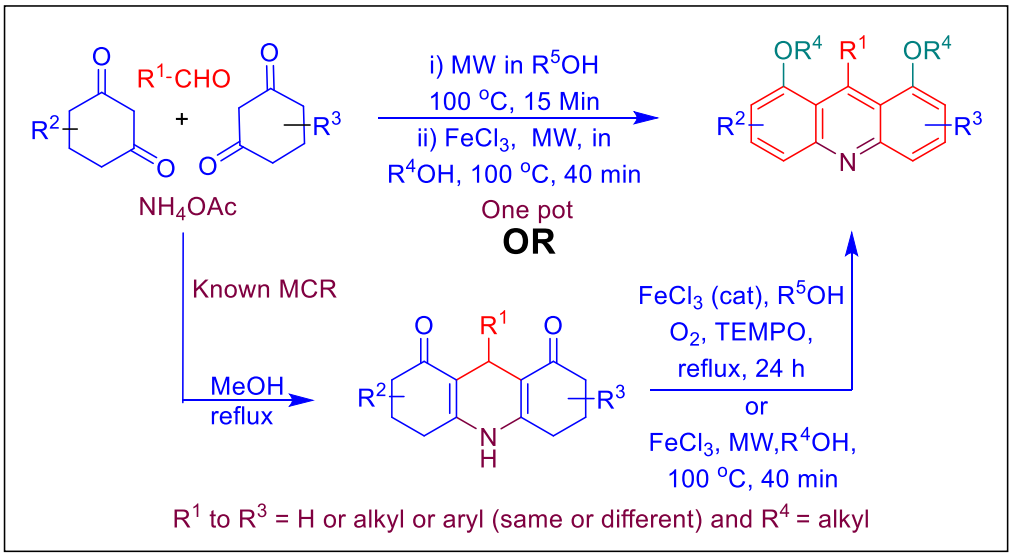

Scheme: 1.12 Schematic representation for the synthesis of acridines.

In stepwise method we first used known MCR for synthesis of hexahydroacridine dione, which then converted to acridine through $FeCl_3$ catalyzed oxidative dehydrogenation by microwave or conventional heating. Whereas, in case of one-pot method we have directly used commercially available MCR constituents; 1,3-cyclohexadiones, aldehydes and ammonium acetate for synthesis of desired acridine through sequential addition of $FeCl_3$ catalyst.

1.5 Results and Discussions

As stated earlier, we have used popular Hantzsch multicomponent reaction for getting easy access to our starting material hexahydroacridine-1, 8-dione **1** using commercially available 1, 3-cyclohexadiones, aldehydes and ammonium acetate. Dehydrogenation of the core dihydropyridine ring is easier and widely reported.[35–37] However, we have not found any report for the dehydrogenation of two peripheral cyclohexene ring. For the oxidative dehydrogenation of the peripheral ring, we were interested in using different inexpensive, easily available and eco-friendly oxidizers, preferably without using any ligand. For that purpose, initially we choose some very commonly used oxidizer available in laboratory and tried to react with **1** in number of different solvents. To start with, we chose to take higher equivalent of oxidizers (5 equiv.) and use microwave heating at 100 ^{o}C for 1 h to observe any noticeable transformation in the reaction as early as possible. Initially we thought polar aprotic or nonpolar solvents might assist the dehydrogenation reaction. Our initial effort with acetonitrile as solvent with different oxidizing agents though successful in oxidizing the middle dihydropyridine ring relatively quickly to generate 1,8-tetrhydroacridinedione, remain invariably unsuccessful in oxidizing the peripheral two cyclohexenone moiety. Similar trends have been observed in dichloromethane, tetrahydrofuran and toluene. Initial disappointment with polar aprotic solvents compelled us to try polar protic solvents like water and alcohol. When we tried the reaction in water using similar reaction condition, in all the cases the starting material **1** was found to remain unreacted after 1 h of microwave heating at 100 ^{o}C. However, we were delighted to find that the same reaction condition using methanol was able to generate a clear different spot when monitored using TLC with different iron (III) and copper (II) oxidizer salts which were used as oxidizer. Though, the amount of conversion to the new product was different

in case of different oxidizers, in all the cases it led to generation of the same product as was evident from their same rf in TLC. The purification of the compound in column chromatography and subsequent NMR spectroscopic study revealed that the generated new compound was indeed acridine but unlike our expectation it generated 1,8-dimethoxy derivative. This encouraging outcome compelled us to think that probably the solvent methanol is participating in the reaction to make it possible. As the reaction was not happening in other solvents but in methanol, to test our hypothesis we were tempted to assess the outcome of the reaction using other alcohols. After screening different oxidizers, we were pleasantly surprised that the most inexpensive and eco-friendly $FeCl_3$ produced the highest yield (73%) in presence of MeOH as the solvent (Entry 13, Table 1.1). To our delight, in case of ethanol as we expected 1,8-diethoxyacridine was obtained with 70% yield. When the same reaction was repeated with other alcohols like propanol, butanol, tert-butanol, in all the cases the reaction went smoothly to generate 1,8-dialkoxy acridines with good yields except in case of bulky tert-butanol, where only the middle ring gets aromatized. The above-mentioned observations clearly indicate that both alcohols and suitable metal catalyst are necessary for the aromatization to acridine derivatives.

Table: 1.1 Optimization of reaction conditions

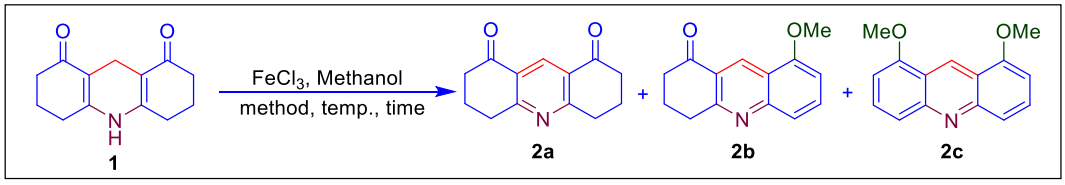

Sl. No.	Reagent and condition				Time	Yield (%)		
	Reagents (equiv.)	Solvent	Method	Temp. (°C)		2a	2b	2c
1	$CuBr_2$ (5 equiv.)	MeOH	MW	100	40 min	40	16	8
2	$Cu(OAc)_2.H_2O$ (5 equiv.)	MeOH	MW	100	40 min	16	0	0
3	$Fe(ClO_4)_3.H_2O$ (5 equiv.)	MeOH	MW	100	40 min	30	25	10

4	$Pd(OAc)_2$ (5 equiv.)	MeOH	MW	100	40 min	20	50	9
5	$FeCl_3$ (5 equiv.)	THF	MW	100	40 min	83	0	0
6	$FeCl_3$ (5 equiv.)	CH_3CN	MW	100	40 min	88	0	0
7	$FeCl_3$ (5 equiv.)	CH_2Cl_2	MW	100	40 min	75	0	0
8	$FeCl_3$ (5 equiv.)	$CHCl_3$	MW	100	40 min	78	0	0
9	$FeCl_3$ (5 equiv.)	MeOH	MW	100	30 min	10	24	38
10	$FeCl_3$ (5 equiv.)	MeOH	MW	100	50 min	0	13	67
11	$FeCl_3$ (7 equiv.)	MeOH	MW	100	40 min	0	4	62
12	$FeCl_3$ (6 equiv.)	MeOH	MW	100	40 min	0	7	66
13	$FeCl_3$ (5 equiv.)	MeOH	MW	100	40 min	0	12	73
14	$FeCl_3$ (4 equiv.)	MeOH	MW	100	40 min	3	29	48
15	$FeCl_3$ (3 equiv.)	MeOH	MW	100	40 min	9	43	26
16	$FeCl_3$ (2 equiv.)	MeOH	MW	100	40 min	21	42	8
17	$FeCl_3$ (1 equiv.)	MeOH	MW	100	40 min	38	13	0
18	$FeCl_3$ (0.5 equiv.)	MeOH	MW	100	40 min	31	5	0
19	TEMPO (5 equiv)	MeOH	MW	100	2 h	90	0	0
20	$FeCl_3$ (1 equiv.), O_2 (1 atm)	MeOH	Conventional	Reflux	36 h	0	36	32
21	$FeCl_3$ (0.5 equiv.), air (1 atm)	MeOH	Conventional	Reflux	24 h	10	46	11
22	$FeCl_3$ (0.5 equiv.), O_2 (1 atm)	MeOH	Conventional	Reflux	24 h	2	40	25
23	$FeCl_3$ (0.5 equiv), Ar (1 atm)	MeOH	Conventional	Reflux	24 h	42	0	0
24	$FeCl_3$ (0.4 equiv), O_2 (1 atm)	MeOH	Conventional	Reflux	24 h	10	46	18
25	$FeCl_3$ (0.2 equiv), O_2 (1 atm)	MeOH	Conventional	Reflux	24 h	21	40	5
26	$FeCl_3$ (1 equiv), O_2 (1 atm), TEMPO (3 equiv)	MeOH	Conventional	Reflux	24 h	0	18	63
27	$FeCl_3$ (0.5 equiv), O_2 (1 atm), TEMPO (3 equiv)	MeOH	Conventional	Reflux	24 h	0	25	44
28	TEMPO (5 equiv)	MeOH	Conventional	Reflux	24 h	86	0	0

With the best combination of solvent and oxidizer in our hand, we became interested in finding the optimized condition for this oxidative aromatization reaction. In order to do that we have performed multiple reactions on our model substrate **1** with different concentration of $FeCl_3$ and analysed the yield percentage of the product after column chromatographic purification (Entry 9-18, Table 1.1). In case of 1 equiv. $FeCl_3$, no desired product was obtained, only 13 % of the **2b** product was formed after 1 h. After the increase of $FeCl_3$ concentration up to 5 equiv., a steady increase of the desired

product **2c** was observed (up to 73%) (Entry 13, Table 1.1). A further increase of oxidizer $FeCl_3$ failed to increase the yield of the product **2c**. On the contrary, the higher equivalent of $FeCl_3$ (more than 5 equiv.) decreased the yield of the product. This is due to the formation of additional side product, 2-Cl 1, 8-dimethoxyacridine in small amount.

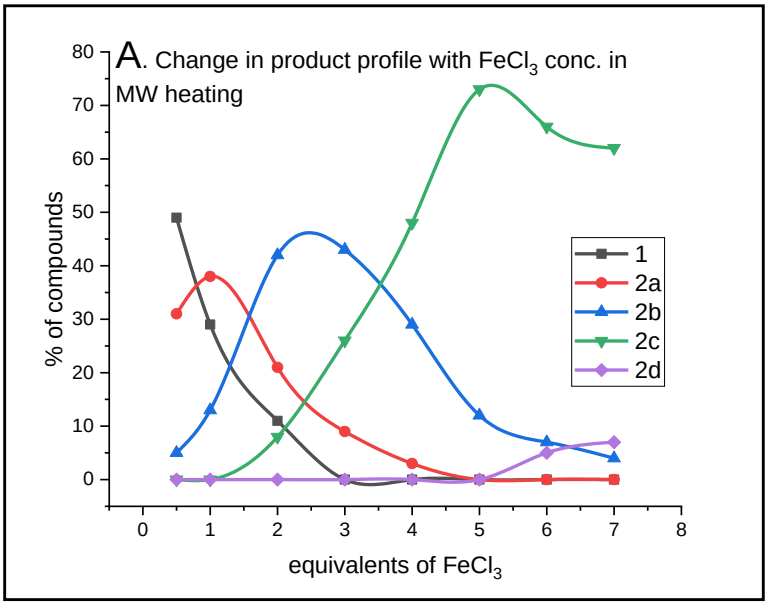

Fig. 1.3 Isolated product profile of oxidative dehydrogenation of 1 after 40 min of MW heating with respect to $FeCl_3$ concentration.

Once the optimization was done, we applied this methodology in various substituted hexahydroacridine-1, 8-dione systems prepared using MCR of different combinations of cyclohexyl diketones, aldehydes and ammonium acetate to check the versatility of this methodology. To our delight, this methodology worked well to generate array of substituted 1,8-dimethoxyacridines, **2c** to **25**, without any difficulty (Fig. 1.4). First, we have checked the effect of the substituents at 9-position of hexahydroacridine-1,8-diones, when there is an electron withdrawing substituents at 9-position of hexahydroacridine 1, 8-diones such as *p*-nitrophenyl **11** (62%), *m*-nitrophenyl **12** (58%), *p*-fluorophenyl **7** (65%) etc., resulted considerable higher yields, compared to

the electron donating substituents at 9-position such as *p*-methoxyphenyl **9** (43%), 3, 5- dimethoxyphenyl **10** (35%), *p*-tolyl **4** (51%) etc., The methyl/phenyl substituents at 3 and 6 positions of the substrates, also contributed higher yields (**16-25**, Fig. 1.4).

One-pot synthetic methods are often preferred in organic synthesis as it provides a much greener, time and cost-efficient alternative to the stepwise method. After successful optimization and substrate scope exploration of synthesis of 1,8-dimethoxyacridines through oxidative aromatization of purified 1,8-hexahydroacridinediones, we became interested in exploring the feasibility of obtaining the same compounds in a one-pot method starting directly from diketones, aldehydes and ammonium acetate. We were pleased to find that, when we conducted one-pot reaction with cyclohexyl-1,3-dione, formaldehyde solution and ammonium acetate in methanol under closed-vessel microwave heating at 100 ^{o}C radiation for 10 min and subsequent addition of $FeCl_3$ followed by similar microwave heating for 40 min, we obtained the compound **2c**, albeit with comparatively lower yield (67%). Lower yield in one-pot method compared to the stepwise method described earlier can easily be explained from the fact that in case of stepwise method we started with pure 1,8-hexahydroacridinediones whereas in case of one-pot method the yield represents the overall yield for both MCR and oxidative aromatization reaction. The encouraging result of **2c** propelled us to explore the efficiency of one-pot synthesis of other substrate combinations. Remarkably, similar efficiency was observed in case of all other cyclohexyl-1,3-diketone and aldehyde combinations. However, as expected, one-pot acridine synthesis using equal mixture of two different diketones invariably resulted in three different products, as in case of **21**, **22** and **25** (Fig 1.4).

Considering huge industrial applicability of acridine derivatives, we became interested in exploring the possibility of the reaction in the conventional heating condition and

subsequent scaling up possibility is such condition. Moreover, comparatively slower conventional reaction might be of great help in exploring the mechanism of the reaction. With those objectives when we tried to carry out the aromatization of **1** with 0.5 equiv. of $FeCl_3$ under refluxing methanol at 1 atm pressure of O_2, indeed the reaction yielded **2c** with 23% yield. As expected, the increased equiv. of $FeCl_3$ to **1** under same reaction condition, the yield of **2c** was found to increase up to 32%. However, addition of TEMPO (3 equiv.) in the reaction mixture found to enhance the yield of **2c** substantially. Earlier we have seen that in absence of $FeCl_3$ TEMPO failed to generate **2c**. That means TEMPO only assist aromatization capability of $FeCl_3$ but it itself is not capable of aromatizing the peripheral rings. To understand the catalytic nature of the reaction when we carried out the reaction in presence of 0.2 equiv. of $FeCl_3$, in argon atmosphere most of the substrate remained unreacted and only part of the **1** got converted to **2a**. When the same reaction was carried out in presence of oxygen atmosphere compound **2c** was generated, but in very little amount. This indicates, in absence of sufficient amount of $FeCl_3$ the molecular oxygen is working as the terminal oxidant. To explore the scaling up possibility of the reaction, when we treated 2 G of **1** with 3 equiv. of $FeCl_3$ in refluxing methanol at 1 atm O_2 pressure, we obtained 1.34 G of **2c** with 61% yield.

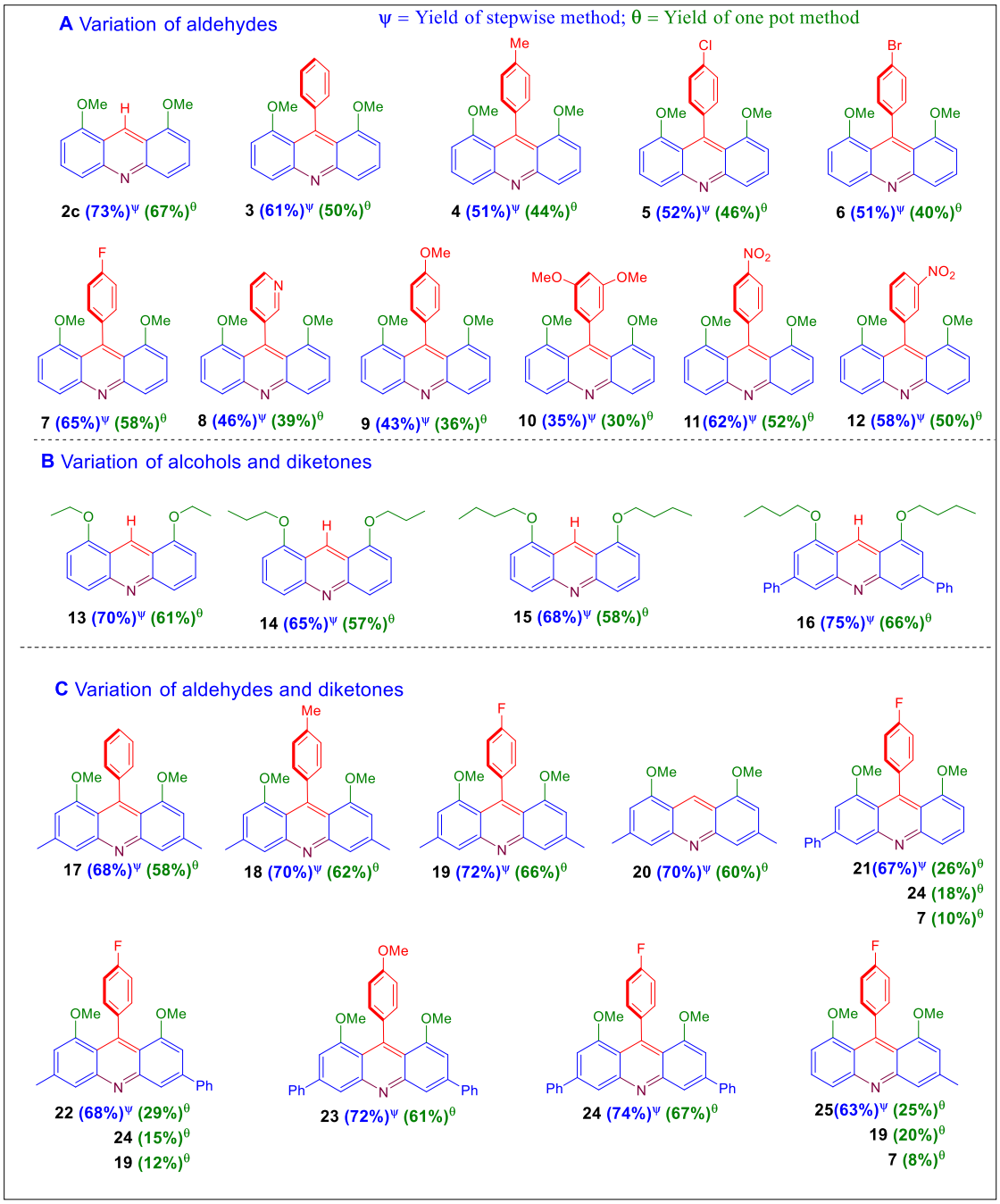

Fig.1.4. Substrate scope of the methodology. *(**A**) Variation in substituents of aldehydes. (**B**) Variations in substituents of alcohols and diketones. (**C**) Variation in substituents of aldehydes and diketones. All the yields presented are isolated yields.*

For exploring the mechanism of this dehydrogenation process as mentioned earlier we have conducted number of different controlled experiments. For precise monitoring of controlled reaction in some cases, we also took the advantage of slower conventional reflux, over faster closed vessel microwave reaction. When we conducted the reaction of **1** in absence of $FeCl_3$ and only in presence of 5 equiv. of TEMPO, we failed to obtain the desired acridine **2c** after 24 h, though the starting material was completely exhausted within few hours to give **2a** as the only product. When the reaction was carried out with $FeCl_3$ in absence of TEMPO, the desired **2c** was obtained as one of the products along with **2a** and **2b**, (Entry 21, Table 1.1), though the reaction progress was slower. From these observations it can be safely concluded that though TEMPO accelerates the first step i.e., generation of **2a**, but it remains ineffective for its further aromatization to **2b** or **2c**, in absence of $FeCl_3$. This observation unambiguously proves the essentiality of $FeCl_3$ for conversion of **1** to **2c**.

To understand the sequential development of the reaction, we used HPLC to examine the contents of the reaction mixture at specific time intervals (Fig. 1.5). At very early stage of the reaction, **2a** emerged as the major product with significant amount of unreacted starting material **1**. As the reaction was given more time or higher equivalents of $FeCl_3$ in MW condition, the product profile gradually shifts toward compounds with **2b** and **2c** having an increasing number of aromatic rings, with gradual depletion of **1** and **2a**. This leads to the conclusion that the reaction initiates with quick aromatization of central 1,4-dihydropyridine ring to generate **2a**. As reflux time with $FeCl_3$ increase, peripheral cyclohexenone rings sequentially get aromatized to yield **2b** and **2c**.

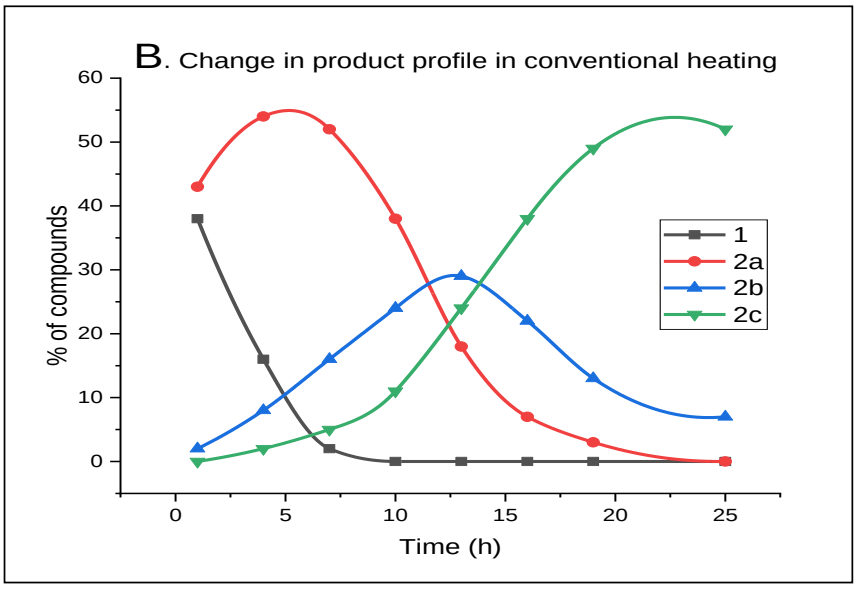

Fig. 1.5 Analysis of product profile with respect to reaction time in conventional reflux with 1 equiv. of $FeCl_3$ in methanol using HPLC

During our product analysis, we have not isolated any product where the peripheral ring got aromatized but alkoxy group at the 1 or 8 position has not been incorporated. Thus, it inferred that the incorporation of alcohols at the carbonyl sites of 1 or 8 is the first step in the aromatization of peripheral cyclohexenones. Also, in none of the case we have isolated any product where the alkoxide group got incorporated at 1 or 8 position but no aromatization of the corresponding ring has taken place. This fact indicates that the methanolic attack at ketone in 1 or 8 position of compound **2a** is the slowest and rate determining step for aromatization of peripheral cyclohexenone rings. Since aromatization was only seen in the presence of $FeCl_3$, we assumed that the Lewis acid nature of $FeCl_3$ promoted the attack of alcohol in ketones. To determine if the role of $FeCl_3$ in this reaction is catalytic, we ran the reaction with 0.5 equiv. of $FeCl_3$ in an open atmosphere for 24 hours and obtained only 11% of **2c** (Entry 21, Table 1.1). When the reaction was performed in argon environment with the same amount of catalyst, the majority of the starting components remained intact after 24 hours (Entry 23, Table

1.1). Although the middle 1,4-dihydropyridine ring of a portion of **1** got aromatized to produce **2a**, this compound was not further oxidized to generate **2b** or **2c**. In contrast, a 25% yield of **2c** is found when the same reaction is conducted in the presence of 1 atm O_2 with same catalyst loading (Entry 22, Table 1.1). These observations indicate that the reaction is catalytic in nature and that molecular oxygen is acting as the terminal oxidant for the regeneration of $FeCl_3$ as catalyst. Based on the aforementioned finding, a probable mechanism for the oxidative dehydrogenation of **1** to **2c** by $FeCl_3$ has been proposed and described as shown in Fig. 1.6.

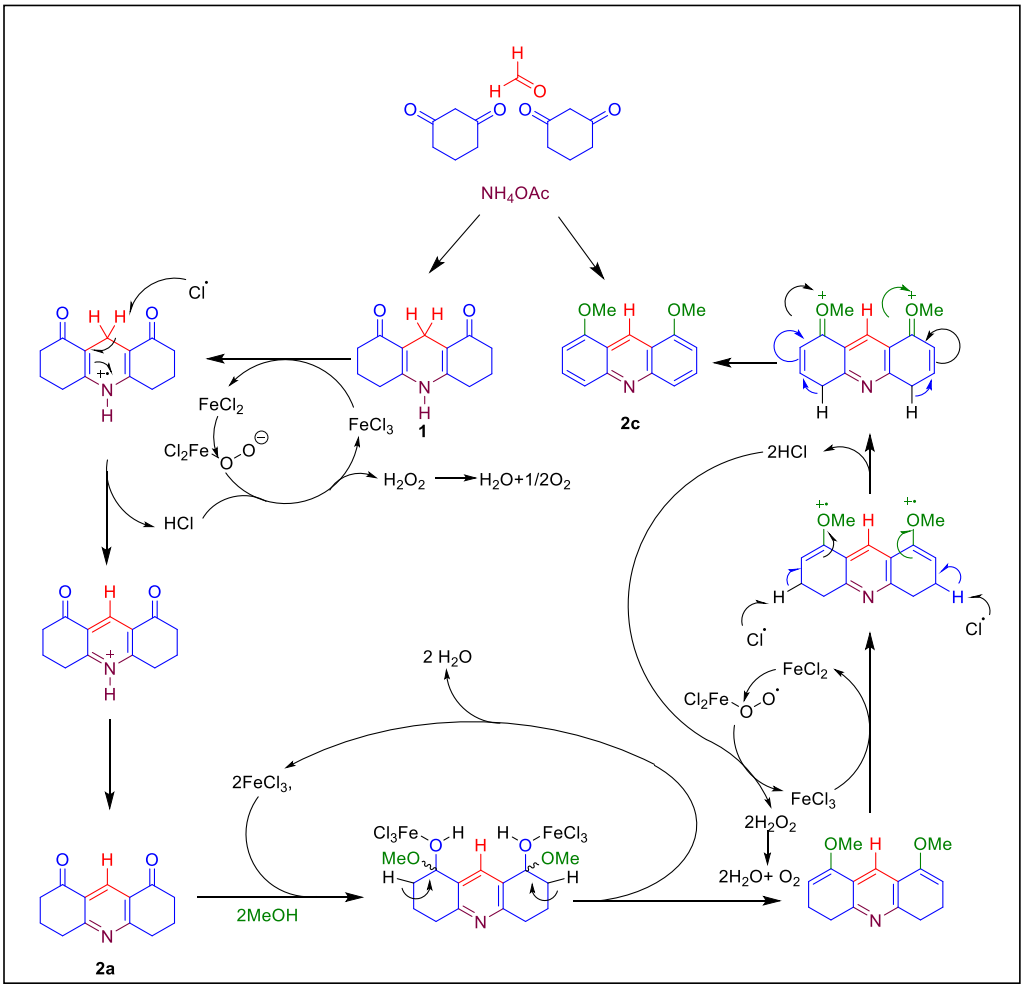

Fig. 1.6 Plausible mechanism for $FeCl_3$ catalyzed oxidative dehydrogenation to acridines.

The conversion process of **1** to **2c** necessitates the elimination of 8 hydrogen atoms and several catalytic cycles, all of which simultaneously require $FeCl_3$ as the catalyst. The significant increase in reaction rate with higher equivalents of $FeCl_3$ (Fig. 1.3; Table 1.1) is thus easily explicable by the timely delivery of catalyst to multiple catalytic cycles concurrently. When 5 equiv. of $FeCl_3$ are employed for the reaction in a sealed microwave environment, all three catalytic cycles can work independently and concurrently to achieve a quicker transformation to **2c**. With a lower equivalent of $FeCl_3$, these stages work sequentially only after catalyst regeneration by molecular oxygen via a catalytic cycle, requiring a longer conversion time to **2c**. Our suggested mechanism also explains the impact of substituents on product yield. The electron-withdrawing substituents at position 9 (*p*-nitrophenyl **11**, *m*-nitrophenyl **12**, *p*-fluorophenyl **7** etc.,) render the central pyridine ring more electron-deficient, hence enhance the electrophilicity of the adjacent ketones at 1 and 8 positions. As a result, the rate-determining $FeCl_3$ assisted nucleophilic attack of alcohol on these more electrophilic carbonyls becomes easier, resulting in higher yields of aromatized product. Similarly, lower yields of electron donating substituents at 9 position such as *p*-tolyl **4**, *p*-methoxyphenyl **9**, 3,5-dimethoxyphenyl **10**, and others can also be explained by sluggish methanolic attack on less electrophilic ketones. Higher yield in case of phenyl/methyl substituents on peripheral rings, as in **16-25**, can also be explained by their resonance/hyperconjugative stabilizing effect on key cationic intermediates (Fig. 1.6) involved in aromatization process.

Formation of fully aromatized 1, 8-dimethoxy acridine compound was confirmed from the proton NMR spectroscopy. The appearance of two doublets for four H and one triplet for two H in aromatic region between δ 6.5-7.5 ppm, confirming the aromatization of two peripheral rings and singlet peak at δ 9.39 ppm represented the

proton present in middle ring of fully aromatized acridine derivative. The attachment of two methoxy groups at 1 and 8 position was confirmed by the presence of one singlet peak at δ 4.10 ppm for six protons, which is the characteristic peak for the methyl group that attached to oxygen.

1.6 Conclusions.

An easy environment-friendly method for the synthesis of substituted acridines has been developed using easily available starting materials 1,3-cyclohexadione, aldehydes and ammonium acetate. This ligand-free methodology enables to produce acridines in presence of eco-friendly $FeCl_3$ as a catalyst using molecular oxygen as a terminal oxidant, which produce water as the only byproduct. Based on the experimental evidences a mechanism has been proposed. In this modular method substituents in each position of the acridines can be altered by changing any particular reactant or solvent. Therefore, this methodology provides better flexibility in construction of acridine ring according to the requirement and hence allow fine tuning of the stereo-electronic properties of the products to suit particular application.

1.7 Experimental Section

1.7.1 General experimental details:

All commercially available compounds were purchased from TCI, Sigma-aldrich and Alfa Aesar. Methanol was dried by using magnesium turning and other alcohols were used as it is received from the company. NMR spectra were recorded on BRUKER AVANCE III 400 (400 MHz for ^{1}H; 100 MHz for ^{13}C) spectrometer. The chemical shifts are given in parts per million (ppm) relative to $CDCl_3$ (7.28 ppm for ^{1}H and 77.00 for ^{13}C) and DMSO-d_6 (2.49 for ^{1}H and 40.09 for ^{13}C). High resolution mass spectra were recorded on Agilent Technologies, Accurate Mass Q-TOF LC/MS G65208. High performance liquid chromatography was performed on Agilent HPLC system 1200 Infinity Series, reverse phase analytical column eluted with a mixture of water and methanol. Normal column chromatography was performed on silica gel (60-120 mesh) purchased from SRL and eluted with petroleum ether and ethyl acetate mixture.

1.7.2 Typical one pot procedure for synthesis of 1,8-dimethoxyacridines:

A dried 10 mL MW tube with a magnetic bar was charged with 1,3-cyclohexanedione (0.4 mmol, 2 equiv.), aldehyde (0.2 mmol, 1equiv.), ammonium acetate (0.3 mmol, 1.5 equiv.) and MeOH (4 mL). Then the tube was closed with a MW tube cap and irradiated under microwave radiation at 100 ^{o}C for 30 min with stirring. After that time period the tube was cooled to room temperature, $FeCl_3$ (5 equiv.) was added to the mixture and kept under microwave radiation for 40 min with stirring. After the reaction mixture reached to room temperature, the reaction solvent MeOH was evaporated and the dried mixture was extracted with $CHCl_3$ (3 x 20 mL). The combined $CHCl_3$ extracts were washed with distilled water and brine solution. The organic layer was passed over anhydrous sodium sulfate and the solvent was evaporated under reduced pressure to

obtain the crude product which was further purified using column chromatography with 10-20% ethyl acetate in petroleum ether.

1.7.3 Typical stepwise method for synthesis of 1,8-dimethoxyacridines:

Construction of hexahydro-1,8-acridinediones: To a 100 mL round bottom flask containing 50 ml of H_2O, 1,3-cyclohexanedione (4 mmol, 2 equiv.), aldehyde (2 mmol, 1 equiv.) and ammonium acetate (3 mmol, 1.5 equiv.) were added to it. The reaction mixture was heated at reflux condition with continuous stirring for 6 h to obtain the product hexahydroacridine-1,8-diones as precipitate. Then the precipitate was filtered through filter paper and dried over P_2O_5 in a vacuum desiccator for next step.

Aromatization to 1,8-dimethoxyacridines: A 100 mL round bottom flask was charged with hexahydroacridine-1,8-dione (0.5 mmol, 1equiv.), MeOH (30 mL) and $FeCl_3$ (81 mg, 0.5 mmol, 1 equiv.), then the mixture was stirred under O_2 atmosphere (approx. 1 atm) in reflux condition for 24 h. After the completion of the reaction (checked by TLC) the mixture was dried under reduced pressure and extracted with $CHCl_3$ (3 x 20 mL). The combined organic extract was dried through anhydrous Na_2SO_4 and finally concentrated through rotary evaporator under reduced pressure. And crude product was purified through column chromatography using silica gel (60-120 mesh) with 10-15% EtOAc in petroleum ether.

1.8 Characterization Data of New Compounds:

1,8-dimethoxyacridine (2c):

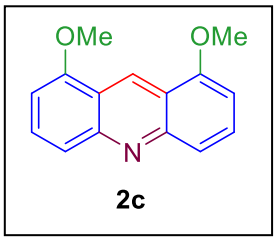

^{1}H NMR ($CDCl_3$, 400 MHz): δ 9.62 (s,1H), 7.81 (d, *J* = 8.9 Hz, 2H), 7.70 (t like, *J* = 7.6, 8.6 Hz, 2H), 6.79 (d, *J* = 7.5 Hz, 2H), 4.10 (s, 6H); ^{13}C NMR ($CDCl_3$, 100 MHz): δ 155.8, 149.7, 130.7, 126.9, 121.2, 119.6, 101.6, 55.8; HRMS: *m/z* (ESI) calculated for ($C_{15}H_{14}NO_2$) $[M+H]^+$: 240.1019, measured: 240.1024.

.

1,8-dimethoxy-9-phenylacridine (3):

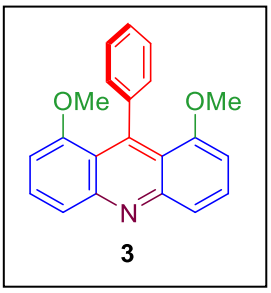

^{1}H NMR (400 MHz, $CDCl_3$) δ 7.85 (d, *J* = 8.7 Hz, 2H), 7.66 (t, *J* = 8.4 Hz, 2H), 7.38-7.33 (m, 3H), 7.25 (d, *J* = 7.9 Hz, 2H), 6.66 (d, *J* = 7.4 Hz, 2H), 3.40 (s, 6H); ^{13}C NMR (100 MHz, $CDCl_3$): δ 157.5, 149.6, 144.3, 130.4, 127.4, 125.4, 125.4, 121.8, 118.9, 104.2, 55.7; HRMS: *m/z* (ESI) calculated for ($C_{21}H_{17}NO_2Na$) $[M+Na]^+$: 338.1151, measured: 338.1153.

1,8-dimethoxy-9-p-tolylacridine (4):

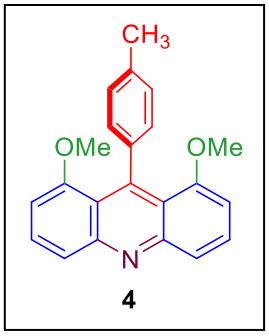

^{1}H NMR (400 MHz, $CDCl_3$) δ 7.85 (d, *J* = 8.8 Hz, 2H), 7.65 (t, *J* = 8.4 Hz, 2H), 7.18 (d, *J* = 8.0 Hz, 2H), 7.13 (d, *J* = 8.0 Hz, 2H), 6.66 (d, *J* = 7.4 Hz, 2H), 3.42 (s, 6H), 2.48 (s,3H); ^{13}C NMR (100 MHz, $CDCl_3$): δ 157.7, 149.7, 141.2, 134.5, 130.2, 127.3, 127.3, 122.0, 119.2, 104.3, 55.7, 21.3; HRMS: *m/z* (ESI) calculated for ($C_{22}H_{20}NO_2$) $[M+H]^+$: 330.1489, measured: 330.1493.

9-(4-cholorophenyl)-1,8-dimethoxyacridine (5):

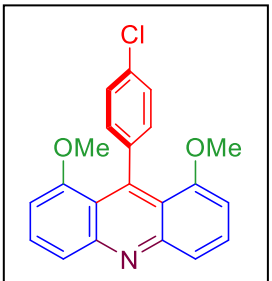

5

^{1}H NMR (400 MHz, $CDCl_3$): δ 7.83 (d, *J* = 8.6 Hz, 2H), 7.64 (t, *J* = 8.5 Hz, 2H), 7.34 (d, *J* = 8.3 Hz, 2H), 7.17 (d, *J* = 8.3 Hz, 2H), 6.65 (d, *J* = 7.6 Hz, 2H), 3.43 (s, 6H); ^{13}C NMR (100 MHz, $CDCl_3$): δ 157.2, 149.5, 142.8, 131.1, 130.5, 128.8, 125.9, 121.8, 118.7, 104.1, 55.5; HRMS: *m/z* (ESI) calculated for ($C_{21}H_{16}ClNO_2Na$) $[M+Na]^+$: 372.0762, measured: 372.0758.

9-(4-bromophenyl)-1,8-dimethoxyacridine (6):

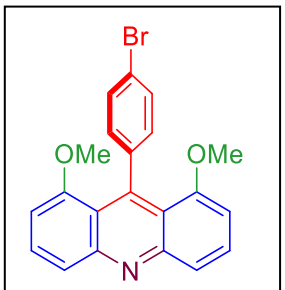

6

^{1}H NMR (400 MHz, $CDCl_3$): δ 7.89 (d, *J* = 8.7 Hz, 2H), 7.68 (t, *J* = 8.1 Hz, 2H), 7.50 (d, *J* = 8.3 Hz, 3H), 7.11 (d, *J* = 8.3 Hz, 2H), 6.67 (d, *J* = 7.6 Hz, 2H), 3.44 (s, 6H);^{13}C NMR (100 MHz, $CDCl_3$): δ 157.1, 149.5, 143.4, 130.5, 129.2, 128.8, 121.8, 119.1, 118.6, 104.1, 55.6; HRMS: *m/z* (ESI) calculated for ($C_{21}H_{17}BrNO_2$) $[M+H]^+$: 394.0443, 396.0422 measured: 394.0440, 396.0423

9-(4-flourophenyl)-1,8-dimethoxyacridine (7):

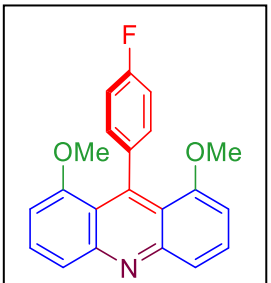

7

^{1}H NMR (400 MHz, $CDCl_3$): δ 7.85 (d, *J* = 8.5 Hz, 2H), 7.66 (t, *J* = 8.4 Hz, 2H), 7.21-7.17 (m, 3H), 7.06 (t, *J* = 8.8 Hz, 2H), 6.66 (d, *J* = 7.5 Hz, 2H), 3.45 (s, 6H); ^{13}C NMR (100 MHz, $CDCl_3$): δ 162.5, 160.1, 157.3, 149.6, 140.1, 130.4, 128.8, 121.9, 118.9, 112.7, 112.5, 104.1, 55.6; HRMS: *m/z* (ESI) calculated for ($C_{21}H_{17}FNO_2$) $[M+H]^+$: 334.1238, measured: 334.1243.

1,8-dimethoxy-9-(pyridine-3-yl)acridine (8):

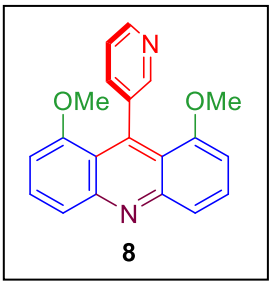

^{1}H NMR (400 MHz, $CDCl_3$): δ 8.63 (d, *J* = 4.8 Hz, 1H), 7.86 (d, *J* = 8.7 Hz, 2H), 7.72 (t, *J* = 7.7 Hz, 1H), 7.65 (t, *J* = 7.8 Hz, 2H), 7.38 (d, *J* = 7.8 Hz 1H), 7.29 (t, *J* = 8.4 Hz, 1H), 6.67 (d, *J* = 7.5 Hz, 2H), 3.42 (s, 6H); ^{13}C NMR (100 MHz, $CDCl_3$): δ 162.5, 156.7, 149.8, 146.7, 143.6, 133.5, 130.4, 123.6, 122.0, 120.6, 118.2, 104.0, 56.0; HRMS: *m/z* for ($C_{20}H_{17}N_2O_2$) (ESI) calculated $[M+H]^+$: 317.1285, measured: 317.1290.

1,8-dimethoxy-9-(4-methoxyphenyl)acridine (9):

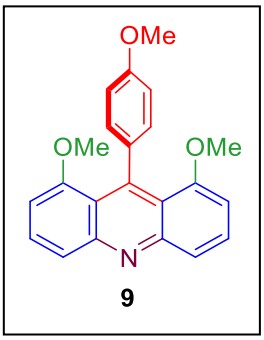

^{1}H NMR (400 MHz, $CDCl_3$): δ 7.88 (d, *J* = 6.7 Hz, 2H), 7.66 (t, *J* = 8.0 Hz, 2H), 7.16 (d, *J* = 8.6 Hz, 2H), 6.95 (d, *J* = 8.5 Hz, 2H), 6.68 (d, *J* = 7.4 Hz, 2H), 3.94 (s, 3H), 3.46 (s, 6H); ^{13}C NMR (100 MHz, $CDCl_3$): δ 158.0, 151.9, 139.3, 133.9, 132.2, 128.6, 128.0, 119.1, 114.1, 111.7, 105.0, 56.0, 55.4; HRMS: *m/z* (ESI) calculated for ($C_{22}H_{19}NNaO_3$) $[M+Na]^+$: 368.1257, measured: 368.1260.

9-(3,5-dimethoxyphenyl)-1,8-dimethoxyacridine (10):

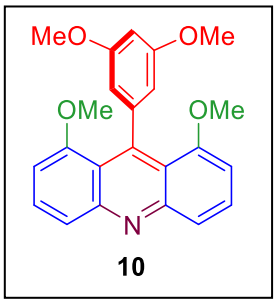

^{1}H NMR (400 MHz, $CDCl_3$): δ 7.84 (d, *J* = 8.6 Hz, 2H), 7.65 (t, *J* = 8.5 Hz, 2H), 6.68 (d, *J* = 7.5 Hz, 2H), 6.52 (t, *J* = 2.2 Hz, 1H), 6.46 (d, *J* = 2.2 Hz, 2H), 3.82 (s, 6H), 3.50 (s, 6H); ^{13}C NMR (100 MHz, $CDCl_3$): δ 159.0, 157.5, 149.5, 146.2, 130.5, 121.6, 118.7, 106.8, 106.5, 104.2, 98.3, 55.9, 55.5; HRMS: *m/z* (ESI) calculated for ($C_{23}H_{22}NO_4$) $[M+H]^+$: 376.1543, measured: 376.1545.

1,8-dimethoxy-9-(4-nitrophenyl)acridine (11):

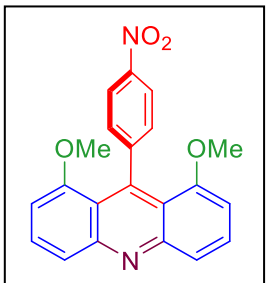

11

^{1}H NMR (400 MHz, $CDCl_3$): δ 8.28 (d, *J* = 8.5 Hz, 2H), 7.86 (d, *J* = 8.7 Hz, 2H), 7.69 (t, *J* = 8.2 Hz, 2H), 7.45 (d, *J* = 8.5 Hz, 2H), 6.68 (d, *J* = 7.6 Hz, 2H), 3.40 (s, 6H); ^{13}C NMR (100 MHz, $CDCl_3$): δ 156.5, 152.3, 149.6, 145.9, 143.3 130.6, 128.5, 122.2, 121.1, 118.0, 104.1, 55.4; HRMS: *m/z* (ESI) calculated for ($C_{21}H_{17}N_2O_4$) $[M+H]^+$: 361.1183, measured: 361.1185.

1,8-dimethoxy-9-(3-nitrophenyl)acridine (12):

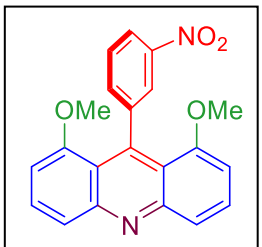

12

^{1}H NMR (400 MHz, $CDCl_3$): δ 8.27 (d, *J* = 10.2 Hz, 1H), 8.17 (t, *J* = 1.8 Hz 1H), 7.88 (d, *J* = 9.5 Hz, 2H), 7.68 (dd, *J* = 8.6, 7.7 Hz, 2H), 7.63 (d, *J* = 6.3 Hz, 1H), 7.54 (t, *J* = 7.9 Hz, 1H) 6.68 (d, *J* = 7.5 Hz, 2H), 3.40 (s, 6H); ^{13}C NMR (100 MHz, $CDCl_3$): δ 156.7, 149.9, 146.4, 133.8, 130.5, 126.5, 122.6, 120.6, 118.4, 104.3, 55.7; HRMS: *m/z* (ESI) calculated for ($C_{21}H_{17}N_2O_4$) $[M+H]^+$: 361.1183, measured: 361.1180.

1,8-diethoxyacridine (13):

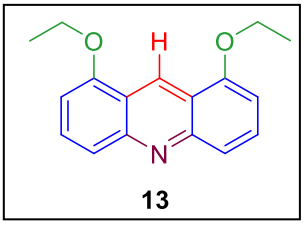

13

^{1}H NMR (400 MHz, $CDCl_3$): δ 9.65 (s, 1H), 7.82 (d, *J* = 8.8 Hz, 2H), 7.69 (t, *J* = 8.6 Hz, 2H), 6.77 (d, *J* = 7.5 Hz, 2H), 4.31 (q, *J* = 7.0 Hz, 4H), 1.65 (t, *J* = 7.0 Hz, 6H); ^{13}C NMR (100 MHz, $CDCl_3$): δ 155.1, 149.4, 130.9, 127.3, 120.7, 119.7, 102.4, 64.1, 14.7; HRMS: *m/z* (ESI) calculated for ($C_{17}H_{17}NNaO_2$) $[M+Na]^+$: 290.1151, measured: 290.1155.

1,8-dipropoxyacridine (14):

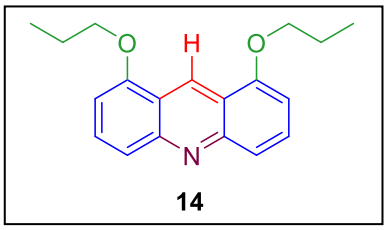

^{1}H NMR (400 MHz, $CDCl_3$): δ 9.66 (s, 1H), 7.80 (d, *J* = 8.8 Hz, 2H), 7.67 (t, *J* = 8.7 Hz, 2H), 6.76 (d, *J* = 7.5 Hz, 2H), 4.19 (t, *J* = 6.4 Hz, 4H), 2.00-2.09 (m, 4H), 1.21 (t, *J* = 7. 4 Hz, 6H); ^{13}C NMR (100 MHz, $CDCl_3$): δ 155.2, 149.7, 130.7, 127.0, 120.9, 119.8, 102.3, 69.9, 22.6, 10.7; HRMS: *m/z* (ESI) calculated for ($C_{19}H_{22}NO_2$) $[M+H]^+$: 296.1645, measured: 296.1641.

1,8-dibutoxyacridine (15):

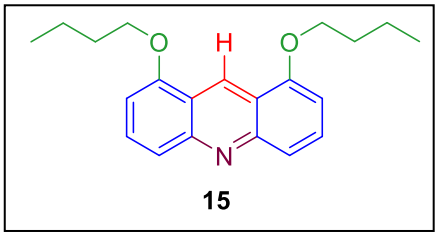

^{1}H NMR (400 MHz, $CDCl_3$): δ 9.68 (s, 1H), 7.83 (d, *J* = 8.8 Hz, 2H), 7.69 (t, *J* = 8.6 Hz, 2H), 6.78 (d, *J* = 7.5 Hz, 2H), 4.25 (t, *J* = 6.2 Hz, 4H), 1.97-2.04 (m, 4H), 1.65-1.75 (m, 4H), 1.10 (t, *J* = 7.4 Hz, 6H); ^{13}C NMR (100 MHz, $CDCl_3$): δ 155.3, 149.3, 131.1, 127.5, 120.5, 119.8, 102.4, 68.3, 31.3, 19.6, 14.0; HRMS: *m/z* (ESI) calculated for ($C_{21}H_{26}NO_2$) $[M+H]^+$: 324.1958, measured: 324.1964.

1,8-dibutoxy-3,6-diphenylacridine (16):

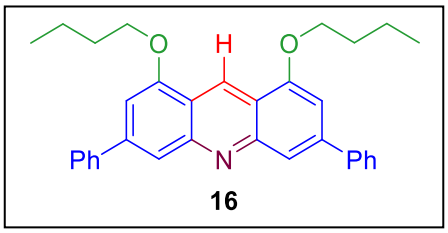

^{1}H NMR (400 MHz, $CDCl_3$) δ 9.61 (s, 1H), 8.04 (s, 2H), 7.85 (d, *J* = 7.4 Hz, 4H), 7.54 (t, *J* = 7.4 Hz, 4H), 7.44 (t, *J* = 7.2 Hz, 2H), 7.05 (s, 2H), 4.34 (t, *J* = 6.2 Hz, 4H), 2.08-2.02 (m, 4H), 1.78-1.69 (m, 4H), 1.13 (t, *J* = 7.4 Hz, 6H). ^{13}C NMR (100 MHz, $CDCl_3$) δ 155.8, 150.5, 143.7, 141.3, 129.1, 128.2, 127.7, 127.5, 119.2, 118.8, 102.9, 68.5, 31.5, 19.8, 14.2. HRMS: *m/z* (ESI) calculated for ($C_{33}H_{34}NO_2$) $[M+H]^+$: 476.2584, measured: 476.2586

1,8-dimethoxy-3,6-dimethyl-9-phenylacridine (17):

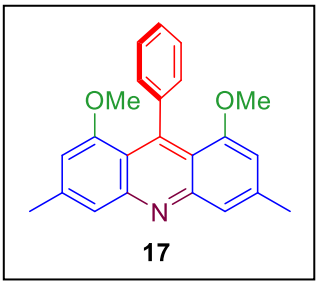

^{1}H NMR (400 MHz, $CDCl_3$): δ 7.68 (s, 2H), 7.37-7.31 (m, 3H), 7.22 (d, *J* = 9.1 Hz, 2H), 6.46 (s, 2H), 3.38 (s, 6H), 2.54 (s, 6H); ^{13}C NMR (100 MHz, $CDCl_3$) δ 157.2, 149.4, 144.2, 141.2, 127.3, 125.7, 125.3, 120.0, 116.9, 106.5, 55.1, 22.4; HRMS: *m/z* (ESI) calculated for ($C_{23}H_{22}NO_2$) $[M+H]^+$: 344.1645, measured: 344.1644.

1,8-dimethoxy-3,6-dimethyl-9-p-tolylacridine (18):

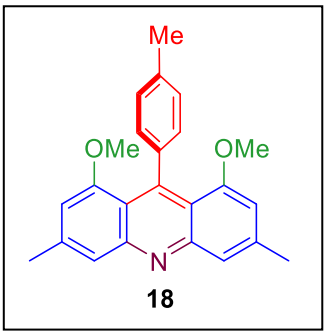

^{1}H NMR (400 MHz, $CDCl_3$): δ 7.60 (s, 2H), 7.17 (d, *J* = 8.0 Hz, 2H), 7.10 (d, *J* = 8.0 Hz, 2H), 6.45 (s, 2H), 3.39 (s, 6H), 2.52 (s, 6H), 2.47 (s, 3H); ^{13}C NMR (100 MHz, $CDCl_3$): δ 157.5, 150.0, 141.3, 141.0, 127.4, 126.5, 127.4, 120.4, 117.3, 106.8, 55.8, 22.5, 21.5; HRMS: *m/z* (ESI) calculated for ($C_{24}H_{24}NO_2$) $[M+H]^+$: 358.1802, measured: 358.1805.

9-(4-fluorophenyl)-1,8-dimethoxy-3,6-dimethylacridine (19):

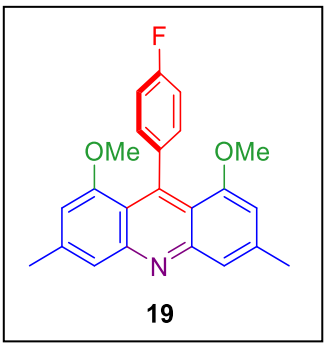

^{1}H NMR (400 MHz, $CDCl_3$): δ 7.61 (s, 2H), 7.18-7.14 (m, 2H), 7.07- 7.03 (m, 2H), 6.46 (s, 2H), 3.42 (s, 6H), 2.54 (s, 6H); ^{13}C NMR (100 MHz, $CDCl_3$): δ 162.7, 160.3, 157.2, 149.9, 141.2, 140.3, 128.9, 120.4, 117.1, 112.8, 112.6, 106.7, 55.7, 22.5; HRMS: *m/z* (ESI) calculated for ($C_{23}H_{20}FNNaO_2$) $[M+Na]^+$: 384.1370, measured: 384.1372.

1,8-dimethoxy-3,6-methylacridine (20):

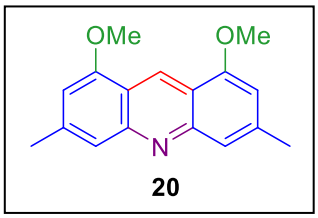

^{1}H NMR (400 MHz, $CDCl_3$): δ 9.49 (s, 1H), 7.62 (s, 2H), 6.61 (s, 2H),4.08 (s, 6H), 2.59 (s, 6H); ^{13}C NMR (100 MHz, $CDCl_3$): δ 155.4, 149.6, 141.5, 126.6, 119.4, 117.6, 104.1, 55.7, 23.0; HRMS: *m/z* (ESI) calculated for ($C_{17}H_{18}NO_2$) $[M+H]^+$: 268.1332, measured: 268.1329.

9-(4-fluorophenyl)-1,8-dimethoxy-3-phenylacridine (21):

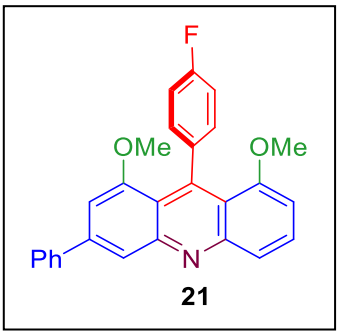

^{1}H NMR (400 MHz, $CDCl_3$): δ 8.09 (s, 1H), 7.83 (t, *J* = 8.2 Hz, 3H), 7.66 (t, *J* = 8.2 Hz, 1 H), 7.53 (t, *J* = 7.5 Hz, 2H), 7.45-7.42 (m, 1H), 7.24-7.21 (m, 2H), 7.09 (t, *J* = 8.8 Hz, 2H), 6.94 (s, 1H), 6.67 (d, *J* = 7.4 Hz 1H), 3.53 (s, 3H), 3.46 (s, 3H); ^{13}C NMR (100 MHz, $CDCl_3$): δ 162.7, 160.3, 157.8, 157.6, 150.4, 150.2, 145.6, 142.8, 140.5, 140.2, 130.6, 129.1, 128.3, 127.5, 122.2, 119.7, 119.1, 118.3, 112.9, 112.7, 104.3, 55.8, 55.8; HRMS: *m/z* (ESI) calculated for ($C_{27}H_{20}FNNaO_2$) $[M+Na]^+$: 432.1370, measured: 432.1373.

9-(4-fluorophenyl)-1,8-dimethoxy-3-methyl-6-phenylacridine (22):

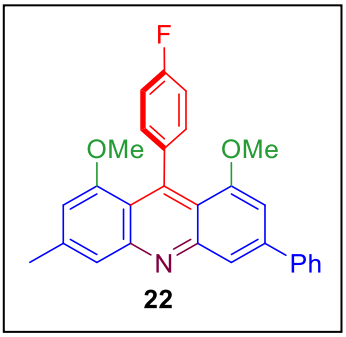

^{1}H NMR (400 MHz, $CDCl_3$): δ 8.06 (s, 1H), 7.82 (d, *J* = 7.5 Hz, 2H), 7.63 (s, 1H), 7.53 (t, *J* = 6.6 Hz, 2 H), 7.44 (t, *J* = 7.2 Hz, 1H), 7.23-7.19 (m, 2H), 7.08 (t, *J* = 8.8 Hz, 2H), 6.90 (s, 1H), 6.49 (s, 1H), 3.52 (s, 3H), 3.45 (s, 3H), 2.56 (s, 3H); ^{13}C NMR (101 MHz, $CDCl_3$): δ 162.7, 160.3, 157.9, 157.1, 150.6, 150.2, 141.3, 140.5, 140.1, 139.5, 129.1, 128.3, 127.5, 120.7, 119.5, 117.9, 117.5, 114.3, 112.9, 112.7, 106.9, 104.0, 77.5, 77.2, 76.9, 55.8, 55.7, 22.9;

HRMS: *m/z* (ESI) calculated for ($C_{28}H_{23}FNO_2$) $[M+H]^+$: 424.1707, measured: 424.1705.

1,8-dimethoxy-9-(4-methoxyphenyl)-3,6-diphenylacridine (23):

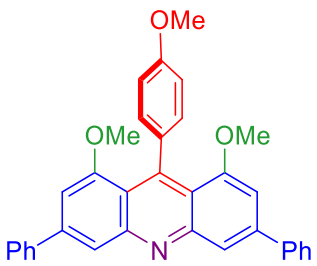

23

^{1}H NMR (400 MHz, $CDCl_3$): δ 8.09 (s,1H), 7.84 (d, *J* = 8.3 Hz, 4H), 7.53 (t, *J* = 7.6 Hz, 4H), 7.44 (t, *J* = 7.3 Hz, 2H), 7.22 (d, *J* = 8.3 Hz, 2H) 6.98-6.94 (d, 4H), 6.95 (s, 2H), 3.96 (s, 3H), 3.55 (s, 6H); ^{13}C NMR (100 MHz, $CDCl_3$): δ 158.2, 158.0, 150.7, 142.8, 140.6, 136.7, 129.1, 128.7, 128.3, 127.5, 119.6, 118.7, 111.6, 104.4, 56.1, 55.6; HRMS: *m/z* (ESI) calculated for ($C_{34}H_{28}NO_3$) $[M+H]^+$: 498.2064, measured: 498.2069.

9-(4-fluorophenyl)-1,8-dimethoxy-3,6-diphenylacridine (24):

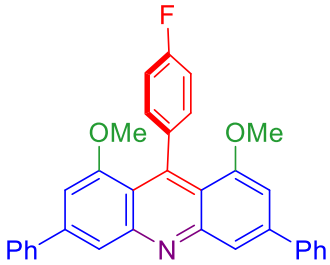

24

^{1}H NMR (400 MHz, $CDCl_3$): δ 8.12 (s,1H), 7.84 (d, *J* = 7.6 Hz, 4H), 7.53 (t, *J* = 7.6 Hz, 4H), 7.44 (t, *J* = 7.3 Hz, 2H), 7.28-7.24 (m, 2H), 7.11 (t, *J* = 8.8 Hz, 2H), 6.94 (s, 2H), 3.54 (s, 6H); ^{13}C NMR (100 MHz, $CDCl_3$): δ 162.8, 160.4, 157.9, 150.4, 143.2, 140.4, 140.0, 129.2, 128.4, 127.5, 119.4, 118.3, 113.0, 112.8, 104.4, 55.9; HRMS: *m/z* (ESI) calculated for ($C_{33}H_{25}FNO_2$) $[M+H]^+$: 486.1864, measured: 486.1869.

9-(4-fluorophenyl)-1,8-dimethoxy-3-methylacridine (25):

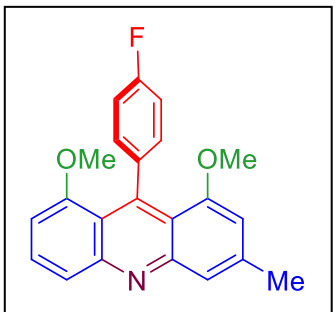

25

^{1}H NMR (400 MHz, $CDCl_3$): δ 7.81 (d, *J* = 8.6 Hz, 1H), 7.65-7.61 (m, 2H), 7.20-7.17 (m, 2H), 7.06 (t, *J* = 8.8 Hz, 2H), 6.64 (d, *J* = 7.5 Hz, 1H), 6.49 (s, 1H), 3.44 (s, 6H), 2.55 (s, 3H); ^{13}C NMR (100 MHz, $CDCl_3$): δ 162.7, 160.3, 157.5, 157.1, 150.1, 145.5, 141.0, 140.3, 130.3, 129.0, 122.1, 120.8, 118.7, 117.6, 112.6, 112.6, 106.9, 104.0, 55.7, 22.5; HRMS: *m/z* (ESI) calculated for ($C_{22}H_{19}FNO_2$) $[M+H]^+$: 348.1394, measured: 348.1400.

References

(1) A. Bernthsen, *Justus LiebigAs Ann. Chem.*, **1884**, 224, 1.

(2) Prasher, P.; Sharma, M. Medicinal Chemistry of Acridine and Its Analogues. *MedChemComm* **2018**, *9* (10), 1589–1618.

(3) Galdino-Pitta, M. R.; Pitta, M. G. R.; Lima, M. C. A.; Galdino, L. S.; Pitta, R. I. Niche for Acridine Derivatives in Anticancer Therapy. *Mini Rev. Med. Chem.* **2013**, *13* (9), 1256–1271.

(4) Makhaeva, G. F.; Lushchekina, S. V.; Boltneva, N. P.; Serebryakova, O. G.; Rudakova, E. V.; Ustyugov, A. A.; Bachurin, S. O.; Shchepochkin, A. V.; Chupakhin, O. N.; Charushin, V. N.; Richardson, R. J. 9-Substituted Acridine Derivatives as Acetylcholinesterase and Butyrylcholinesterase Inhibitors Possessing Antioxidant Activity for Alzheimer's Disease Treatment. *Bioorg. Med. Chem.* **2017**, *25* (21), 5981–5994.

(5) Wang, C.; Fu, J.; Yao, K.; Xue, K.; Xu, K.; Pang, X. Acridine-Based Fluorescence Chemosensors for Selective Sensing of Fe3+ and Ni2+ Ions. *Spectrochim. Acta. A. Mol. Biomol. Spectrosc.* **2018**, *199*, 403–411.

(6) Dai, Q.; Liu, H.; Gao, C.; Li, W.; Zhu, C.; Lin, C.; Tan, Y.; Yuan, Z.; Jiang, Y. A One-Step Synthesized Acridine-Based Fluorescent Chemosensor for Selective Detection of Copper(II) Ions and Living Cell Imaging. *New J. Chem.* **2017**, *42* (1), 613–618.

(7) Chatterjee, S.; Kumar, G. S. Binding of Fluorescent Acridine Dyes Acridine Orange and 9-Aminoacridine to Hemoglobin: Elucidation of Their Molecular

Recognition by Spectroscopy, Calorimetry and Molecular Modeling Techniques. *J. Photochem. Photobiol. B* **2016**, *159*, 169–178.

(8) Darzynkiewicz, Z.; Juan, G.; Srour, E. F. Differential Staining of DNA and RNA. *Curr. Protoc. Cytom.* **2004**, *30* (1), 7.3.1-7.3.16.

(9) Liu, X.; Karsili, T. N. V.; Sobolewski, A. L.; Domcke, W. Photocatalytic Water Splitting with the Acridine Chromophore: A Computational Study. *J. Phys. Chem. B* **2015**, *119* (33), 10664–10672.

(10) Qin, P.; Paek, S.; Dar, M. I.; Pellet, N.; Ko, J.; Grätzel, M.; Nazeeruddin, M. K. Perovskite Solar Cells with 12.8% Efficiency by Using Conjugated Quinolizino Acridine Based Hole Transporting Material. *J. Am. Chem. Soc.* **2014**, *136* (24), 8516–8519.

(11) Cho, A.-N.; Chakravarthi, N.; Kranthiraja, K.; Reddy, S. S.; Kim, H.-S.; Jin, S.-H.; Park, N.-G. Acridine-Based Novel Hole Transporting Material for High Efficiency Perovskite Solar Cells. *J. Mater. Chem. A* **2017**, *5* (16), 7603–7611.

(12) Wainwright, M. Acridine-a Neglected Antibacterial Chromophore. *J. Antimicrob. Chemother.* **2001**, *47* (1), 1–13.

(13) Tonelli, M.; Vettoretti, G.; Tasso, B.; Novelli, F.; Boido, V.; Sparatore, F.; Busonera, B.; Ouhtit, A.; Farci, P.; Blois, S.; Giliberti, G.; La Colla, P. Acridine Derivatives as Anti-BVDV Agents. *Antiviral Res.* **2011**, *91* (2), 133–141.

(14) Giorgio, E.; Tanaka, K.; Ding, W.; Krishnamurthy, G.; Pitts, K.; Ellestad, G. A.; Rosini, C.; Berova, N. Theoretical Simulation of the Electronic Circular Dichroism Spectrum of Calicheamicin. *Bioorg. Med. Chem.* **2005**, *13* (17), 5072–5079.

(15) Dolphin, G. T.; Chierici, S.; Ouberai, M.; Dumy, P.; Garcia, J. A Multimeric Quinacrine Conjugate as a Potential Inhibitor of Alzheimer's β-Amyloid Fibril Formation. *ChemBioChem* **2008**, *9* (6), 952–963.

(16) Gelus, N.; Hamy, F.; Bailly, C. Molecular Basis of HIV-1 TAR RNA Specific Recognition by an Acridine Tat-Antagonist. *Bioorg. Med. Chem.* **1999**, *7* (6), 1075–1079.

(17) Taraporewala, I. B.; Cessac, J. W.; Chanh, T. C.; Delgado, A. V.; Schinazi, R. F. HIV-1 Neutralization and Tumor Cell Proliferation Inhibition in Vitro by Simplified Analogs of Pyrido[4,3,2-Mn]Thiazolo[5,4-b]Acridine Marine Alkaloids. *J. Med. Chem.* **1992**, *35* (15), 2744–2752.

(18) Ketron, A. C.; Denny, W. A.; Graves, D. E.; Osheroff, N. Amsacrine as a Topoisomerase II Poison: Importance of Drug–DNA Interactions. *Biochemistry* **2012**, *51* (8), 1730–1739.

(19) Byvaltsev, V. A.; Bardonova, L. A.; Onaka, N. R.; Polkin, R. A.; Ochkal, S. V.; Shepelev, V. V.; Aliyev, M. A.; Potapov, A. A. Acridine Orange: A Review of Novel Applications for Surgical Cancer Imaging and Therapy. *Front. Oncol.* **2019**, *9*, 925.

(20) George, K. P. Quinacrine Mustard--a Selective Fluorescent Stain for the Y Chromosome in Human Tissues for Routine Cytogenetic Screening. *Stain Technol.* **1971**, *46* (1), 34–36.

(21) Gniazdowski, M.; Szmigiero, L. Nitracrine and Its Congeners—An Overview. *Gen. Pharmacol. Vasc. Syst.* **1995**, *26* (3), 473–481.

(22) Afzal, A.; Sarfraz, M.; Wu, Z.; Wang, G.; Sun, J. Integrated Scientific Data Bases Review on Asulacrine and Associated Toxicity. *Crit. Rev. Oncol. Hematol.* **2016**, *104*, 78–86.

(23) Tajima, K.; Matsuo, K.; Yamada, H.; Seki, S.; Fukui, N.; Shinokubo, H. Acridino[2,1,9,8-Klmna]Acridine Bisimides: An Electron-Deficient π-System for Robust Radical Anions and n-Type Organic Semiconductors. *Angew. Chem. Int. Ed.* **2021**, *60* (25), 14060–14067.

(24) Li, C.; Sun, P.; Yan, L.; Pan, Y.; Cheng, C.-H. Synthesis and Electroluminescent Properties of Ir Complexes with Benzo[c]Acridine or 5,6-Dihydro-Benzo[c]Acridine Ligands. *Thin Solid Films* **2008**, *516* (18), 6186–6190.

(25) Lian, Y.; Hummel, J. R.; Bergman, R. G.; Ellman, J. A. Facile Synthesis of Unsymmetrical Acridines and Phenazines by a Rh(III)-Catalyzed Amination/Cyclization/Aromatization Cascade. *J. Am. Chem. Soc.* **2013**, *135* (34), 12548–12551.

(26) Wang, T.-J.; Chen, W.-W.; Li, Y.; Xu, M.-H. Facile Synthesis of Acridines via Pd(0)-Diphosphine Complex-Catalyzed Tandem Coupling/Cyclization Protocol. *Org. Biomol. Chem.* **2015**, *13* (23), 6580–6586.

(27) Huang, Z.; Yang, Y.; Xiao, Q.; Zhang, Y.; Wang, J. Auto-Tandem Catalysis: Synthesis of Acridines by Pd-Catalyzed C=C Bond Formation and C(Sp^2)-N Cross-Coupling. *Eur. J. Org. Chem.* **2012**, *2012* (33), 6586–6593.

(28) Tsvelikhovsky, D.; Buchwald, S. L. Synthesis of Heterocycles via Pd-Ligand Controlled Cyclization of 2-Chloro- *N* -(2-Vinyl)Aniline: Preparation of Carbazoles,

Indoles, Dibenzazepines, and Acridines. *J. Am. Chem. Soc.* **2010**, *132* (40), 14048–14051.

(29) Rogness, D. C.; Larock, R. C. Synthesis of Acridines by the [4 + 2] Annulation of Arynes and 2-Aminoaryl Ketones. *J. Org. Chem.* **2010**, *75* (7), 2289–2295.

(30) Wang, M.; Fan, Q.; Jiang, X. Nitrogen–Iodine Exchange of Diaryliodonium Salts: Access to Acridine and Carbazole. *Org. Lett.* **2018**, *20* (1), 216–219.

(31) Guo, H.-M.; Mao, R.-Z.; Wang, Q.-T.; Niu, H.-Y.; Xie, M.-S.; Qu, G.-R. Pd(II)-Catalyzed One-Pot, Three-Step Route for the Synthesis of Unsymmetrical Acridines. *Org. Lett.* **2013**, *15* (21), 5460–5463.

(32) Wu, H.; Zhang, Z.; Ma, N.; Liu, Q.; Liu, T.; Zhang, G. Synthesis of Acridines from *o* -Aminoaryl Ketones and Arylboronic Acids by Copper Trifluoroacetate-Mediated Relay Reactions. *J. Org. Chem.* **2018**, *83* (20), 12880–12886.

(33) Shen, J.; Liu, X.; Wang, L.; Chen, Q.; He, M. Rh(III)-Catalyzed Synthesis of Unsymmetrical Acridines from Aldehydes and Azides Using Transient Directing Strategy in Biomass-Derived γ -Valerolactone. *Synth. Commun.* **2018**, *48* (11), 1354–1362.

(34) Biswas, A.; Sarkar, S.; Samanta, R. Rh^{III} -Catalyzed Straightforward Synthesis of Benzophenanthroline and Benzophenanthrolinone Derivatives Using Anthranils. *Chem. – Eur. J.* **2019**, *25* (12), 3000-3004.

(35) Jia, X.; Yu, L.; Huo, C.; Wang, Y.; Liu, J.; Wang, X. Catalytic Aromatization of 1,4-Dihydropyridines by Radical Cation Salt Prompted Aerobic Oxidation. *Tetrahedron Lett.* **2014**, *55* (1), 264–266.

(36) Bagley, M.; Lubinu, M. Microwave-Assisted Oxidative Aromatization of Hantzsch 1,4-Dihydro-pyridines Using Manganese Dioxide. *Synthesis* **2006**, *2006* (8), 1283–1288.

(37) Liu, D.; Gui, J.; Wang, C.; Lu, F.; Yang, Y.; Sun, Z. Oxidative Aromatization of Hantzsch 1,4-Dihydropyridines Catalyzed by Ferric Perchlorate in Ionic Liquids with Air. *Synth. Commun.* **2010**, *40* (7), 1004–1008.

(38) Izawa, Y.; Pun, D.; Stahl, S. S. Palladium-Catalyzed Aerobic Dehydrogenation of Substituted Cyclohexanones to Phenols. *Science* **2011**, *333* (6039), 209–213.

(39) Diao, T.; Pun, D.; Stahl, S. S. Aerobic Dehydrogenation of Cyclohexanone to Cyclohexenone Catalyzed by Pd(DMSO)2(TFA)2: Evidence for Ligand-Controlled Chemoselectivity. *J. Am. Chem. Soc.* **2013**, *135* (22), 8205–8212.

(40) Pun, D.; Diao, T.; Stahl, S. S. Aerobic Dehydrogenation of Cyclohexanone to Phenol Catalyzed by Pd(TFA)2/2-Dimethylaminopyridine: Evidence for the Role of Pd Nanoparticles. *J. Am. Chem. Soc.* **2013**, *135* (22), 8213–8221.

(41) Zhang, Z.; Hashiguchi, T.; Ishida, T.; Hamasaki, A.; Honma, T.; Ohashi, H.; Yokoyama, T.; Tokunaga, M. Aerobic Oxidation of Cyclohexanones to Phenols and Aryl Ethers over Supported Pd Catalysts. *Org. Chem. Front.* **2015**, *2* (6), 654–660.

(42) Jin, X.; Taniguchi, K.; Yamaguchi, K.; Mizuno, N. Au–Pd Alloy Nanoparticles Supported on Layered Double Hydroxide for Heterogeneously Catalyzed Aerobic Oxidative Dehydrogenation of Cyclohexanols and Cyclohexanones to Phenols. *Chem. Sci.* **2016**, *7* (8), 5371–5383.

(43) Zhang, J.; Jiang, Q.; Yang, D.; Zhao, X.; Dong, Y.; Liu, R. Reaction-Activated Palladium Catalyst for Dehydrogenation of Substituted Cyclohexanones to Phenols and H2 without Oxidants and Hydrogen Acceptors. *Chem. Sci.* **2015**, *6* (8), 4674–4680.

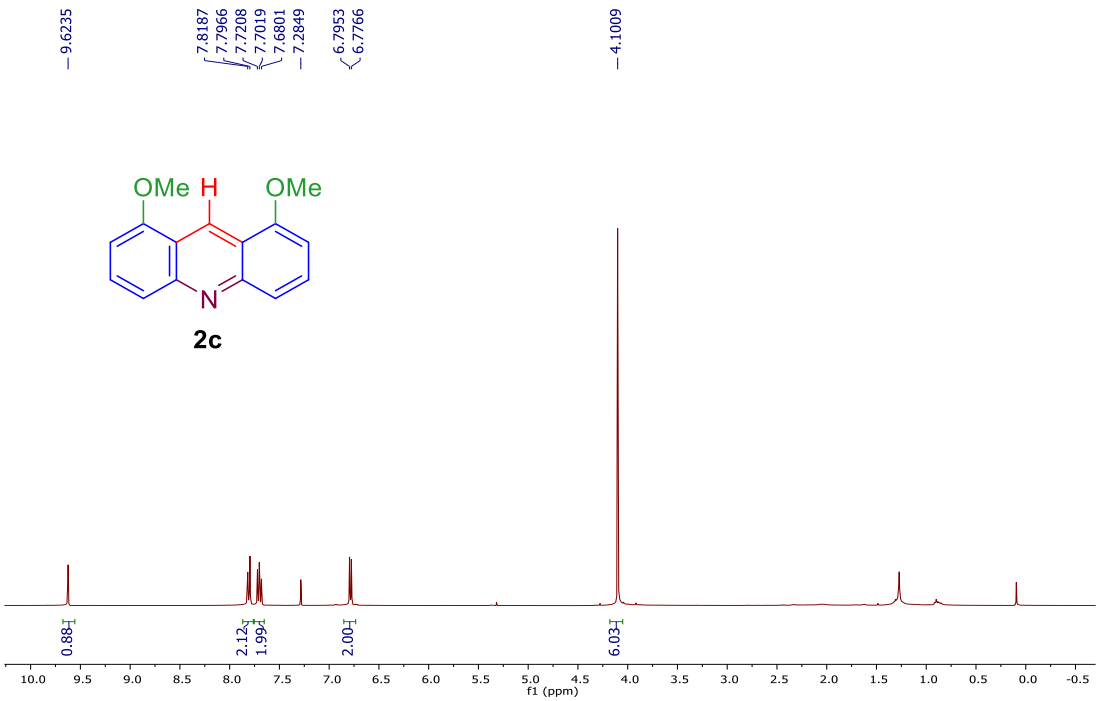

^{1}H NMR ($CDCl_3$, 400 MHz) spectrum of 1,8-dimethoxyacridine (2c).

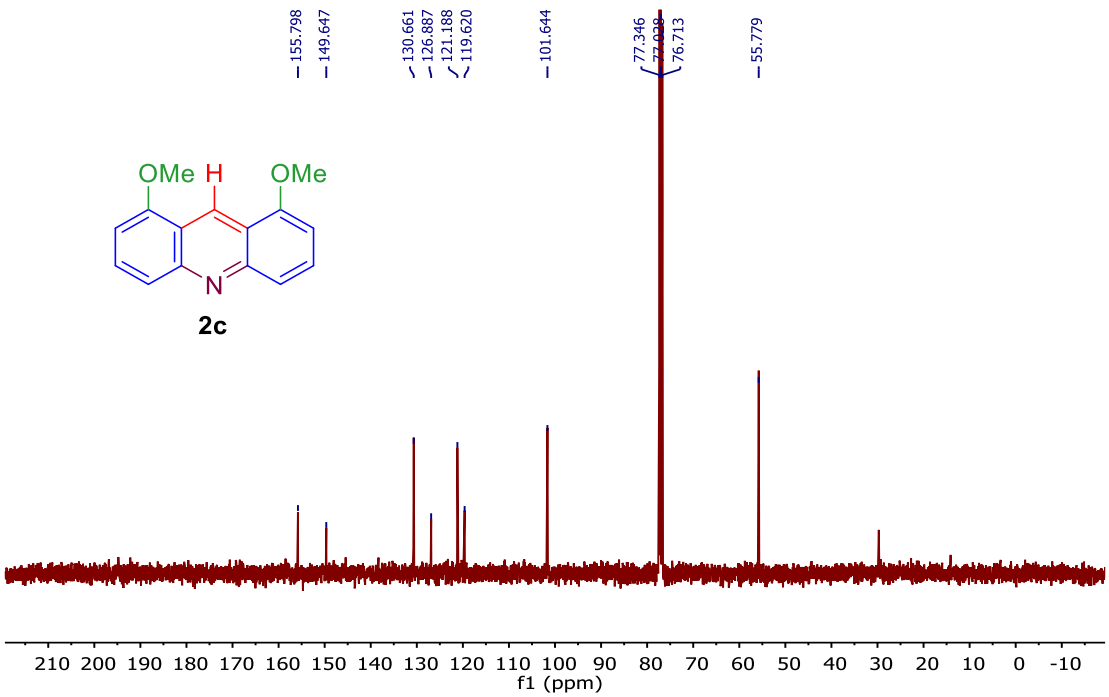

^{13}C NMR ($CDCl_3$, 100 MHz) spectrum of 1,8-dimethoxyacridine (2c).

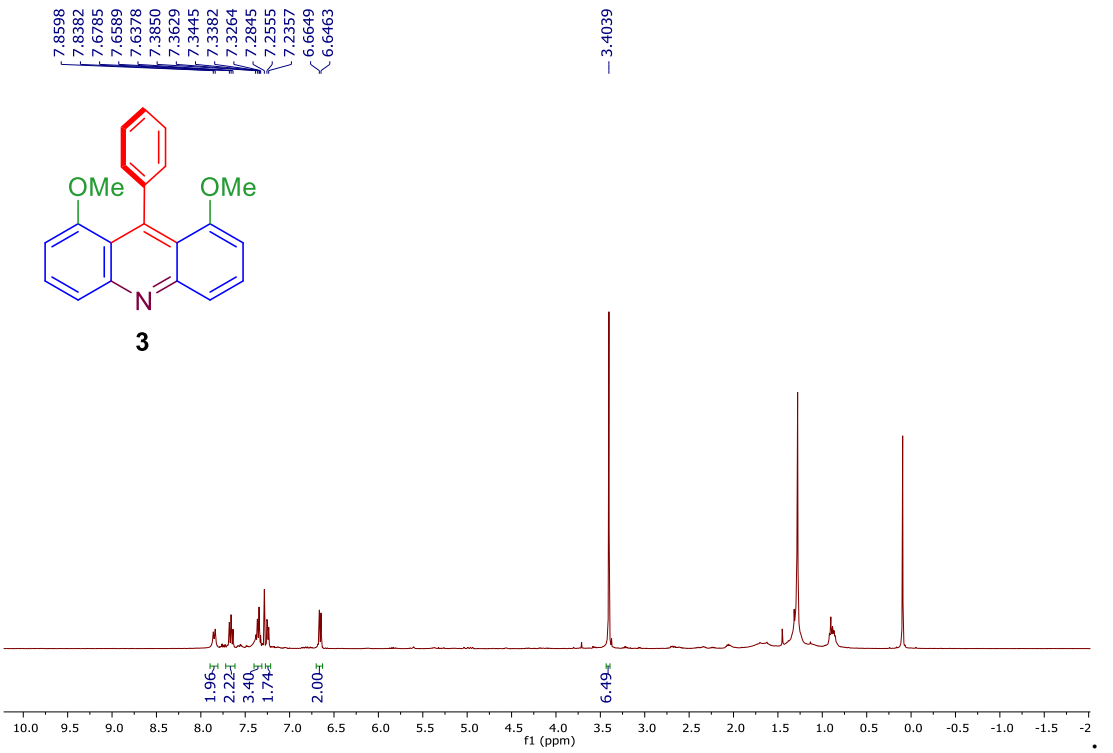

^{1}H NMR ($CDCl_3$, 400 MHz) spectrum of 1,8-dimethoxy-9-phenylacridine (3).

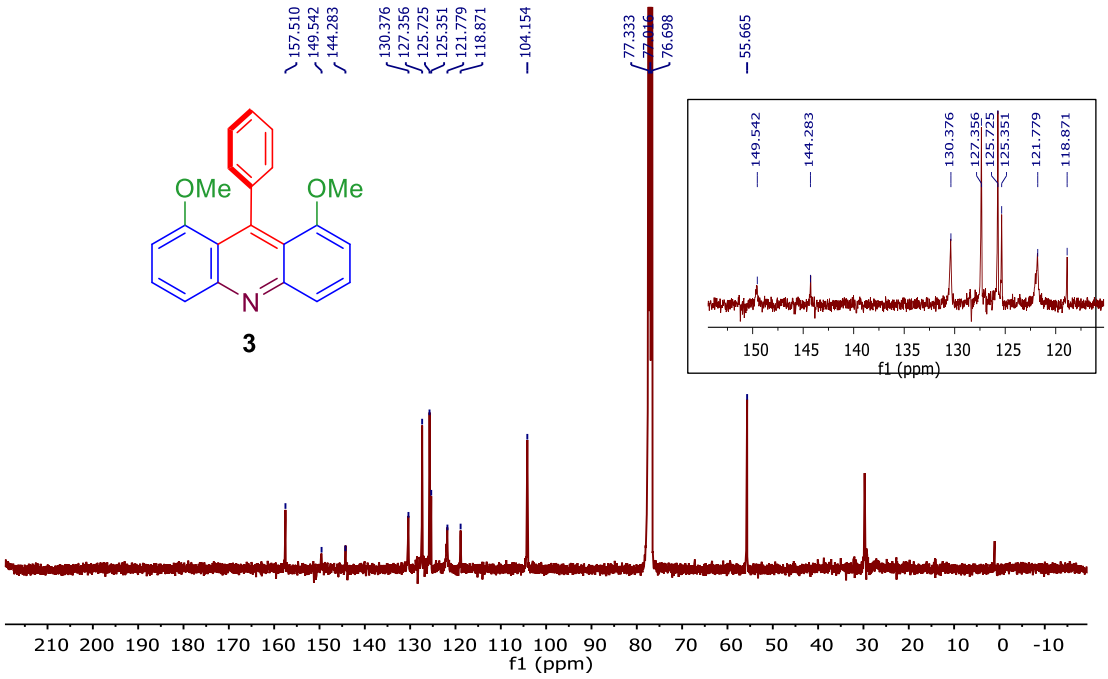

^{13}C NMR ($CDCl_3$, 100 MHz) spectrum of 1,8-dimethoxy-9-phenylacridine (3).

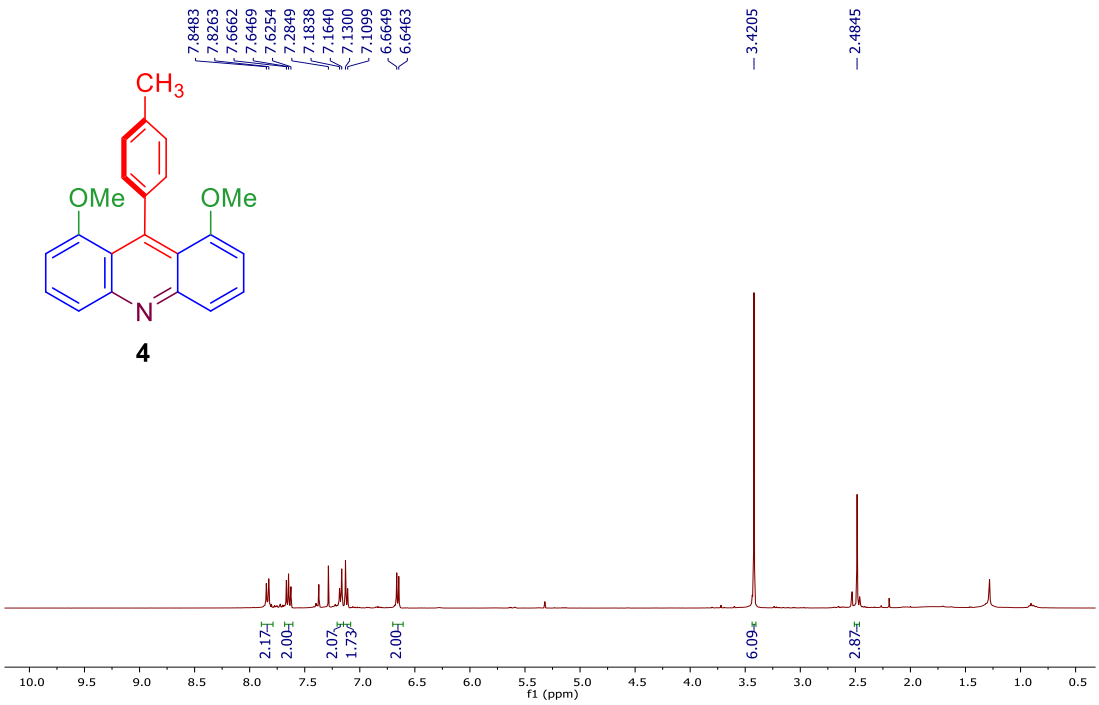

^{1}H NMR ($CDCl_3$, 400 MHz) spectrum of 1,8-dimethoxy-9-p-tolylacridine (4).

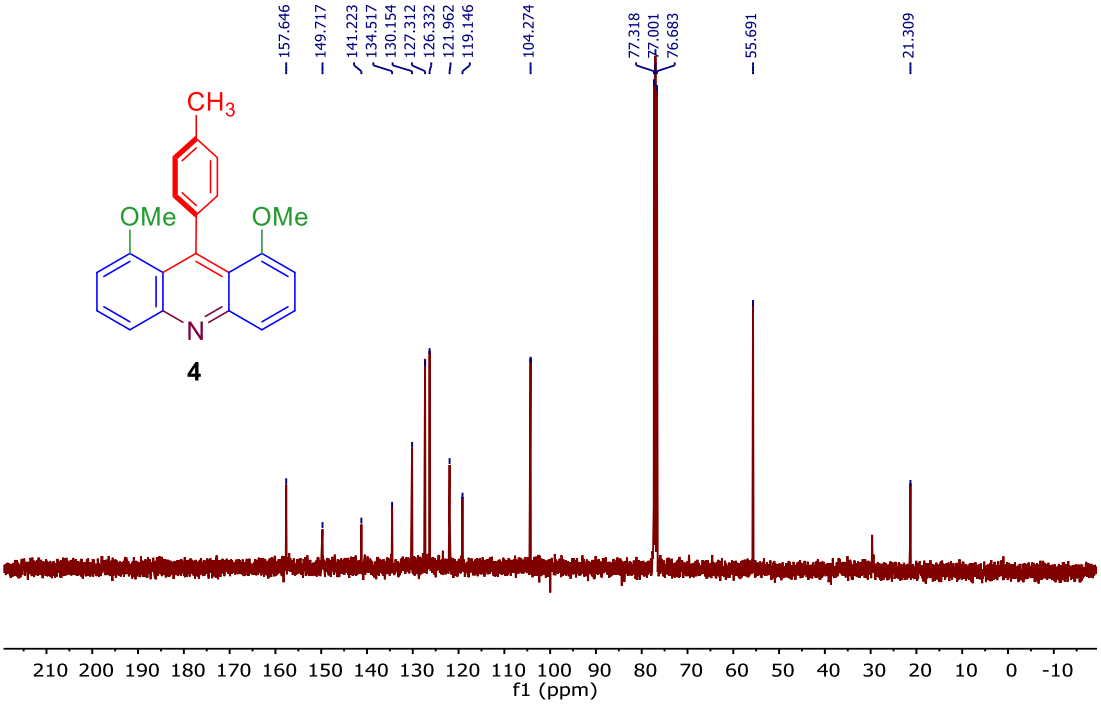

^{13}C NMR ($CDCl_3$, 100 MHz) spectrum of 1,8-dimethoxy-9-p-tolylacridine (4).

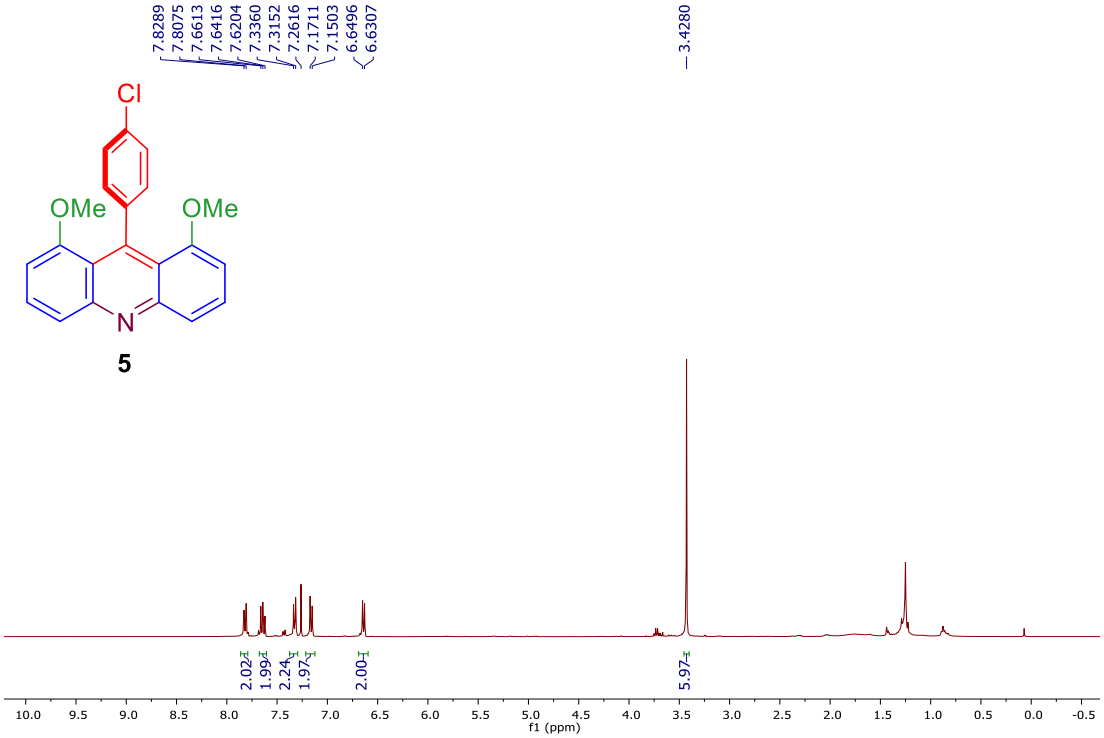

^{1}H NMR ($CDCl_3$, 400 MHz) spectrum of 9-(4-cholorophenyl)-1,8-dimethoxyacridine (5).

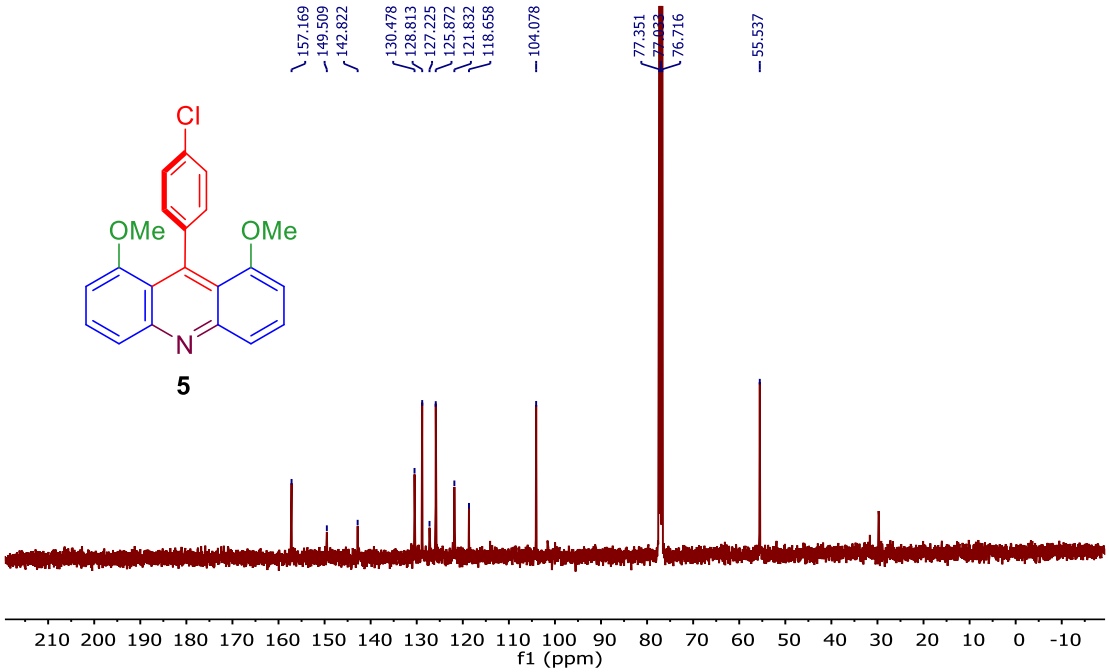

^{13}C NMR ($CDCl_3$, 100 MHz) spectrum of 9-(4-cholorophenyl)-1,8-dimethoxyacridine (5).

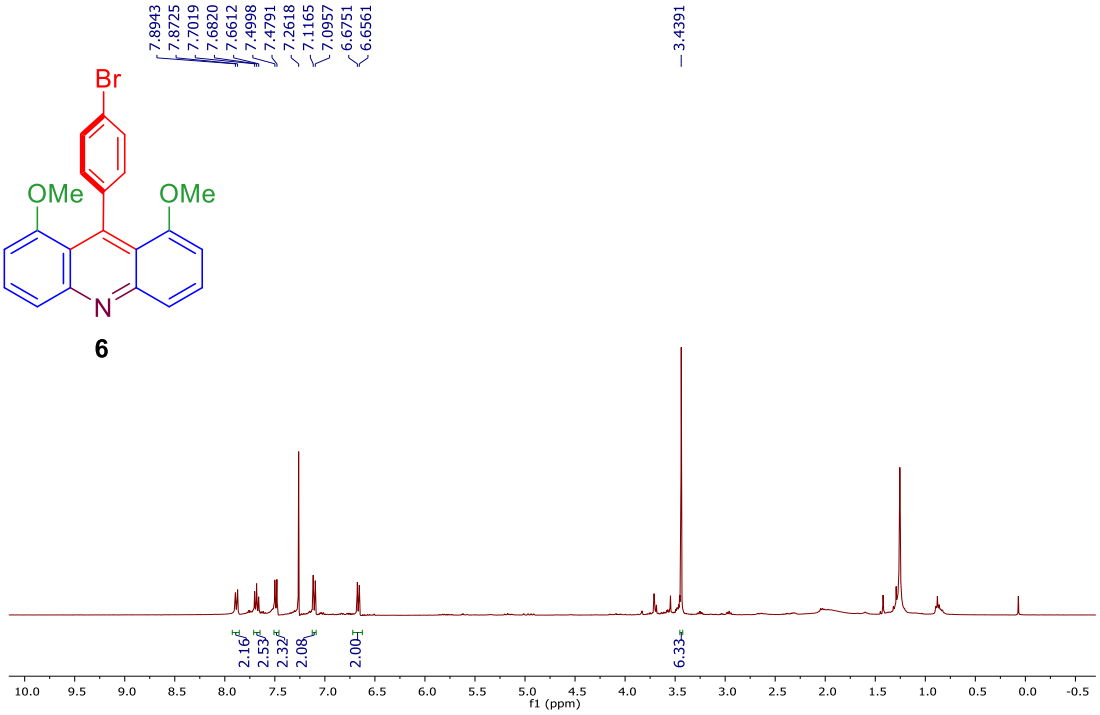

^{1}H NMR ($CDCl_3$, 400 MHz) spectrum of 9-(4-bromophenyl)-1,8-dimethoxyacridine (6).

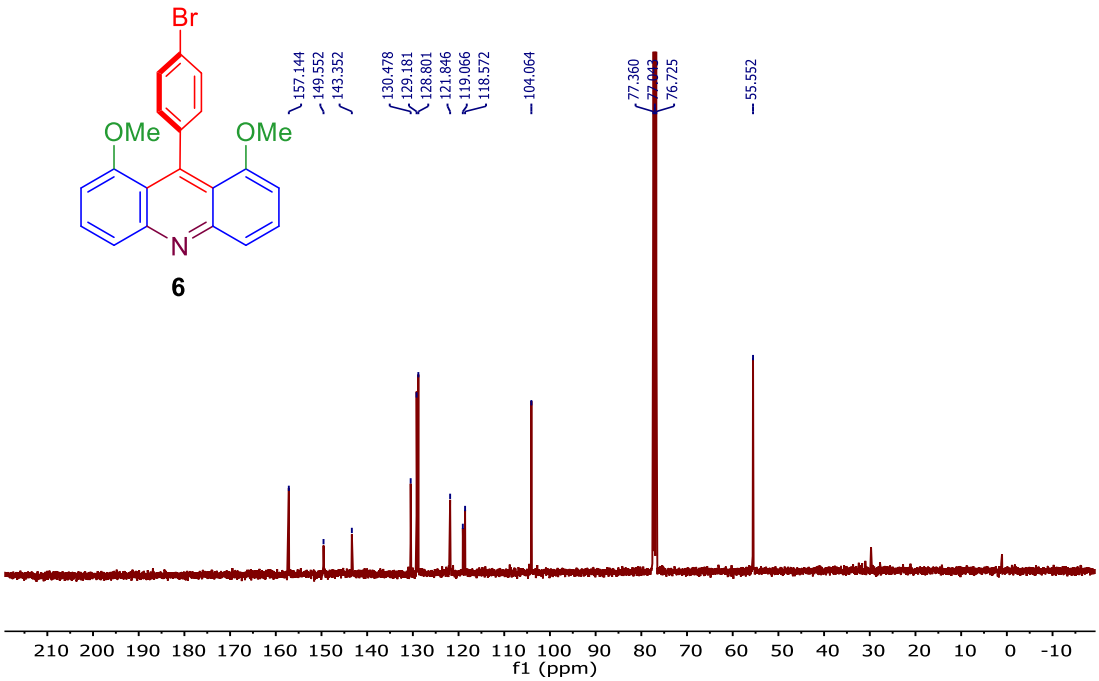

^{13}C NMR ($CDCl_3$, 100 MHz) spectrum of 9-(4-bromophenyl)-1,8-dimethoxyacridine (6).

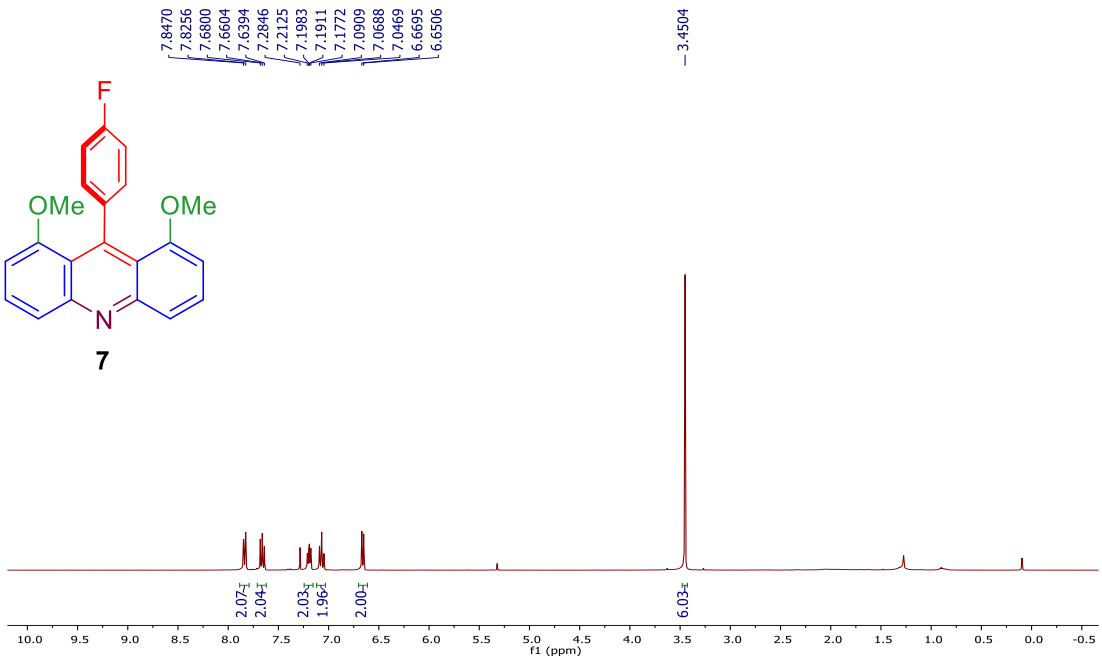

^{1}H NMR ($CDCl_3$, 400 MHz) spectrum of 9-(4-flourophenyl)-1,8-dimethoxyacridine (7).

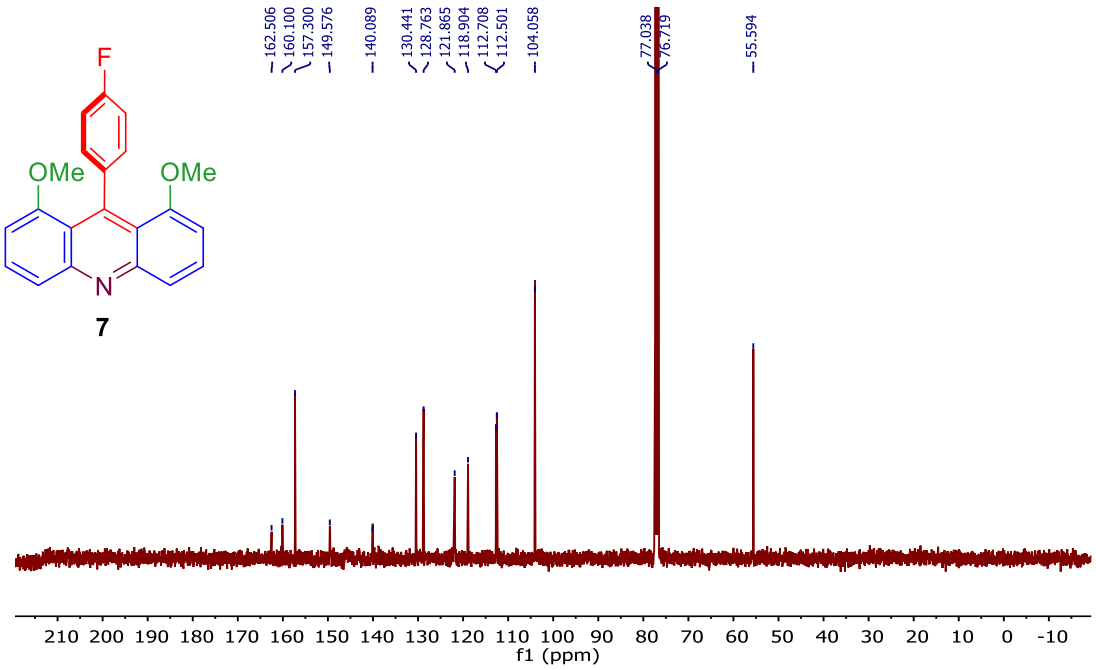

^{13}C NMR ($CDCl_3$, 100 MHz) spectrum of 9-(4-flourophenyl)-1,8-dimethoxyacridine (7).

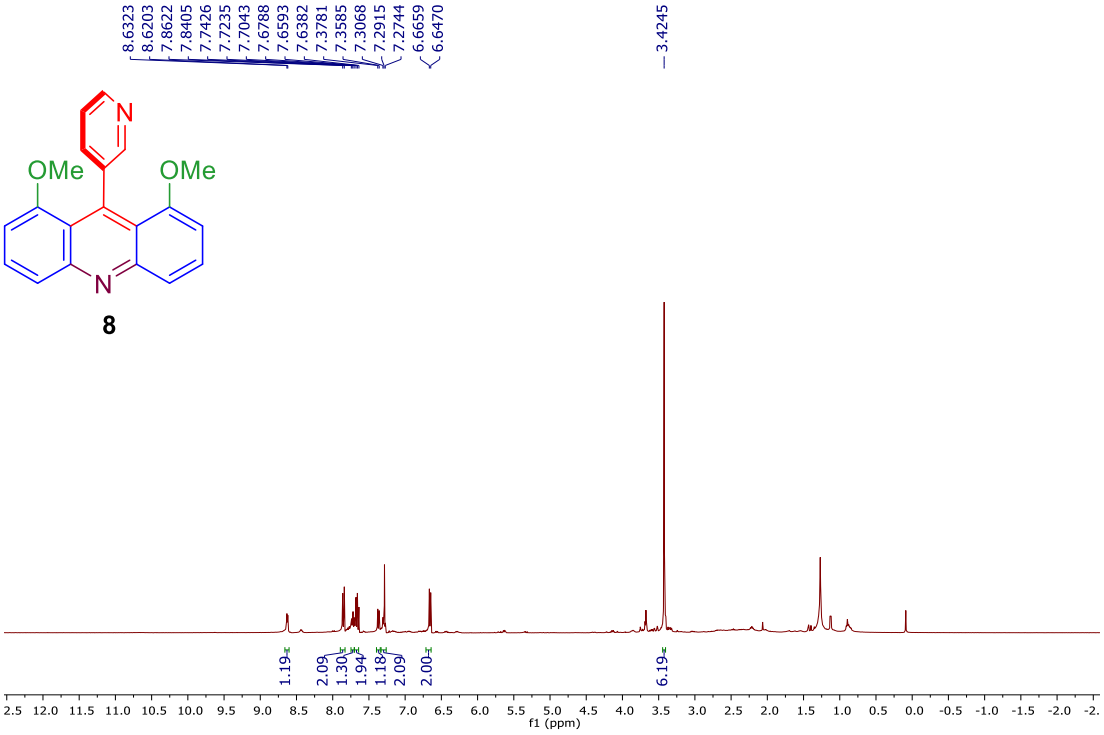

^{1}H NMR ($CDCl_3$, 400 MHz) spectrum of 1,8-dimethoxy-9-(pyridine-3-yl)acridine (8)

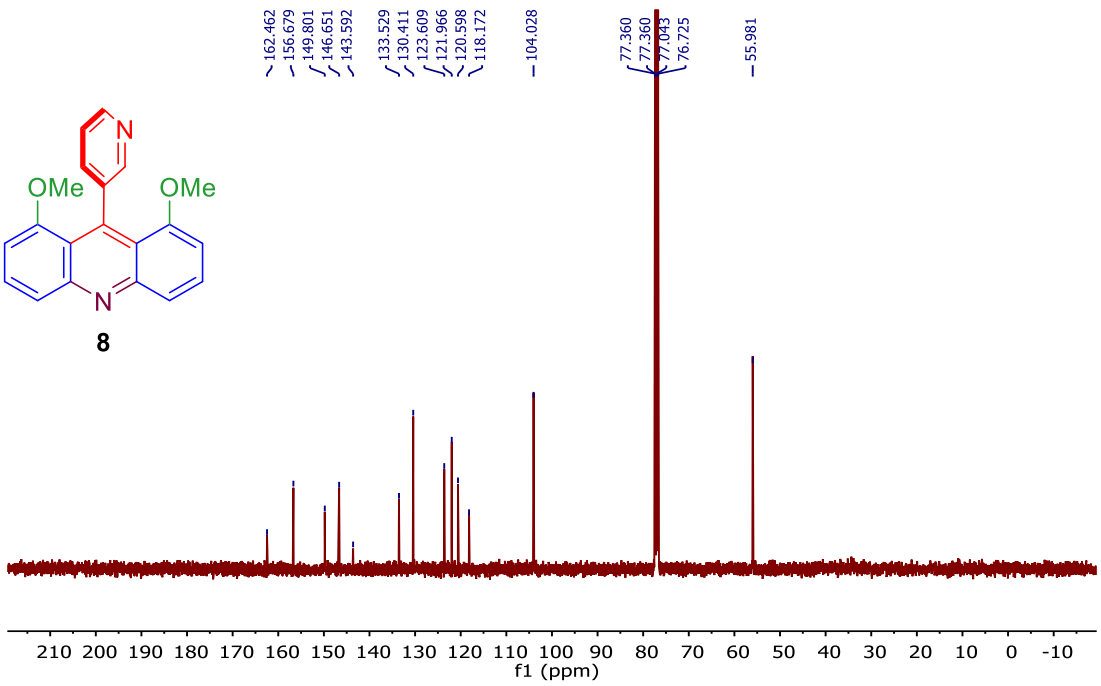

^{13}C NMR ($CDCl_3$, 100 MHz) spectrum of 1,8-dimethoxy-9-(pyridine-3-yl)acridine (8)

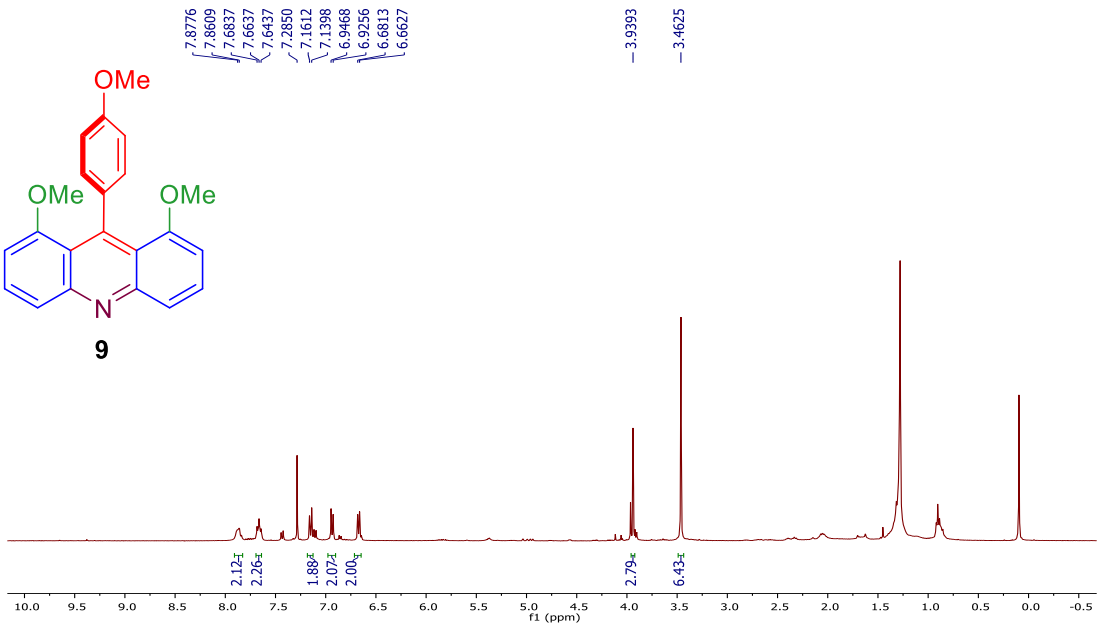

^{1}H NMR ($CDCl_3$, 400 MHz) spectrum of 1,8-dimethoxy-9-(4-methoxyphenyl)acridine (9).

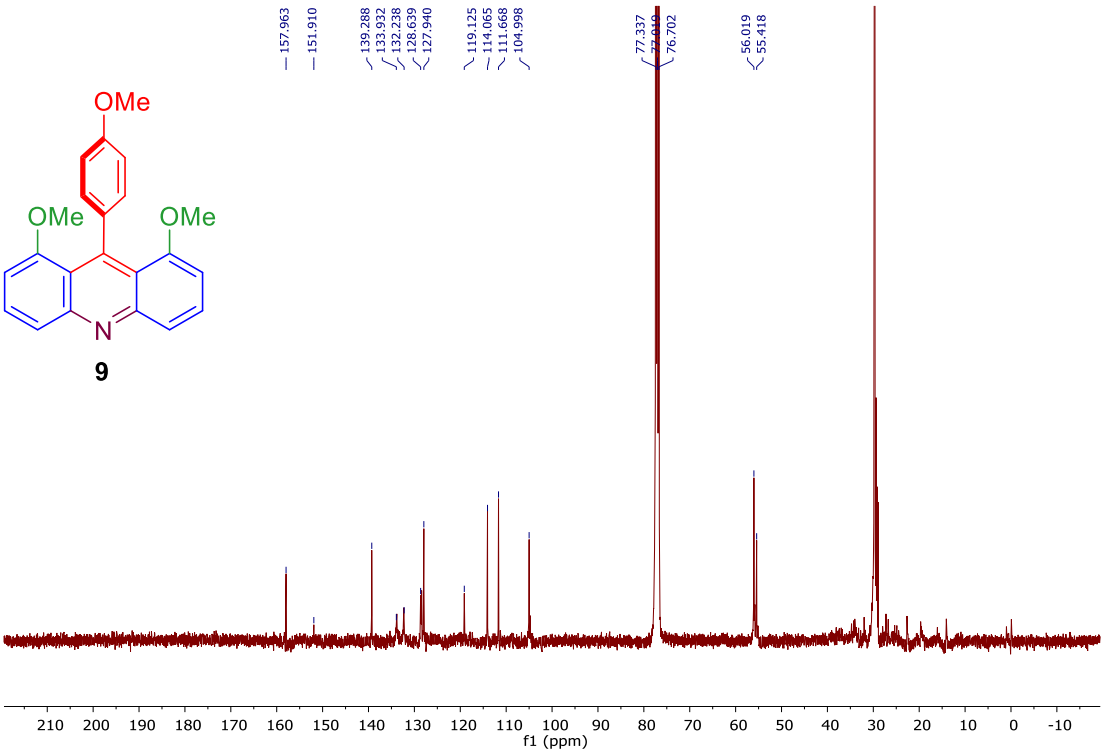

^{13}C NMR ($CDCl_3$, 100 MHz) spectrum of 1,8-dimethoxy-9-(4-methoxyphenyl)acridine (9).

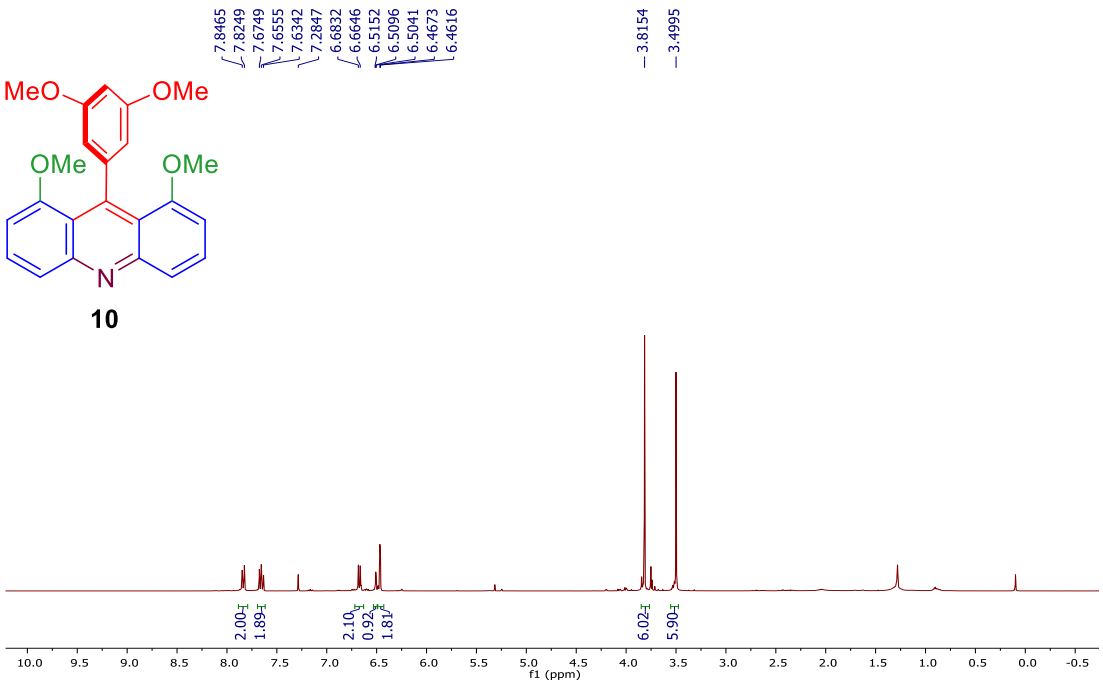

^{1}H NMR ($CDCl_3$, 400 MHz) spectrum of 9-(3,5-dimethoxyphenyl)-1,8-dimethoxyacridine (10).

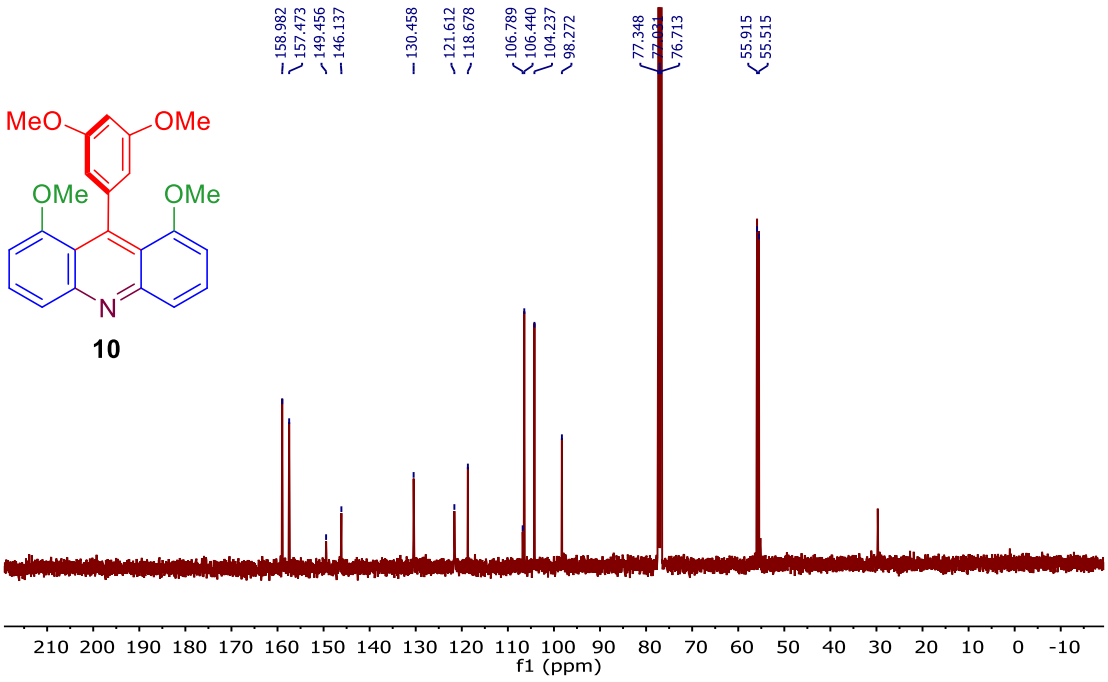

^{13}C NMR ($CDCl_3$, 100 MHz) spectrum of 9-(3,5-dimethoxyphenyl)-1,8-dimethoxyacridine (10).

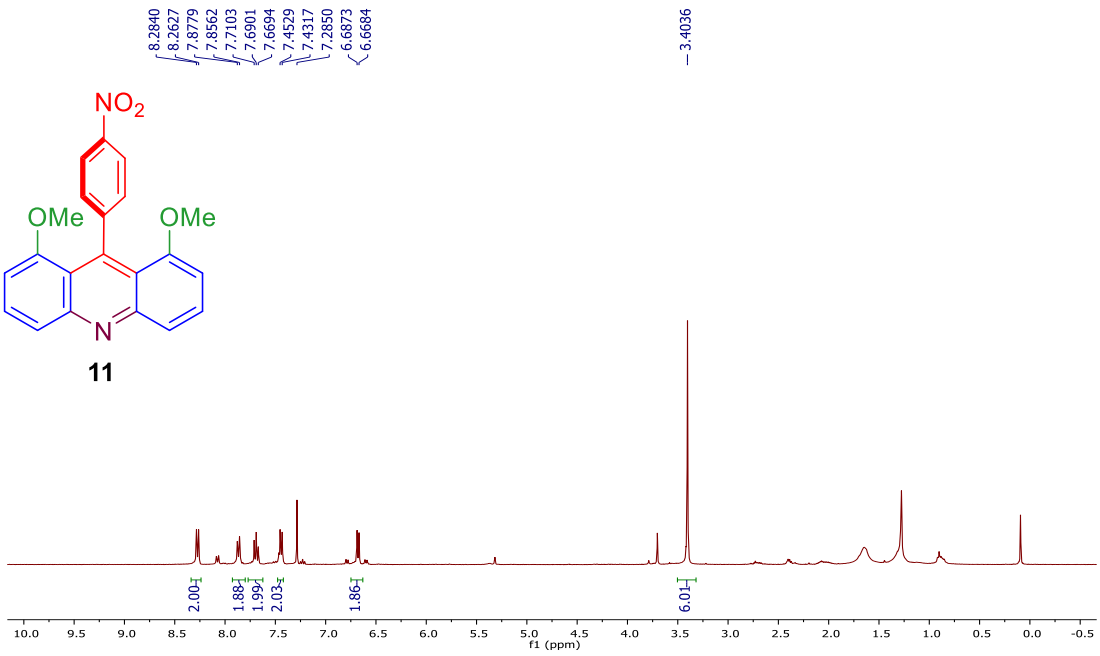

^{1}H NMR ($CDCl_3$, 400 MHz) spectrum of 1,8-dimethoxy-9-(4-nitrophenyl)acridine (11).

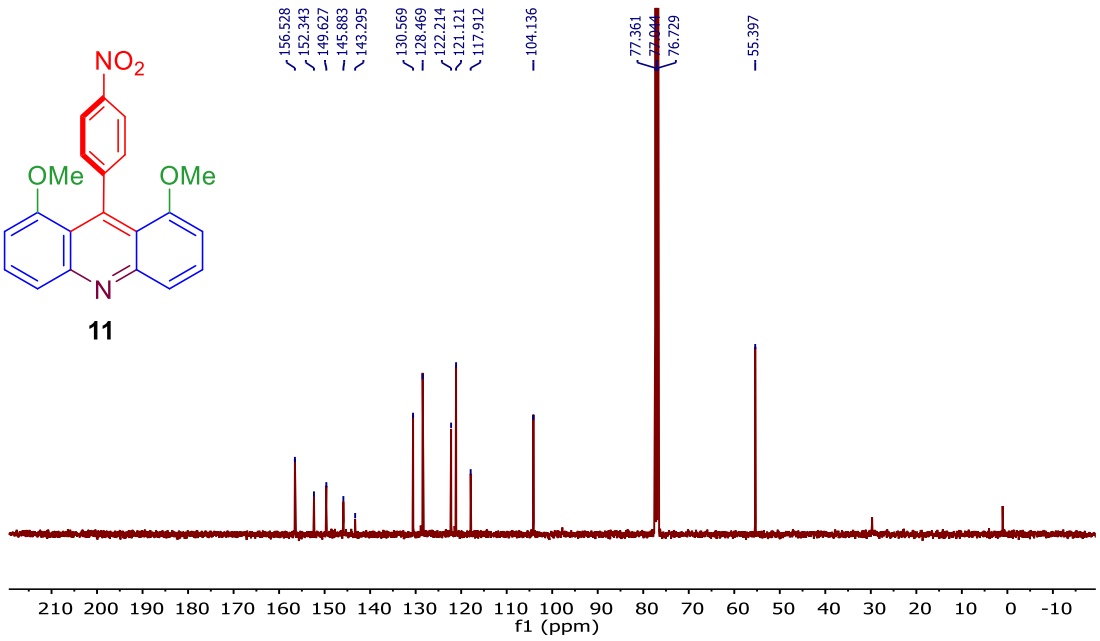

^{13}C NMR ($CDCl_3$, 100 MHz) spectrum of 1,8-dimethoxy-9-(4-nitrophenyl)acridine (11).

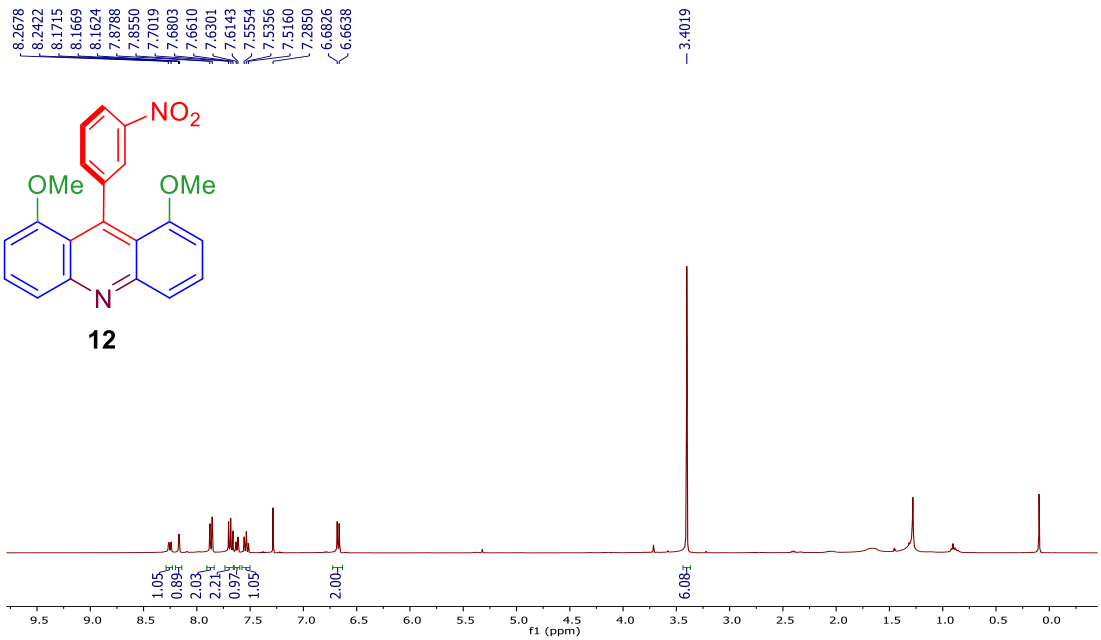

^{1}H NMR ($CDCl_3$, 400 MHz) spectrum of 1,8-dimethoxy-9-(3-nitrophenyl)acridine (12).

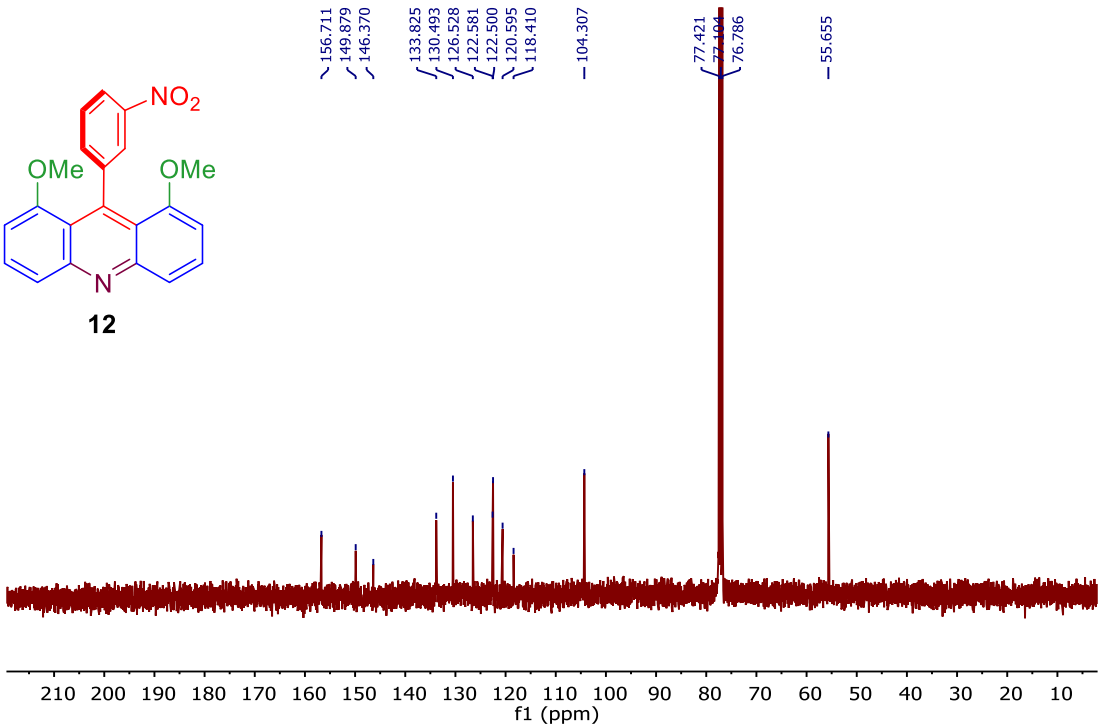

^{13}C NMR ($CDCl_3$, 100 MHz) spectrum of 1,8-dimethoxy-9-(3-nitrophenyl)acridine (12).

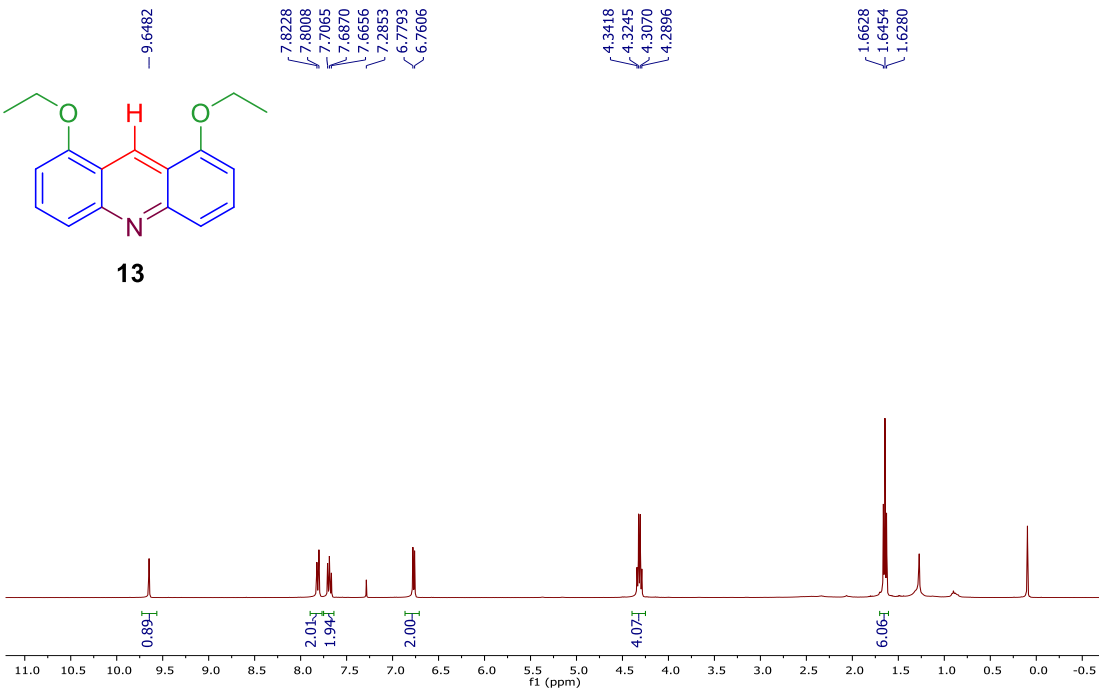

^{1}H NMR ($CDCl_3$, 400 MHz) spectrum of 1,8-diethoxyacridine (13).

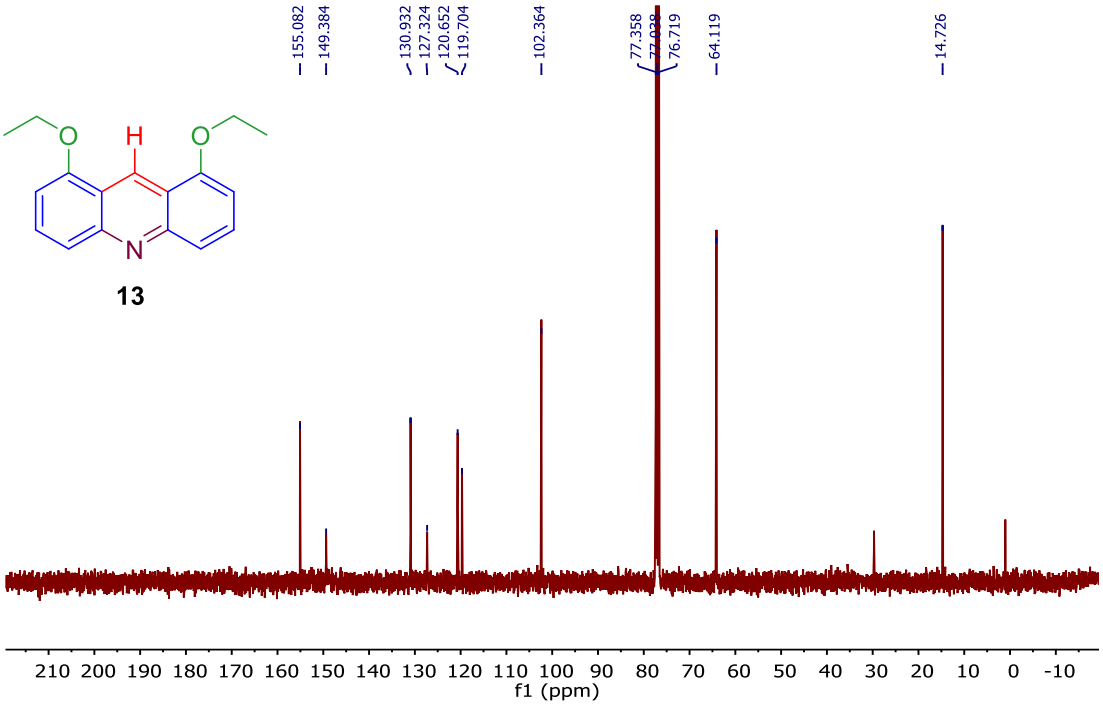

^{13}C NMR ($CDCl_3$, 100 MHz) spectrum of 1,8-diethoxyacridine (13).

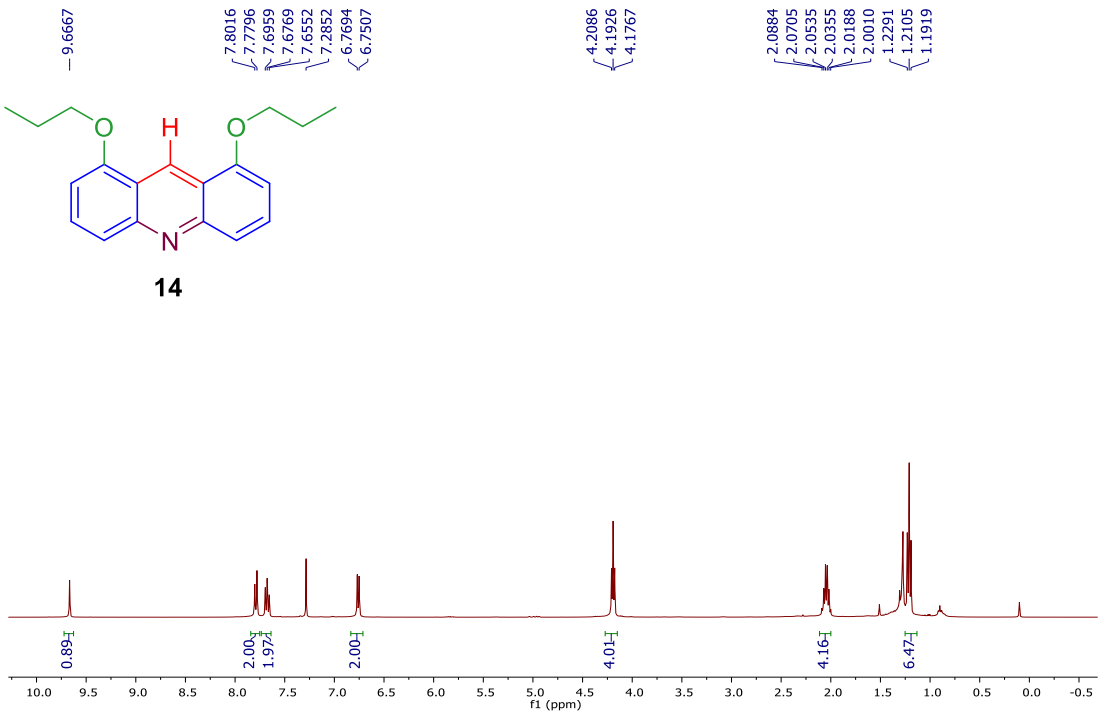

^{1}H NMR ($CDCl_3$, 400 MHz) spectrum of 1,8-dipropoxyacridine (14).

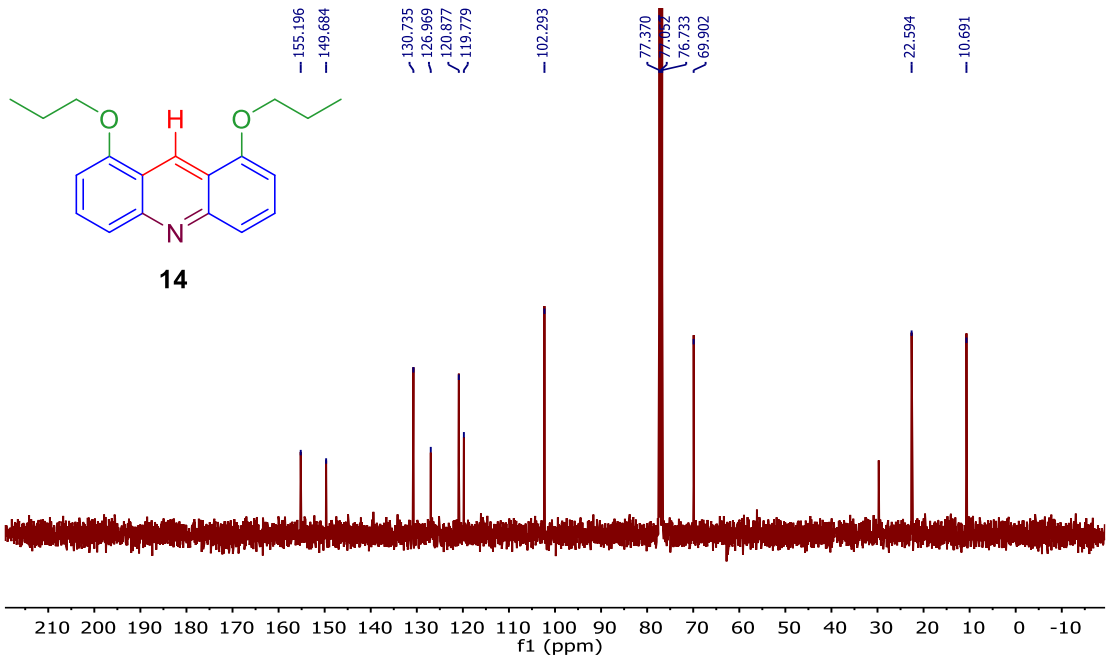

^{13}C NMR ($CDCl_3$, 100 MHz) spectrum of 1,8-dipropoxyacridine (14).

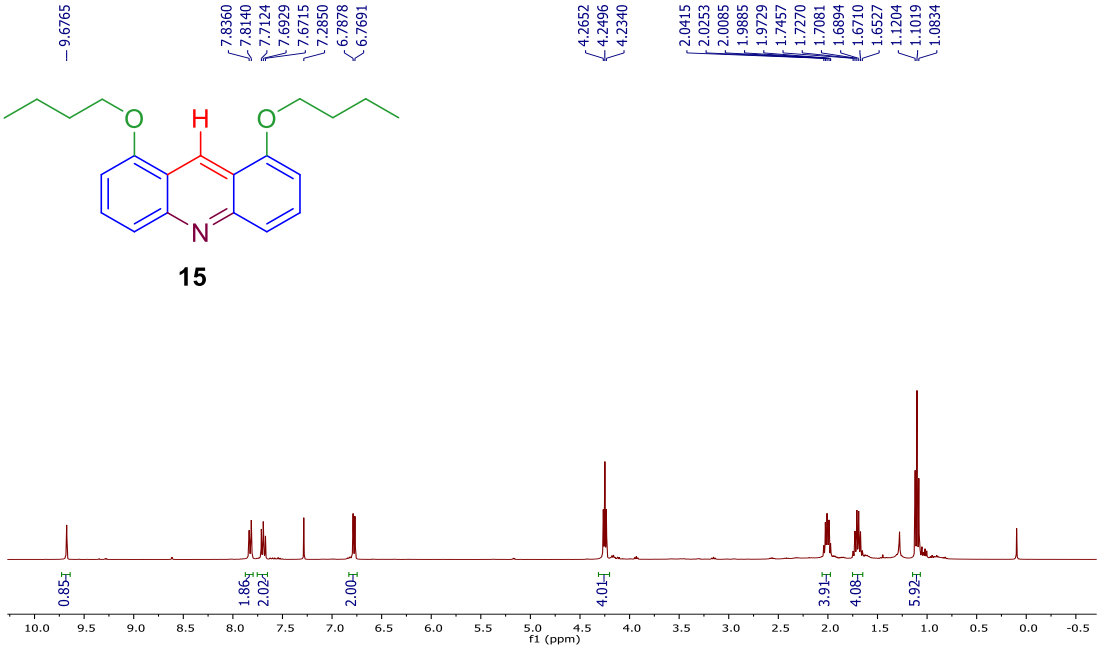

^{1}H NMR ($CDCl_3$, 400 MHz) spectrum of 1,8-dibutoxyacridine (15).

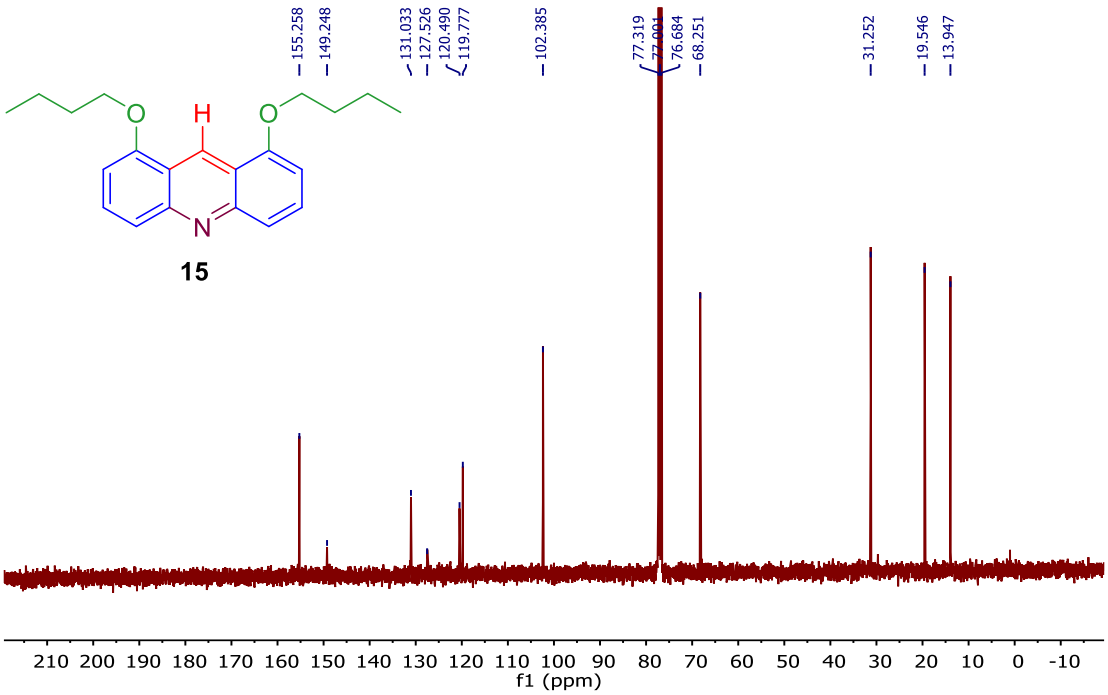

^{13}C NMR ($CDCl_3$, 100 MHz) spectrum of 1,8-dibutoxyacridine (15).

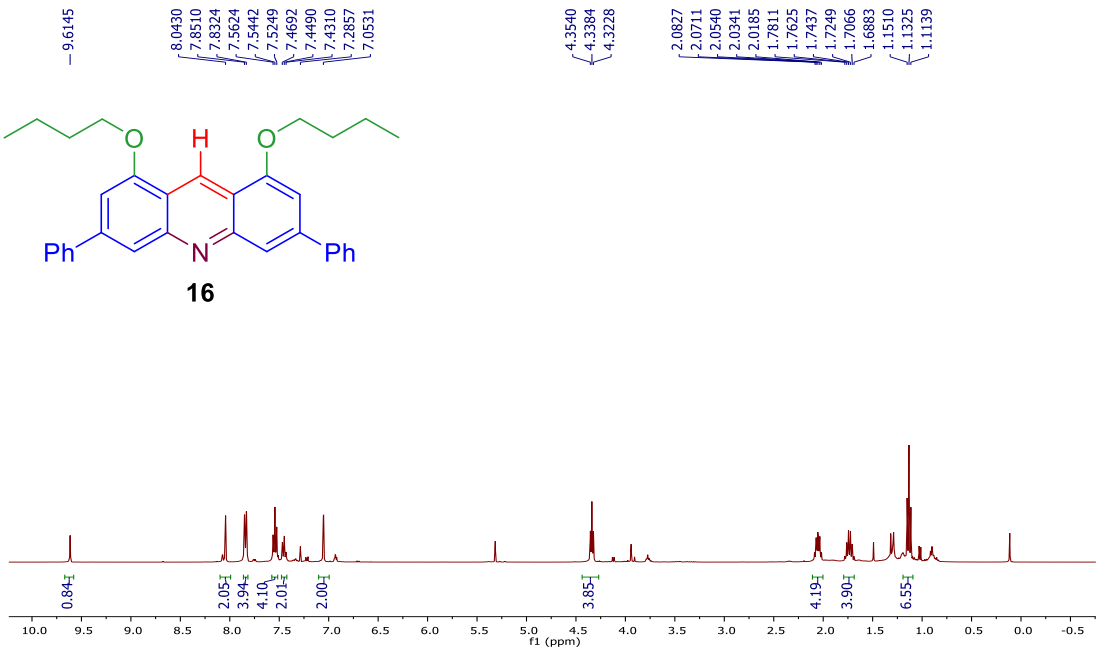

^{1}H NMR ($CDCl_3$, 400 MHz) spectrum of 1,8-dibutoxy-3,6-diphenylacridine (16).

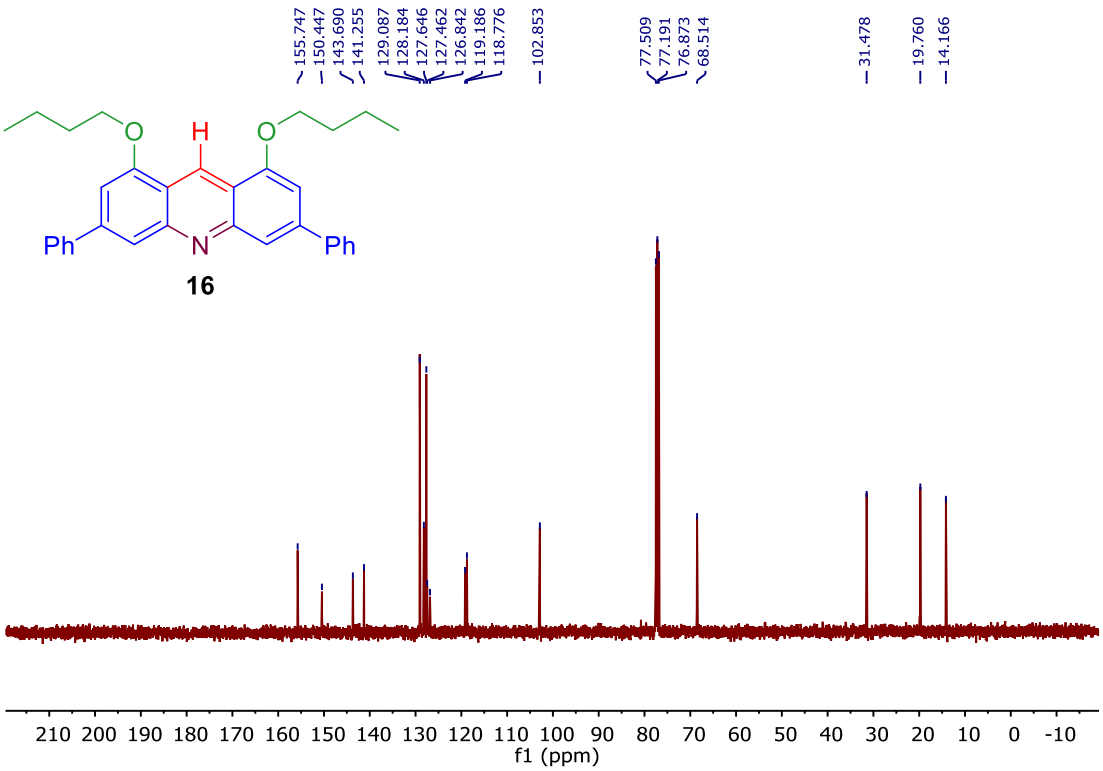

^{13}C NMR ($CDCl_3$, 100 MHz) spectrum of 1,8-dibutoxy-3,6-diphenylacridine (16).

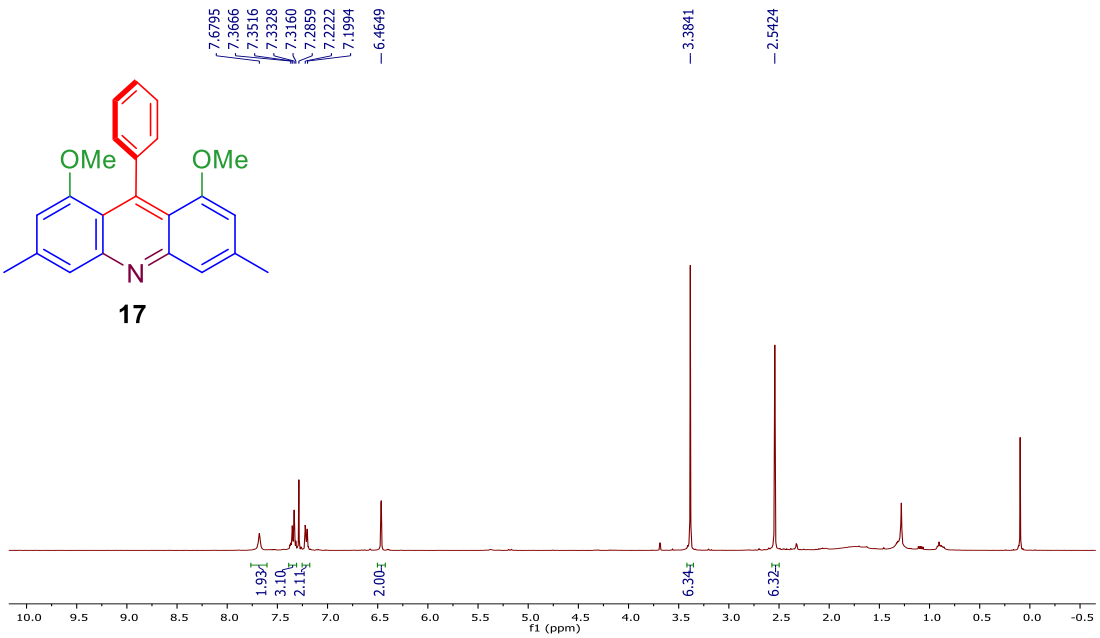

^{1}H NMR ($CDCl_3$, 100 MHz) spectrum of 1,8-dimethoxy-3,6-dimethyl-9-phenylacridine (17).

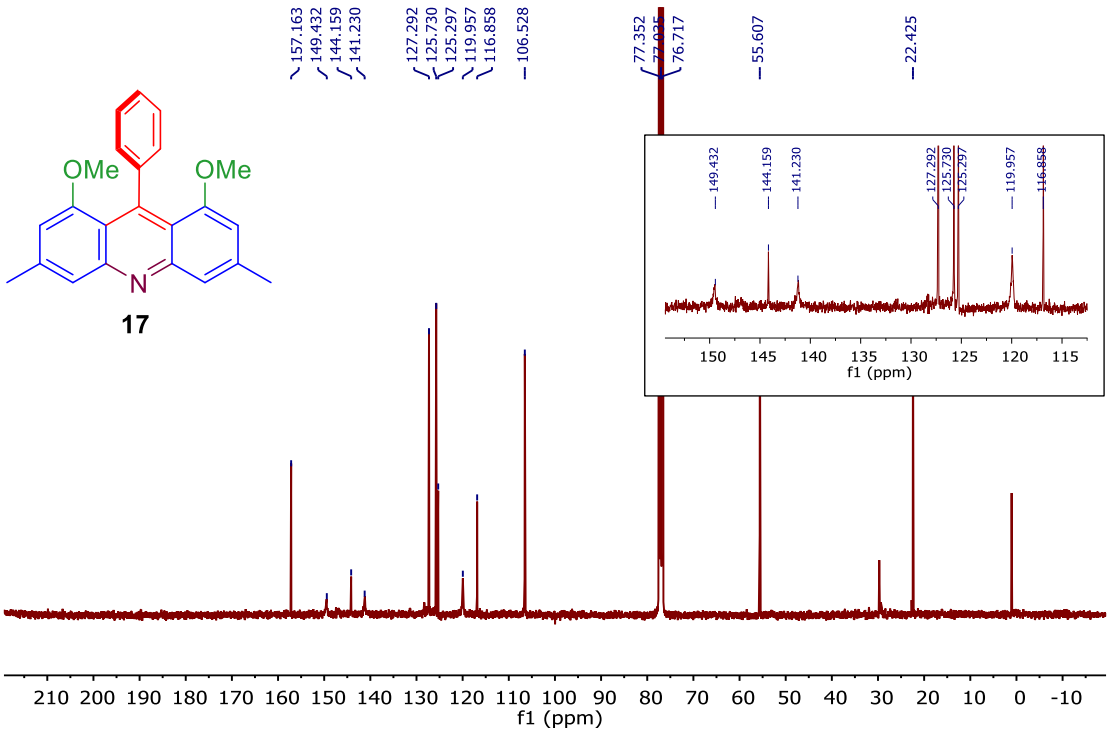

^{13}C NMR ($CDCl_3$, 100 MHz) spectrum of 1,8-dimethoxy-3,6-dimethyl-9-phenylacridine (17).

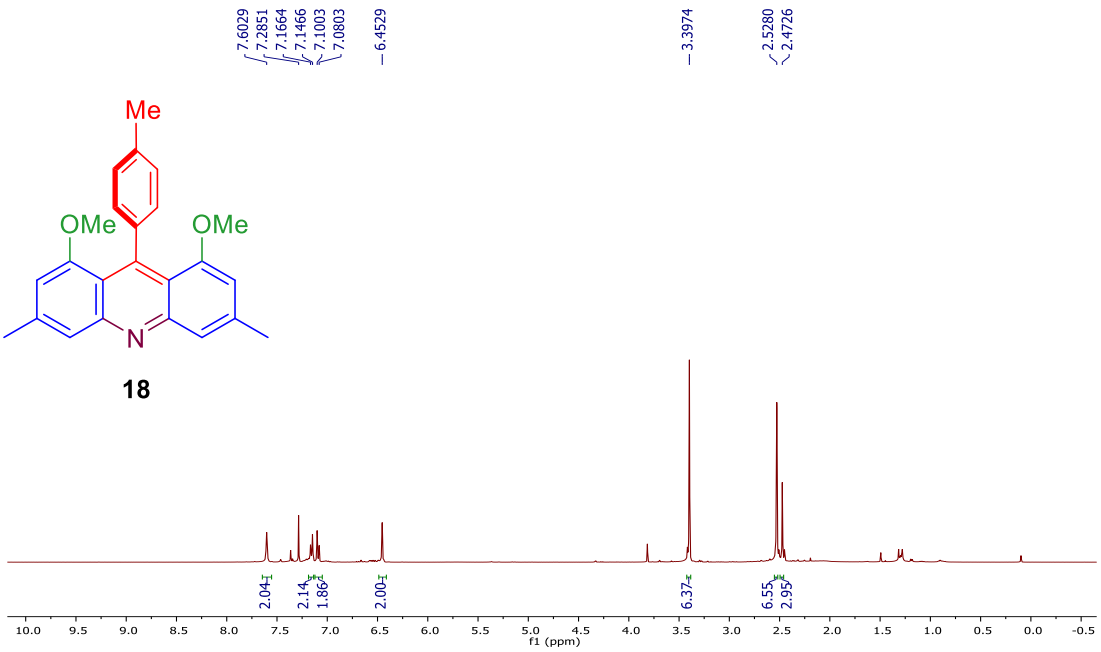

^{1}H NMR ($CDCl_3$, 400 MHz) spectrum of 1,8-dimethoxy-3,6-dimethyl-9-p-tolylacridine (18).

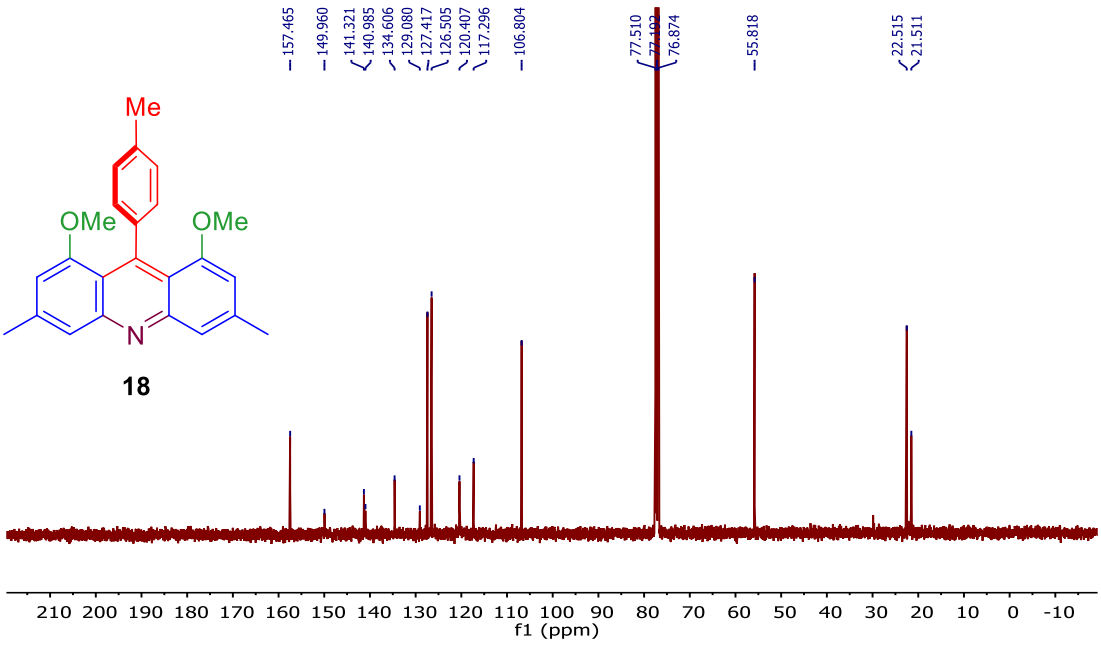

^{13}C NMR ($CDCl_3$, 100 MHz) spectrum of 1,8-dimethoxy-3,6-dimethyl-9-p-tolylacridine (18).

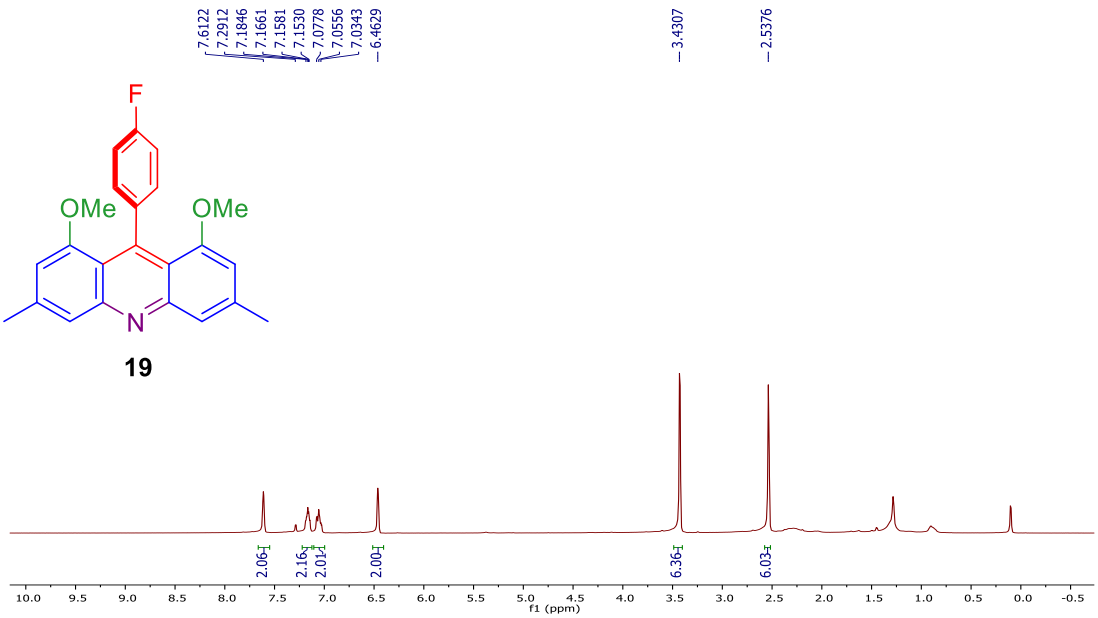

^{1}H NMR ($CDCl_3$, 400 MHz) spectrum of 9-(4-fluorophenyl)-1,8-dimethoxy-3,6-dimethylacridine (19).

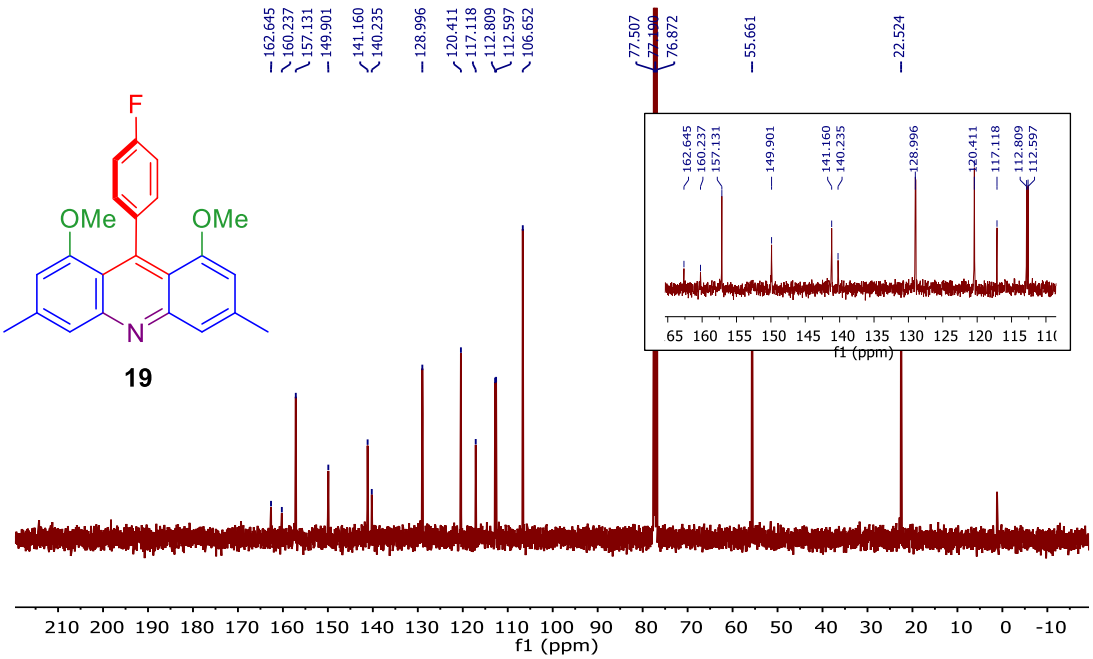

^{13}C NMR ($CDCl_3$, 100 MHz) spectrum of 9-(4-fluorophenyl)-1,8-dimethoxy-3,6-dimethylacridine (19).

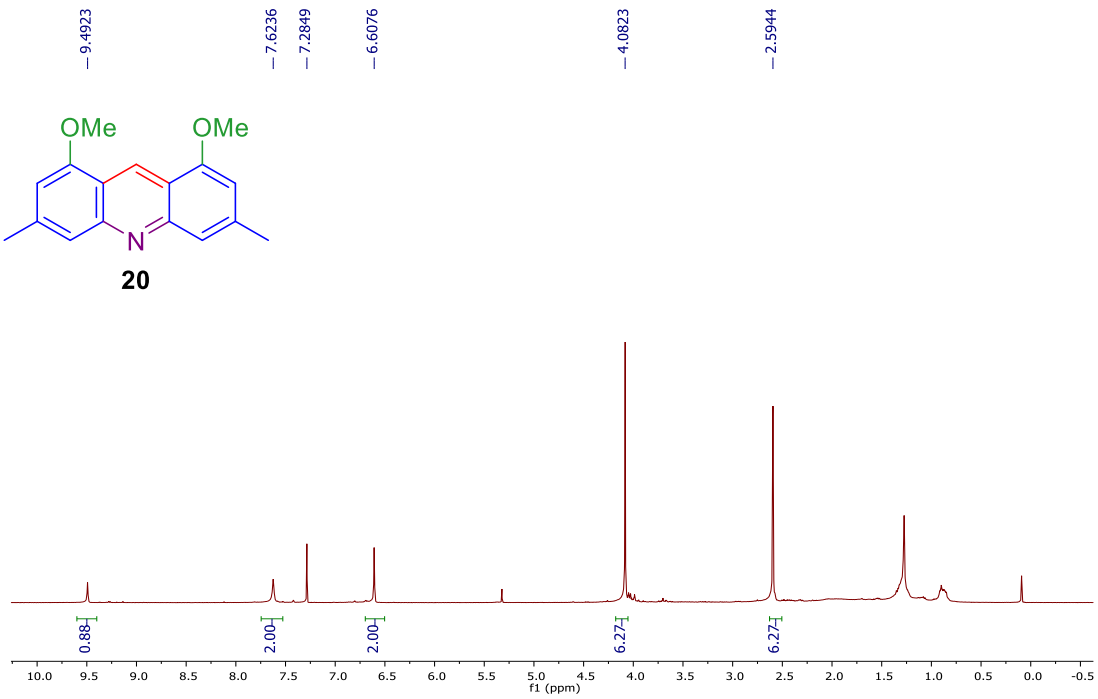

^{1}H NMR ($CDCl_3$, 400 MHz) spectrum of 1,8-dimethoxy-3,6-dimethylacridine (20).

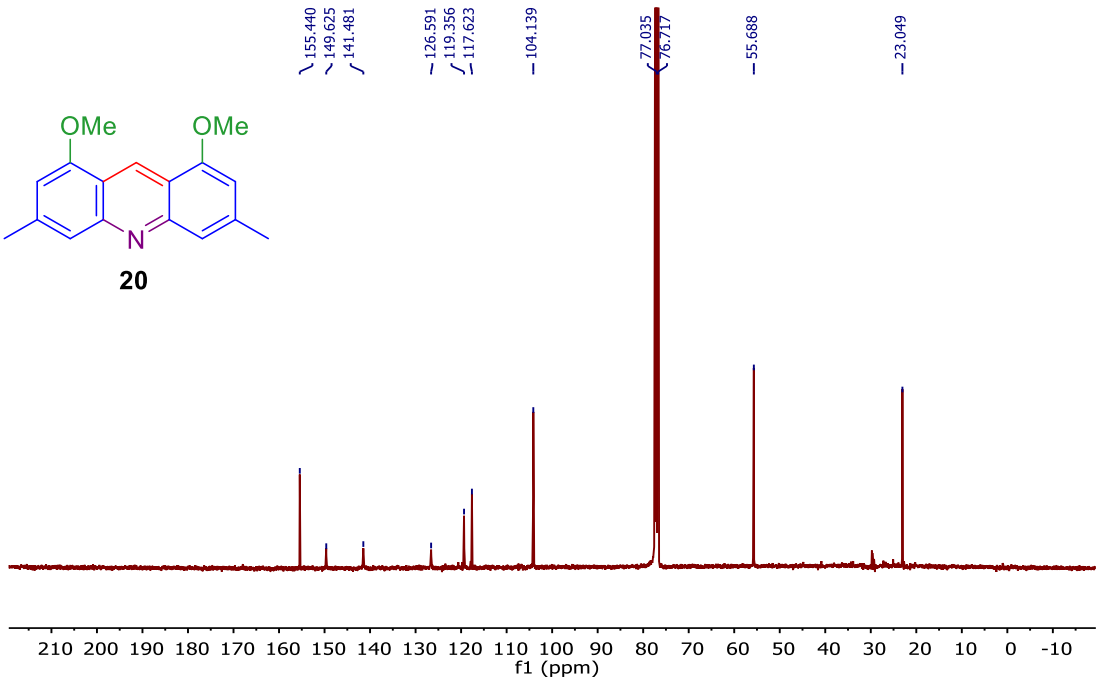

^{13}C NMR ($CDCl_3$, 100 MHz) spectrum of 1,8-dimethoxy-3,6-dimethylacridine (20).

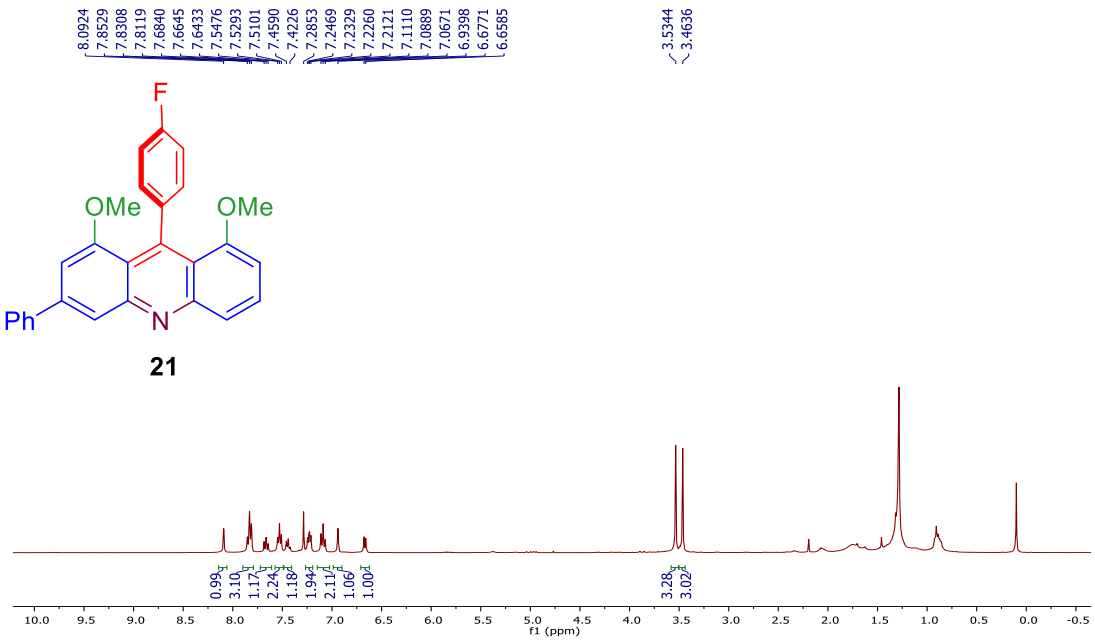

^{1}H NMR ($CDCl_3$, 400 MHz) spectrum of 9-(4-fluorophenyl)-1,8-dimethoxy-3-phenylacridine (21).

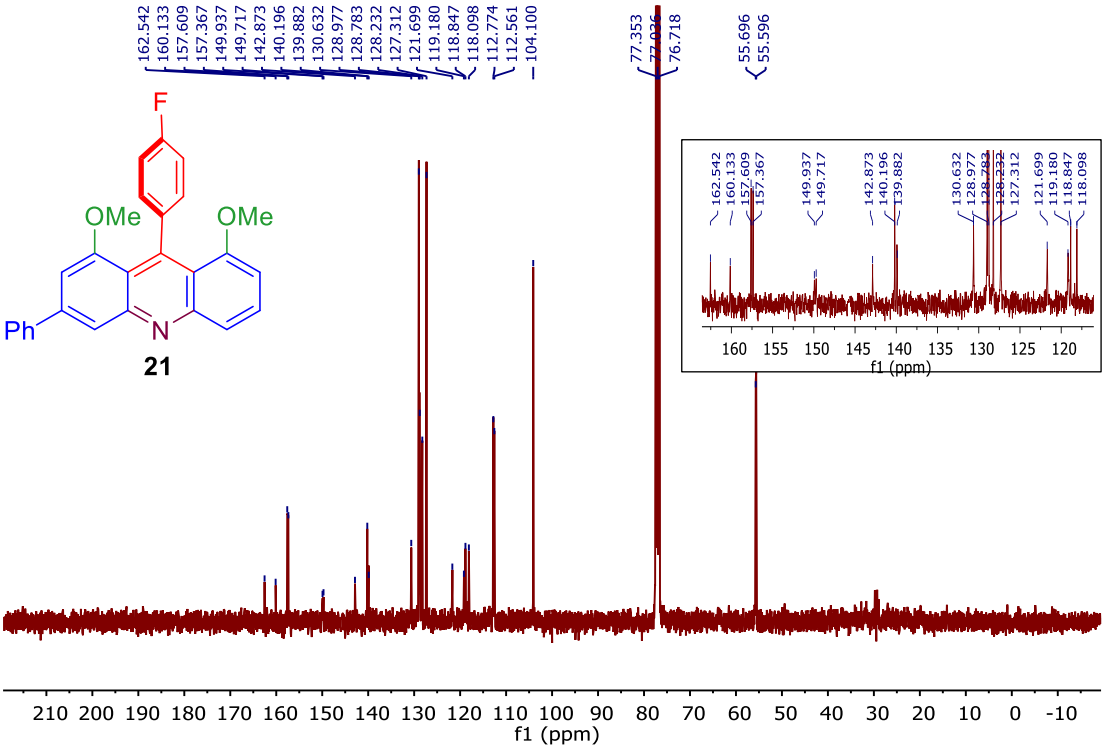

^{13}C NMR ($CDCl_3$, 100 MHz) spectrum of 9-(4-fluorophenyl)-1,8-dimethoxy-3-phenylacridine (21).

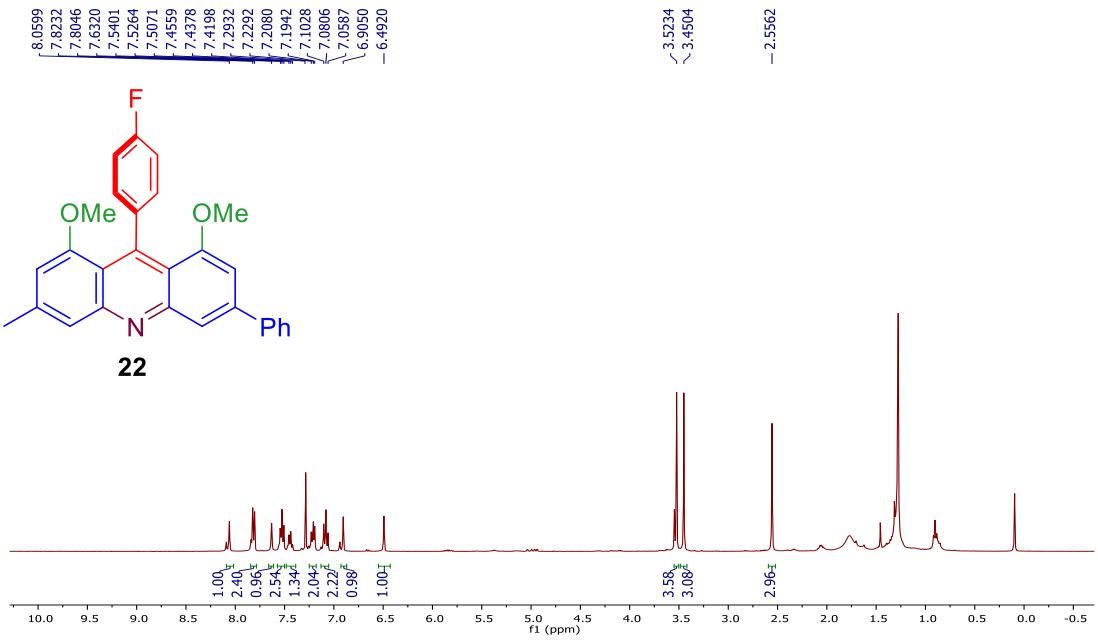

^{1}H NMR($CDCl_3$, 400 MHz) spectrum of 9-(4-fluorophenyl)-1,8-dimethoxy-3-methyl-6-phenylacridine (22).

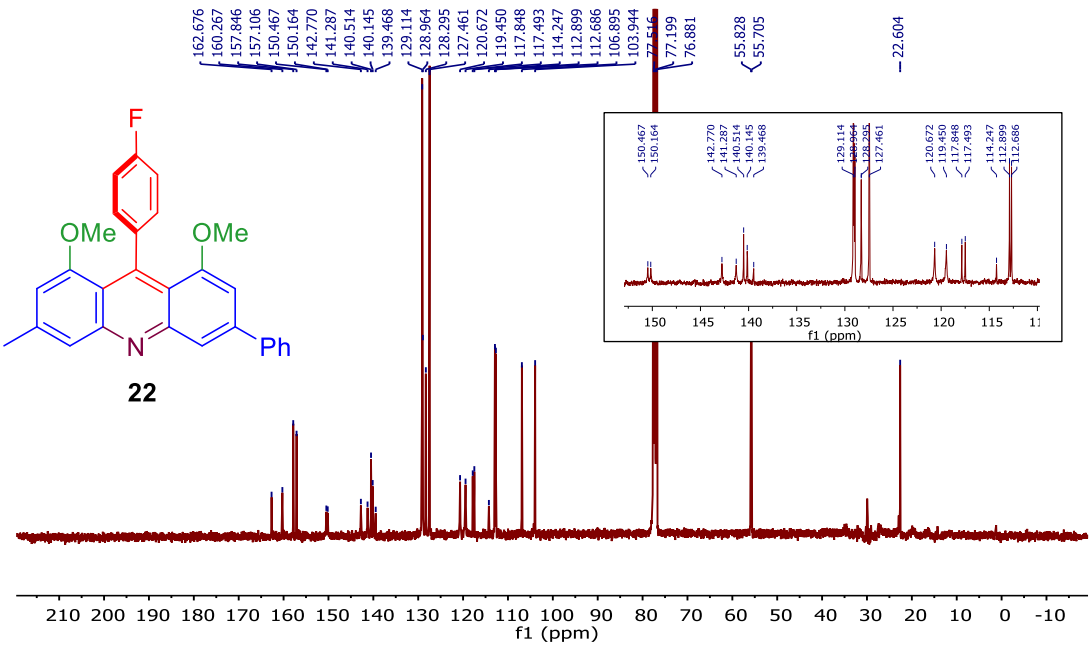

^{13}C NMR ($CDCl_3$, 100 MHz) spectrum of 9-(4-fluorophenyl)-1,8-dimethoxy-3-methyl-6-phenylacridine (22).

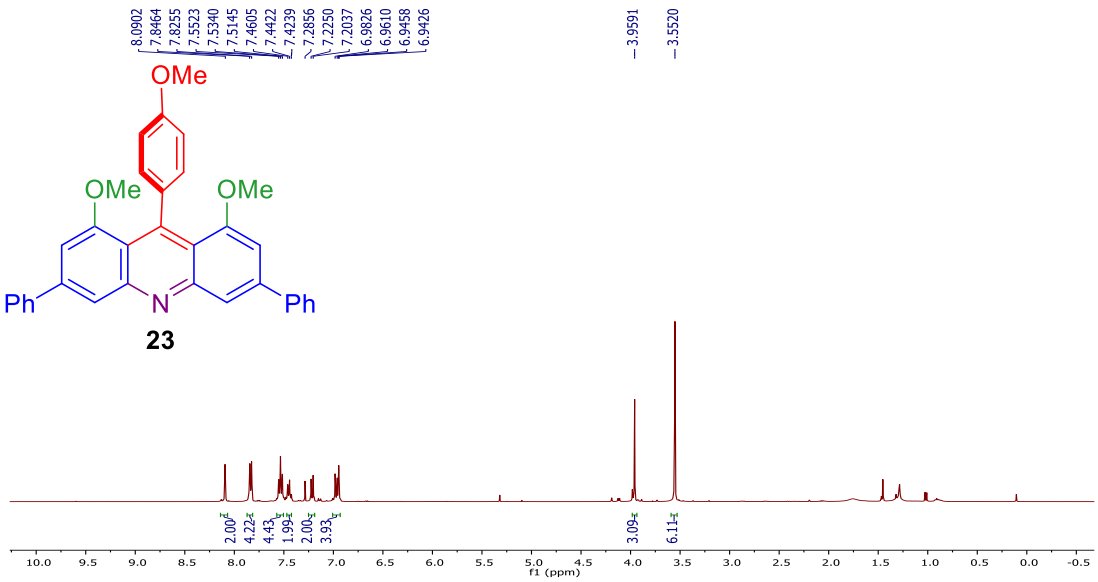

^{1}H NMR ($CDCl_3$, 400 MHz) spectrum of 1,8-dimethoxy-9-(4-methoxyphenyl)-3,6-diphenylacridine (23).

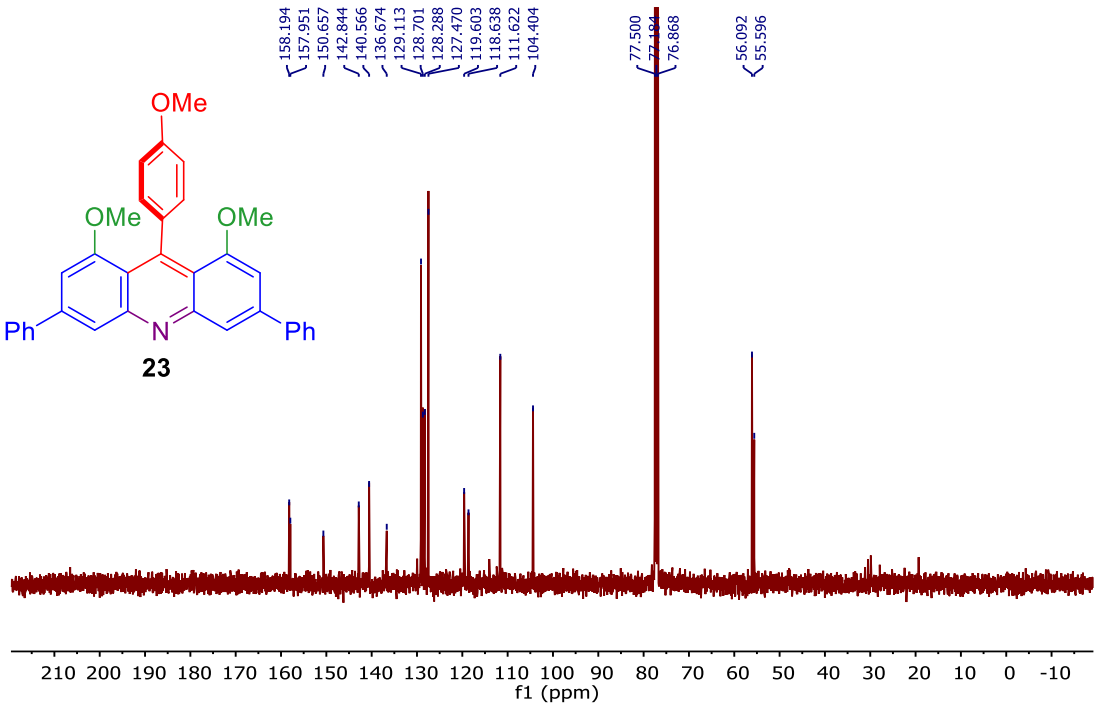

^{13}C NMR ($CDCl_3$, 100 MHz) spectrum of 1,8-dimethoxy-9-(4-methoxyphenyl)-3,6-diphenylacridine (23).

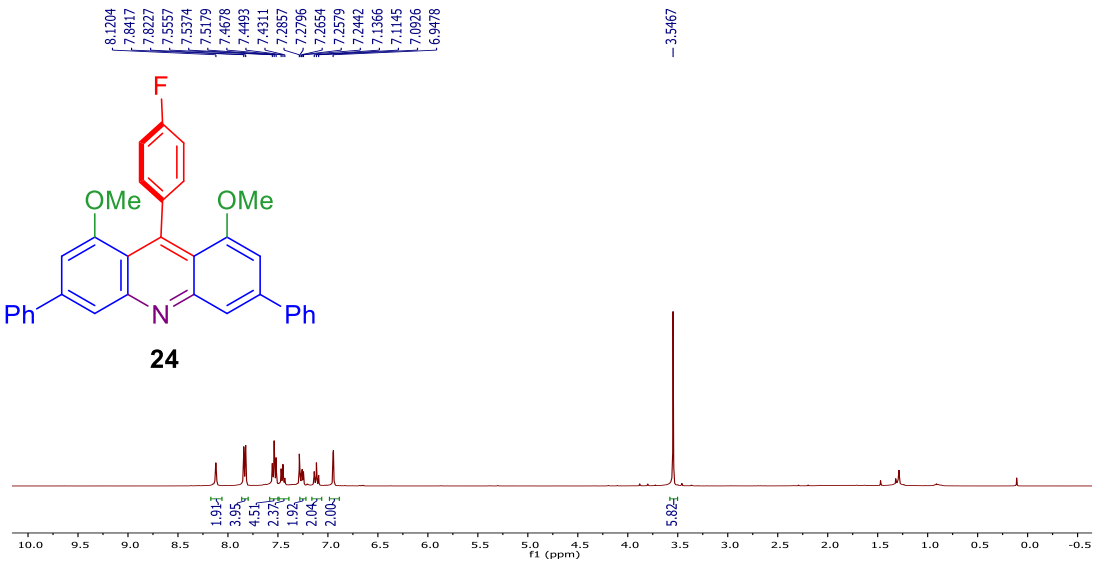

^{1}H NMR ($CDCl_3$, 400 MHz) spectrum of 9-(4-fluorophenyl)-1,8-dimethoxy-3,6-diphenylacridine (24).

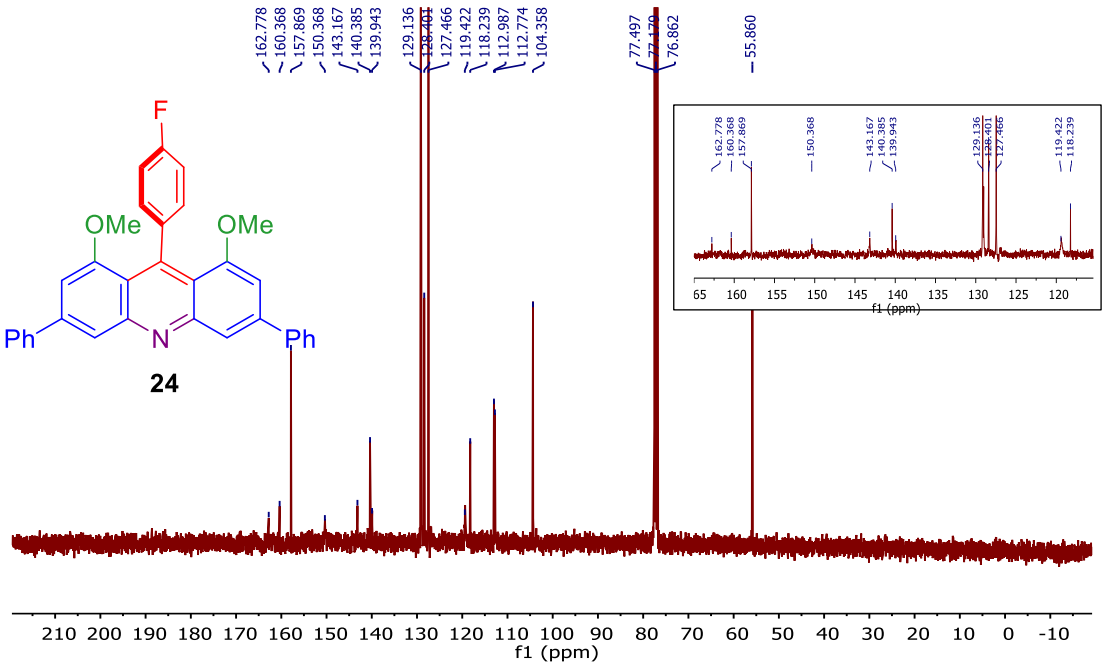

^{13}C NMR ($CDCl_3$, 100 MHz) spectrum of 9-(4-fluorophenyl)-1,8-dimethoxy-3,6-diphenylacridine (24).

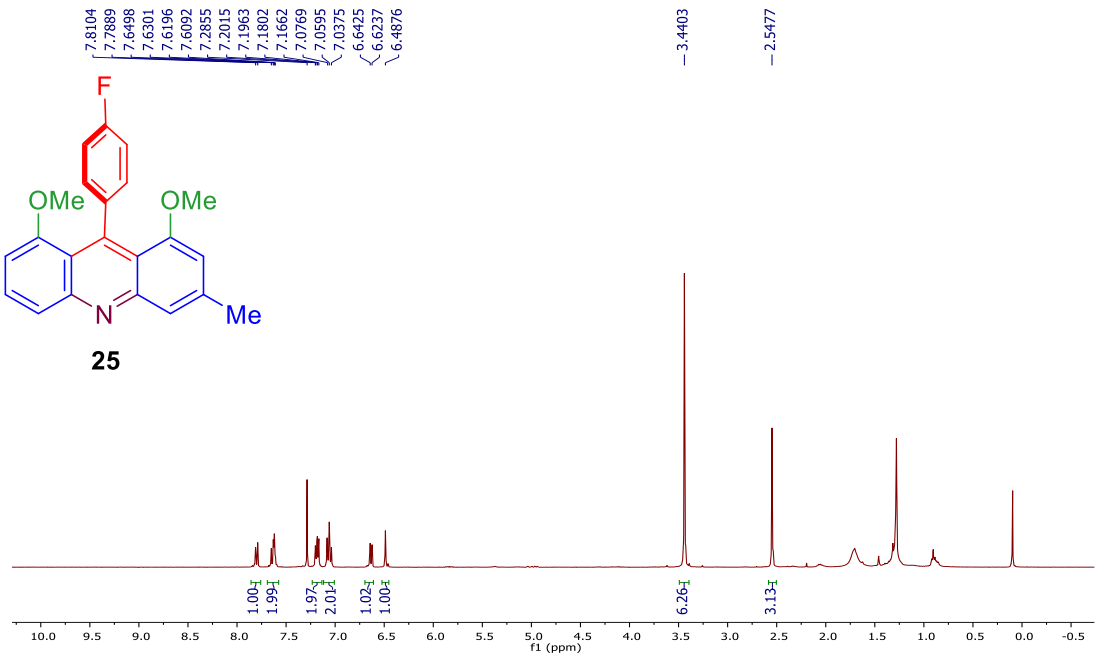

^{1}H NMR ($CDCl_3$, 400 MHz) spectrum of 9-(4-fluorophenyl)-1,8-dimethoxy-3-methylacridine (25).

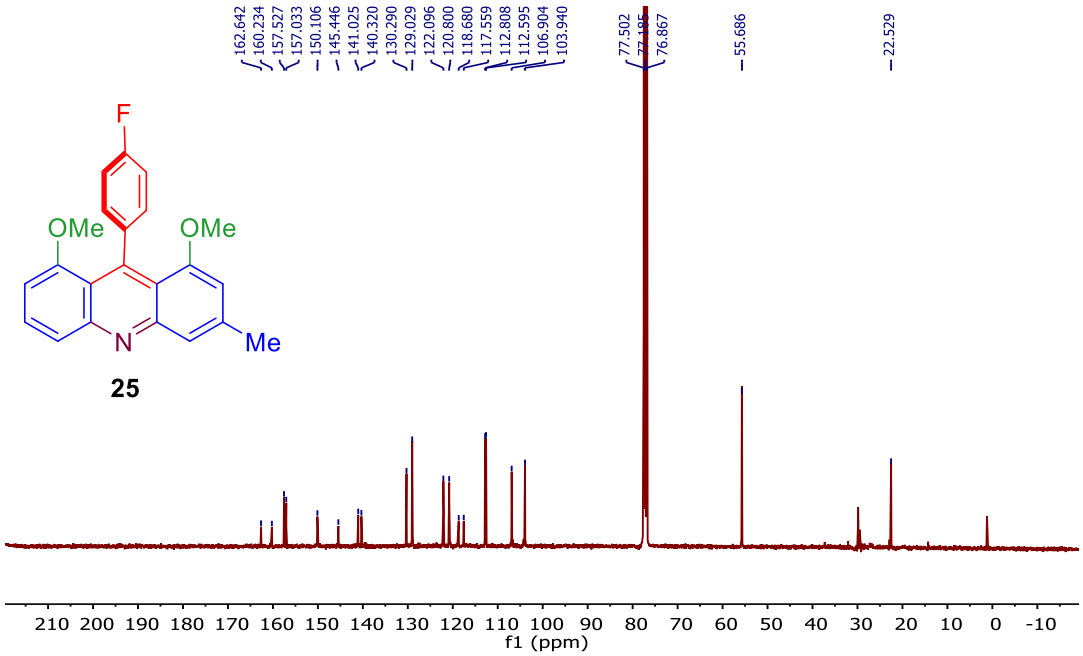

^{13}C NMR ($CDCl_3$, 100 MHz) spectrum of 9-(4-fluorophenyl)-1,8-dimethoxy-3-methylacridine (25)

Chapter-2 Visible light mediated synthesis of quinolin-2(*1H*)-ones from quinoline *N*-oxides

2.1 Introduction.

Quinolin-2(*1H*)-ones and their analogues represent an important class of aza-heterocycles due to their ubiqutousness in pharmaceuticals[1–4] and bioactive natural products[5–7] and their usefulness as intermediates in organic synthesis.[8] Quinolin-2(*1H*)-ones containing scaffolds are one of the very common pharmacophores currently being used for many new drug discovery research. Compounds with quinolone moiety display broad range of intriguing bioactivity as antitumor agents,[9–12] CDK5 inhibitor,[1] endothelin receptor antagoists,[13] angiotensin II receptor antagonists,[14] p38aMAP kinase inhibitors,[15] and antibiotics.[16–18] Many quinolin-2(*1H*)-ones are also frequently used as efficient fluorescent markers[19,20] for peptides, amino polysaccharides, and amino carbohydrates. Due to their practical and industrial utility, chemists have expended considerable effort towards the development of numerous efficient and economic synthetic methods.

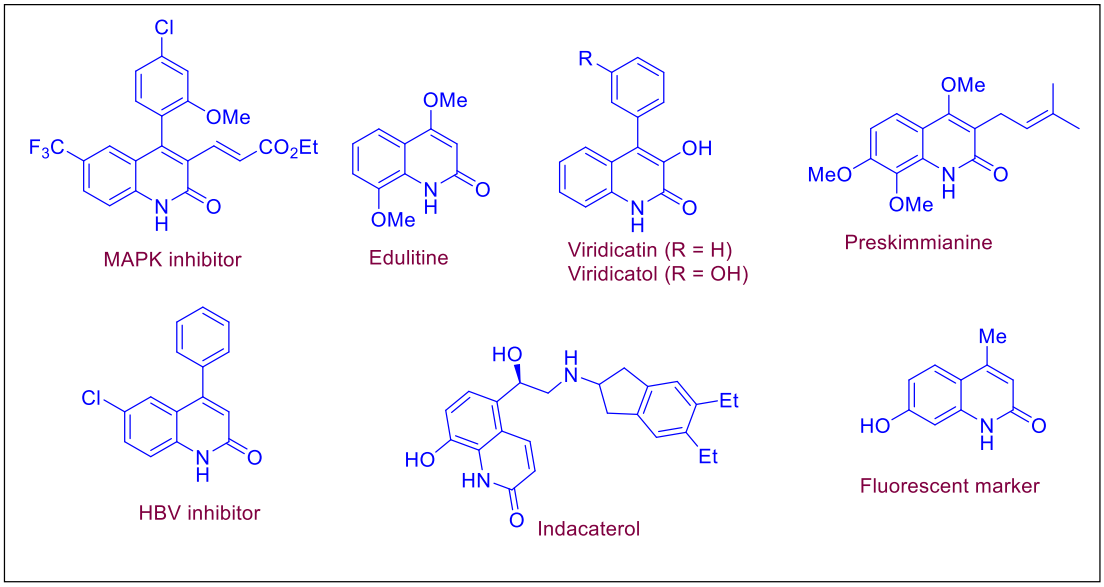

Fig. 2.1 Natural products and bioactive drugs containing a quinoline-2(1H)-one moiety.

All these previous synthetic approaches can be divided into two major categories: (i) through the building of quinolone rings starting from suitably pre-functionalized aromatic precursors[21–24] and (ii) through the ortho-hydroxylation of quinoline *N*-oxides using some suitable activating agents.[25–27] The use of pre-functionalized precursor, generally associated with the inherent difficulty to synthesize, use of transition metals complexes (such as palladium, cobalt, copper and nickel), harsh reaction conditions and sometimes lower yields make the ring construction approach less attractive in terms of sustainability and efficiency. On the other hand, synthesis of quinolin-2(*1H*)-ones from easily accessible *N*-oxides makes the second approach more efficient and cost effective. But these Riessert-Henze type approaches require stoichiometric amount of activating agents such as MsCl, TsCl, PhC(O)Cl, PyBrOP etc., which produces significant amounts of hazardous water-soluble waste. Few early approaches also tried to obtain quinolin-2(*1H*)-ones through high-energy UV-light irradiation on quinoline *N*-oxides to obtain desired 2-quinolones under reagent-free conditions.[28–30] However, the use of high-energy UV-light generates a mixture of products with a very low yield of 2-quinolones and multiple undesirable byproducts as the major components.[31,32] Moreover, due to the use of high energy UV-light these methods are not suitable for UV labile substituents like nitro, carbonyls, alkenes etc. Thus, the harsh reaction conditions, low yield of the desired quinolone in a complex mixture of major byproducts and limited substrate scope, makes this method synthetically unattractive. Therefore, development of a simple, more efficient, mild and ecofriendly synthetic method for quinolin-2(*1H*)-ones bears significant importance. Visible light photoredox catalysis has displayed revolutionary impact in organic synthetic by providing much easier, cleaner and greener alternative to many strategically important conventional organic transformations. Since its initial introduction in organic synthesis a decade ago

through expensive heavy metal complexes as catalyst[33] it has voyaged through an extremely fruitful journey by providing practical and environmental benign solution to numerous difficulties commonly faced in conventional transformations. With time, the visible-light catalysis becoming more mature, greener and sustainable through the application of many more effective, inexpensive and eco-friendly organo-photocatalysts. In this chapter we have described effective use of one such acridinium based organocatalyst, recently developed in our laboratory, for the synthesis of variety of quinolin-2(*1H*)-ones starting from easily accessible quinoline *N*-oxides. Before, going to the discussion of the current work, a brief overview of how visible-light photocatalysis works and review of some important synthetic advancement towards quinolin-2(*1H*)-ones till date have been reviewed to make the discussion more comprehensible.

2.2 A brief introduction of visible-light photocatalysis:

Visible light is a renewable source of energy abundantly available from sun. In nature, plants use the photons energy available from sunlight in photosynthesis for the synthesis of carbohydrates from CO_2 and water. Mimicking such green synthesis have remained a perennial quest for the synthetic chemists. However, most of the common substrates and reagents are capable of absorbing light only in the high energy in the ultra-violet region. Though UV-light has been used for a large number of synthetic transformations earlier, the high energy UV-light are often not compatible with many functional groups and create highly reactive intermediates which ultimately leads to the formation of many byproducts.[31,32] To protect living being or other substance from high energy UV-light, these reactions often need special protective equipments and reaction set-up. The application of visible light in organic synthesis is done through the use of a photocatalysts which can absorb lower-energy photons to assume excited state and can

exchange that energy or electron to organic substrates to invoke selective chemical transformations.[34,35] This capability of exciting selective bonds or group in the organic substrate incapable of absorbing in low energy visible light has revolutionaized the field of organic synthesis by providing a mild, highly tolerant, efficient and greener alternative to many strategically important organic transformations.

Mechanistically these catalytic processes take simple yet intuitive path laid in photochemistry. Upon irradiation of visible light, the photocatalyst goes to the singlet exited state S_1 from singlet ground state S_0. The S_1 state can then either return to ground state S_0 through radiative fluorescence process, or it can go to the triplet exited state T_1 through spin inversion via a nonradiative inter system crossing (ISC) process. The T_1 state can relax to initial state S_0 via a spin-forbidden radiative process known as phosphorescence or it can initiate a photochemical reaction through photoinduced electron transfer (PET) depending on their exited state reduction potential or direct energy transfer (EnT) to the ground-state molecule.

Due to the inverted spin state the excited T_1 state have comparatively higher life-time, which either follow a radiative spin-forbidden phosphorescence process or can initiate a photochemical reaction through photoinduced electron transfer (PET/photoredox) or direct energy transfer (EnT) on collision with suitable substrates.

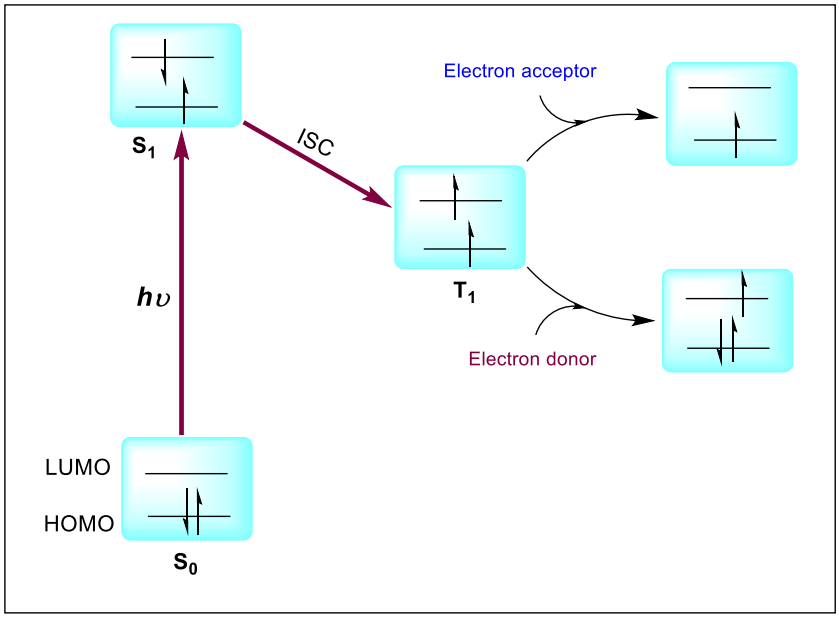

Fig.2.2 Schematic representation of photoinduced electron transfer process.

Most of the photo-redox reactions proceed through one of the two mechanistic way shown in the Fig. 2.3 depending upon the nature of the substrates.[36] In reduction quenching cycle the reduction potential of the exited catalyst $E^{*}_{red}(cat^{*}/cat^{\bullet-})$ must be higher (more positive) than the oxidation potential of the substrate $E_{ox}(sub^{\bullet+}/sub)$, so that it can grab an electron from the substrate. And the reduced form of catalyst later oxidized by the substrate intermediate or by some other oxidizing agent to get back into the initial position of the catalyst. Conversely, in oxidative quenching cycle the oxidation potential of exited photocatalyst $E^{*}_{ox}(cat^{\bullet+}/cat^{*})$ must be lower (more negative) than the reduction potential of substrate $E_{red}(sub/sub^{\bullet-})$. Generally depending on their reduction and oxidation potential in the exited state (**PC***), photocatalysts can grab an electron from the substrate or it can donate an electron to substrate in the quenching step. Later in the generation step photocatalyst gets back to its ground state by taking or donating an electron from the substrate intermediate or some other reagent present in the reaction. In energy transfer mechanism, first the photocatalyst gets

excited by absorbing energy from visible light and then the excited photocatalyst directly transfers this energy to the substrate for the chemical reactions.

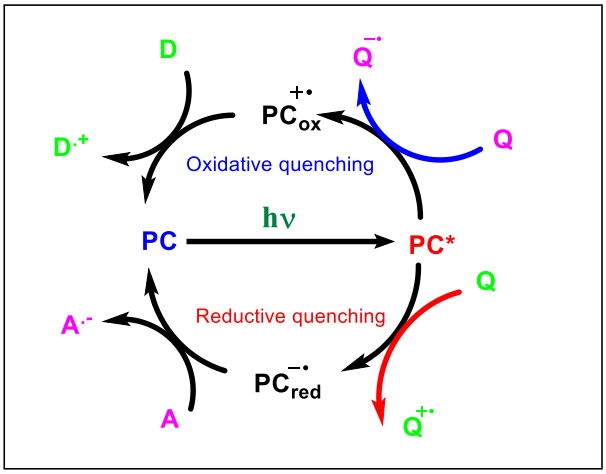

Fig. 2.3 Mechanistic pathways of photo-redox catalysis reaction.

The use of acridinium based organophotocatalysts[37,38] in organic synthesis is gradually becoming more popular compared to the expensive transition metal based photocatalysts because it offers a nontoxic, cost-effective and metal free alternatives. Here we have used one of the most efficient acridinium based photocatalyst (**PC-5**), developed by our group, for above-mentioned reagent-free synthesis of quinoline-2(*1H*)-ones starting from inexpensive and easily obtainable quinoline *N*-oxides.

2.3 Literature Review.

Due to their importance, many methods have been reported for the synthesis of quinolin-2(*1H*)-ones till date using different strategies, starting materials and reagents. Herein, we have discussed about some of the recently reported important synthetic methods by different groups.

Xue-Wei Liu group[39] described a Pd-catalyzed synthesis of quinolin-2(*1H*)-ones using substituted anilines and ethyl acrylates as their starting materials at 100 ^{o}C. In this work the authors proposed a three step C-H activation/C-C bond formation/cyclization cascade mechanism in presence of $Pd(OAc)_2$. In this protocol, after the screening of different oxidants and additives, they found that the combination of $Na_2S_2O_8$ as the terminal oxidant and TsOH. H_2O resulted in the maximum yield. With the help of this methodology, they also synthesized the biological active compound Tipifarnib in just five steps process.

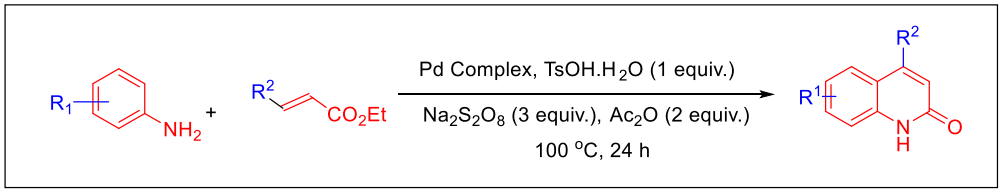

Scheme: 2.1 A synthetic route to 2-quinolines via Pd-catalyzed C-H activation.

An efficient route has been developed for the synthesis of 4-substituted quinoline-2(*1H*)-ones by M. Jeganmohan group[40] using [{$RuCl_2$(p-cymene)}$_2$] as a catalyst at 130 ^{o}C for 24 h. In this methodology, the authors proposed an *ortho*-alkenylation/cyclization mechanism, where in the first step addition of alkenyl group occurred through C-H activation and in the second step intramolecular cyclization happened in presence of carboxylic acid. A further extension of this methodology, a

halogen group was introduced at C-3 position of quinolones by using *N*-bromosuccinimide (NBS) or *N*-chlorosuccinimide (NCS).

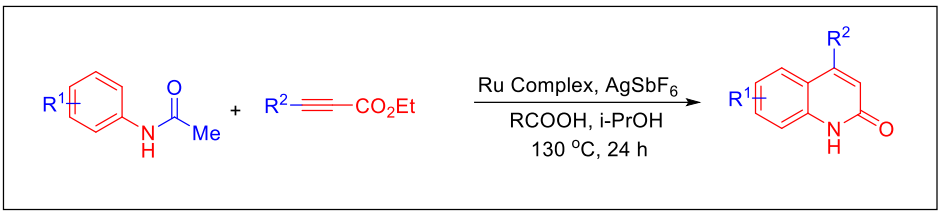

Scheme: 2.2 Ruthenium-catalyzed synthesis of 2-quinolones.

A catalytic synthetic route has been developed for the synthesis of 4-aryl substituted quinoline-2(*1H*)-ones by T. Doi group[41] through an intramolecular C-H amination functionalization process. After the screening of different metal catalysts, the authors found that the combination of $PdCl_2$ and $Cu(OAc)_2$ in catalytic amount resulted the highest yield (88%) in O_2 atmosphere. Although this methodology does not require any reagent for the formation of 2-quinolones but high temperature (120 ^oC) and longer reaction time (14-48 h) decreases the efficiency and substrate scope of this method.

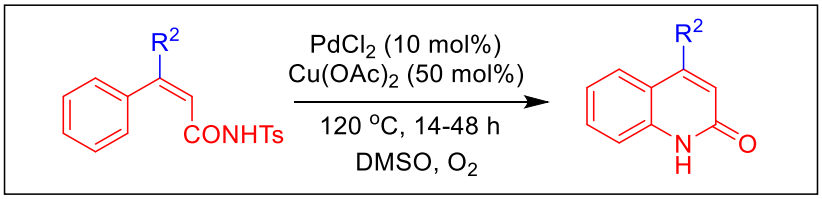

Scheme 2.3 A palladium-catalysed synthetic route to quinoline-2(1H)-ones via an intramolecular amidation reaction.

A cascade synthesis of disubstituted isoquinolin-1(*2H*)-ones has been reported by Y. Zhao group[42] using 2-halobenzamides and β-keto esters in presence of CuI as the catalyst at 80 ^oC temperature. They reported that high reaction temperature is essential for this methodology to get the desired product. The authors also reported that this ligand free methodology enabled to produce different 3,4 substituted isoquinolone derivatives with excellent yields. In this work a series of Cu-catalysts were examined

by the authors and they found that only CuI gave the maximum yield, whereas the other catalysts like CuBr, $CuCl_2$ resulted lower or no yields.

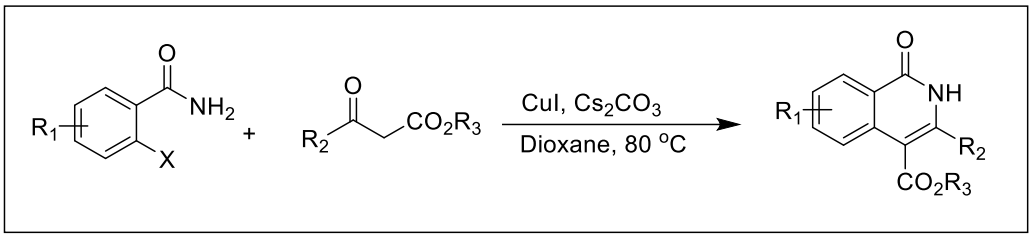

Scheme: 2.4 A one-pot copper catalyzed synthesis of isoquinolin-1(2H)-ones.

Zhaoyan Zheng *et. al.*,[43] in 2008 developed a methodology for the synthesis of substituted isoquinolin-1(*2H*)-ones through cyclization reactions using diethyl(2-iodoaryl)malonates, imidoyl chlorides and carbon monoxide using $Pd(OAc)_2$ as the catalyst. They also reported that the presence of phosphine ligand played a vital role for the formation of the products. After examining a range of phosphine ligands they found that only tri(2,6-dimethoxyphenyl)phosphine (TDMPP) resulted the highest yield (47%). Further, the addition of hindered base *N*,*N*-diisopropylethylamine afforded a little better yield of the product.

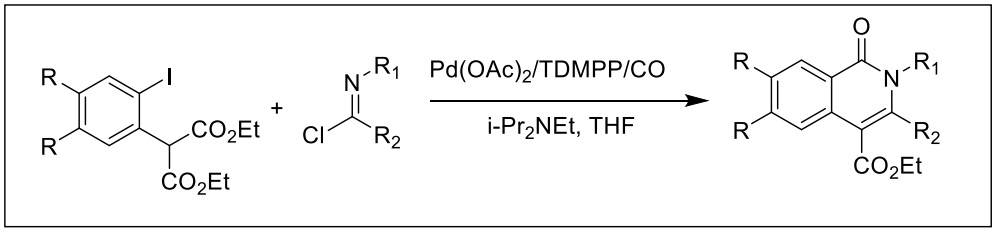

Scheme: 2.5 An efficient Pd-catalyzed route to isoquinolin-1(2H)-ones.

In 2017 Long-Yong Xie *et. al.*,[44] reported a fast synthesis of quinoline-2(*1H*)-ones from quinoline *N*-oxides at room temperature. In this methodology, initially they used TsCl as an activating agent and H_2O as a nucleophile as well as solvent, which resulted 86% yield of the product. Later on, after screening different activating agents such as MsCl,

Ac_2O, PhC(O)Cl, Ms_2O etc. they found that MsCl resulted the highest yield (99%) with least reaction time. A proposed mechanism for the formation of 2-quinolone has been outlined by the authors where quinoline *N*-oxide was first activated by MsCl through the formation of O-S bond and in the next step nucleophilic attack by H_2O to activated *N*-oxide occurred for the formation of 2-hydroxyl quinoline. Though this reaction is quite fast but the use of MsCl in stoichiometric amount produced water soluble hazardous byproduct that makes this methodology less sustainable.

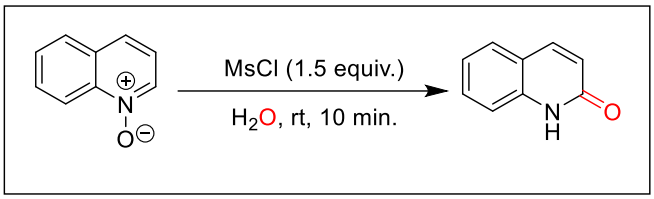

Scheme: 2.6 A fast and aqueous synthesis of quinoline-2(1H)-ones under milder conditions.

A Pd-catalyzed synthesis of quinolin-2(*1H*)-ones has been reported by Xiao-Feng Wu group[45] using quinoline *N*-oxides as a starting material at 120 ^{o}C for 16 h.. The authors examined different Pd(II) catalysts along with DIAD as the optimized activating agent and found that $PdCl_2$ produced the highest yield using acetonitrile as the solvent, while the screening of other metal oxidants such as $Cu(OAc)_2$ and $Mn(OAc)_3.H_2O$ didn't produce satisfactory yields. They also found that the presence of organic oxidants such as DTBP and benzoquinone resulted better yields.

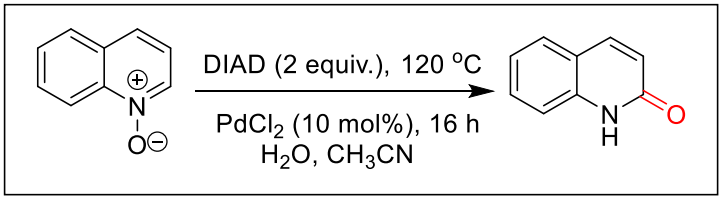

Scheme: 2.7 Palladium-catalyzed synthesis of Quinoline-2(1H)-ones.

A general procedure for the synthesis of hydroxyazines from azine *N*-oxides has been developed by Peng Yu group.[46] In this methodology the authors used phosphonium salt PyBroP as the activating agent for the nucleophilic attack at C-2 position of pyridine. For the hydroxylation initially they have used tetrabutylammonium hydroxide as a base, which resulted trace amount of final product, later on the combination of NaOAc/H_2O enabled to produce the highest yield (80%).

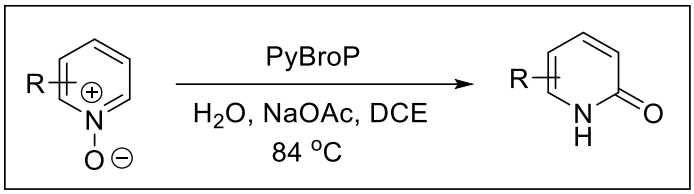

Scheme 2.8 A general synthesis of hydroxyazines from azine N-oxides.

Y. Wu group[25], in the year 2017 developed a methodology for the synthesis of *N*-mehoxyquinolin-2(*1H*)-ones using *N*-methoxyquinoline-1-ium as their staring material in presence of NaOH in dioxane as the solvent. After the screening of different mixed solvent systems, they found that dioxane/H_2O system resulted the maximum yield, whereas the other solvent systems such as DMF/H_2O and CH_3OH/H_2O resulted lower yields.

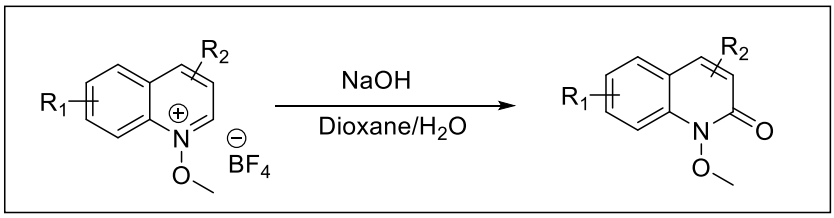

Scheme 2.9 A facile synthesis of N-methoxyquinolin-2(1H)-ones from N-methoxyquinoline-1-ium

.

2.4 Limitations of previous methods:

As mentioned earlier, synthesis of quinolin-2(*1H*)-ones through ring construction mostly required difficult-to-prepare suitably pre-factionalized aromatic systems, suitable co-precursors, heavy metal complex catalyst, additives, high temperature and long reaction time. Moreover, these reactions often involve multiple low yielding reaction steps and thus require more energy, resources and create significant environmental hazards. Conversely, quinolin-2(*1H*)-ones synthesis through Reissert-Henze type of synthesis from quinoline *N*-oxides though much efficient and faster, they require stoichiometric or excess activating agents which ultimately results in generation of considerable water-soluble hazardous byproducts. Therefore, an efficient and greener synthetic protocol for synthesis of quinolin-2(*1H*)-ones is highly desirable. In order to develop a mild eco-friendly synthesis of quinolin-2(*1H*)-ones we anticipated a visible-light catalytic isomerization of quinoline *N*-oxide in reagent-free condition at room temperature. If successful, the reaction can provide a very atom-economic, milder, byproduct-free, greener alternative to all reported synthesis. With that target in mind, we could develop a reagent-free visible-light catalytic synthesis of quinolin-2(*1H*)-ones using very low loading of inexpensive acridinium based organocatalysts.

2.5 Current synthetic scheme:

In this chapter, an efficient, reagent-free visible-light catalytic method has been developed for the synthesis of 2-quinolones/1-isoquinolones from easily available quinoline/isoquinolines *N*-oxides using a newly developed acridinium based organo-photocatalyst **PC-5**. The reaction happens under blue light exposure in very low catalyst loading (0.5 mol%) and DMSO solvent at ambient temperature to generate array of quinolones with up to 95% yield.

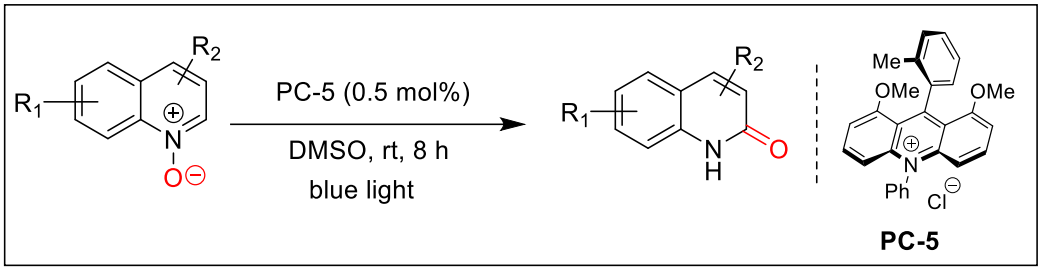

Scheme: 2.10 Schematic representation for the synthesis of quinoline-2(1H)-ones from quinoline N-oxides.

2.6 Results and discussions:

Quinolines are naturally abundant and commercially available compounds. Corresponding *N*-oxides of these quinolines are easily accessible through simple room temperature stirring with inexpensive peroxide reagents. Considering their cheap and easily accessibility we planned our synthesis of quinolin-2(*1H*)-ones using corresponding quinoline *N*-oxides. We started our journey of visible-light photochemical synthesis of quinolin-2(*1H*)-ones by choosing unsubstituted quinoline-*N*-oxide **1a** as our model substrate. To explore the feasibility of the anticipated reaction, we choose an efficient commercially available iridium complex based photocatalyst **PC-1** and acetonitrile as the solvent under blue LED light at room temperature. We were delighted to find that our very first effort successfully resulted in the desired 2-quinolone product **2a** with yield 73% in 8 h. When we tried the reaction in other less polar aprotic solvents like THF, DCM or nonpolar solvents like toluene (Entry 6 and 7, Table 2.1), in all the cases we obtained desired product but with much lower yield compared to the yield obtained in acetonitrile as solvent. Realizing the fact that the lesser yield of the reaction in less polar solvents can also partly be due to the less solubility of highly polar substrate quinoline *N*-oxide **1a,** we tried to conduct the reaction in more polar aprotic and comparatively greener solvent DMSO. To our delight we found for this transformation under same reaction conditions give much better yield (89% yield) compared to acetonitrile (Entry 14, Table 2.1). However, our effort to synthesize the product **2a** in polar protic solvent water failed to produce the product **2a** even after 24 h. Considering the high boiling point, broad range solubility and environment-friendly nature of the solvent, we choose DMSO as the optimized solvent for this photocatalytic transformation. After selecting the optimized solvent, we became interested in selecting the most suitable photocatalyst for the reaction. For optimization

we selected some commercially available expensive heavy metal complex-based catalysts like Ir-photocatalysts **PC-1** and **PC-2**, Ru-photocatalyst **PC-3**, commercially available organophotocatalysts, Fukuzumi catalyst **PC-4** and an organophotocatalyst **PC-5** (Fig. 2.4) developed by our group. After the screening of photocatalysts, the best result was obtained in presence of inexpensive and easily synthesizable acridinium based photocatalyst **PC-5** under the same reaction condition. It was also observed that 0.5 mol% of **PC-5** displayed more effectiveness (Entry 14, Table 2.1) compared to 1

Table 2.1 Optimization of reaction conditions

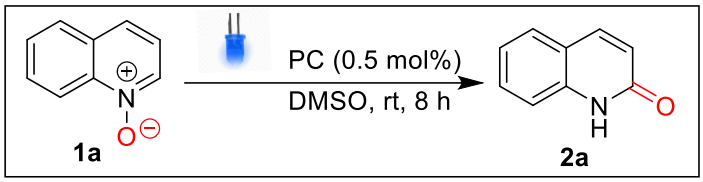

Entry	Catalyst (mol%)	Solvent	Time	Yield (%)
1	PC 1(1 mol%)	CH_3CN	8 h	73
2	PC 1(1 mol%)	DMSO	8 h	82
3	PC 5(1 mol%)	CH_3CN	8 h	81
4	PC 5(1 mol%)	H_2O	24 h	ND
5	PC 5(1 mol%)	MeOH	24 h	trace
6	PC 5(1 mol%)	Toluene	8 h	77
7	PC 5(1 mol%)	DCM	8 h	50
8	PC 5(1 mol%)	DMSO	8 h	90
9	PC 5(0.5 mol%)	DMSO	8 h	89
10	PC 5(0.5 mol%)	DMSO	5 h	65
11	PC 5(0.5 mol%)	DMSO	10 h	89
12	PC 5(0.2 mol%)	DMSO	8 h	50
13	PC 5(0.5 mol%)[a]	DMSO	8 h	86
14	PC 5(0.5 mol%)[b]	DMSO	8 h	89
15	PC 5(1 mol%)[c]	DMSO	24 h	ND
16	-	DMSO	24 h	ND
17	PC 2(1 mol%)	DMSO	8 h	71
18	PC 3(1 mol%)	DMSO	8 h	51
19	PC 4(1 mol%)	DMSO	8 h	54

[a]in presence of O_2, [b]in presence of Argon, [c]in absence of light, ND means not detected

mol% iridium (**PC-1** and **PC-2**) and ruthenium (**PC-3**) based expensive heavy metal complexes or the Fukuzumi catalyst (**PC-4**). Further to confirm the significance of photocatalyst in this methodology, we carried out this reaction in absence of photocatalyst and we observed that no desired product was obtained after 24 h. This confirmed that the photocatalyst is absolutely necessary for the reaction. We also performed the reaction in dark condition in presence of photocatalyst **PC-5** and found that no reaction happened even after 24 h. From these observations we concluded that the presence of blue light is necessary for the activation of photocatalyst.

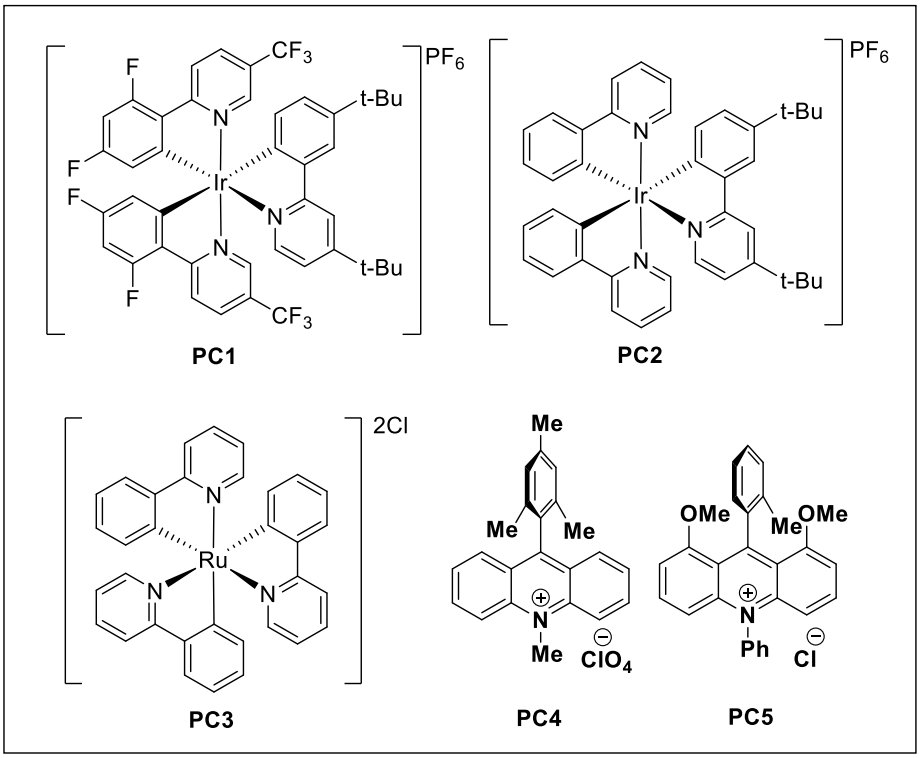

Fig. 2.4 Photocatalysts used for the optimization of reaction.

After optimizing the reaction conditions, we explored the versatility of this methodology using different substituted quinoline and isoquinoline *N*-oxides. The reactions went well with excellent yields irrespective of the electron rich, electron-poor, sterically hindered and the position of the substituents on the substrates. A series of

different functional groups including alkoxy (**9**, **10** and **11**), alkyl (**4**, **5**, **18** and **21**), halides (**3**, **12**, **15**, **16**, **17** and **20**), amide (**19**), hydroxyl (**8**), alkenyl (**7**), ester (**14**) and labile acetal (**6**) groups were compatible with this reaction conditions, which indicates the mildness of this developed methodology. From the obtained yields of the products (Fig. 2.5) it is evident that the steric effect of the substituents seems to play a prominent role compared to the electronic effect on the reaction yield. For example, presence of

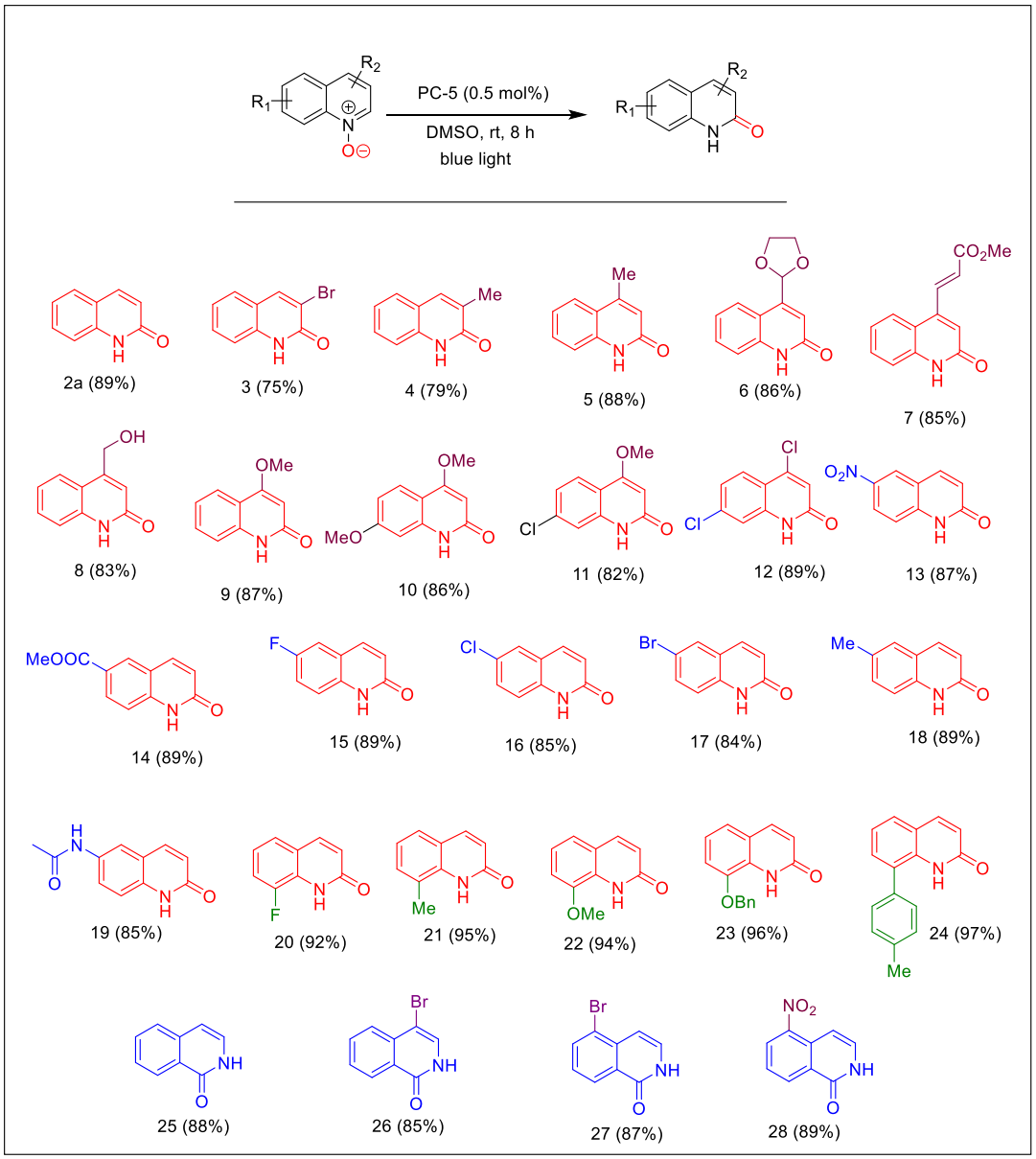

Fig. 2.5 substrate scope for the formation of 2-quinolones.

either of electron donating methyl and electron withdrawing bromine groups at C-3 position resulted almost similar yields of 2-quinolone. All the substituents at C-4 position of quinoline *N*-oxides produced better yields compared to C-3 substituents irrespective of the nature of the substituents. Again, quinoline *N*-oxides with substituents at C-6 were found to produce higher yields compared to the C-3 and C-4. The best yield was obtained in case of substituents at C-8 position of quinoline *N*-oxides and it was also observed that more bulkier substituents like tolyl substituent produced higher yields than the less bulky substituents at same position. The probable reason for higher yield of 8-tolyl quinoline *N*-oxide is due to the close proximity of bulky substituent at peri-position assists in the formation of oxaziridine by pushing *N*-oxide towards C-2. This methodology also worked very well for substituted isoquinoline *N*-oxides with equal efficiency.

To understand the mechanism of the reaction we carried out some controlled experiments. To confirm whether the carbonyl oxygen of our product quinolone is coming from other external sources like water, air, etc., or not; we performed the reaction in anhydrous acetonitrile solvent with different partial pressure of oxygen. In three different vials, same amount of quinoline *N*-oxide was dissolved in an equal amount of dry acetonitrile. The solvent of these vials was then saturated with (i) O_2 gas, (ii) Ar gas and (iii) air with 2 mol% H_2O respectively and we checked the rate of the reactions by NMR spectroscopy and it was found that the argon saturated solution of quinoline *N*-oxide resulted higher reaction rate to that in air with 2% H_2O or O_2 gas saturated dehydrated acetonitrile solution. From the above observations we can easily conclude that the carbonyl oxygen at C-2 position of quinolone is being transferred from *N*-oxide either through intramolecular or intermolecular transformation. To know the intra or intermolecular nature of oxygen atom transfer we performed three different

photo reactions with different concentration of quinoline *N*-oxide in dry acetonitrile using 0.5 mol% of catalyst **PC-5**. The progress of the reactions was checked by ^{1}H NMR spectroscopy at different time intervals. In case of intermolecular oxygen atom transfer process, the higher concentrated solution of **1a** was expected to show the higher

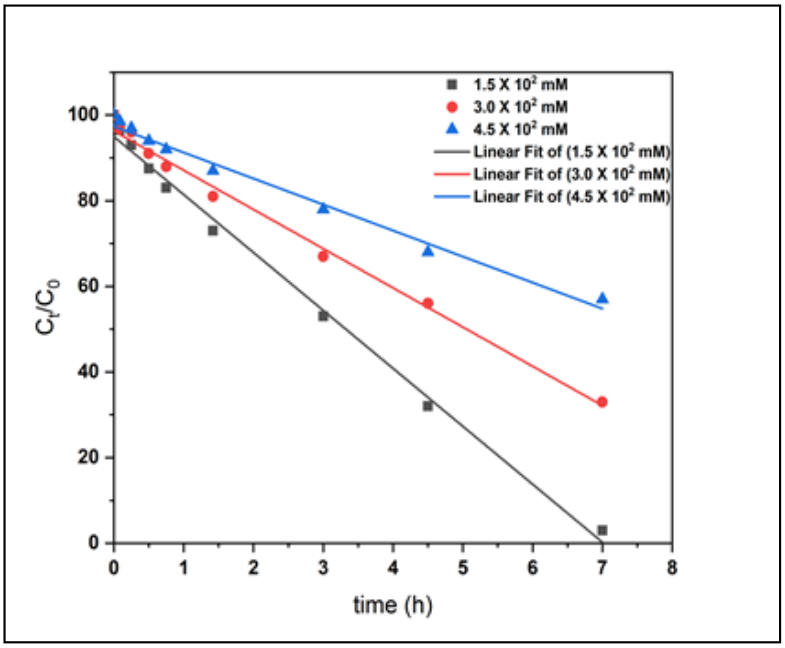

Fig. 2.6 Concentration dependent change in rate of the reaction.

reaction rate as compared to lower concentrated solution of **1a**. On the contrary in our case the solution of lowest concentrated quinoline *N*-oxide was found to give fastest reaction rate with the same reaction conditions (Fig. 2.6). We also checked the absorbance of quinoline *N*-oxide by UV-visible spectrometer and we observed that it has very negligible absorbance in blue light region (400-450 nm) which confirmed that the slow reaction rate of the higher concentrated solution is not due to the less penetration of visible light in presence of 0.5 mol% photocatalyst. From these observations we concluded that the intramolecular oxygen transfer is happening to produce the product quinolin-2(*1H*)-one **2a**. To confirm the nature of the photocatalytic

transformation, whether it occurs through energy transfer (EnT) or single electron transfer (SET) mechanism, we have calculated the excited state redox potential of the catalyst **PC-5** $E^{*}_{red}(cat^{*}/cat^{\bullet-})$ = 1.97 V *vs.* SCE, which is higher than that of the ground state oxidation potential of the quinoline *N*-oxide **1a** $E_{ox}(sub^{\bullet+}/sub)$ = 1.24 V *vs.* SCE. Therefore, the exited photocatalyst **PC-5** can take an electron from the substrate to

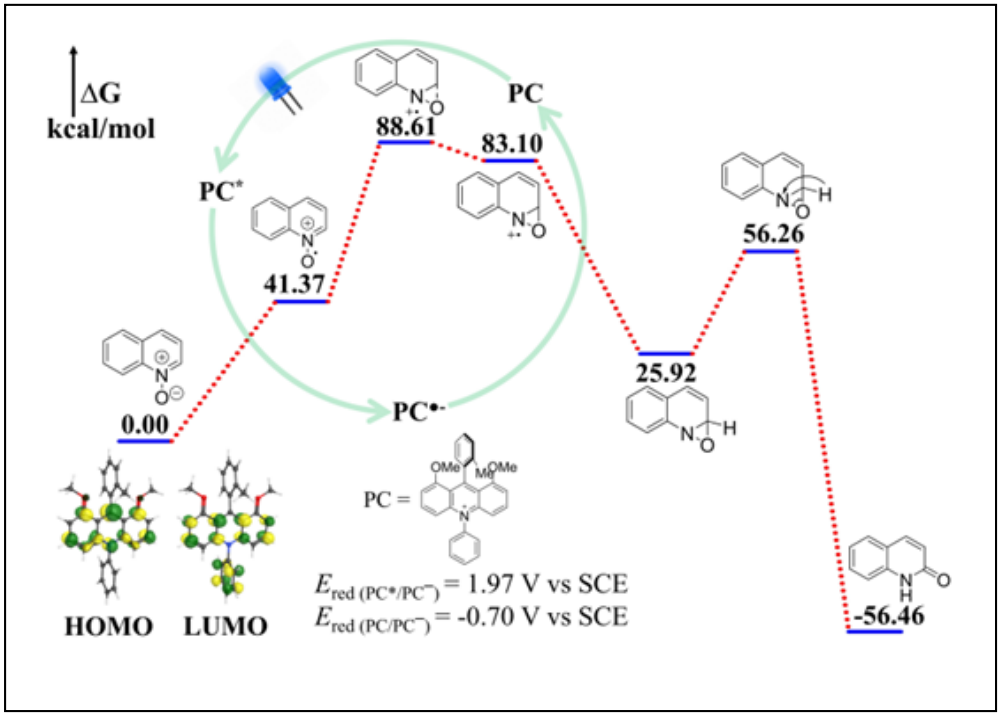

Fig. 2.7 Computed Gibbs free energy profile for photocatalytic synthesis of quinolin-2(1H)-one.

generate a highly unstable quinolinium-oxo radical. We also calculated the triplet state energies of the light absorbing donor **PC-5** (194.9 kJ) and the acceptor **1a** (185.25 kJ), which suggested that there is a possibility of energy transfer from higher triplet energy photocatalyst **PC-5** to lower triplet energy acceptor quinoline *N*-oxide **1a**. But in Dexter energy transfer mechanism, a good overlap between the emission spectra of the donor and the absorption spectra of the acceptor is required, which is absent in our donor and acceptor system. Therefore, a single electron transfer mechanism is more feasible for

this reaction. Unfortunately, the radical trapping experiment by TEMPO during the reaction remained unsuccessful. However, the addition of TEMPO (1 equiv.) was found to competitively inhibit the reaction which resulted only 43% yield of the desired product **2a**.

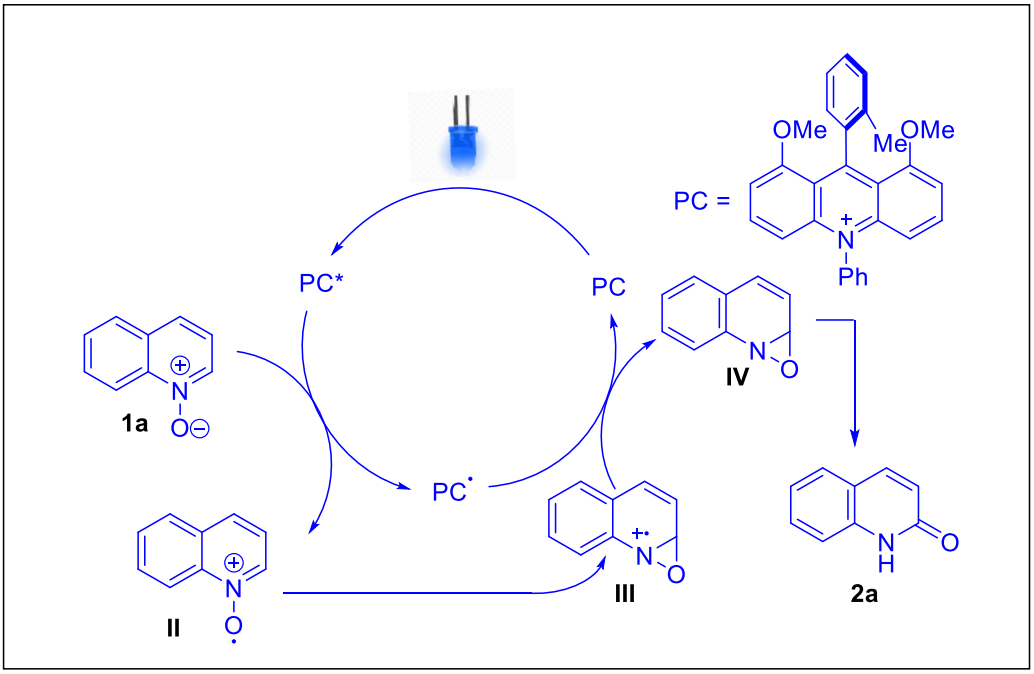

Fig. 2.8 Proposed mechanism for visible light photoredox catalytic synthesis of Quinolin-2(1H)-ones.

Based on the above experimental evidences and TD-DFT Gibb's free energy calculations by Gaussian 16 at M06-2X/6-311G(d,p) level of theory, we proposed a SET mechanism as shown in Fig. 2.8. In presence of visible light, the excited photocatalyst (**PC***) grabs an electron from quinoline *N*-oxide to make it a highly reactive nucleophilic quinolinium *N*-oxo radical, which ultimately resulted in the formation of oxaziridine radical cation ring **III** by attacking the adjacent electrophilic C-2 centre. Then this radical cation **III** accepts an electron from the singly occupied LUMO of the photocatalyst to form a neutral and unstable oxaziridine **IV**. The three membered oxaziridine ring of **IV** finally isomerizes to form a stable amide bond

through simultaneous hydride migration to produce the corresponding quinoline 2(1*H*)-one **2a** as our final product.

2.7 Conclusions

An efficient, eco-friendly and straightforward method has been developed for the synthesis of quinoline-2(*1H*)-ones using visible light. This highly atom-economic and metal-free approach does not require any stoichiometric or excess reagents and consequently does not produce any undesirable byproduct. The milder reaction conditions of this methodology can tolerate labile functional groups as well as protecting groups. Being the only organo-photocatalytic method with a very low catalyst loading, excellent yield and hassle-free clean methodology, it provides a sustainable alternative to all transition-metal/reagent based traditional methods reported so far. The substrate scope of the reaction has been demonstrated through successful conversion of 28 different substituted quinoline/isoquinoline *N*-oxides to corresponding quinolones. Based on the controlled experimental evidences, reduction potential and energy calculation a mechanistic pathway has been proposed for this transformation.

2.8 Experimental Section:

2.8.1 General experimental details:

All commercially available compounds were purchased from Sigma-aldrich, TCI and other commercial suppliers and used as received. NMR spectra were recorded on BRUKER AVANCE III 400 (400 MHz for ^{1}H; 100 MHz for ^{13}C) spectrometer. The chemical shifts are given in parts per million (ppm) relative to $CDCl_3$ (7.28 ppm for ^{1}H and 77.00 for ^{13}C) and DMSO-d_6 (2.49 for ^{1}H and 40.09 for ^{13}C). High resolution mass spectra were recorded on Agilent Technologies, Accurate Mass Q-TOF LC/MS G65208. Normal column chromatography was performed on silica gel (60-120 mesh) purchased from SRL and eluted with petroleum ether and ethyl acetate mixture.

2.8.2 General procedure for the synthesis of substituted quinoline *N*-oxides.

To a 100 mL round bottom flask, corresponding quinoline substrates (5 mmol) and m-chloroperbenzoic acid (7.5 mmol, 1.5 equiv.) were added in 50 mL CH_2Cl_2. The reaction mixture was stirred at room temperature for 10 hours. Upon completion of the reaction, the mixture was extracted with CH_2Cl_2 (20 mL x 3), dried over Na_2SO_4 and concentrated under reduced pressure. The crude product was purified by column chromatography (eluted with 0 to 10 % methanol in chloroform) on silica gel to obtain quinoline *N*-oxides.

2.8.3 General procedure for the synthesis of quinoline-2(*1H*)-one:

A 4 mL screw cap vial with a small magnetic bar was charged with quinoline *N*-oxide (0.4 mmol, 58 mg), 1,8-dimethoxy-10-phenyl-9-(o-tolyl)acridin-10-ium chloride (PC 4, 0.002 mmol, 0.9 mg) and DMSO (3 mL). The vial was then sealed with plastic screw

cap and placed on stirring plate and irradiated with a 40 W blue LED for 8 hours at room temperature. Upon completion of the reaction (as monitored by TLC), the reaction mixture was concentrated under reduced pressure using lyophilizer. The reduced residue was purified by column chromatography (gradient eluent of EtOAc/petroleum ether: 1/2 to 3/1) on silica gel to afford quinolone as a white solid.

2.9 Characterization Data of Compounds:

quinolin-2(1H)-one(2a):

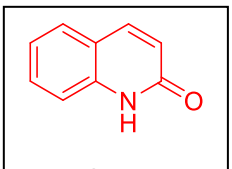

2a

^{1}H NMR (400 MHz, DMSO-d_6) δ 11.87 (s, 1H), 7.89 (d, J = 9.5 Hz, 1H), 7.63 (d, J = 7.7 Hz, 1H), 7.48 (t, J = 7.7 Hz, 1H), 7.34 (d, J = 8.2 Hz, 1H), 7.15 (t, J = 7.5 Hz, 1H), 6.52 (d, J = 9.5 Hz, 1H). ^{13}C NMR (100 MHz, DMSO-d_6) δ 162.45, 140.87, 139.25, 130.85, 128.32, 122.31, 122.09, 119.65, 115.70. HRMS: m/z (ESI) calculated for (C_9H_7NO) $[M+H]^+$: 146.0600, measured: 146.0623.

3-bromoquinolin-2(1H)-one (3):

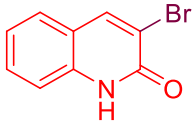

3

^{1}H NMR (400 MHz, DMSO-d_6) δ 12.06 (s, 1H), 8.51 (s, 1H), 7.68 (d, J = 7.7 Hz, 1H), 7.55 (t, J = 8.2 Hz, 1H), 7.34 (d, J = 8.2 Hz, 1H), 7.22 (t, J = 7.5 Hz, 1H). ^{13}C NMR (100 MHz, DMSO-d_6) δ 158.15, 142.18, 138.65, 131.21, 127.80, 122.79, 119.87, 117.55, 115.70. HRMS: m/z (ESI) calculated for (C_9H_6BrNO) $[M+H]^+$: 223.9705 and 225.9685, measured: 223.9682 and 225.9705.

3-methylquinolin-2(1H)-one (4):

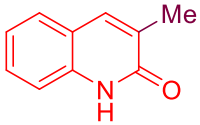

4

^{1}H NMR (400 MHz, Chloroform-d) δ 10.95 (s, 1H), 7.67 (s, 1H), 7.53 (d, J = 7.7 Hz, 1H), 7.47 (t, J = 6.9 Hz, 1H), 7.33 (d, J = 7.4 Hz, 1H), 7.22 (t, J = 7.4 Hz, 1H), 2.31 (s, 3H). ^{13}C NMR (100 MHz, $CDCl_3$) δ 164.14, 137.42, 137.34, 130.21, 129.32, 126.97, 122.49, 120.36, 115.30, 16.80. HRMS: m/z (ESI) calculated for ($C_{10}H_9NO$) $[M+H]^+$: 160.0757, measured: 106.0783.

4-methylquinolin-2(1H)-one (5):

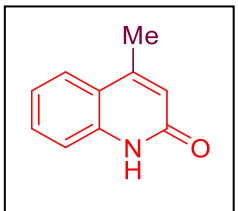

5

^{1}H NMR (400 MHz, Chloroform-*d*) δ 12.88 (s, 1H), 7.68 (d, *J* = 8.0 Hz, 1H), 7.50 (d, *J* = 6.0 Hz, 2H), 7.31 – 7.15 (m, 1H), 6.61 (s, 1H), 2.52 (s, 3H). ^{13}C NMR (100 MHz, $CDCl_3$) δ 164.56, 149.34, 138.29, 130.50, 124.35, 122.49, 120.43, 116.74, 19.19. HRMS: m/z (ESI) calculated for ($C_{10}H_9NO$) $[M+H]^+$: 160.0757, measured: 160.0793.

4-(1,3-dioxolan-2-yl)quinolin-2(1H)-one:

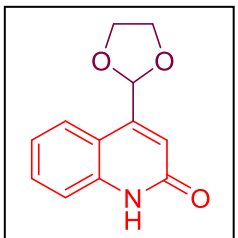

6

^{1}H NMR (400 MHz, Chloroform-*d*) δ 12.45 (s, 1H), 7.94 (d, *J* = 7.7 Hz, 1H), 7.55 (t, *J* = 7.6 Hz, 1H), 7.48 (d, *J* = 7.6 Hz, 1H), 7.31 – 7.24 (m, 1H), 7.00 (s, 1H), 6.30 (s, 1H), 4.15 (s, 4H). ^{13}C NMR (100 MHz, $CDCl_3$) δ 164.32, 147.57, 138.89, 130.63, 125.03, 122.73, 117.96, 117.88, 116.61, 100.25, 65.39. HRMS: m/z (ESI) calculated for ($C_{12}H_{11}NO$) $[M+H]^+$: 218.2315, measured: 218.2297.

methyl (E)-3-(2-oxo-1,2-dihydroquinolin-4-yl)acrylate (7):

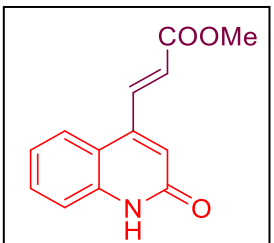

7

^{1}H NMR (400 MHz, Chloroform-*d*) δ 11.54 (s, 1H), 7.59 – 7.51 (m, 2H), 7.40 (d, *J* = 8.1 Hz, 1H), 7.26 – 7.17 (m, 2H), 6.61 (s, 1H), 6.35 (d, *J* = 12.1 Hz, 1H), 3.63 (s, 3H). ^{13}C NMR (100 MHz, $CDCl_3$) δ 165.10, 147.62, 138.33, 138.18, 130.82, 125.16, 125.10, 122.73, 119.53, 118.60, 116.48, 51.68. HRMS: m/z (ESI) calculated for ($C_{13}H_{11}NO_3$) $[M+H]^+$: 230.0812, measured: 230.0823.

4-(hydroxymethyl)quinolin-2(1H)-one (8):

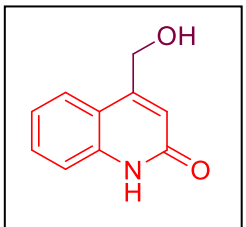

8

^{1}H NMR (400 MHz, DMSO-d_6) δ 11.63 (s, 1H), 7.65 (d, J = 8.1 Hz, 1H), 7.49 (t, J = 7.7 Hz, 1H), 7.32 (d, J = 8.1 Hz, 1H), 7.17 (t, J = 7.6 Hz, 1H), 6.55 (s, 1H), 5.50 (t, J = 5.6 Hz, 1H), 4.76 (d, J = 5.5 Hz, 2H). ^{13}C NMR (100 MHz, DMSO-d_6) δ 162.35, 151.75, 139.16, 130.60, 124.15, 122.04, 117.77, 115.96, 60.02. HRMS: m/z (ESI) calculated for ($C_{10}H_9NO_2$) $[M+H]^+$: 176.0706, measured: 176.0719.

4-methoxyquinolin-2(1H)-one (9):

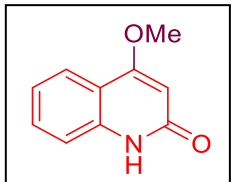

9

^{1}H NMR (400 MHz, Chloroform-d) δ 12.17 (s, 1H), 7.88 (d, J = 7.7 Hz, 1H), 7.51 (t, J = 7.1 Hz, 1H), 7.40 (d, J = 8.2 Hz, 1H), 7.20 (t, J = 7.6 Hz, 1H), 6.04 (s, 1H), 3.97 (s, 3H). ^{13}C NMR (100 MHz, $CDCl_3$) δ 166.27, 165.03, 138.26, 131.18, 122.71, 122.21, 116.12, 115.52, 95.87, 55.98. HRMS: m/z (ESI) calculated for ($C_{10}H_9NO_2$) $[M+H]^+$: 176.0706, measured: 176.0693.

4,7-dimethoxyquinolin-2(1H)-one (10):

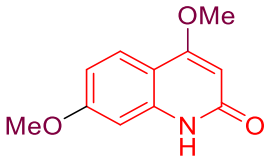

10

^{1}H NMR (400 MHz, DMSO-d_6) δ 11.33 (s, 1H), 7.65 (d, J = 8.8 Hz, 1H), 6.87 (s, 1H), 6.76 (d, J = 7.7 Hz, 1H), 5.73 (s, 1H), 3.89 (s, 3H), 3.79 (s, 3H). ^{13}C NMR (100 MHz, DMSO-d_6) δ 164.18, 163.89, 161.87, 140.89, 124.17, 110.59, 108.79, 98.59, 94.67, 56.44, 55.80. HRMS: m/z (ESI) calculated for ($C_{11}H_{11}NO_3$) $[M+H]^+$: 206.0812, measured: 206.0817.

7-chloro-4-methoxyquinolin-2(1H)-one (11):

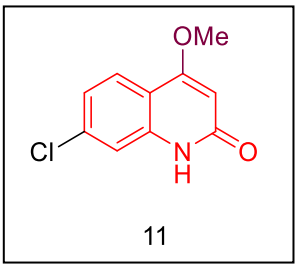

^{1}H NMR (400 MHz, DMSO-d_6) δ 11.57 (s, 1H), 7.75 (d, J = 8.4 Hz, 1H), 7.40 (s, 1H), 7.19 (d, J = 8.1 Hz, 1H), 5.90 (s, 1H), 3.92 (s, 3H). ^{13}C NMR (100 MHz, DMSO-d_6) δ 163.69, 163.16, 139.78, 135.82, 124.69, 122.01, 114.96, 113.86, 97.40, 56.77. HRMS: m/z (ESI) calculated for ($C_{10}H_8ClNO_2$) $[M+H]^+$: 210.0316, measured: 210.0351.

4,7-dichloroquinolin-2(1H)-one (12):

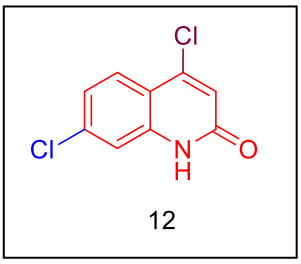

^{1}H NMR (400 MHz, DMSO-d_6) δ 12.07 (s, 1H), 7.81 (d, J = 8.6 Hz, 1H), 7.37 (s, 1H), 7.30 (d, J = 8.6 Hz, 1H), 6.82 (s, 1H). ^{13}C NMR (100 MHz, DMSO-d_6) δ 160.82, 143.97, 139.86, 136.83, 127.04, 123.15, 122.01, 116.58, 115.39. HRMS: m/z (ESI) calculated for ($C_9H_5Cl_2NO$) $[M+H]^+$: 213.9821, measured: 213.9836.

6-nitroquinolin-2(1H)-one (13):

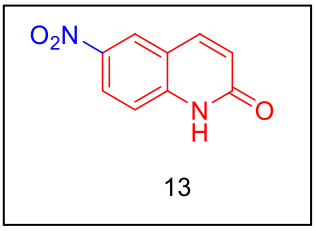

^{1}H NMR (400 MHz, DMSO-d_6) δ 12.32 (s, 1H), 8.63 (s, 1H), 8.27 (d, J = 9.1 Hz, 1H), 8.08 (d, J = 9.6 Hz, 1H), 7.42 (d, J = 9.1 Hz, 1H), 6.64 (d, J = 9.6 Hz, 1H). ^{13}C NMR (100 MHz, DMSO-d_6) δ 162.40, 143.72, 141.85, 140.53, 125.42, 124.70, 124.26, 118.95, 116.52. HRMS: m/z (ESI) calculated for ($C_9H_6N_2O_3$) $[M+H]^+$: 191.0451, measured: 191.0472.

methyl 2-oxo-1,2-dihydroquinoline-6-carboxylate (14):

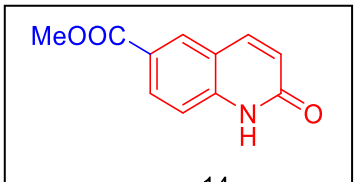

14

^{1}H NMR (400 MHz, DMSO-d_6) δ 12.04 (s, 1H), 8.31 (s, 1H), 8.03 (t, J = 8.6 Hz, 2H), 7.37 (d, J = 8.6 Hz, 1H), 6.57 (d, J = 9.6 Hz, 1H), 3.86 (s, 3H). ^{13}C NMR (100 MHz, DMSO-d_6) δ 166.17, 162.52, 142.59, 140.87, 131.05, 130.37, 123.35, 123.23, 119.14, 115.88, 52.51. HRMS: m/z (ESI) calculated for ($C_{11}H_9NO_3$) $[M+H]^+$: 204.0655, measured: 204.0643.

6-fluoroquinolin-2(1H)-one (15):

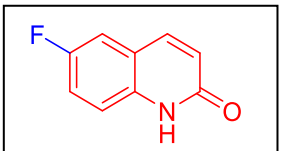

15

^{1}H NMR (400 MHz, DMSO-d_6) δ 11.84 (s, 1H), 7.89 (d, J = 9.6 Hz, 1H), 7.55 (dd, J = 9.2, 2.8 Hz, 1H), 7.41 (td, J = 8.8, 2.8 Hz, 1H), 7.32 (dd, J = 9.0, 4.9 Hz, 1H), 6.57 (d, J = 9.6 Hz, 1H). ^{13}C NMR (100 MHz, DMSO-d_6) δ 162.11, 158.52, 156.16, 139.90, 136.04, 123.66, 120.16, 118.95, 118.71, 117.39, 113.22, 112.99. HRMS: m/z (ESI) calculated for (C_9H_6FNO) $[M+H]^+$: 164.0506, measured: 164.0492.

6-chloroquinolin-2(1H)-one (16):

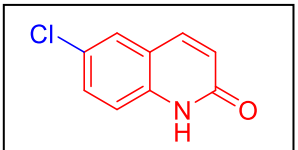

16

^{1}H NMR (400 MHz, DMSO-d_6) δ 11.90 (s, 1H), 7.87 (d, J = 9.6 Hz, 1H), 7.77 (s, 1H), 7.52 (d, J = 8.8 Hz, 1H), 7.30 (d, J = 8.8 Hz, 1H), 6.56 (d, J = 9.6 Hz, 1H). ^{13}C NMR (100 MHz, DMSO-d_6) δ 162.17, 139.66, 138.04, 130.66, 127.33, 126.01,

123.63, 120.71, 117.43. HRMS: m/z (ESI) calculated for (C_9H_6ClNO) $[M+H]^+$: 180.0211, measured: 180.0219.

6-bromoquinolin-2(1H)-one (17):

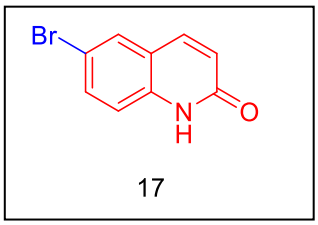

17

^{1}H NMR (400 MHz, DMSO-d_6) δ 11.85 (s, 1H), 7.92 (s, 1H), 7.88 (d, J = 9.6 Hz, 1H), 7.64 (d, J = 10.9 Hz, 1H), 7.26 (d, J = 8.8 Hz, 1H), 6.55 (d, J = 9.6 Hz, 1H). ^{13}C NMR (100 MHz, DMSO-d_6) δ 162.07, 139.58, 138.42, 133.31, 130.35, 123.61, 121.28, 117.73, 113.76. HRMS: m/z (ESI) calculated for (C_9H_6BrNO) $[M+H]^+$: 223.9705 and 225.9685, measured: 223.9718 and 225.9691

6-methylquinolin-2(1H)-one (18):

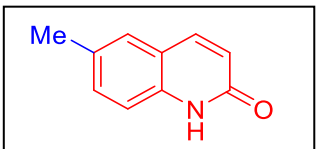

18

^{1}H NMR (400 MHz, Chloroform-d) δ 12.26 (s, 1H), 7.79 (d, J = 9.5 Hz, 1H), 7.37 (d, J = 8.7 Hz, 3H), 6.72 (d, J = 9.5 Hz, 1H), 2.44 (s, 3H). ^{13}C NMR (100 MHz, $CDCl_3$) δ 164.39, 140.87, 136.40, 132.31, 132.10, 127.39, 121.24, 119.92, 115.99, 20.91. HRMS: m/z (ESI) calculated for ($C_{10}H_9NO$) $[M+H]^+$: 160.0757, measured: 160.0762.

N-(2-oxo-1,2-dihydroquinolin-6-yl)acetamide (19):

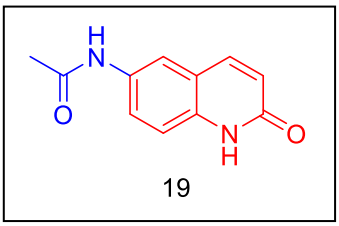

^{1}H NMR (400 MHz, DMSO-d_6) δ 11.66 (s, 1H), 9.99 (s, 1H), 7.97 (s, 1H), 7.86 (d, J = 9.6 Hz, 1H), 7.56 (d, J = 8.8 Hz, 1H), 7.24 (d, J = 8.8 Hz, 1H), 6.48 (s, 1H), 2.05 (s, 3H). ^{13}C NMR (100 MHz, DMSO-d_6) δ 168.62, 162.09, 140.56, 135.38, 134.01, 123.23, 122.72, 119.48, 117.61, 115.84, 24.31. HRMS: m/z (ESI) calculated for ($C_{11}H_{10}N_2O_2$) $[M+H]^+$: 203.0815, measured: 203.0821.

8-fluoroquinolin-2(1H)-one (20):

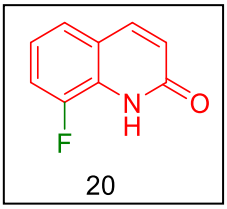

^{1}H NMR (400 MHz, Chloroform-d) δ 10.56 (s, 1H), 7.79 (d, J = 10.7 Hz, 1H), 7.37 (d, J = 7.9 Hz, 1H), 7.33 – 7.25 (m, 1H), 7.21 – 7.12 (m, 1H), 6.76 (d, J = 9.6 Hz, 1H). ^{13}C NMR (100 MHz, $CDCl_3$) δ 162.62, 150.59, 148.14, 140.11, 127.32, 123.29, 123.20, 122.15, 121.51, 115.65, 115.48. HRMS: m/z (ESI) calculated for (C_9H_6FNO) $[M+H]^+$: 164.0506, measured: 164.0513.

8-methylquinolin-2(1H)-one (21):

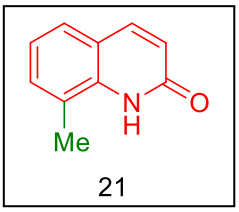

^{1}H NMR (400 MHz, Chloroform-d) δ 10.02 (s, 1H), 7.79 (d, J = 9.5 Hz, 1H), 7.44 (d, J = 7.8 Hz, 1H), 7.37 (d, J = 7.3 Hz, 1H), 7.14 (t, J = 7.6 Hz, 1H), 6.69 (d, J = 9.5 Hz, 1H), 2.54 (s, 3H). ^{13}C NMR (100 MHz, $CDCl_3$) δ 163.45, 141.35, 136.88, 131.84, 126.09, 123.23, 122.29, 121.40, 119.70, 16.86. HRMS: m/z (ESI) calculated for ($C_{10}H_9NO$) $[M+H]^+$: 160.0757, measured: 160.0781.

8-methoxyquinolin-2(1H)-one (22):

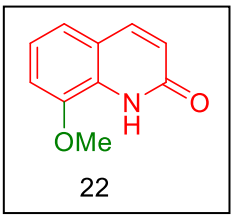

^{1}H NMR (400 MHz, Chloroform-*d*) δ 9.43 (s, 1H), 7.74 (d, *J* = 9.5 Hz, 1H), 7.22 – 7.08 (m, 2H), 6.99 (d, *J* = 9.1 Hz, 1H), 6.68 (d, *J* = 9.5 Hz, 1H), 3.99 (s, 3H). ^{13}C NMR (100 MHz, $CDCl_3$) δ 162.15, 145.56, 140.46, 128.54, 122.53, 122.21, 120.01, 119.58, 110.16, 56.02. HRMS: m/z (ESI) calculated for ($C_{10}H_9NO_2$) $[M+H]^+$: 176.0706, measured: 176.0716.

8-(benzyloxy)quinolin-2(1H)-one (23):

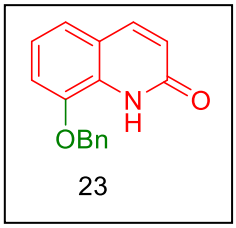

^{1}H NMR (400 MHz, Chloroform-*d*) δ 9.28 (s, 1H), 7.76 (d, *J* = 9.6 Hz, 1H), 7.51 – 7.36 (m, 5H), 7.19 (d, *J* = 6.7 Hz, 1H), 7.14 (t, *J* = 7.8 Hz, 1H), 7.08 (d, *J* = 9.0 Hz, 1H), 6.69 (d, *J* = 9.6 Hz, 1H), 5.21 (s, 2H). ^{13}C NMR (100 MHz, $CDCl_3$) δ 162.03, 144.61, 140.46, 135.61, 128.85, 127.89, 122.60, 122.20, 120.19, 119.87, 111.45, 71.06. HRMS: m/z (ESI) calculated for ($C_{16}H_{13}NO_2$) $[M+H]^+$: 252.1019, measured: 252.1030.

8-(p-tolyl)quinolin-2(1H)-one (24):

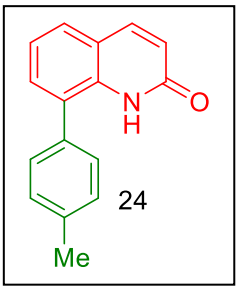

^{1}H NMR (400 MHz, Chloroform-*d*) δ 8.85 (s, 1H), 7.83 (d, *J* = 9.6 Hz, 1H), 7.57 (d, *J* = 6.8 Hz, 1H), 7.44 (d, *J* = 7.4 Hz, 1H), 7.39 – 7.24 (m, 5H), 6.67 (d, *J* = 9.6 Hz, 1H), 2.47 (s, 3H). ^{13}C NMR (100 MHz, $CDCl_3$) δ 162.45, 141.00, 138.66, 135.43, 132.82, 131.40, 130.28, 129.07, 128.73, 127.26, 122.41, 121.81, 120.00, 21.21. HRMS: m/z (ESI) calculated for ($C_{16}H_{13}NO$) $[M+H]^+$: 236.1070, measured: 236.1052.

isoquinolin-1(2H)-one (25):

25

^{1}H NMR (400 MHz, Chloroform-*d*) δ 11.08 (s, 1H), 8.44 (d, *J* = 8.1 Hz, 1H), 7.71 (t, *J* = 7.5 Hz, 1H), 7.60 (d, *J* = 7.8 Hz, 1H), 7.54 (t, *J* = 7.6 Hz, 1H), 7.20 (d, *J* = 7.0 Hz, 1H), 6.61 (d, *J* = 7.1 Hz, 1H). ^{13}C NMR (100 MHz, $CDCl_3$) δ 164.20, 138.11, 132.76, 127.49, 127.35, 126.91, 126.27, 126.03, 106.89. HRMS: m/z (ESI) calculated for (C_9H_7NO) $[M+H]^+$: 146.0600, measured: 146.0989.

4-bromoisoquinolin-1(2H)-one (26):

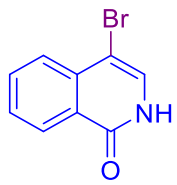

26

^{1}H NMR (400 MHz, DMSO-d_6) δ 11.56 (s, 1H), 8.24 (d, *J* = 7.7 Hz, 1H), 7.87 (t, *J* = 7.7 Hz, 1H), 7.77 (d, *J* = 8.0 Hz, 1H), 7.61 (t, *J* = 7.6 Hz, 1H), 7.55 (s, 1H). ^{13}C NMR (100 MHz, DMSO-d_6) δ 161.45, 136.15, 133.95, 130.58, 128.09, 127.87, 126.93, 125.82, 98.02. HRMS: m/z (ESI) calculated for (C_9H_6BrNO) $[M+H]^+$: 223.9705 and 225.9685, measured: 223.9699 and 225.9707

5-bromoisoquinolin-1(2H)-one (27):

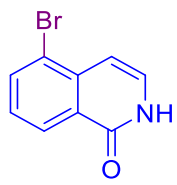

27

^{1}H NMR (400 MHz, Chloroform-*d*) δ 11.32 (s, 1H), 8.48 – 8.37 (m, 1H), 7.96 (d, *J* = 7.8 Hz, 1H), 7.38 (t, *J* = 7.9 Hz, 1H), 7.31 – 7.24 (m, 1H), 6.97 (d, *J* = 7.4 Hz, 1H). ^{13}C NMR (100 MHz, DMSO-d_6) δ 162.65, 137.25, 137.09, 130.26, 128.21, 127.04, 126.92, 120.57,

104.98. HRMS: m/z (ESI) calculated for (C_9H_6BrNO) $[M+H]^+$: 223.9705 and 225.9685, measured: 223.9723 and 225.9689

5-nitroisoquinolin-1(2H)-one (28):

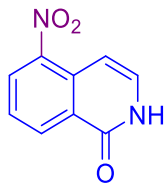

28

^{1}H NMR (400 MHz, DMSO-d_6) δ 12.32 (s, 1H), 8.63 (s, 1H), 8.27 (d, J = 9.1 Hz, 1H), 8.08 (d, J = 9.6 Hz, 1H), 7.42 (d, J = 9.1 Hz, 1H), 6.64 (d, J = 9.6 Hz, 1H). ^{13}C NMR (100 MHz, DMSO-d_6) δ 162.40, 143.72, 141.85, 140.53, 125.42, 124.70, 124.26, 118.95, 116.52. HRMS: m/z (ESI) calculated for ($C_9H_6N_2O_3$) $[M+H]^+$: 191.0451, measured: 191.0432.

References

(1) Zhong, W.; Liu, H.; Kaller, M. R.; Henley, C.; Magal, E.; Nguyen, T.; Osslund, T. D.; Powers, D.; Rzasa, R. M.; Wang, H.-L.; Wang, W.; Xiong, X.; Zhang, J.; Norman, M. H. Design and Synthesis of Quinolin-2(1H)-One Derivatives as Potent CDK5 Inhibitors. *Bioorg. Med. Chem. Lett.* **2007**, *17* (19), 5384–5389.

(2) Konecny, G. E.; Winterhoff, B.; Guorong, E. Y.; Qi, J.; Le, J.; Shi, M.; Dugan, M.; Linnartz, R.; Finn, R. S.; Slamon, D. J. Abstract 3589: Dovitinib (TKI258), a Multikinase Inhibitor of FGFR, PDGFR, and VEGFR Tyrosine Kinases, Induces Growth Inhibition in Endometrial Carcinoma Cells. *Cancer Res.* **2011**, *71* (8_Supplement), 3589.

(3) Beattie, D.; Beer, D.; Bradley, M. E.; Bruce, I.; Charlton, S. J.; Cuenoud, B. M.; Fairhurst, R. A.; Farr, D.; Fozard, J. R.; Janus, D.; Rosethorne, E. M.; Sandham, D. A.; Sykes, D. A.; Trifilieff, A.; Turner, K. L.; Wissler, E. An Investigation into the Structure–Activity Relationships Associated with the Systematic Modification of the B2-Adrenoceptor Agonist Indacaterol. *Bioorg. Med. Chem. Lett.* **2012**, *22* (19), 6280–6285.

(4) Weiss, J.; Theile, D.; Dvorak, Z.; Haefeli, W. E. Interaction Potential of the Multitargeted Receptor Tyrosine Kinase Inhibitor Dovitinib with Drug Transporters and Drug Metabolising Enzymes Assessed in Vitro. *Pharmaceutics* **2014**, *6* (4), 632–650.

(5) Simonetti, S. O.; Larghi, E. L.; Kaufman, T. S. The 3,4-Dioxygenated 5-Hydroxy-4-Aryl-Quinolin-2(1H)-One Alkaloids. Results of 20 Years of Research, Uncovering a New Family of Natural Products. *Nat. Prod. Rep.* **2016**, *33* (12), 1425–1446.

(6) Mou, X.-F.; Liu, X.; Xu, R.-F.; Wei, M.-Y.; Fang, Y.-W.; Shao, C.-L. Scopuquinolone B, a New Monoterpenoid Dihydroquinolin-2(1H)-One Isolated from the Coral-Derived Scopulariopsis Sp. Fungus. *Nat. Prod. Res.* **2018**, *32* (7), 773–776.

(7) Chung, H. S.; Woo, W. S. A Quinolone Alkaloid with Antioxidant Activity from the Aleurone Layer of Anthocyanin-Pigmented Rice. *J. Nat. Prod.* **2001**, *64* (12), 1579–1580.

(8) Chilin, A.; Marzano, C.; Baccichetti, F.; Simonato, M.; Guiotto, A. 4-Hydroxymethyl- and 4-Methoxymethylfuro[2,3-h]Quinolin-2(1H)-Ones: Synthesis and Biological Properties. *Bioorg. Med. Chem.* **2003**, *11* (7), 1311–1318.

(9) End, D. W.; Smets, G.; Todd, A. V.; Applegate, T. L.; Fuery, C. J.; Angibaud, P.; Venet, M.; Sanz, G.; Poignet, H.; Skrzat, S.; Devine, A.; Wouters, W.; Bowden, C. Characterization of the Antitumor Effects of the Selective Farnesyl Protein Transferase Inhibitor R115777 in Vivo and in Vitro. *Cancer Res.* **2001**, *61* (1), 131–137.

(10) Chen, Y.-L.; Chung, C.-H.; Chen, I.-L.; Chen, P.-H.; Jeng, H.-Y. Synthesis and Cytotoxic Activity Evaluation of Indolo-, Pyrrolo-, and Benzofuro-Quinolin-2(1H)-Ones and 6-Anilinoindoloquinoline Derivatives. *Bioorg. Med. Chem.* **2002**, *10* (8), 2705–2712.

(11) Angibaud, P. R.; Venet, M. G.; Filliers, W.; Broeckx, R.; Ligny, Y. A.; Muller, P.; Poncelet, V. S.; End, D. W. Synthesis Routes Towards the Farnesyl Protein Transferase Inhibitor ZARNESTRATM. *Eur. J. Org. Chem.* **2004**, *2004* (3), 479–486.

(12) Kraus, J. M.; Verlinde, C. L. M. J.; Karimi, M.; Lepesheva, G. I.; Gelb, M. H.; Buckner, F. S. Rational Modification of a Candidate Cancer Drug for Use Against Chagas Disease. *J. Med. Chem.* **2009**, *52* (6), 1639–1647.

(13) Mederski, W. W. K. R.; Osswald, M.; Dorsch, D.; Christadler, M.; Schmitges, C.-J.; Wilm, C. 1,4-Diaryl-2-Oxo-1,2-Dihydro-Quinoline-3-Carboxylic Acids as Endothelin Receptor Antagonists. *Bioorg. Med. Chem. Lett.* **1997**, *7* (14), 1883–1886.

(14) W. K. R. Mederski, W.; Beier, N.; Labitzke, E.; Radunz, H.-E.; Rauschenbach-Ruess, K.; Schneider, B. Synthesis of 7-Ethyl-1,2-Dihydroquinolin-2-Ones as Angiotensin II Receptor Antagonists. *HETEROCYCLES* **1994**, *39* (1), 117.

(15) Peifer, C.; Urich, R.; Schattel, V.; Abadleh, M.; Röttig, M.; Kohlbacher, O.; Laufer, S. Implications for Selectivity of 3,4-Diarylquinolinones as P38αMAP Kinase Inhibitors. *Bioorg. Med. Chem. Lett.* **2008**, *18* (4), 1431–1435.

(16) Anderson, M. E.; Mazur, A.; Yang, T.; Roden, D. M. Potassium Current Antagonist Properties and Proarrhythmic Consequences of Quinolone Antibiotics. *J. Pharmacol. Exp. Ther.* **2001**, *296* (3), 806–810.

(17) Heeb, S.; Fletcher, M. P.; Chhabra, S. R.; Diggle, S. P.; Williams, P.; Cámara, M. Quinolones: From Antibiotics to Autoinducers. *FEMS Microbiol. Rev.* **2011**, *35* (2), 247–274.

(18) Khamkhenshorngphanuch, T.; Kulkraisri, K.; Janjamratsaeng, A.; Plabutong, N.; Thammahong, A.; Manadee, K.; Na Pombejra, S.; Khotavivattana, T. Synthesis and Antimicrobial Activity of Novel 4-Hydroxy-2-Quinolone Analogs. *Molecules* **2020**, *25* (13), 3059.

(19) Kovalska, V. B.; Volkova, K. D.; Manaev, A. V.; Losytskyy, M. Yu.; Okhrimenko, I. N.; Traven, V. F.; Yarmoluk, S. M. 2-Quinolone and Coumarin Polymethines for the Detection of Proteins Using Fluorescence. *Dyes Pigments* **2010**, *84* (2), 159–164.

(20) Chen, Y.; Wei, X.-R.; Sun, R.; Xu, Y.-J.; Ge, J.-F. The Fluorescent Biomarkers for Lipid Droplets with Quinolone-Coumarin Unit. *Org. Biomol. Chem.* **2018**, *16* (41), 7619–7625.

(21) Li, X.; Li, X.; Jiao, N. Rh-Catalyzed Construction of Quinolin-2 (1 H)-Ones via C–H Bond Activation of Simple Anilines with CO and Alkynes. *J. Am. Chem. Soc.* **2015**, *137* (29), 9246–9249.

(22) Zhu, F.; Li, Y.; Wang, Z.; Wu, X.-F. Iridium-Catalyzed Carbonylative Synthesis of Halogen-Containing Quinolin-2 (1H)-Ones from Internal Alkynes and Simple Anilines. *Adv. Synth. Catal.* **2016**, *358* (21), 3350–3354.

(23) Bellam, M.; Gundluru, M.; Sarva, S.; Chadive, S.; Netala, V. R.; Tartte, V.; Cirandur, S. R. Synthesis and Antioxidant Activity of Some New N-Alkylated Pyrazole-Containing Benzimidazoles. *Chem. Heterocycl. Compd.* **2017**, *53* (2), 173–178.

(24) Kim, J.; Moon, Y.; Lee, S.; Hong, S. A Pd-Catalyzed One-Pot Dehydrogenative Aromatization and Ortho-Functionalization Sequence of N-Acetyl Enamides. *Chem. Commun.* **2014**, *50* (24), 3227–3230.

(25) Gao, X.; Liang, A.; Li, J.; Zou, D.; Wu, Y.; Wu, Y. A Facile and Environmental Friendly Strategy for the Synthesis of N-Methoxyquinolin-2(1H)-Ones. *Tetrahedron Lett.* **2017**, *58* (20), 1917–1920.

(26) Jeong, H. J.; Chae, S.; Jeong, K.; Namgoong, S. K. The Diverse One-Pot Reactions of 2-Quinolylzincates: Homologation, Electrophilic Trapping, Hydroxylation, and Arylation Reactions. *Eur. J. Org. Chem.* **2018**, *2018* (45), 6343–6349.

(27) DeRuiter, J.; Brubaker, A. N.; Whitmer, W. L.; Stein, J. L. Synthesis and Aldose Reductase Inhibitory Activity of Substituted 2-Oxoquinoline-1-Acetic Acid Derivatives. *J. Med. Chem.* **1986**, *29* (10), 2024–2028.

(28) Ishikawa, M.; Yamada, S.; Hotta, H.; Kaneko, C. Photochemistry of the N-Oxides of Azanaphthalene and Their Substituted Derivatives. *Chem. Pharm. Bull. (Tokyo)* **1966**, *14* (10), 1102–1107.

(29) Kaneko, C.; Yamada, Sa.; Yokoe, I.; Ishikawa, M. Structures of the Stable Photo-Products Derived from Quinoline 1-Oxides and Quinoxaline 1-Oxides. *Tetrahedron Lett.* **1967**, *8* (20), 1873–1877.

(30) Kaneko, C.; Yokoe, I.; Ishikawa, M. Photochemical Reaction of 2-Cyanoquinoline 1-Oxides with Amines: A New Approach to N-Aminocarbostyrils. *Tetrahedron Lett.* **1967**, *8* (51), 5237–5240.

(31) Buchardt, O.; Kumler, P. L.; Lohse, C.; Theander, O.; Lindberg, A. A.; Jansen, G.; Lamm, B.; Samuelsson, B. Photochemical Studies. XIII. The Liquid Phase Photolysis of Quinoline N-Oxides Unsubstituted in the 2-Position. *Acta Chem. Scand.* **1969**, *23*, 159–170.

(32) Buchardt, O.; Jensen, B.; Larsen, I. K.; Levstek, I.; Eržen, V.; Blinc, R.; Paušak, S.; Ehrenberg, L.; Dumanović, J. Photochemical Studies. VIII. The Formation of Benz[d]-1,3-Oxazepines in the Photolysis of Quinoline N-Oxides in Solution. *Acta Chem. Scand.* **1967**, *21*, 1841–1854.

(33) Prier, C. K.; Rankic, D. A.; MacMillan, D. W. C. Visible Light Photoredox Catalysis with Transition Metal Complexes: Applications in Organic Synthesis. *Chem. Rev.* **2013**, *113* (7), 5322–5363.

(34) Tucker, J. W.; Stephenson, C. R. J. Shining Light on Photoredox Catalysis: Theory and Synthetic Applications. *J. Org. Chem.* **2012**, *77* (4), 1617–1622.

(35) Xuan, J.; Xiao, W.-J. Visible-Light Photoredox Catalysis. *Angew. Chem. Int. Ed.* **2012**, *51* (28), 6828–6838.

(36) Zeitler, K. Photoredox Catalysis with Visible Light. *Angew. Chem. Int. Ed.* **2009**, *48* (52), 9785–9789.

(37) Romero, N. A.; Nicewicz, D. A. Organic Photoredox Catalysis. *Chem. Rev.* **2016**, *116* (17), 10075–10166.

(38) Ravelli, D.; Dondi, D.; Fagnoni, M.; Albini, A. Photocatalysis. A Multi-Faceted Concept for Green Chemistry. *Chem. Soc. Rev.* **2009**, *38* (7), 1999–2011.

(39) Wu, J.; Xiang, S.; Zeng, J.; Leow, M.; Liu, X.-W. Practical Route to 2-Quinolinones via a Pd-Catalyzed C–H Bond Activation/C–C Bond Formation/Cyclization Cascade Reaction. *Org. Lett.* **2015**, *17* (2), 222–225.

(40) Manikandan, R.; Jeganmohan, M. Ruthenium-Catalyzed Cyclization of Anilides with Substituted Propiolates or Acrylates: An Efficient Route to 2-Quinolinones. *Org. Lett.* **2014**, *16* (13), 3568–3571.

(41) Inamoto, K.; Saito, T.; Hiroya, K.; Doi, T. Palladium-Catalyzed Intramolecular Amidation of C(Sp2)−H Bonds: Synthesis of 4-Aryl-2-Quinolinones. *J. Org. Chem.* **2010**, *75* (11), 3900–3903.

(42) Wang, F.; Liu, H.; Fu, H.; Jiang, Y.; Zhao, Y. An Efficient One-Pot Copper-Catalyzed Approach to Isoquinolin-1(2 *H*)-One Derivatives. *Org. Lett.* **2009**, *11* (11), 2469–2472.

(43) Zheng, Z.; Alper, H. Palladium-Catalyzed Carbonylation−Decarboxylation of Diethyl(2-Iodoaryl)Malonates with Imidoyl Chlorides: An Efficient Route to Substituted Isoquinolin-1(2 *H*)-Ones. *Org. Lett.* **2008**, *10* (21), 4903–4906.

(44) Xie, L.-Y.; Duan, Y.; Lu, L.-H.; Li, Y.-J.; Peng, S.; Wu, C.; Liu, K.-J.; Wang, Z.; He, W.-M. Fast, Base-Free and Aqueous Synthesis of Quinolin-2 (1H)-Ones under Ambient Conditions. *ACS Sustain. Chem. Eng.* **2017**, *5* (11), 10407–10412.

(45) Peng, J.-B.; Chen, B.; Qi, X.; Ying, J.; Wu, X.-F. Palladium-Catalyzed Synthesis of Quinolin-2 (1 H)-Ones: The Unexpected Reactivity of Azodicarboxylate. *Org. Biomol. Chem.* **2018**, *16* (10), 1632–1635.

(46) Wang, D.; Zhao, J.; Wang, Y.; Hu, J.; Li, L.; Miao, L.; Feng, H.; Désaubry, L.; Yu, P. A General and Efficient Synthesis of 2-Pyridones, 2-Quinolinones, and 1-Isoquinolinones from Azine *N* -Oxides. *Asian J. Org. Chem.* **2016**, *5* (12), 1442–1446.

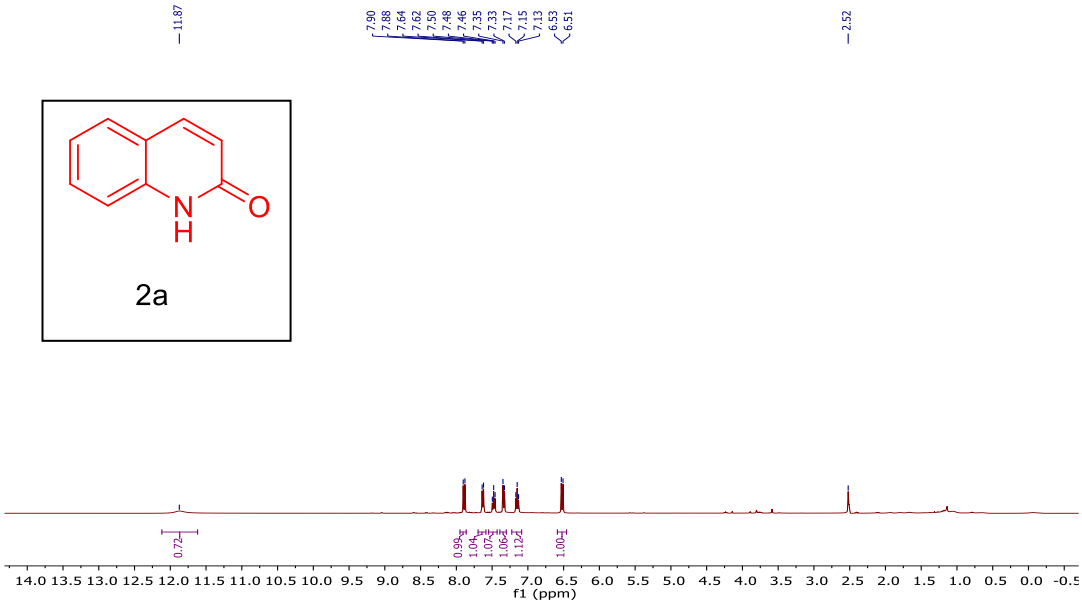

^{1}H NMR ($CDCl_3$, 400 MHz) spectrum of **quinolin-2(1H)-one (2a).**

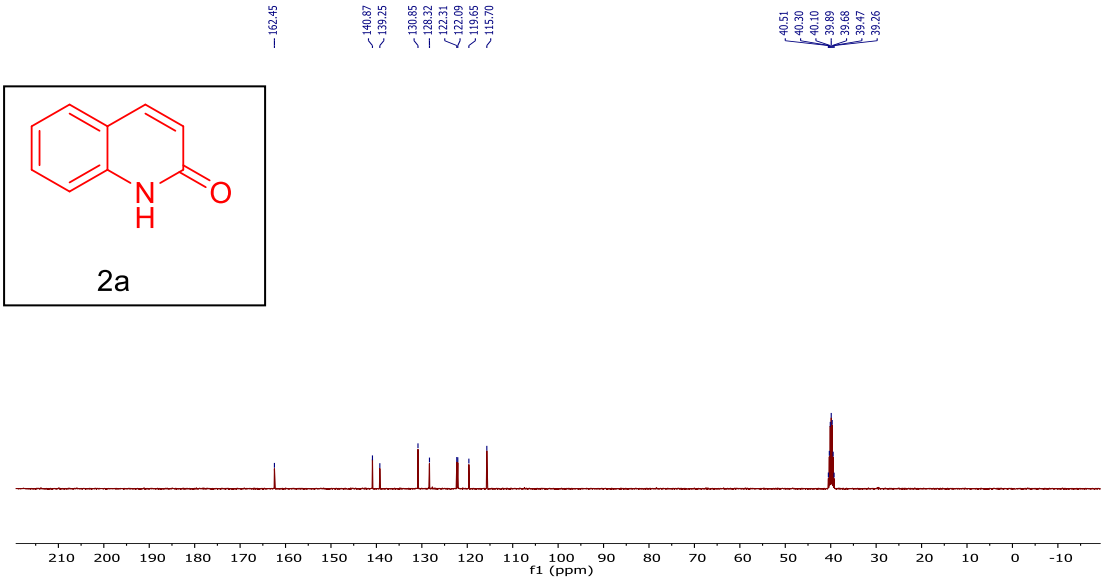

^{13}C NMR ($CDCl_3$, 100 MHz) spectrum of **quinolin-2(1H)-one (2a).**

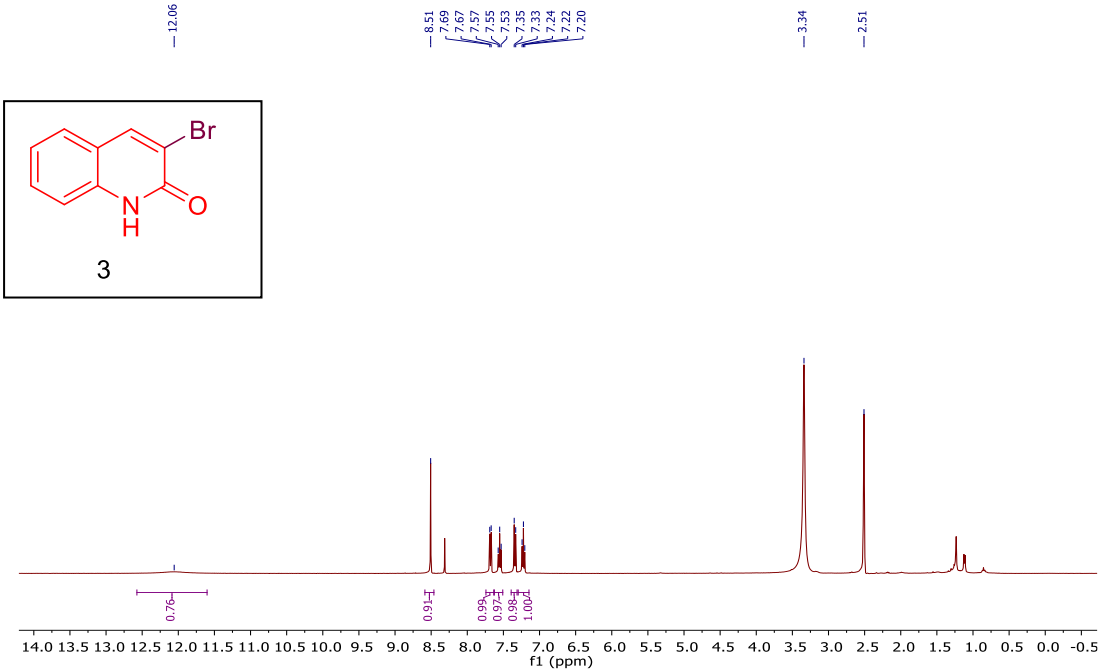

^{1}H NMR (DMSO-d$_6$, 400 MHz) spectrum of **3-bromoquinolin-2(1H)-one (3).**

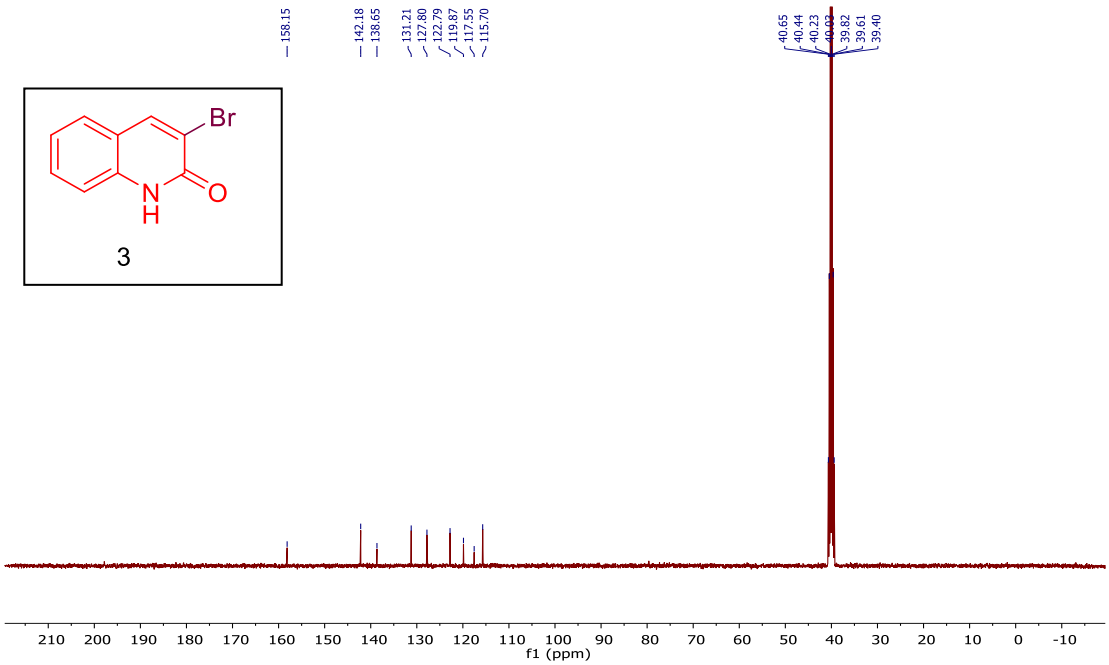

^{13}C NMR (DMSO-d$_6$, 100 MHz) spectrum of **3-bromoquinolin-2(1H)-one (3).**

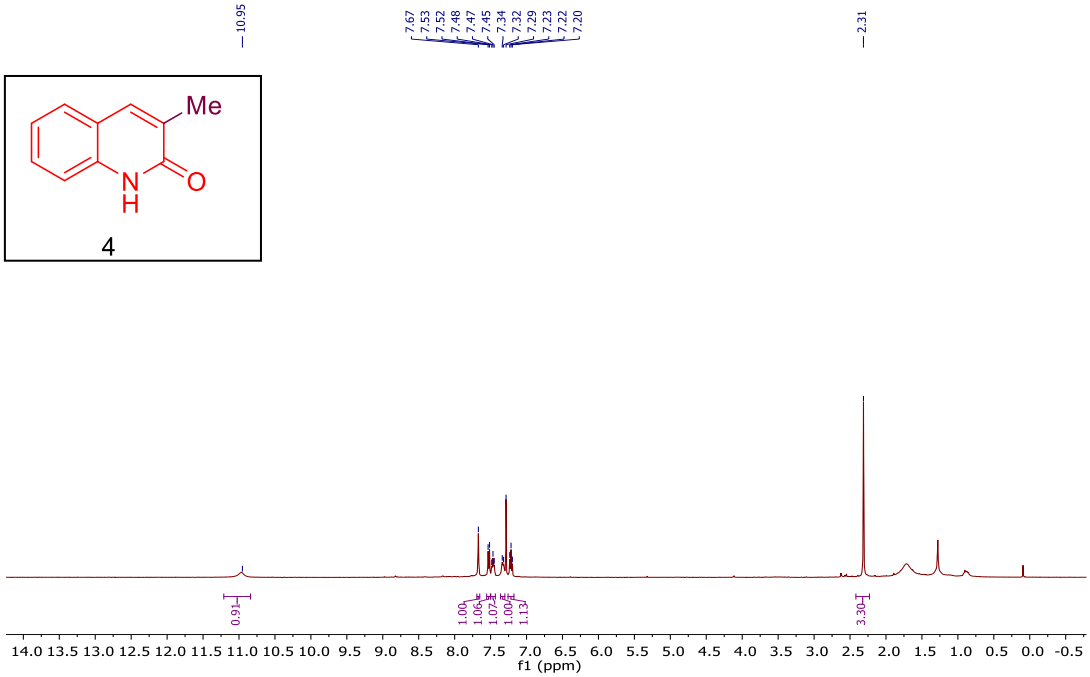

^{1}H NMR ($CDCl_3$, 400 MHz) spectrum of **3-methylquinolin-2(1H)-one (4).**

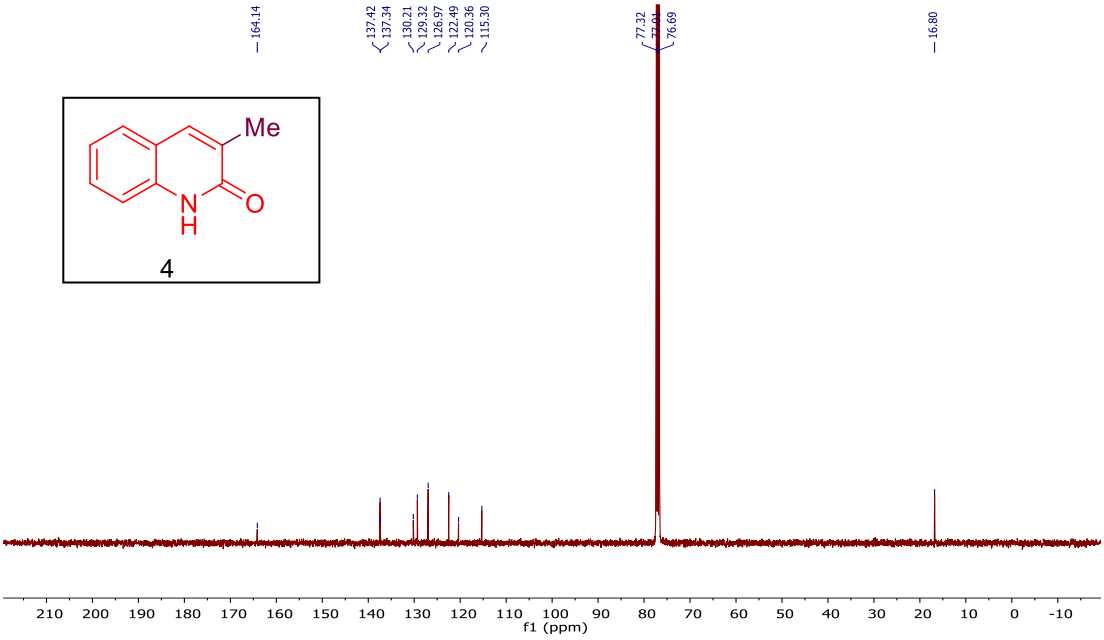

^{13}C NMR ($CDCl_3$, 100 MHz) spectrum of **3-methylquinolin-2(1H)-one (4).**

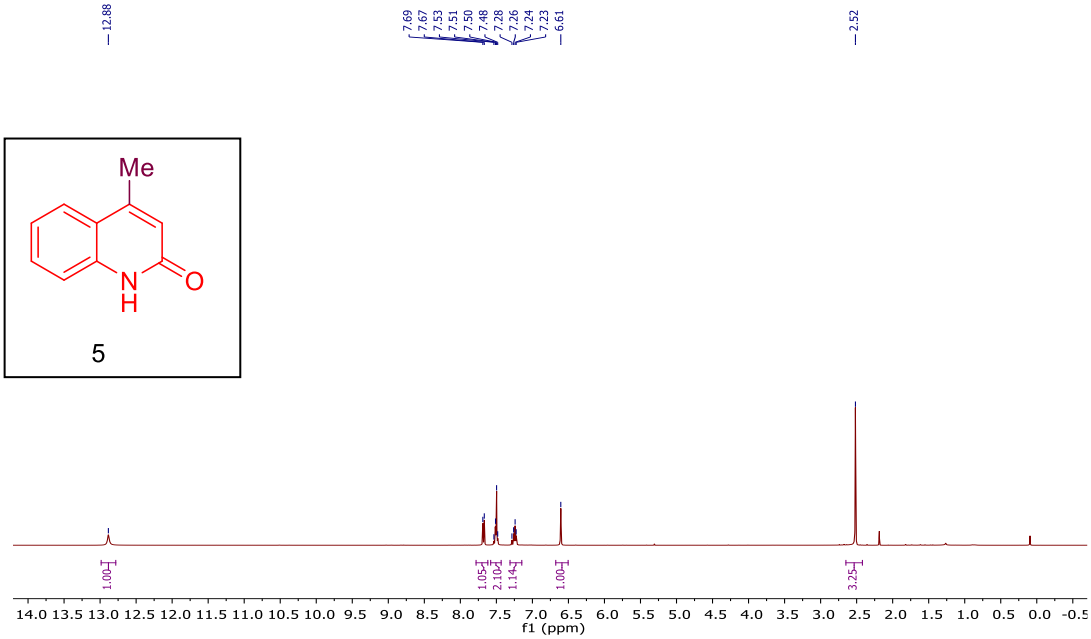

^{1}H NMR ($CDCl_3$, 400 MHz) spectrum of **4-methylquinolin-2(1H)-one (5).**

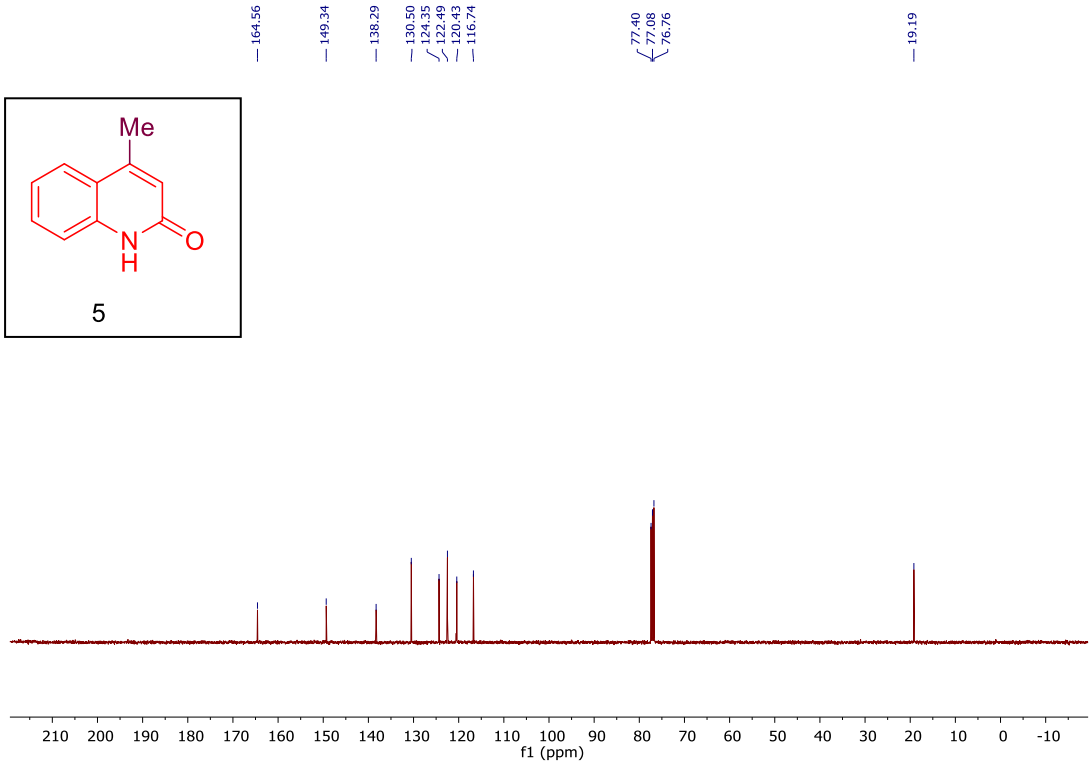

^{13}C NMR ($CDCl_3$, 100 MHz) spectrum of **4-methylquinolin-2(1H)-one (5).**

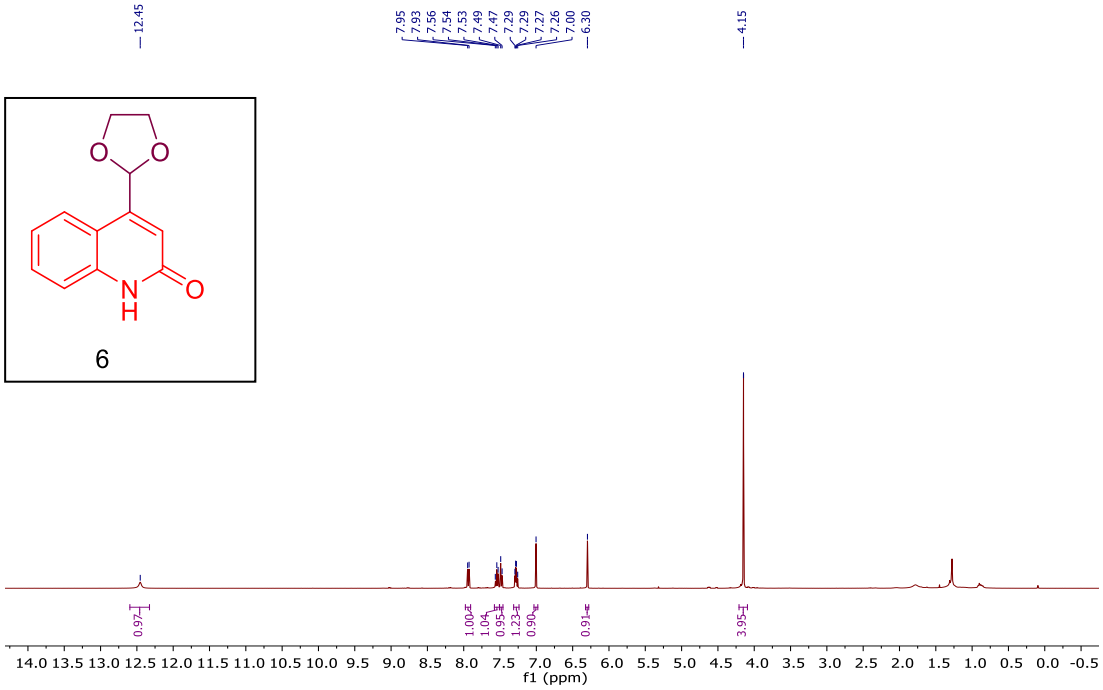

^{1}H NMR ($CDCl_3$, 400 MHz) spectrum of **4-(1,3-dioxolan-2-yl)quinolin-2(1H)-one (6).**

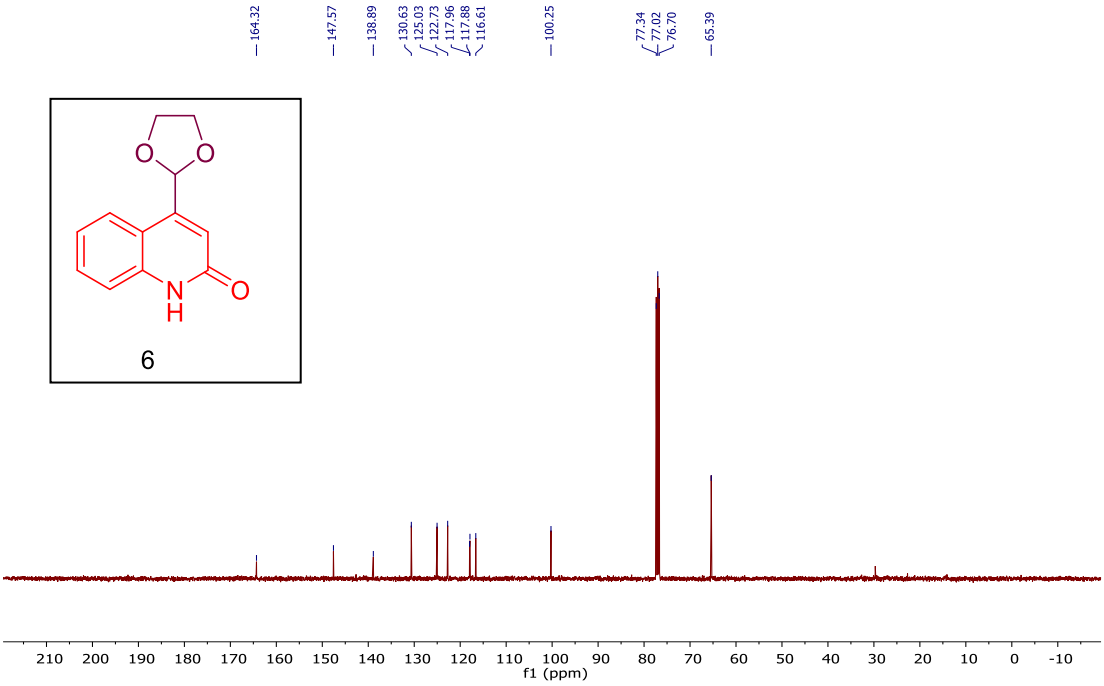

^{13}C NMR ($CDCl_3$, 100 MHz) spectrum of **4-(1,3-dioxolan-2-yl)quinolin-2(1H)-one (6).**

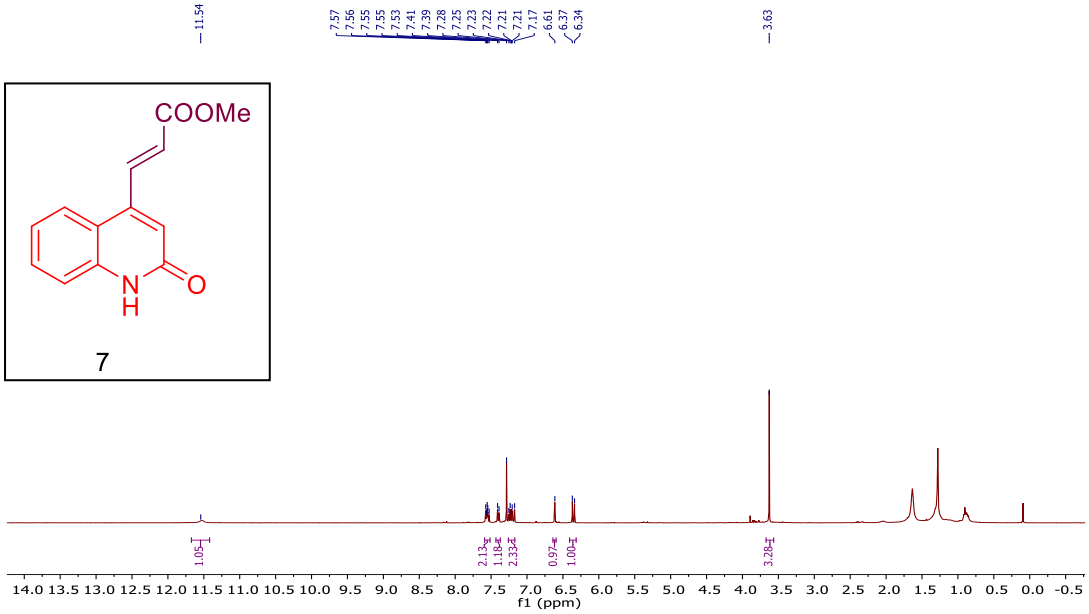

^{1}H NMR ($CDCl_3$, 400 MHz) spectrum of **methyl (E)-3-(2-oxo-1,2-dihydroquinolin-4-yl)acrylate (7).**

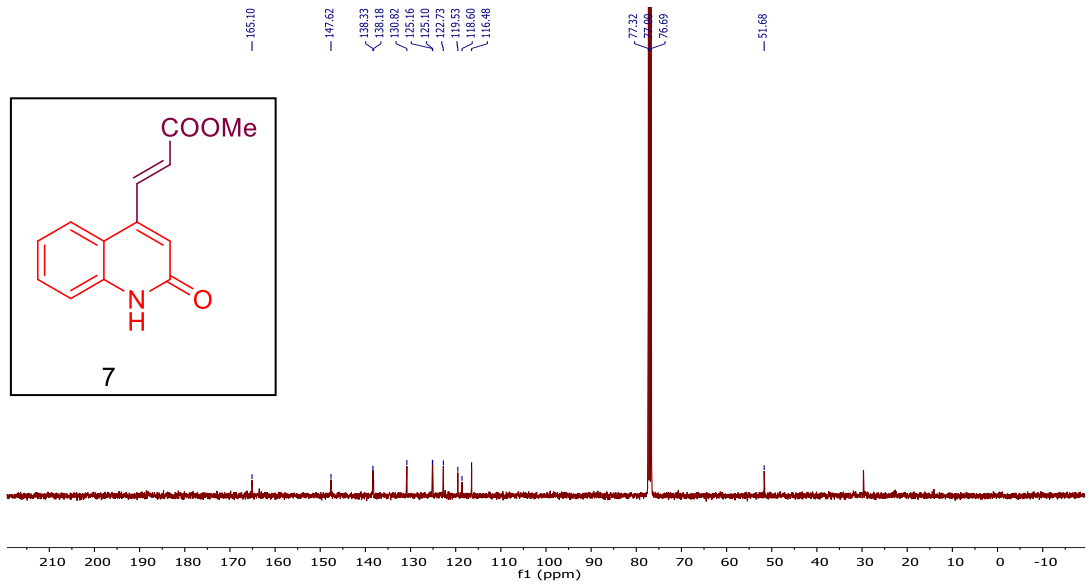

^{13}C NMR ($CDCl_3$, 100 MHz) spectrum of **methyl (E)-3-(2-oxo-1,2-dihydroquinolin-4-yl)acrylate (7).**

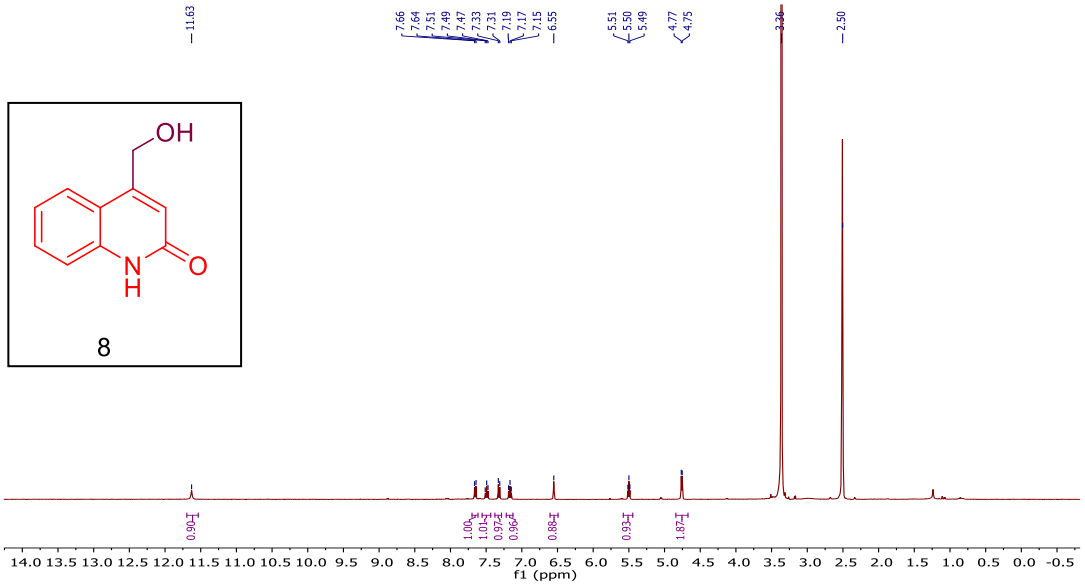

^{1}H NMR (DMSO-d_6, 400 MHz) spectrum of **4-(hydroxymethyl)quinolin-2(1H)-one (8).**

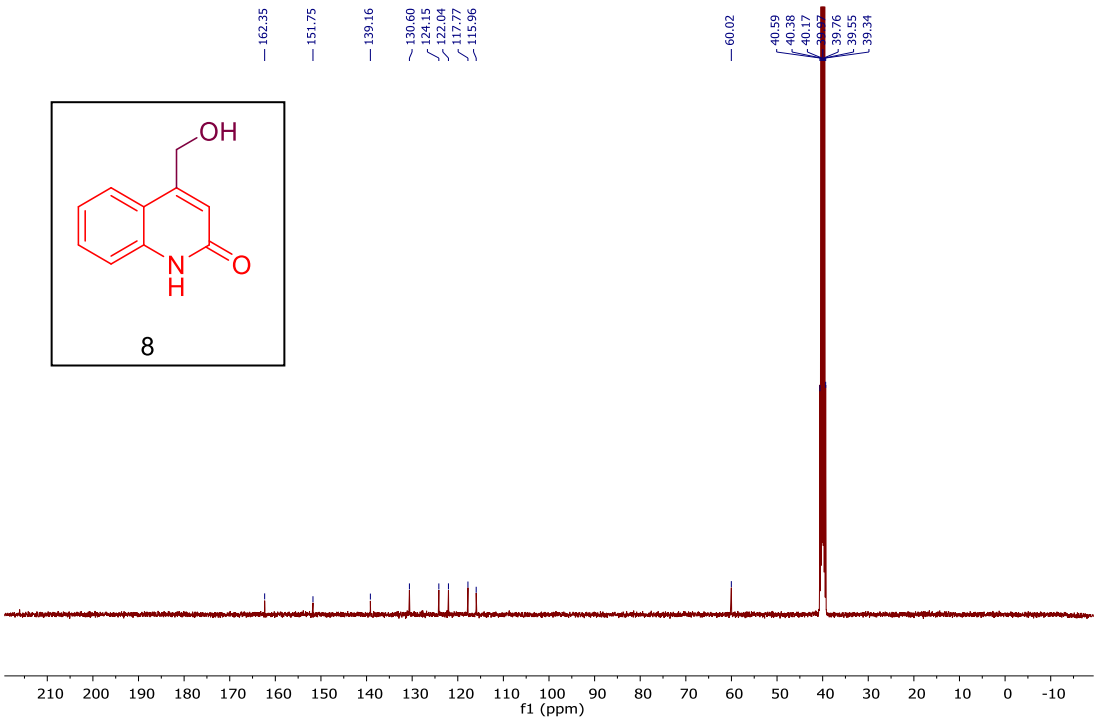

^{13}C NMR (DMSO-d_6, 100 MHz) spectrum of **4-(hydroxymethyl)quinolin-2(1H)-one (8).**

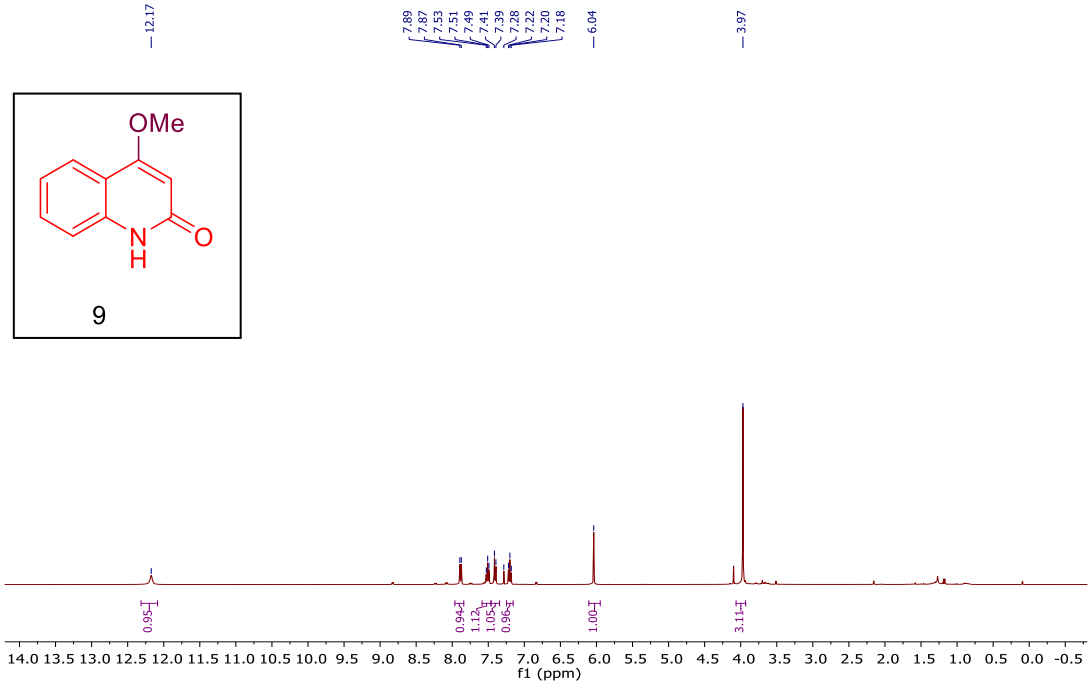

^{1}H NMR ($CDCl_3$, 100 MHz) spectrum of **4-methoxyquinolin-2(1H)-one (9).**

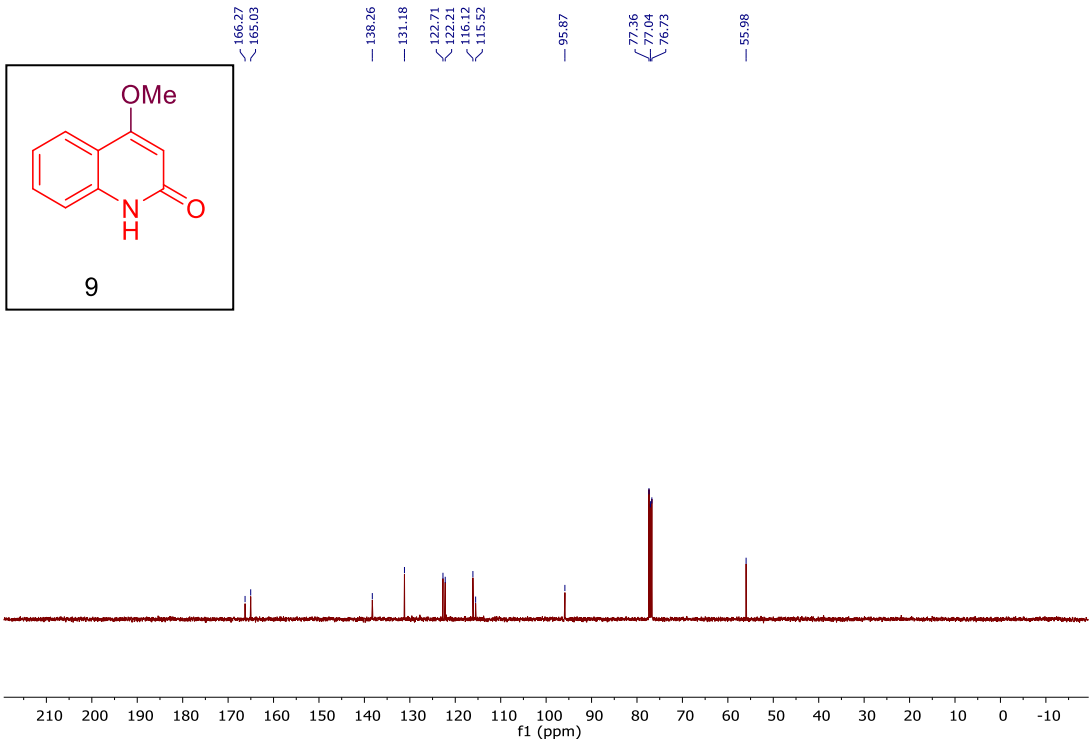

^{13}C NMR ($CDCl_3$, 100 MHz) spectrum of **4-methoxyquinolin-2(1H)-one (9).**

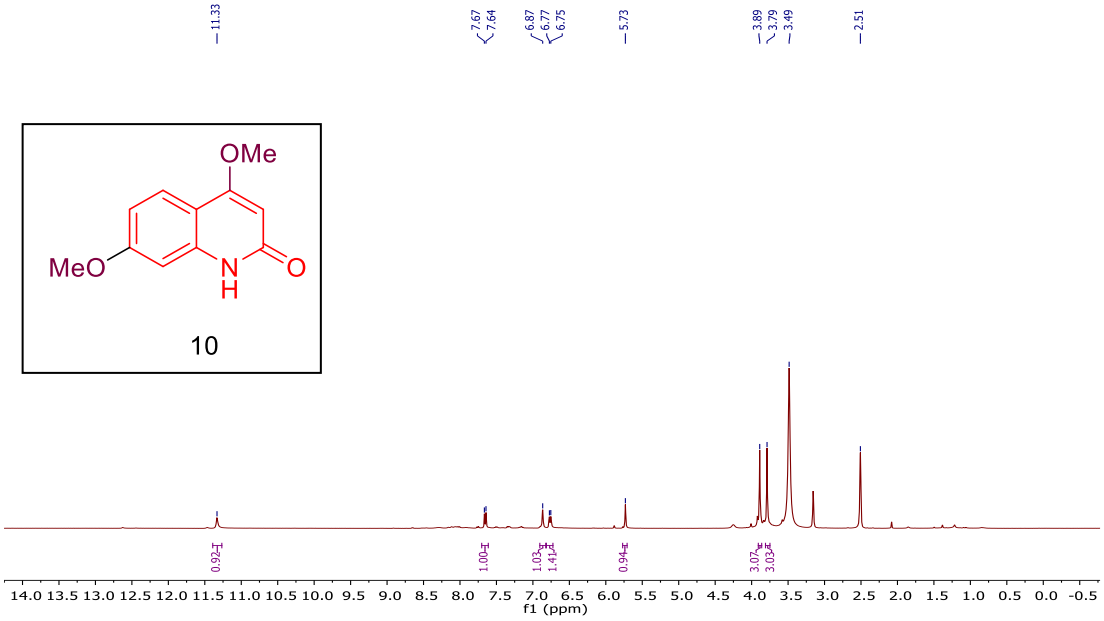

^{1}H NMR (DMSO-d_6, 400 MHz) spectrum of **4,7-dimethoxyquinolin-2(1H)-one (10).**

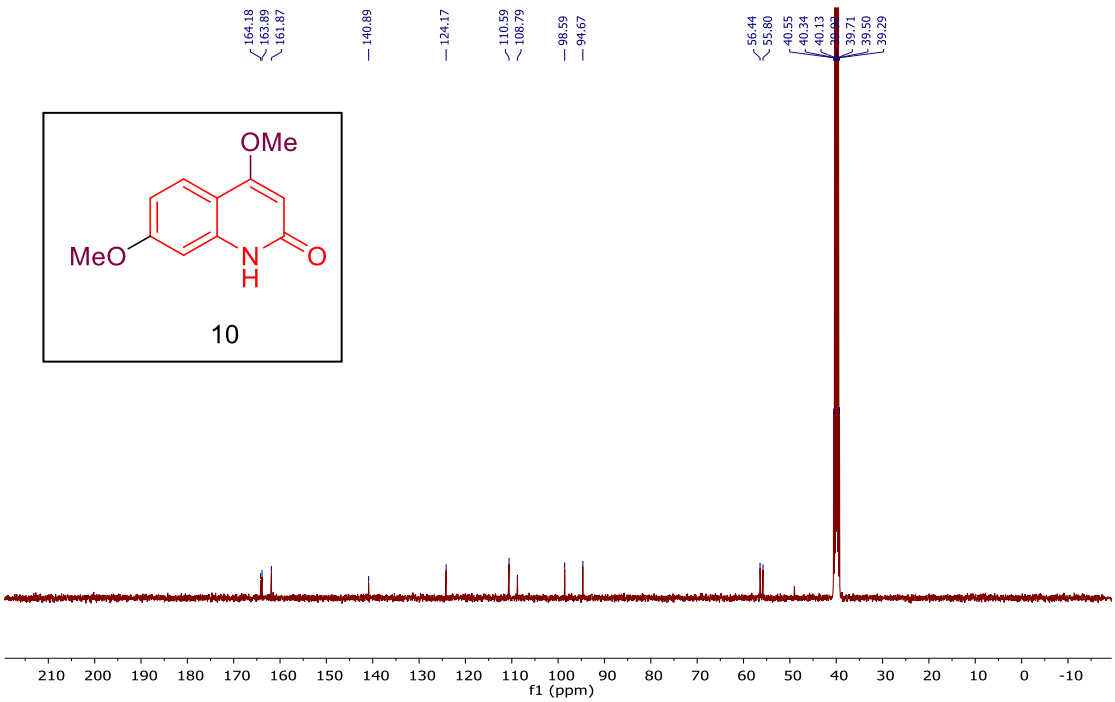

^{13}C NMR (DMSO-d_6, 100 MHz) spectrum of **4,7-dimethoxyquinolin-2(1H)-one (10).**

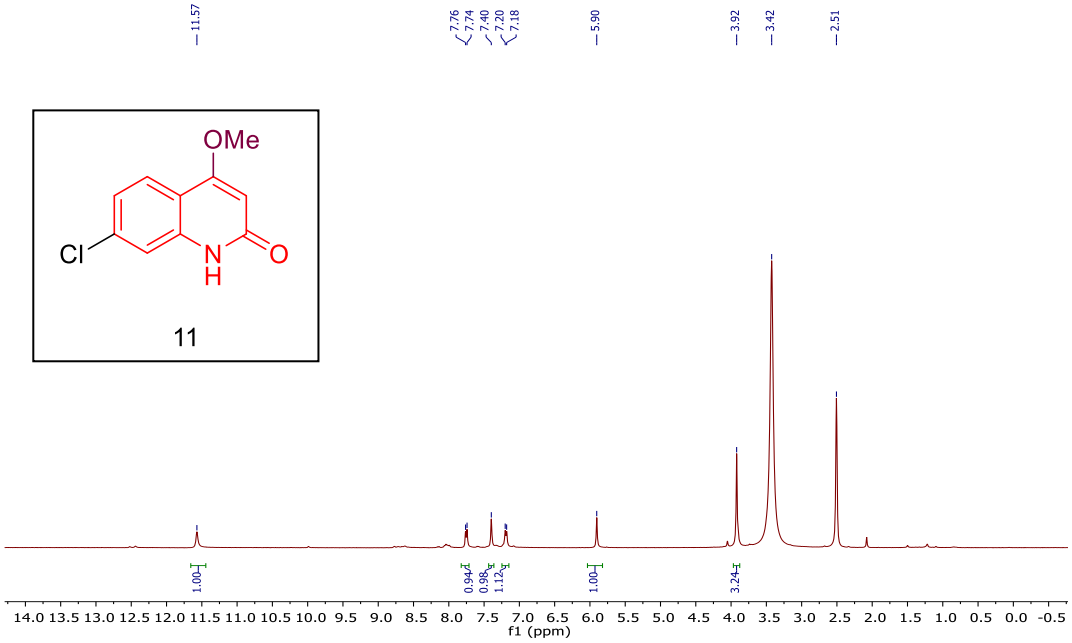

^{1}H NMR (DMSO-d_6, 400 MHz) spectrum of **7-chloro-4-methoxyquinolin-2(1H)-one (11).**

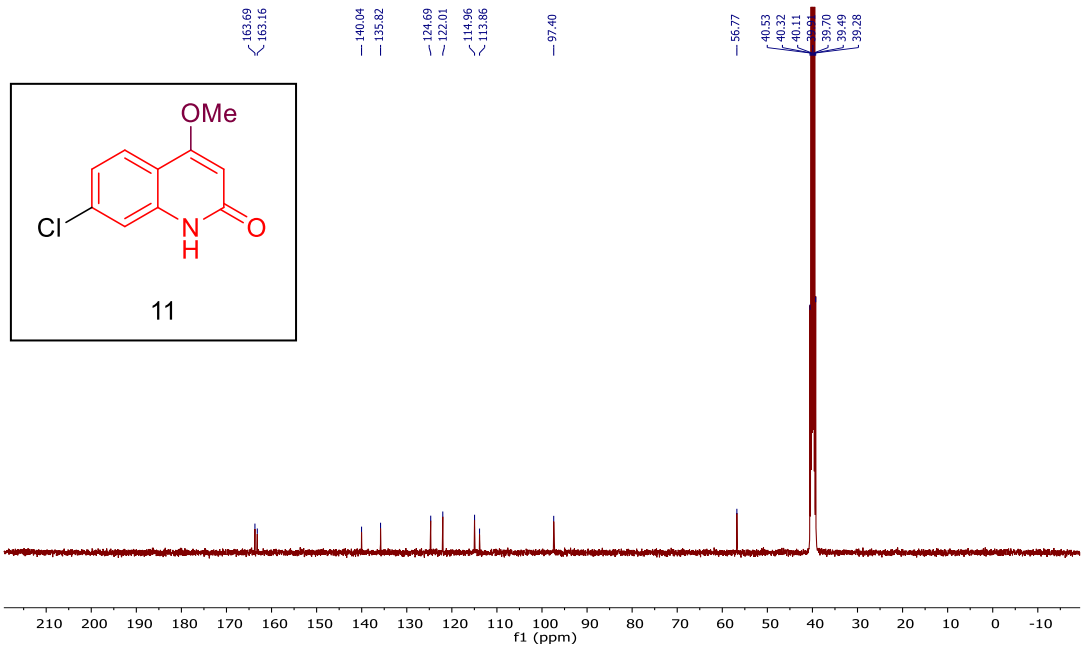

^{13}C NMR (DMSO-d_6, 100 MHz) spectrum of **7-chloro-4-methoxyquinolin-2(1H)-one (11).**

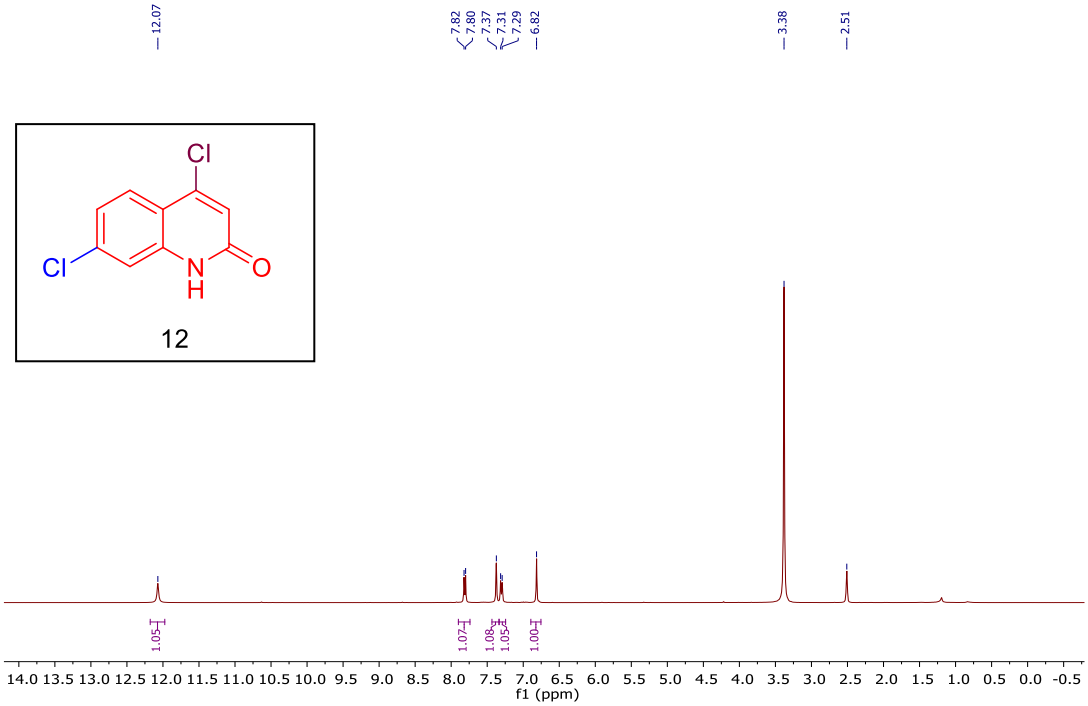

^{1}H NMR (DMSO-d_6, 400 MHz) spectrum of **4,7-dichloroquinolin-2(1H)-one (12).**

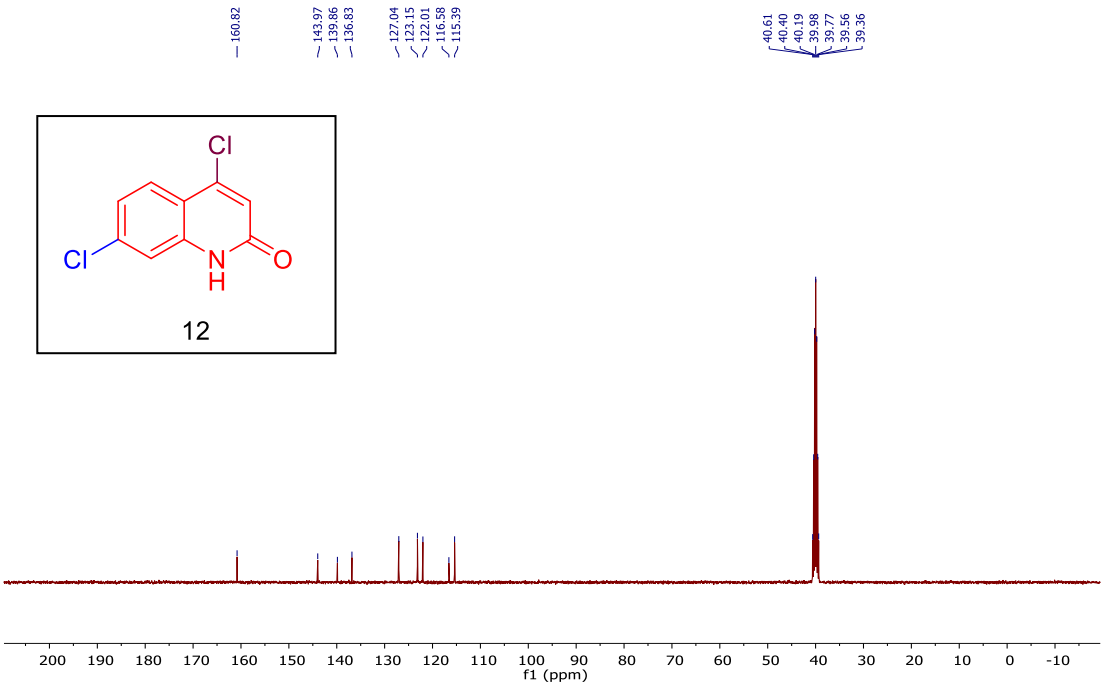

^{13}C NMR (DMSO-d_6, 100 MHz) spectrum of **4,7-dichloroquinolin-2(1H)-one (12).**

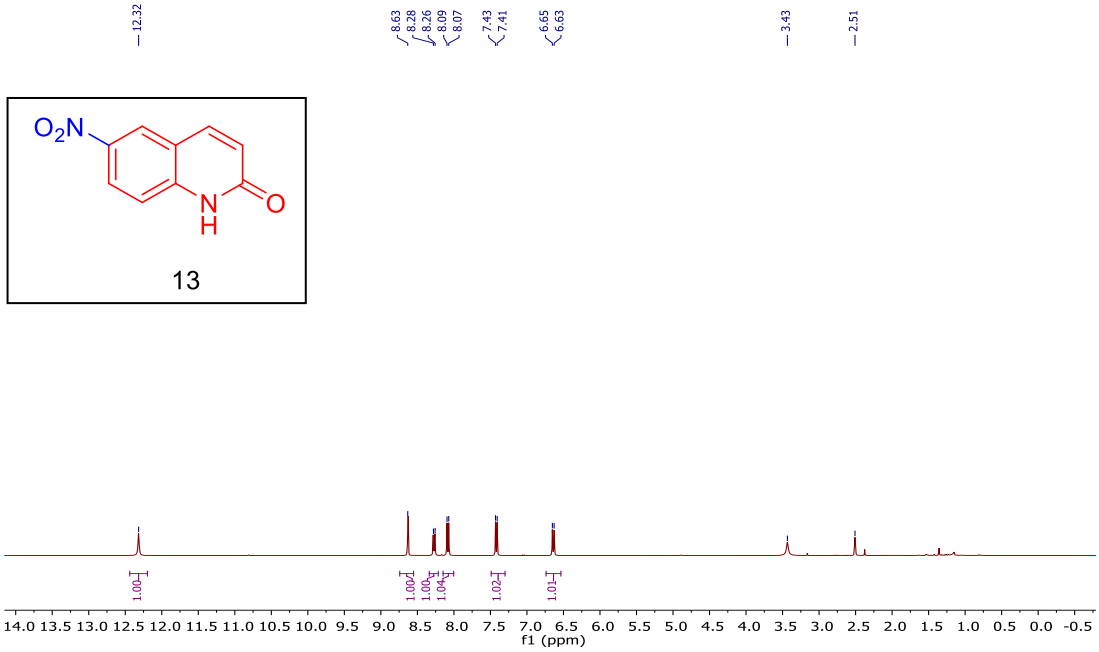

^{1}H NMR(DMSO-d_6, 400 MHz) spectrum of **6-nitroquinolin-2(1H)-one (13).**

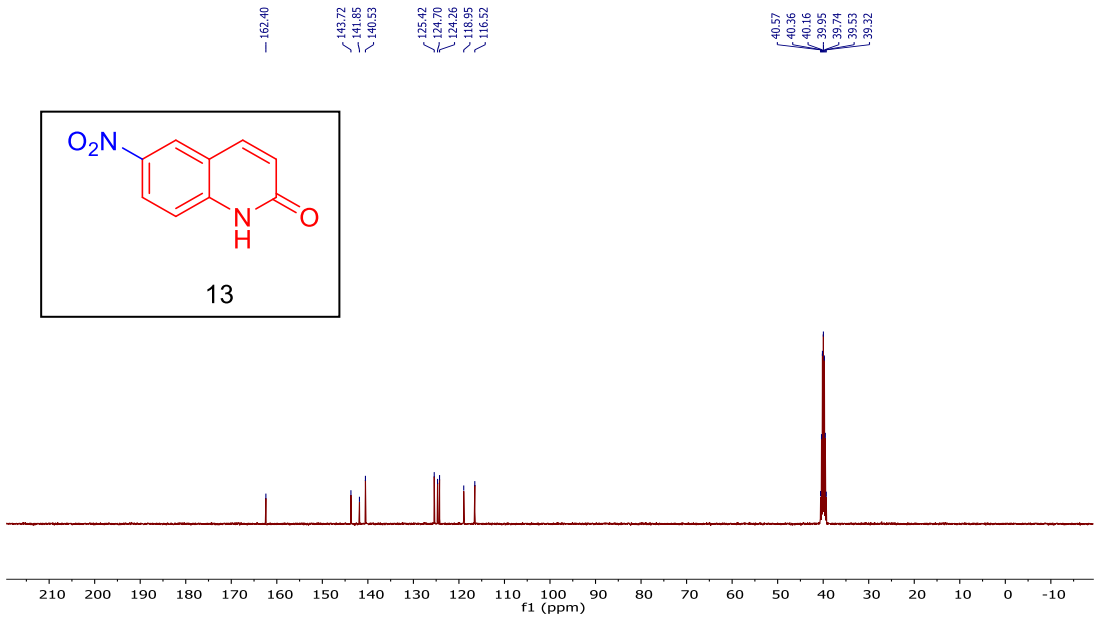

^{13}C NMR (DMSO-d_6, 100 MHz) spectrum of **6-nitroquinolin-2(1H)-one (13).**

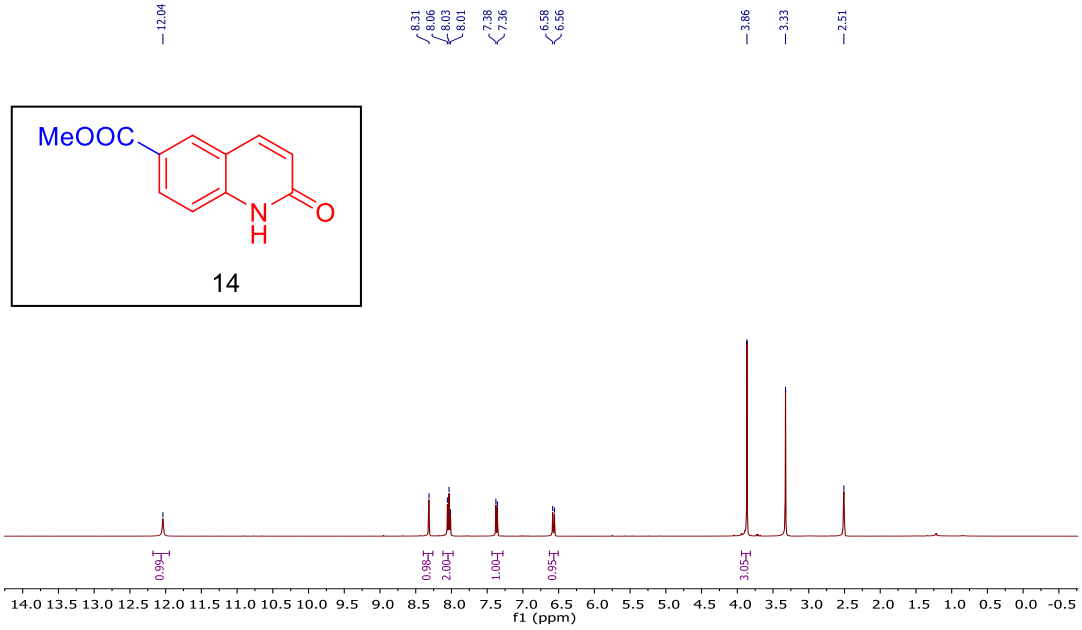

^{1}H NMR (DMSO-d_6, 400 MHz) spectrum of **methyl 2-oxo-1,2-dihydroquinoline-6-carboxylate (14).**

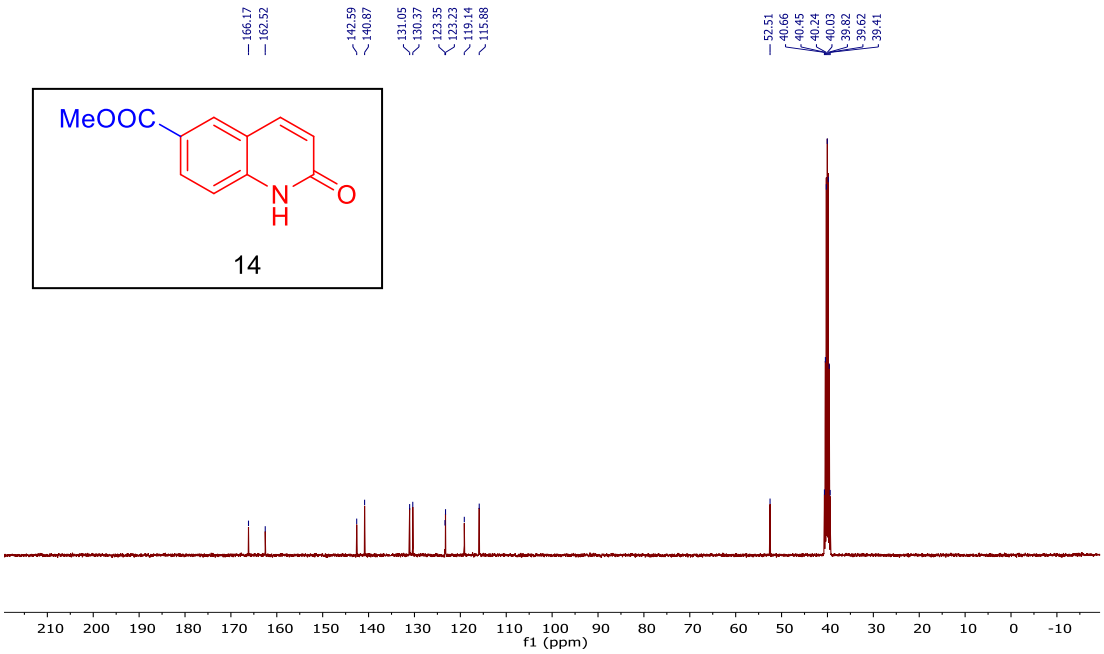

^{13}C NMR (DMSO-d_6, 100 MHz) spectrum of **methyl 2-oxo-1,2-dihydroquinoline-6-carboxylate (14).**

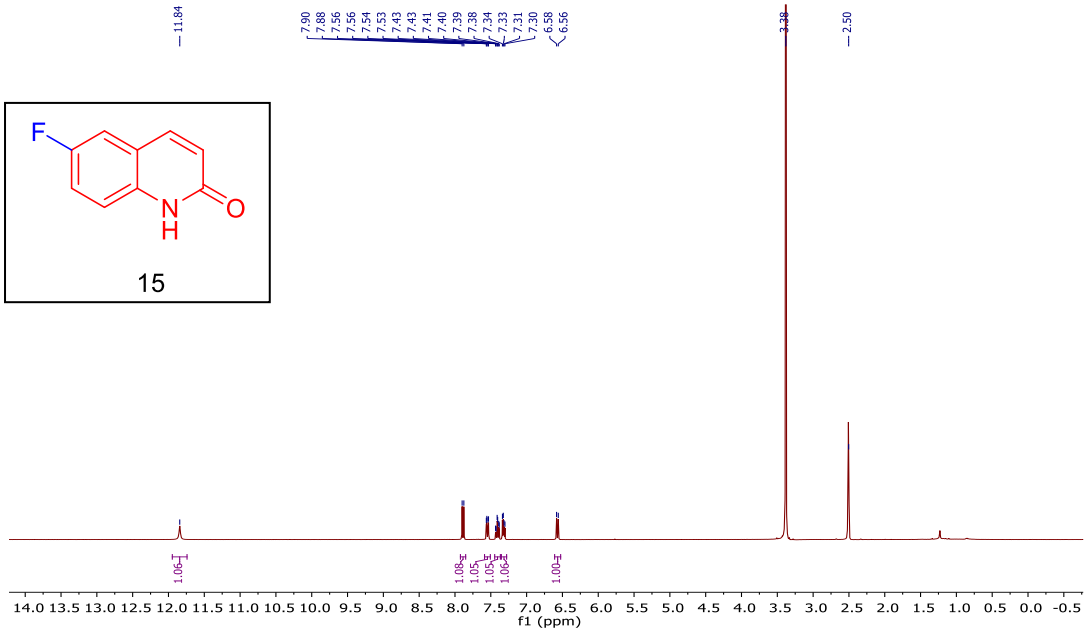

^{1}H NMR (DMSO-d_6, 400 MHz) spectrum of **6-fluoroquinolin-2(1H)-one (15).**

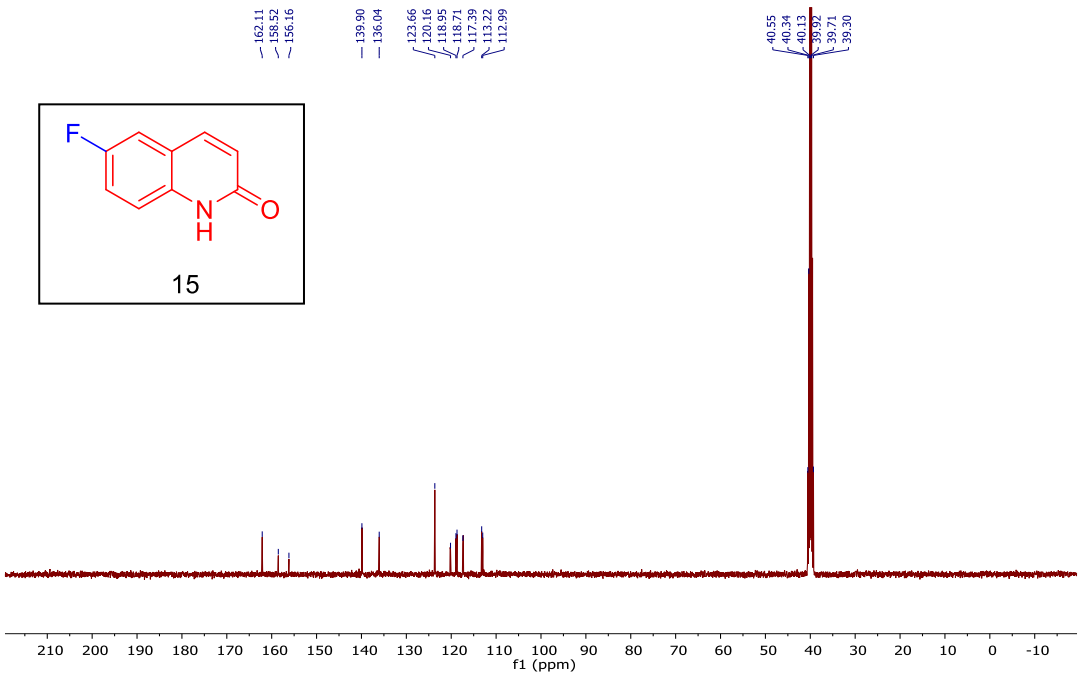

^{13}C NMR (DMSO-d_6, 100 MHz) spectrum of **6-fluoroquinolin-2(1H)-one (15).**

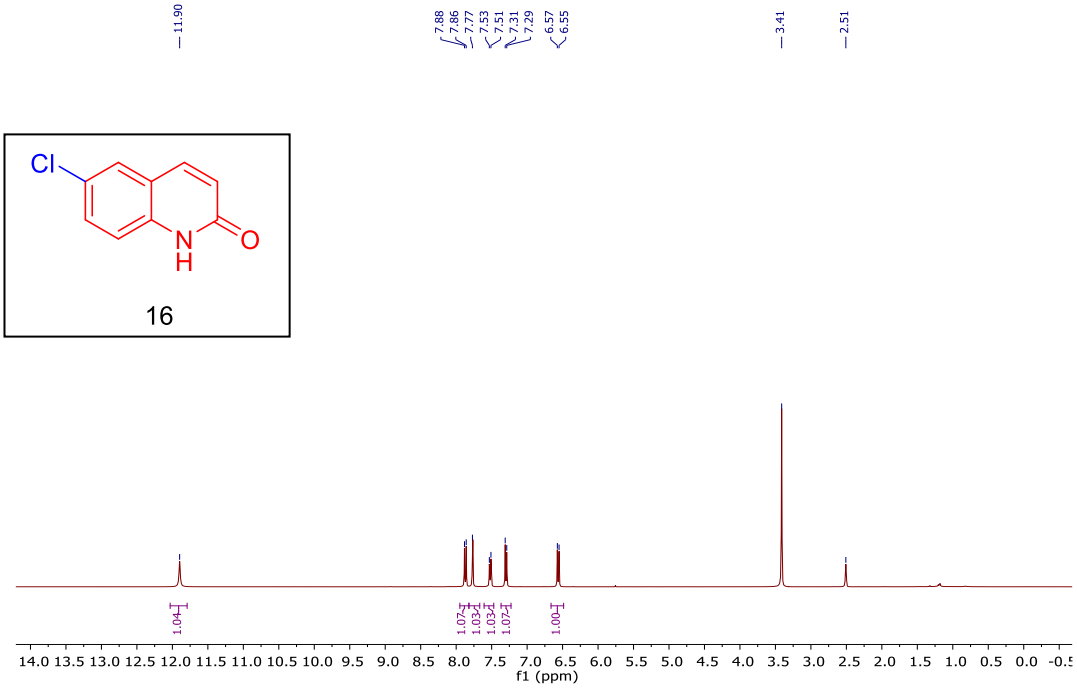

^{1}H NMR (DMSO-d_6, 400 MHz) spectrum of **6-chloroquinolin-2(1H)-one (16).**

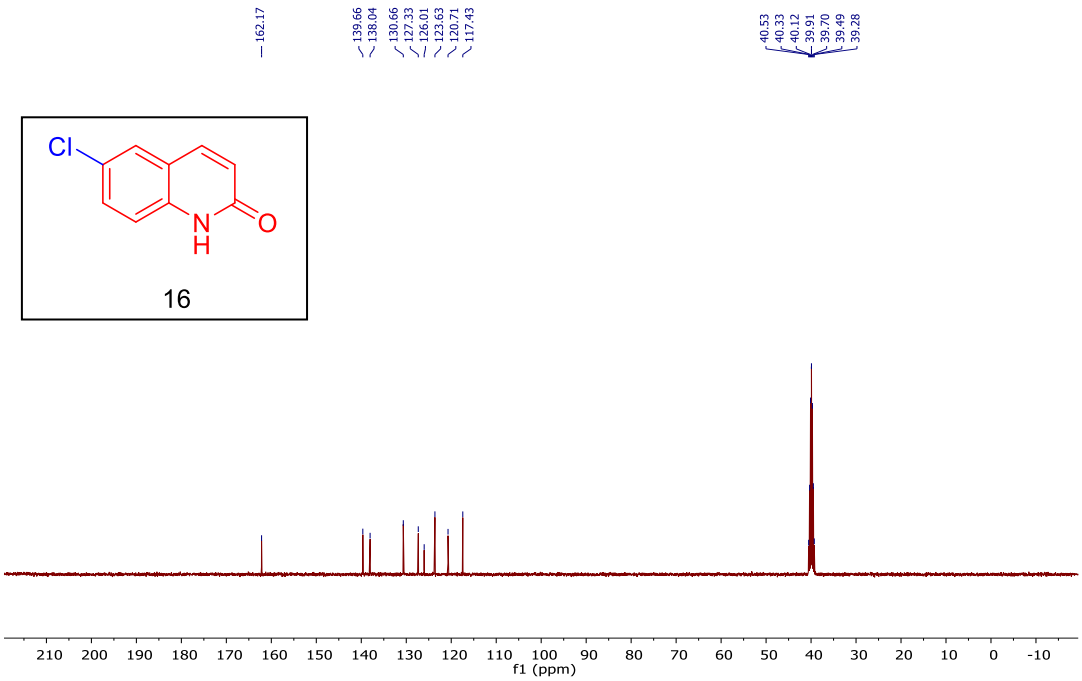

^{13}C NMR (DMSO-d_6, 100 MHz) spectrum of **6-chloroquinolin-2(1H)-one (16).**

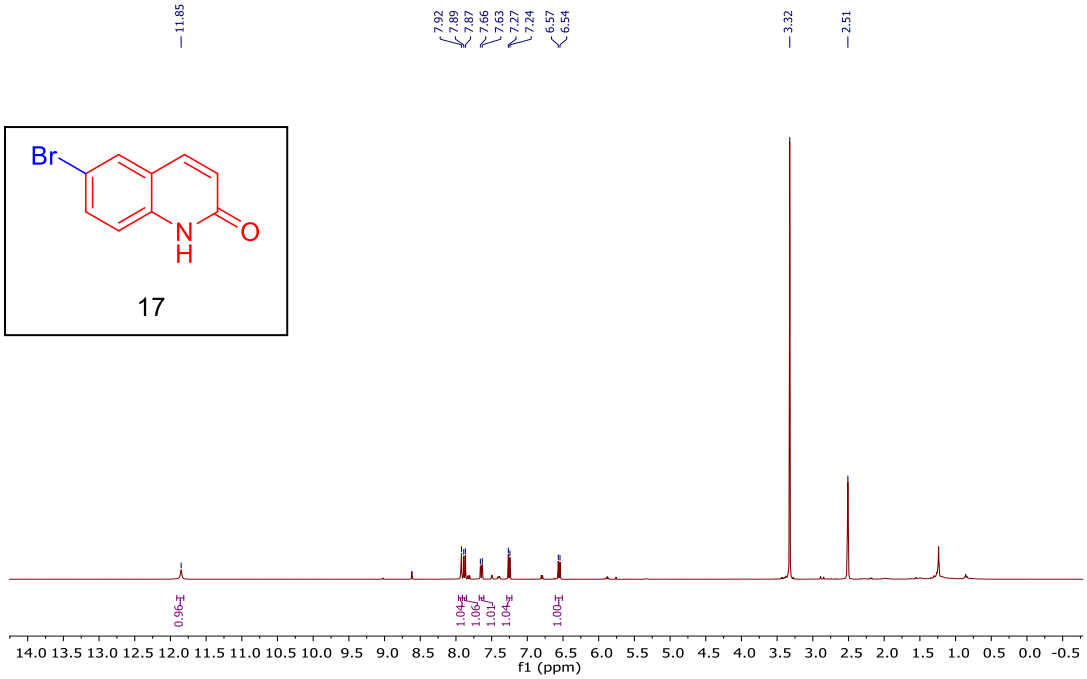

^{1}H NMR (DMSO-d_6, 400 MHz) spectrum of **6-bromoquinolin-2(1H)-one (17).**

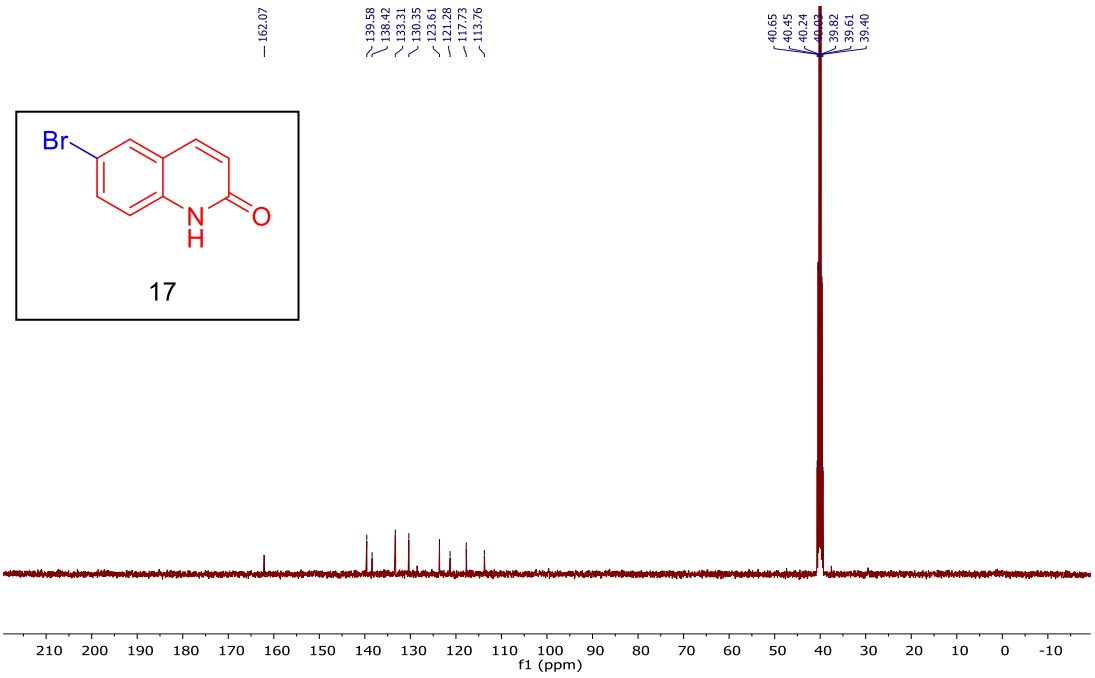

^{13}C NMR (DMSO-d_6, 100 MHz) spectrum of **6-bromoquinolin-2(1H)-one (17).**

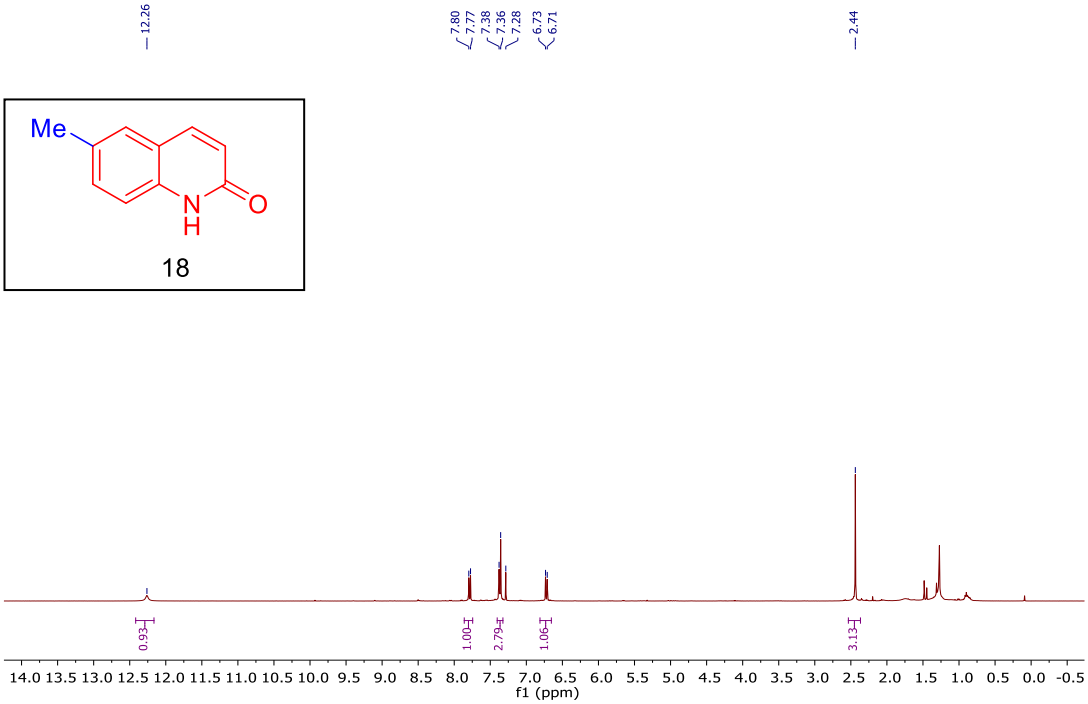

^{1}H NMR ($CDCl_3$, 400 MHz) spectrum of **6-methylquinolin-2(1H)-one (18).**

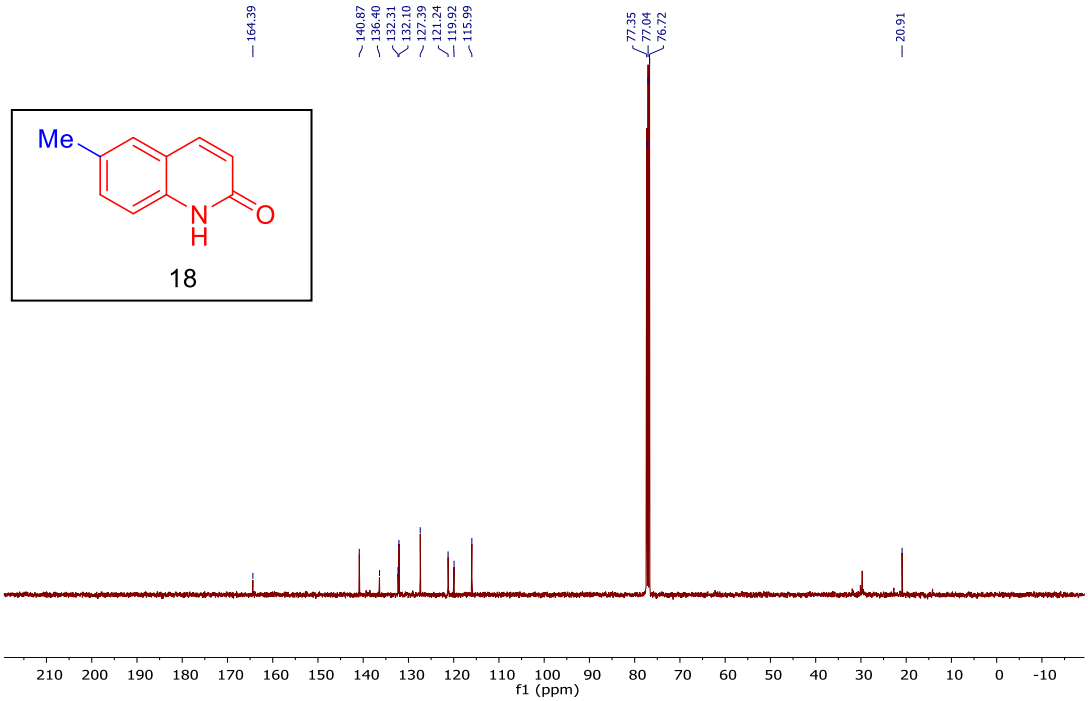

^{13}C NMR ($CDCl_3$, 100 MHz) spectrum of **6-methylquinolin-2(1H)-one (18).**

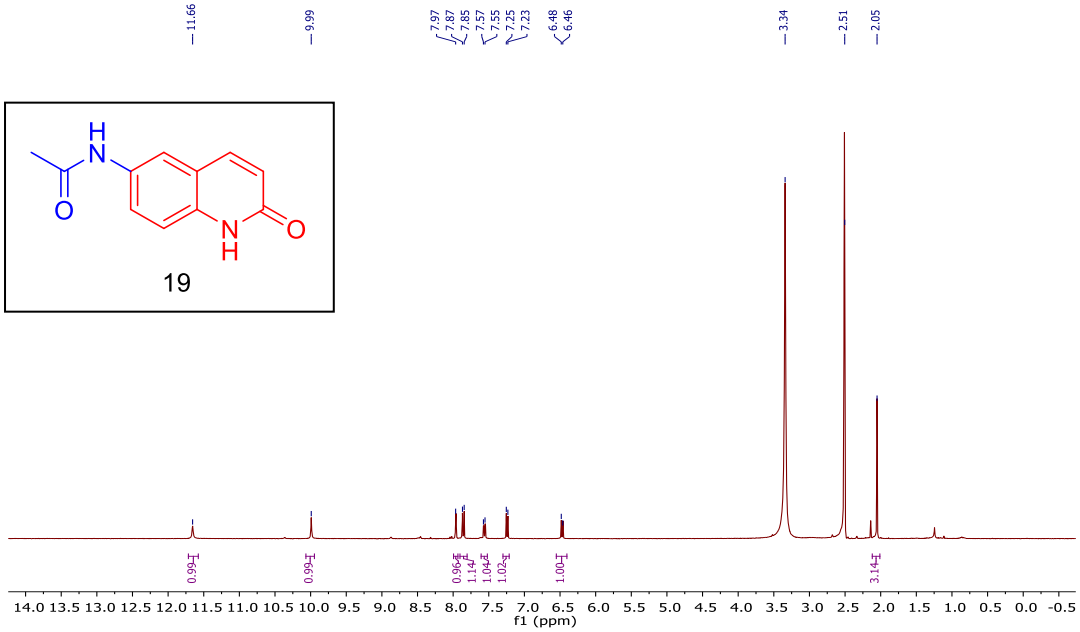

^{1}H NMR (DMSO-d_6, 400 MHz) spectrum of **N-(2-oxo-1,2-dihydroquinolin-6-yl)acetamide (19).**

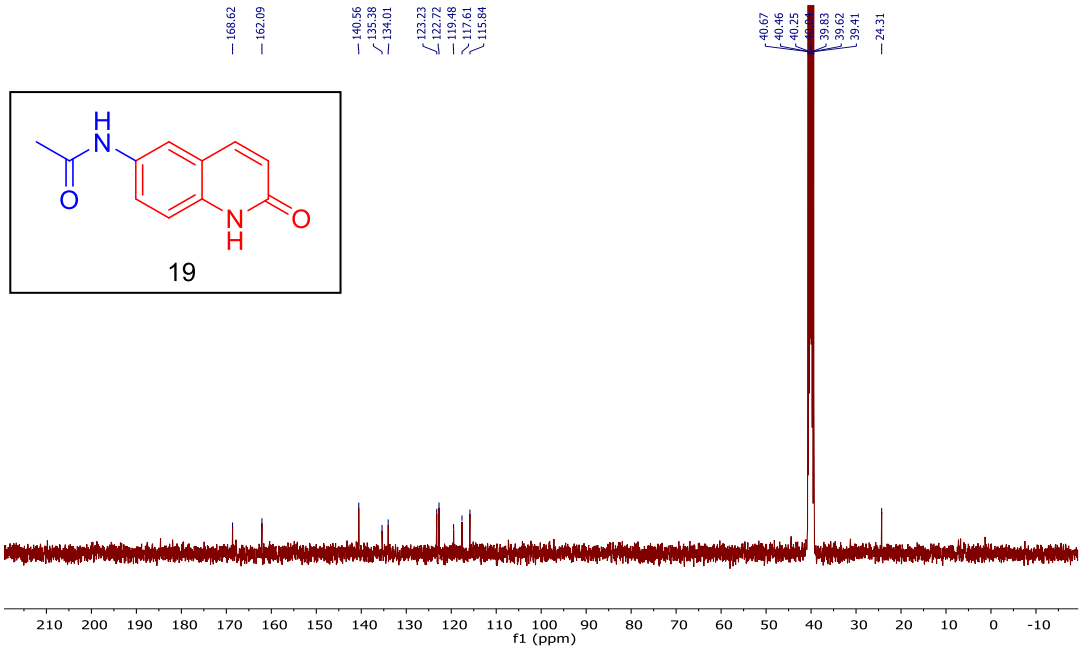

^{13}C NMR (DMSO-d_6, 100 MHz) spectrum of **N-(2-oxo-1,2-dihydroquinolin-6-yl)acetamide (19).**

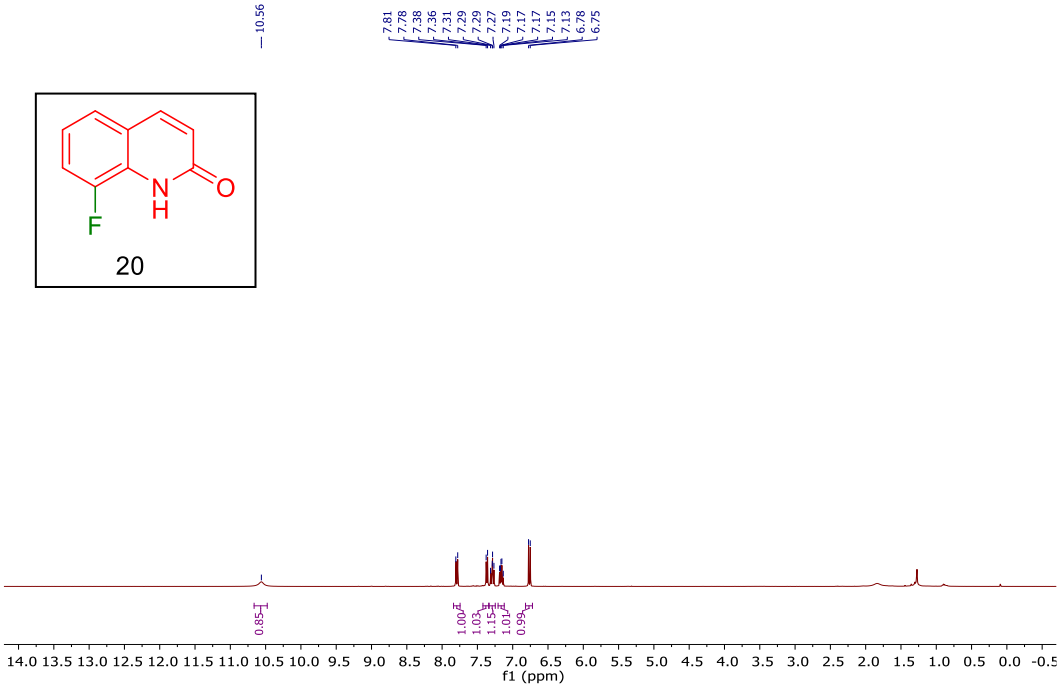

^{1}H NMR ($CDCl_3$, 400 MHz) spectrum of **8-fluoroquinolin-2(1H)-one (20).**

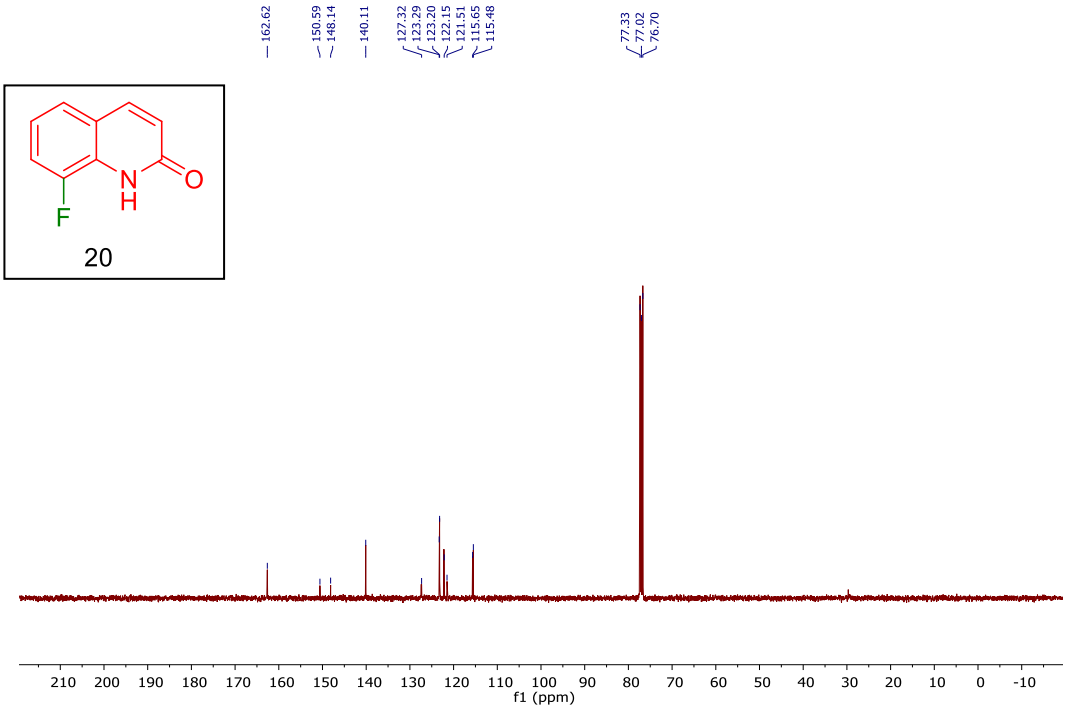

^{13}C NMR ($CDCl_3$, 100 MHz) spectrum of **8-fluoroquinolin-2(1H)-one (20)**

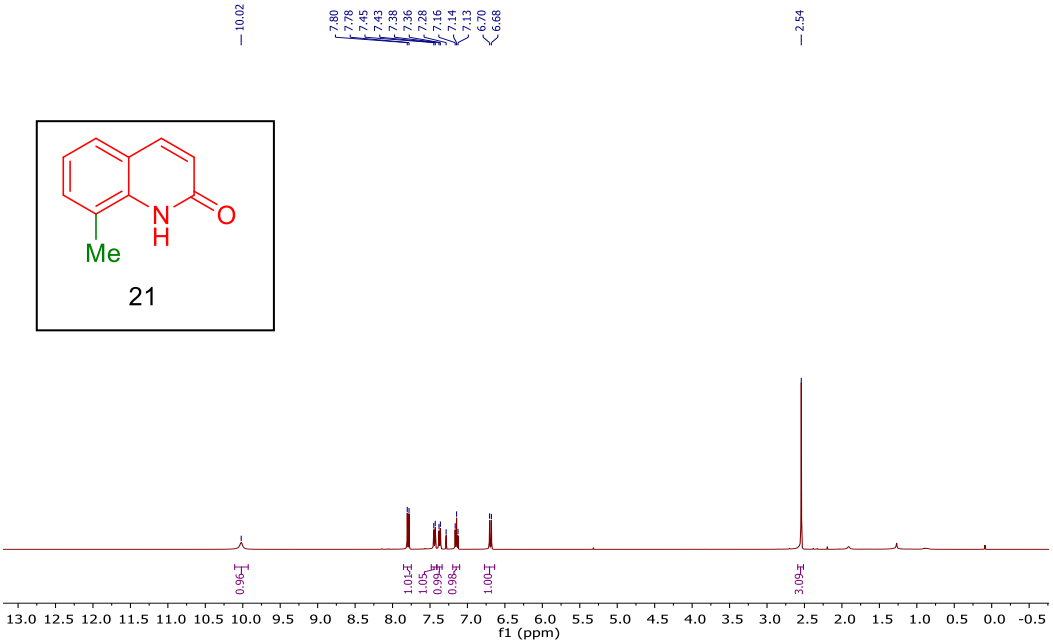

^{1}H NMR ($CDCl_3$, 400 MHz) spectrum of **8-methylquinolin-2(1H)-one (21).**

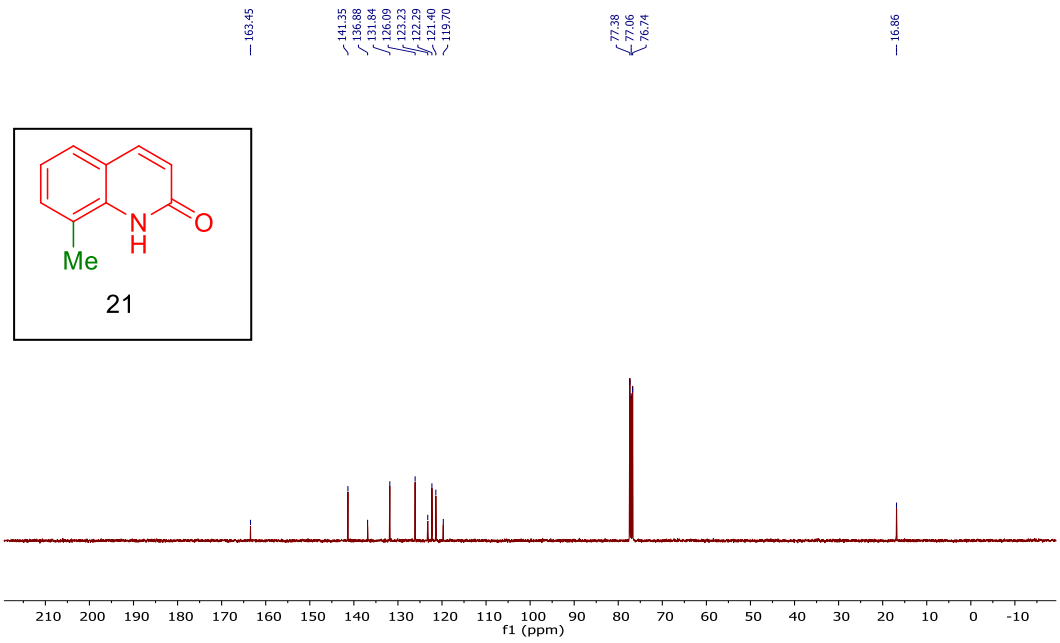

^{13}C NMR ($CDCl_3$, 100 MHz) spectrum of **8-methylquinolin-2(1H)-one (21).**

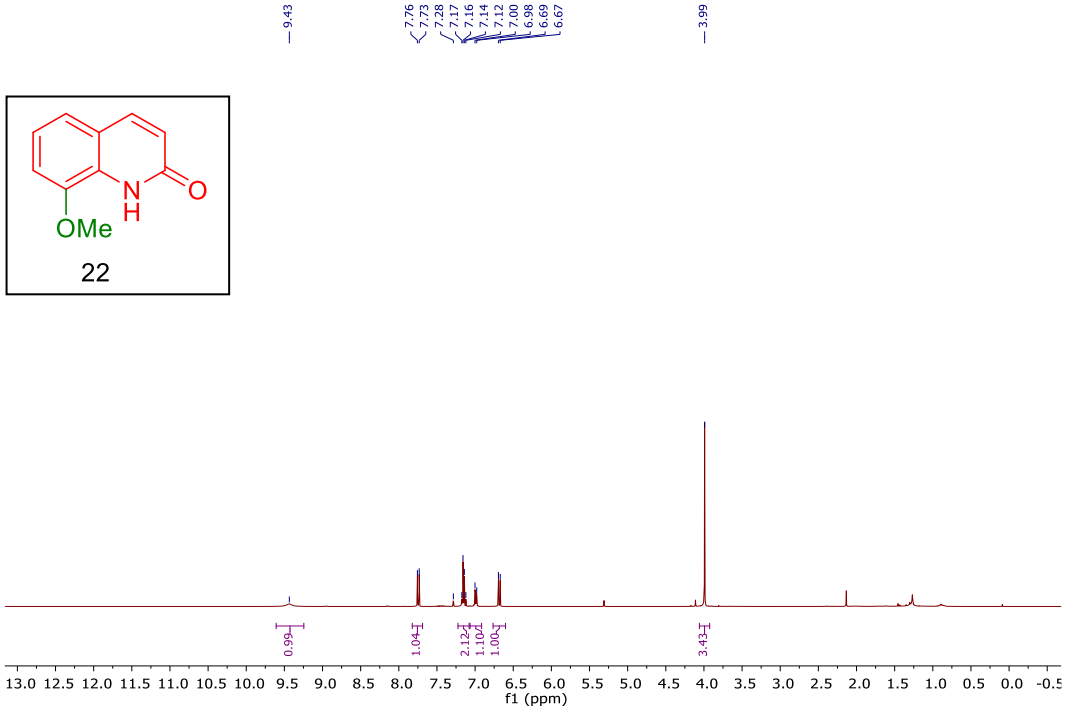

^{1}H NMR ($CDCl_3$, 400 MHz) spectrum of **8-methoxyquinolin-2(1H)-one (22).**

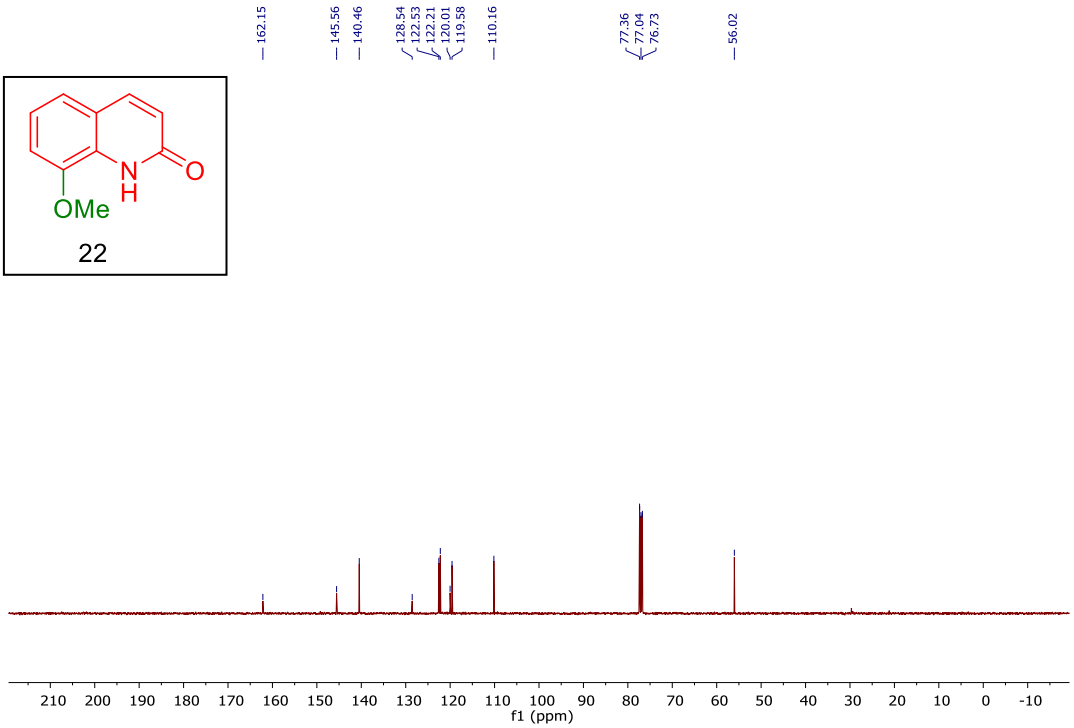

^{13}C NMR ($CDCl_3$, 100 MHz) spectrum of **8-methoxyquinolin-2(1H)-one (22).**

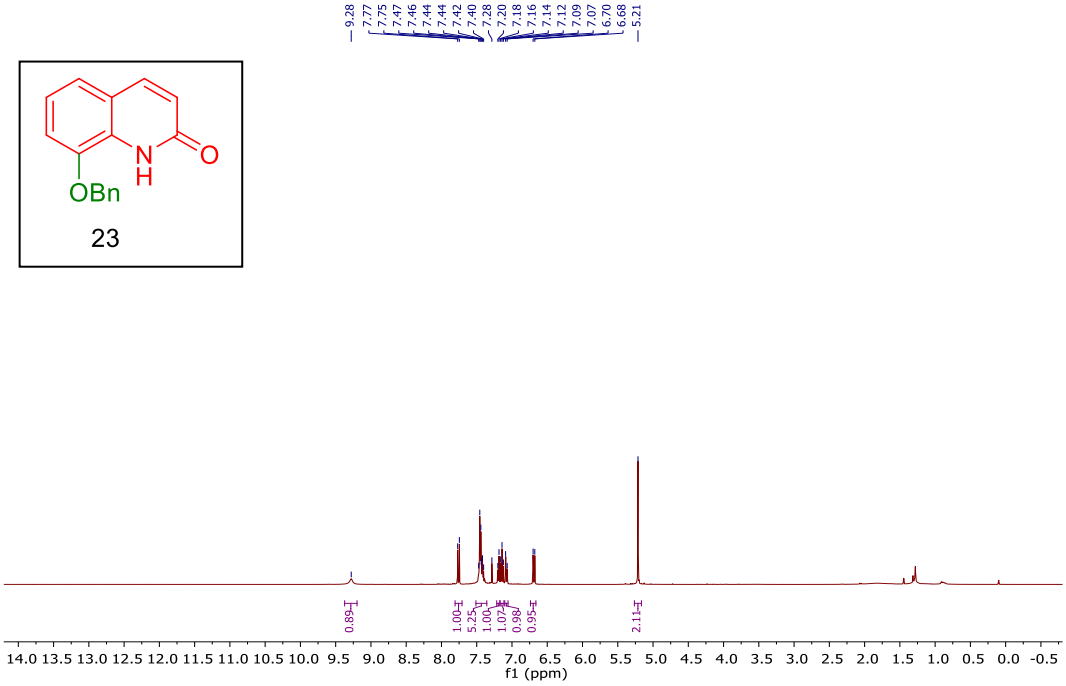

^{1}H NMR ($CDCl_3$, 400 MHz) spectrum of **8-(benzyloxy)quinolin-2(1H)-one (23).**

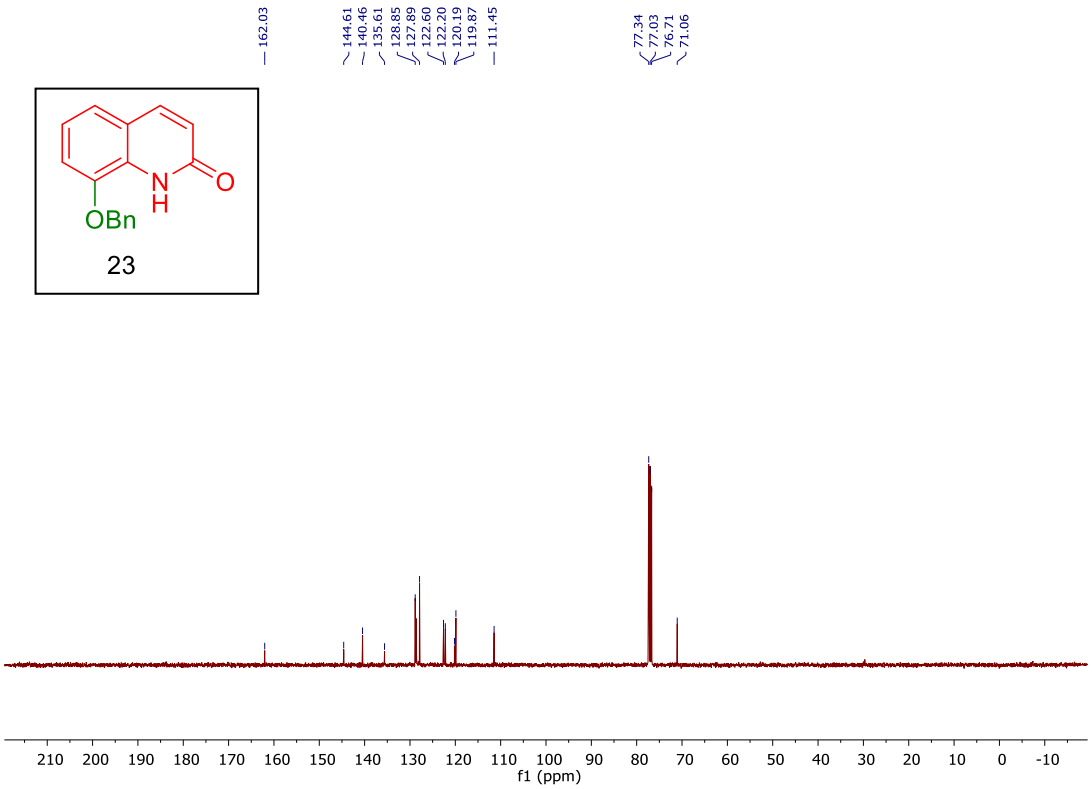

^{13}C NMR ($CDCl_3$, 100 MHz) spectrum of **8-(benzyloxy)quinolin-2(1H)-one (23).**

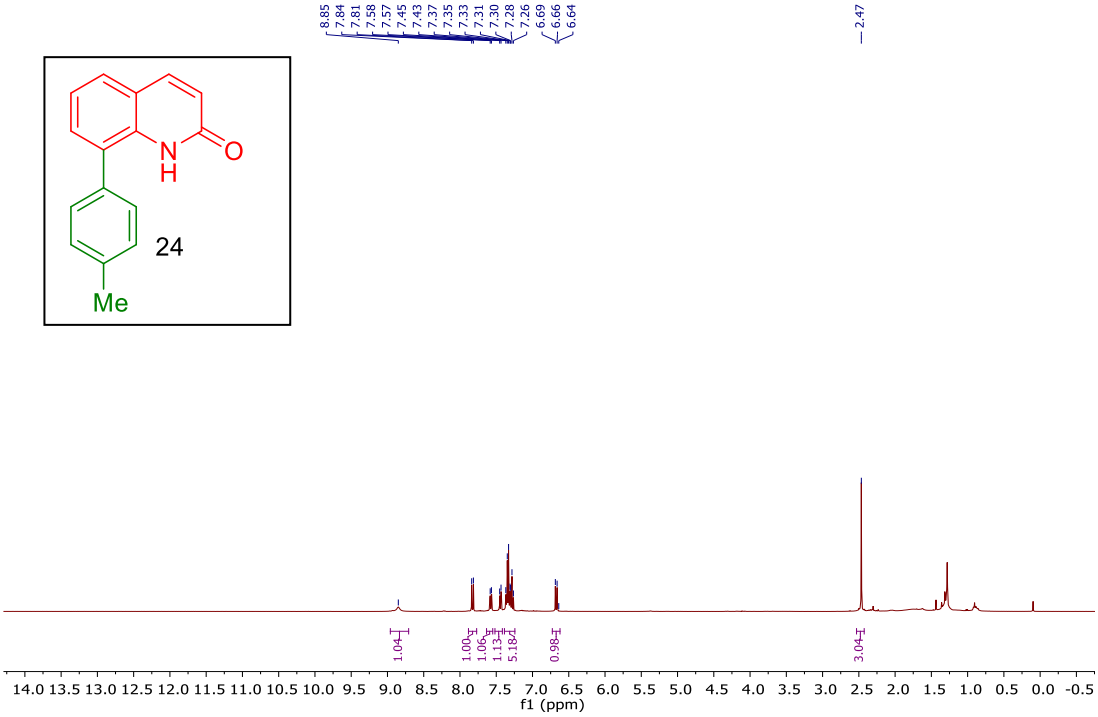

^{1}H NMR ($CDCl_3$, 400 MHz) spectrum of **8-(p-tolyl)quinolin-2(1H)-one (24).**

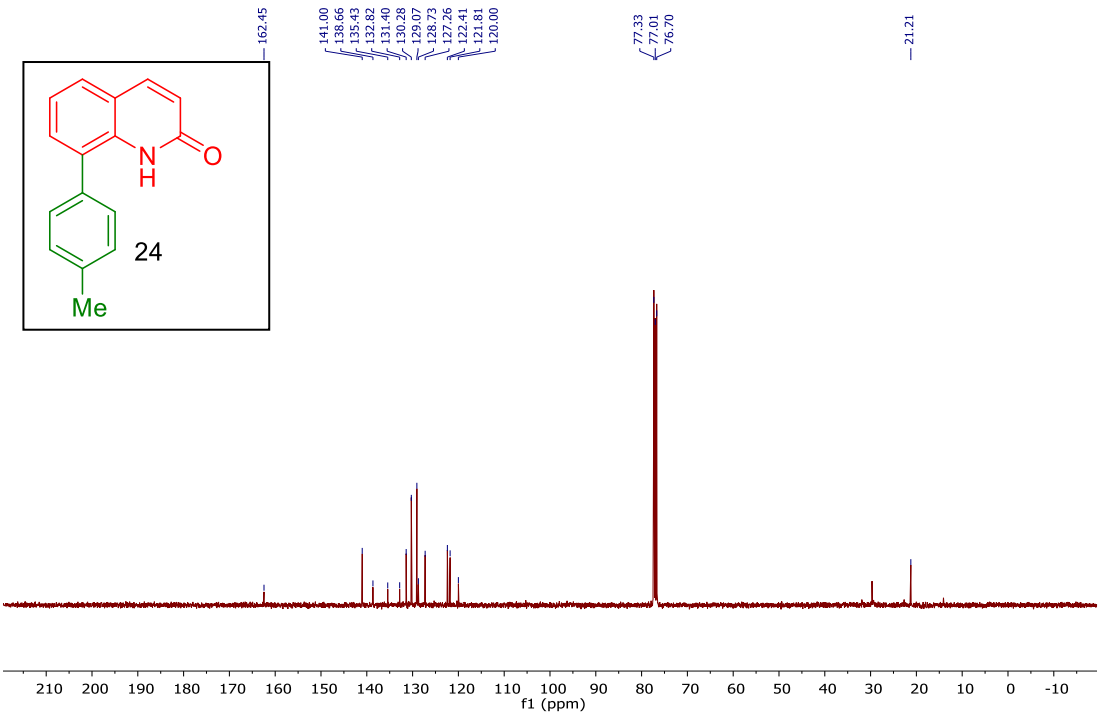

^{13}C NMR ($CDCl_3$, 100 MHz) spectrum of **8-(p-tolyl)quinolin-2(1H)-one (24).**

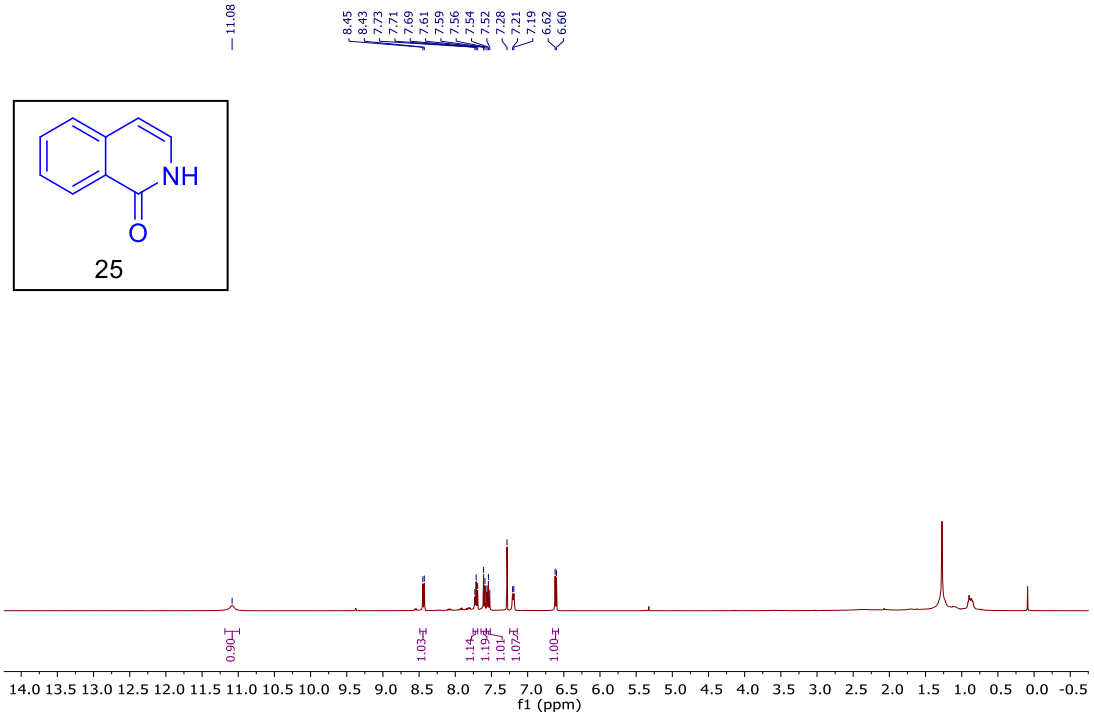

^{1}H NMR ($CDCl_3$, 400 MHz) spectrum of **isoquinolin-1(2H)-one (25).**

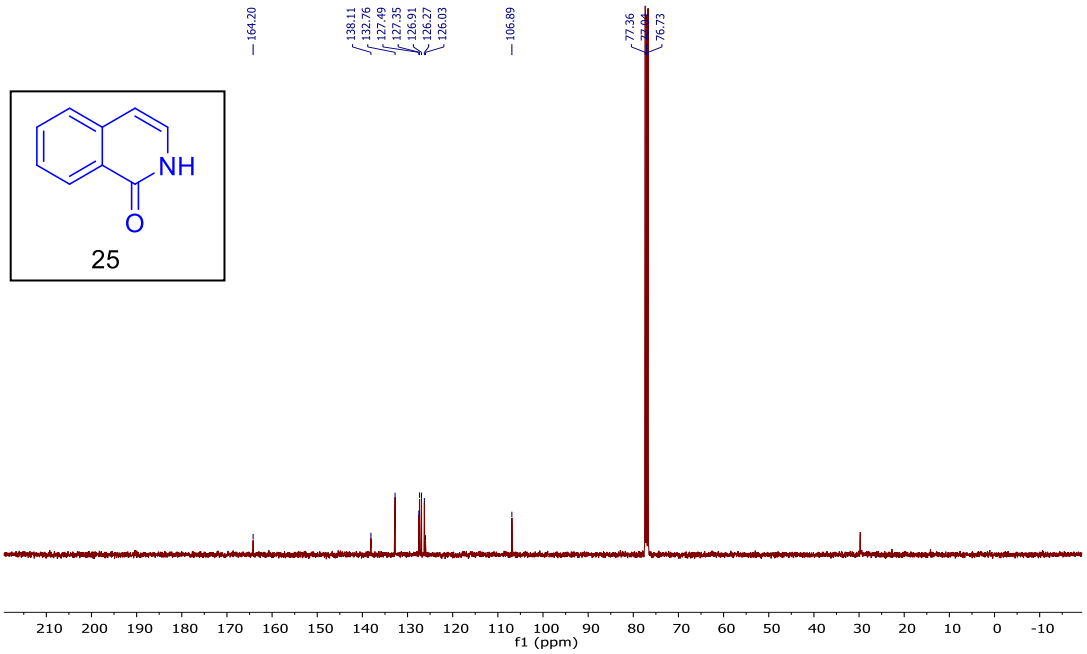

^{13}C NMR ($CDCl_3$, 100 MHz) spectrum of **isoquinolin-1(2H)-one (25).**

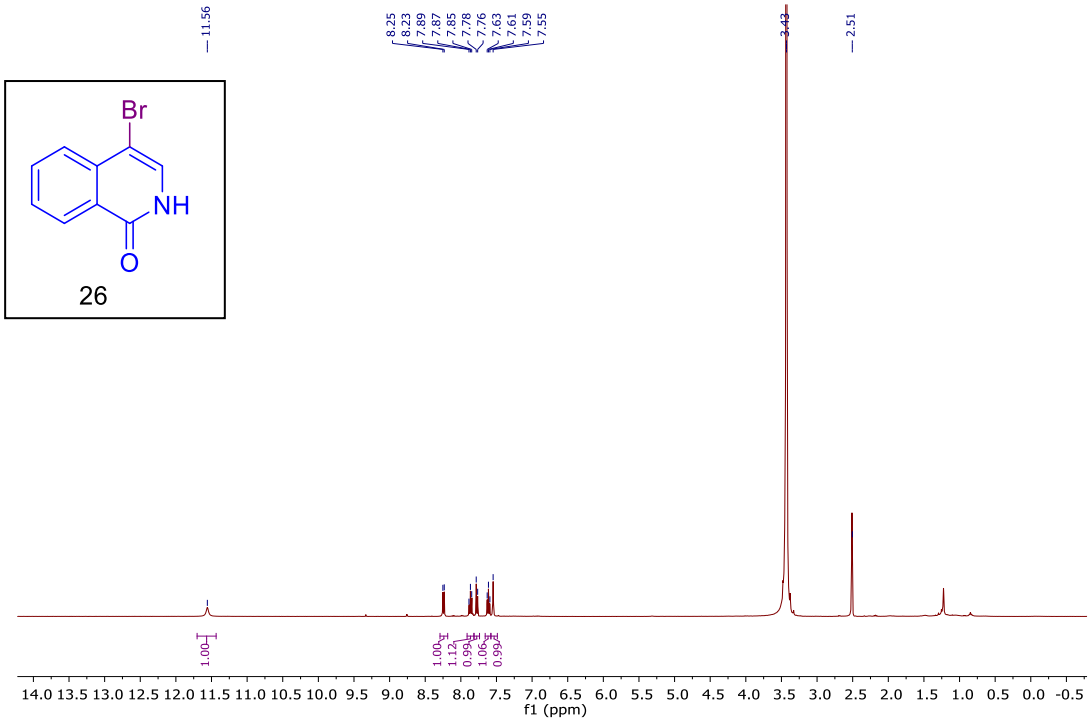

^{1}H NMR (DMSO-d_6, 400 MHz) spectrum of **4-bromoisoquinolin-1(2H)-one (26).**

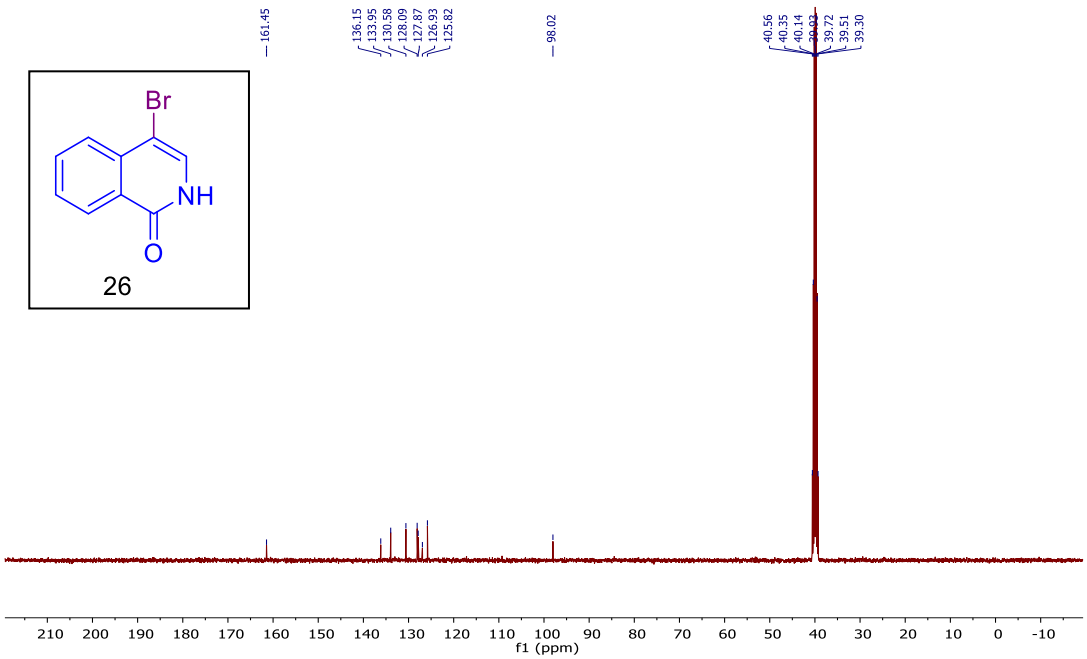

^{13}C NMR (DMSO-d_6, 100 MHz) spectrum of **4-bromoisoquinolin-1(2H)-one (26).**

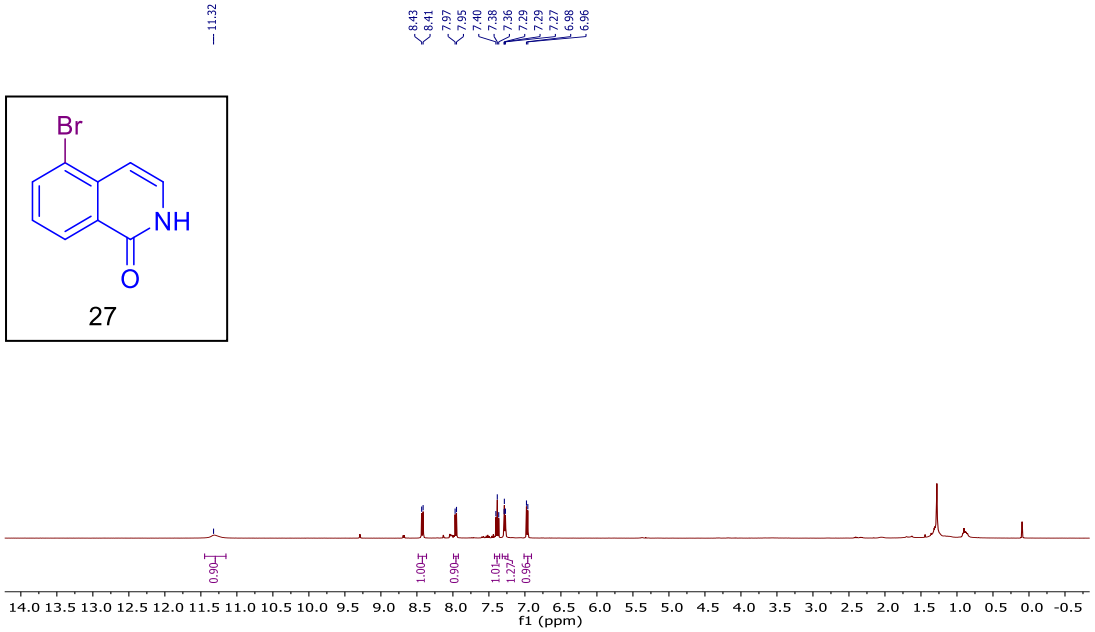

^{1}H NMR (DMSO-d_6, 400 MHz) spectrum of **5-bromoisoquinolin-1(2H)-one (27).**

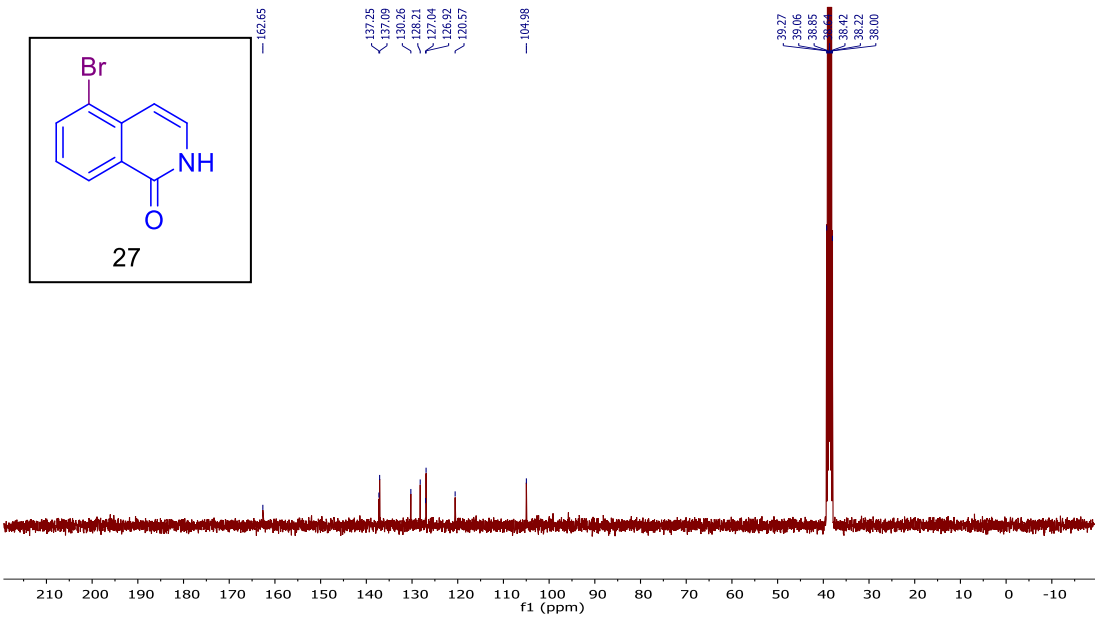

^{13}C NMR (DMSO-d_6, 100 MHz) spectrum of **5-bromoisoquinolin-1(2H)-one (27).**

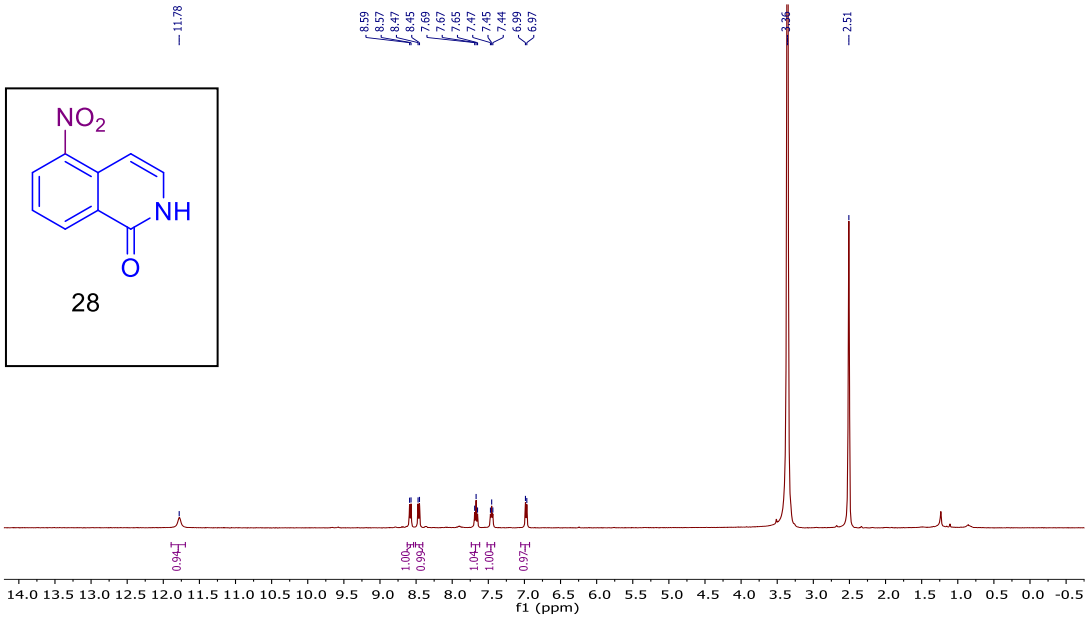

^{1}H NMR (DMSO-d_6, 400 MHz) spectrum of **5-nitroisoquinolin-1(2H)-one (28).**

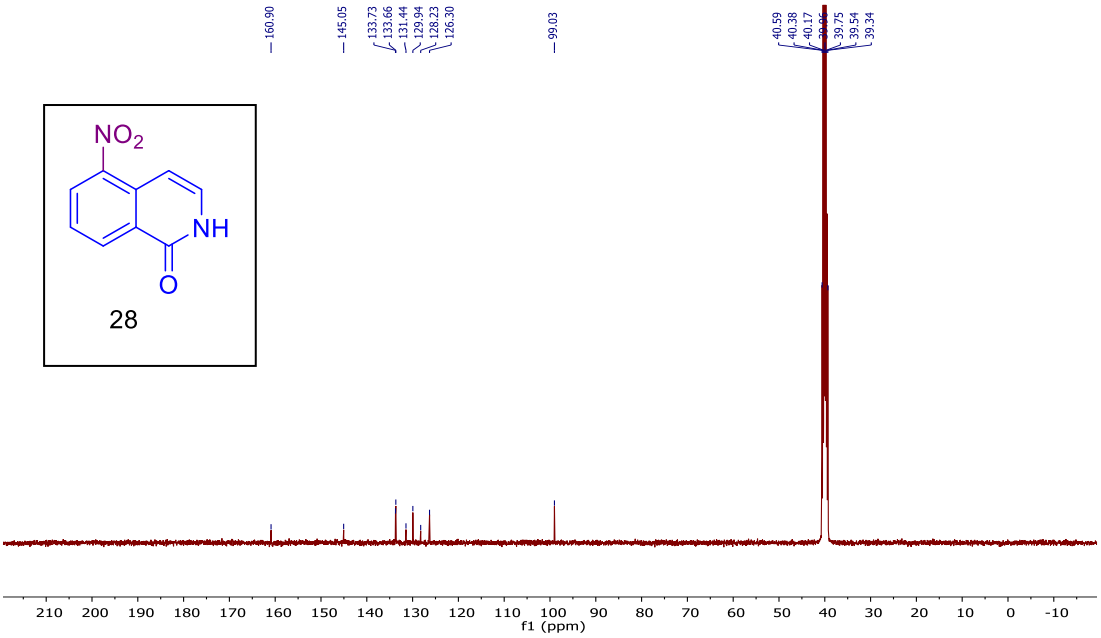

^{13}C NMR (DMSO-d_6, 100 MHz) spectrum of **5-nitroisoquinolin-1(2H)-one (28).**

Chapter-3 Visible light mediated deoxygenation of hetero aryl *N*-oxides

3.1 Introduction

Azaheterocycles containing pyridines and quinolines are very commonly encountered moieties in bioactive compounds/natural products,[1-6] common chemicals, ligands[7 8] and value-added materials.[9] Suitable site-selective functionalization of these electron deficient aza-heterocycles often require activating and directing capability of corresponding *N*-oxides.[10,11] In many cases *N*-oxides are used for distant functionalization through metal catalyzed C-H activation. After the directed functionalization of aromatic rings, it is often required to remove the *N*-oxide to get the desired aromatic aza-heterocycles for various applications mentioned above.

Consequently, development of mild and chemo-selective method for the removal of these oxides from nitrogen in presence of other functional groups/oxide have crucial importance. Over the past few decades, chemists are trying to develop some efficient and greener methods for the deoxygenation of aza-aryl *N*-oxides, due to their large-scale application in organic syntheses as well as in medicinal chemistry. Conventional methods that are used for the deoxygenation processes often require the oxo-philic reagents with harsh reaction conditions,[12–15] which are not suitable for the substrates with labile functional groups or protecting groups. Also, most of these reactions use excess reagent for successful deoxygenation, therefore they are not eco-friendly in nature. Keeping that in mind, we became interested in developing an efficient, cost-effective and eco-friendly method for the deoxygenation of *N*-oxides of aromatic azaheterocycles. Recently, Lee and Wangelin groups have reported some visible-light photocatalyzed chemo selective deoxygenation of heteroaromatic *N*-oxides using Ru and Ir-complex based photocatalysts. However, use of the expensive heavy metal catalysts makes the reaction cost-ineffective and unsustainable for bulk scale use. Organo-photocatalysts are considered as the sustainable and cost-effective alternative

to heavy transition metal complexes in photochemical reactions. Among the various types of organo-photocatalysts, acridinium based photo catalysts have drawn considerable attention in organic transformation due to their high reduction potential and longer lifetimes in the exited state.[16] In this chapter, we have presented a metal-free, atom economic, visible-light catalytic synthetic protocol for room temperature oxygen removal from *N*-oxides using very low loading of inexpensive acridinium based organo-photocatalyst Mes-Acr-Ph$^+$ BF_4^-.

Before describing our work, in the following section we have briefly discussed some of the recent and relevant works to highlight the significance of the current work.

3.2 Literature review:

A deoxygenation method for the deoxygenation of aza-aromatic *N*-oxides has been developed by R. R. Gonzalez group[17] by utilizing benzyl alcohol as the solvent. After the screening of different solvent systems and bases, the authors found that only the combination of benzyl alcohol/sodium hydroxide was capable to produce the desired product with excellent yields at 30 ^{o}C, whereas, the presence of other solvents such as MeOH, EtOH or *n*-BuOH needed high temperature (120 ^{o}C) for the deoxygenation process.

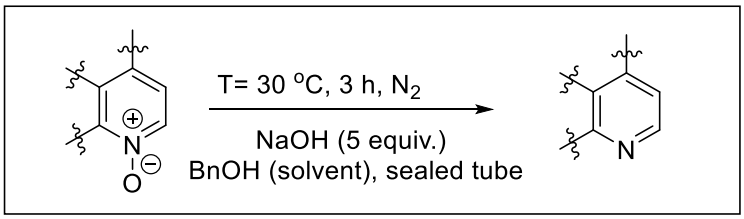

Scheme 3.1 Metal-free deoxygenation of aza-aromatic N-oxides.

A molybdenum-catalyzed chemoselective deoxygenation of heteroaromatic *N*-oxides has been developed by R. Sanz group[18] using pinacol as an oxo-acceptor. In presence of $MoO_2Cl_2(dma)_2$, pinacol first coordinates with the Mo(VI) to form pinacolate-complex which then leads to the formation of oxomolybdenium(IV) complex through an oxidative cleavage of pinacol ligand. Later on, displacement of acetone ligand by *N*-oxide afforded to a new complex which then resulted into re-oxidized and regenerated molybdenum catalyst by releasing the deoxygenated pyridine product. This methodology enabled the cleavage of N-O bond in different substituted quinoline, isoquinoline and pyridine N-oxides under microwave heating condition at 130 ^{o}C.

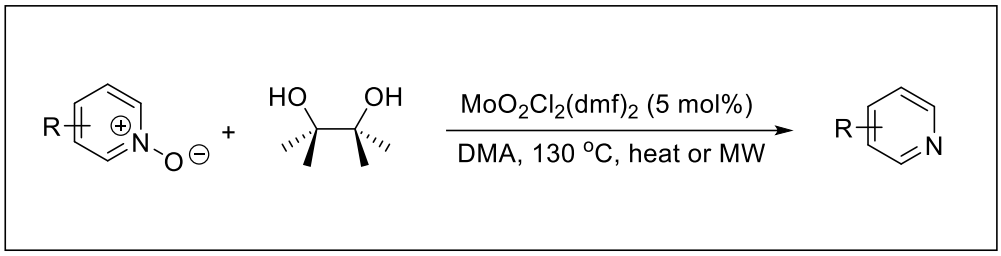

Scheme 3.2 Molybdenum-catalyzed deoxygenation of heteroaromatic N-oxides.

A Cu-catalyzed deoxygenation of *N*-oxides has been reported by J. Jeong *et. al.*,[15] through an oxygen atom transfer mechanism. In this methodology, methyl phenyldiazoacetate was used for the cleavage of N-O bond as an oxygen acceptor. In presence of $Cu(OTf)_2$, diazoacetate first formed copper-carbenoid and then the electrophilic center of in situ generated carbenoid was attacked by oxygen atom of *N*-oxide to form an oxonium ylide, which subsequently resulted in the deoxygenation products, quinoline and benzoyl formate. Although, milder reaction conditions of this methodology tolerate various functional groups but substrates with the functional groups like hydroxyl and amine are not compatible with this method.

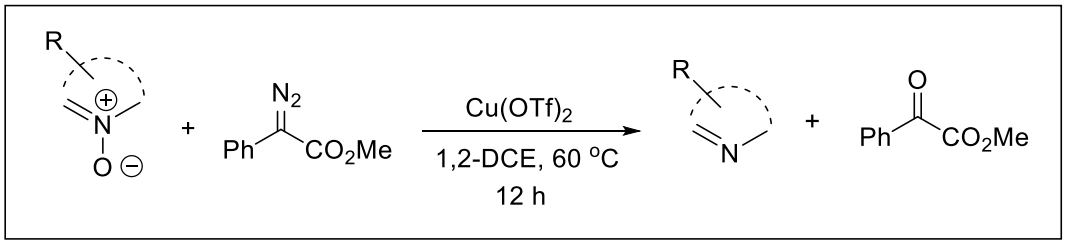

Scheme 3.3 Cu-catalyzed deoxygenation of N-heterocyclic N-oxides.

S. Donck *et. al.*,[19] reported a deoxygenation method for the cleavage of N-O in different *N*-heterocycle *N*-oxides using gold-hybrid carbon nano tube (AuCNT) as the catalyst. To confirm the mechanism, they did an isotope labelling experiment using $PhMe_2SiD$ as the reducing agent. After ^{2}H-NMR spectroscopy, they found that incorporation of D occurred at C-2 position of quinoline. Based on this result, they proposed a mechanism

where first $PhMe_2SiD$ undergoes oxidative Si-D addition on surface of AuCNT. Then the activated silane species reacts with the *N*-oxide with transfer of deuteride at C-2 position. The intermediate then rearomatizes with elimination of silanol to afford deuterated deoxy product quinoline.

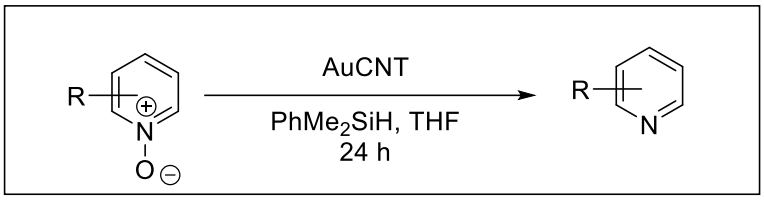

Scheme 3.4 Deoxygenation of aza-heterocycle N-oxides using gold-hybrid carbon nano tube.

A chemoselective deoxygenation of pyridine and amine *N*-oxides method has been developed by R. D. Young group[20] using rhodium pincer complexes in presence of isopropanol in neat condition. The resulting complexes after deoxygenation exhibit η^2 C=O coordination of keto POP pincer ligand, which need to be reduced to regenerate the POP pincer complex. For the reduction of η^2 C=O linkage, a series of reducing agents have been tested and they found that 10 equiv. of *i*-PrOH reduced 90% of the carbonyl linkage, whereas other reducing agents such as H_2 and $SiHEt_3$ resulted no conversion.

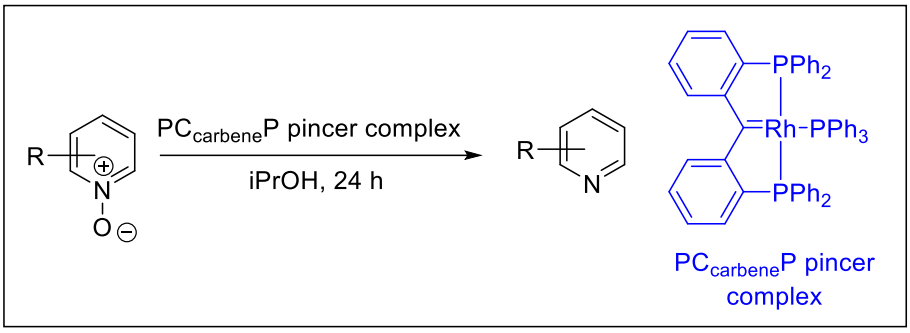

Scheme 3.5 Catalytic deoxygenation of pyridine N-oxides using rhodium POP pincer complex.

In the year 2018, J. H. Lee group[21] reported a transition metal photocatalyzed chemo-selective deoxygenation of aza-heterocycle *N*-oxides under blue light irradiation at room temperature in presence of 30 equiv. of hydrazine hydrate as hydrogen source. They found that in such condition, Ru-photocatalyst is capable of producing quinolines from quinoline-*N*-oxides with good yield. However, a more expensive Ir-based catalyst with higher reduction potential is required for the deoxygenation of pyridine *N*-oxides under the same reaction conditions. In this methodology, the use of excess amount of hydrazine hydrate (30 equiv.) as a hydrogen source makes this procedure less atom-economic and environmentally hazardous.

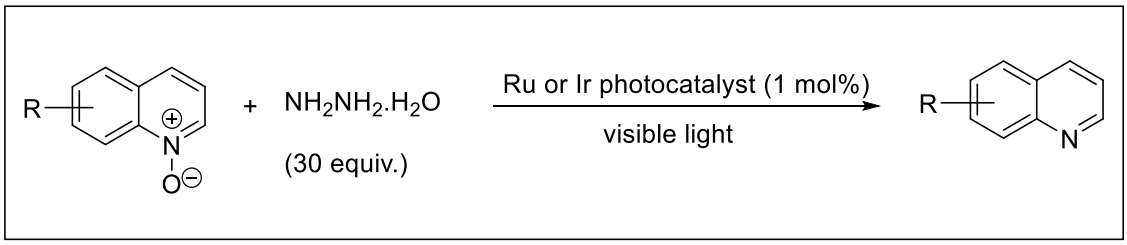

Scheme: 3.6 Visible-light photocatalyzed deoxygenation of aza-heterocycle N-oxides.

A metal-free methodology has been developed by Gupta *et. al.*,[22] for the deoxygenation of amine oxides and sulfoxides to their corresponding amines and sulfides using iodine

as catalyst. They observed that the reaction goes well in DMSO solvent and required 100 ^{o}C temperature and $K_2S_2O_8$ as an oxidizing agent. However, the use of high temperature and strong oxidant $K_2S_2O_8$ narrows the substrate scope of the method. Other solvent systems like- DCM, CH_3CN and DMF were tested but in none of the cases a better yield has been observed.

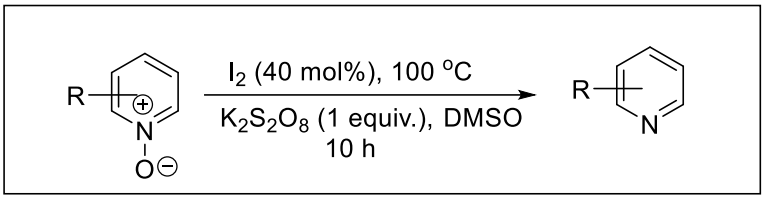

Scheme: 3.7 A metal-free approach to deoxygenation of pyridine N-oxides.

A. J. Wangelin group[23] in the year 2020, reported a catalyst-free deoxygenation process for the deoxygenation of heteroaryl *N*-oxides in presence of visible light at room temperature. They proposed that the deoxygenation reaction takes place through an electron donor–acceptor complex formation between Hantzsch ester and substrate, which absorbs visible light to undergo photoinduced electron and proton transfer between the substrate and esters to afford the product. Although the absence of transition metal photocatalysts made this process less expensive however, the use of Hantzsch ester in stoichiometric amount makes the separation method for the final deoxygenated product more difficult and less atom-economic.

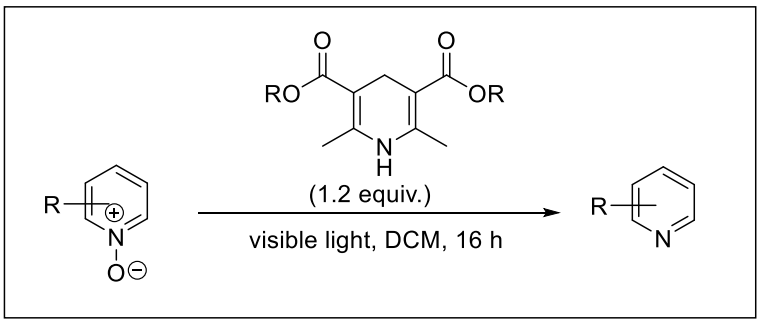

Scheme: 3.8 Catalyst-free N-deoxygenation by Hantzsch ester as reducing agent.

In 2021, J. H. Lee group[24] developed a methodology for chemoselective deoxygenation of aza-aryl *N*-oxides under blue light irradiation at room temperature. For this photocatalytic method they used transition metal Ir or Ru catalyst and Hantzsch ester as a reductant in stoichiometric amount. Like their previous work, in this work also they reported that only Ir-catalyst is suitable for the deoxygenation of substituted pyridinium *N*-oxides under the same reaction conditions.

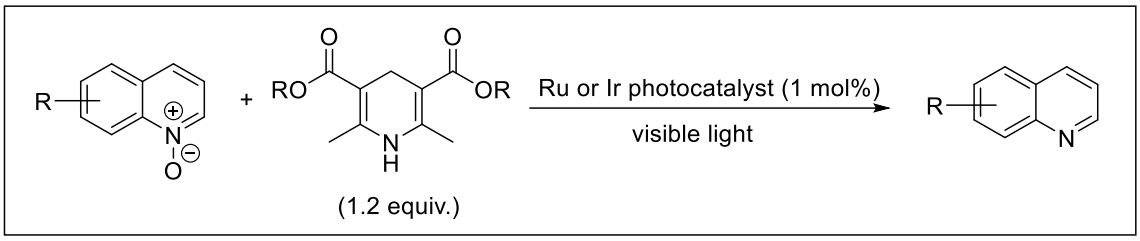

Scheme: 3.9 A chemo-selective deoxygenation of N-heterocyclic N-oxides.

3.3 Synthetic scheme:

In this chapter, an efficient, metal-free visible-light catalytic method for chemoselective deoxygenation of aza-aromatic *N*-oxides under has been developed using Mes-Acr-Ph$^+$ BF_4^- **PC-1** as photocatalyst in presence of di-isoporopyl amine (DIPA), as a hydrogen source. The reaction uses blue LED for efficient deoxygenation of *N*-oxides of various azaheterocycles at room temperature in acetonitrile solvent within 8 h to give up to 90% yield.

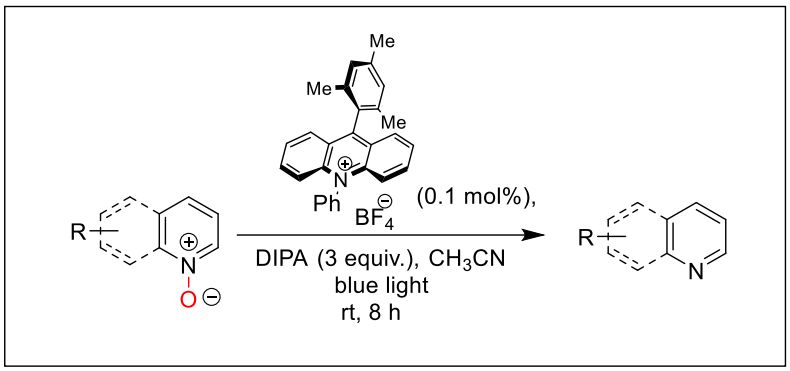

Scheme:3.10 Schematic representation for the deoxygenation of aza-aromatic N-oxides.

3.4 Results and discussions:

Initially, to investigate the feasibility of the deoxygenation of *N*-oxides, we took quinoline *N*-oxide as our model substrate and Mes-Acr-Ph$^+$BF$_4^-$ **(PC-1)** as the organo-photocatalyst. When the reaction was conducted in acetonitrile, after 12 h of blue LED exposure at room temperature, only trace amount of the quinoline *N*-oxide **1a** got deoxygenated to give quinoline **2a**. However, when di-isopropyl amine (DIPA) was added in 1:1 ratio with the substrate as a reductive quencher and reductive hydrogen source, after 8 h of blue LED light exposure, partial deoxygenation of *N*-oxides took place to give 33% of desired quinoline **2a**. Further, increase in the DIPA concentration to 3:1 ratio with substrate increases the yield drastically to generate 91% of **2a** in 8 h of blue LED exposure at room temperature stirring. When other reductive quenchers like, hydrazine hydrate (3:1) is used the reaction failed to display similar efficiency. A series of solvent systems were tested and acetonitrile was found to be the best one among them, whereas the other solvent systems such as DMSO and DCM resulted lower yields of the deoxygenated product (Entry 2 and 3, Table 3.1). Apart from our optimized photocatalyst **PC-1**, other organo-photosensitizers, Eosin and Rose Bengal were also tested but none of the cases, satisfactory yield was obtained (Entry 9 and 10, Table 3.1). Furthermore, the controlled experiment was performed and we found that in absence of blue light, the reaction did not take place. This observation confirmed that the blue light is essential as the energy source for the deoxygenation process. We also performed the reaction in absence of organo-photocatalyst under blue light irradiation, which yielded only 15% of the desired product. Further, this operationally simple protocol can be performed very well under ambient reaction conditions, which do not require any rigorous dry solvent, inert atmosphere or special reaction set up.

Table 3.1 Evaluation of reaction conditions

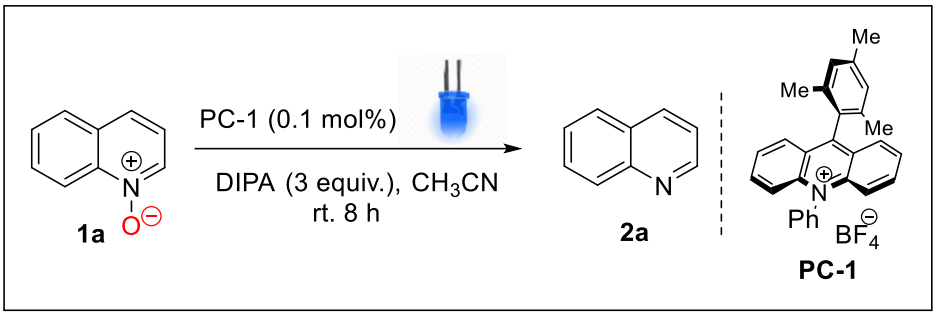

Entry	Deviation from standard conditions	Yield (%)
1	none	91
2	DMSO as solvent	80
3	DCM as solvent	68
4	Without PC-1	24
5	Without DIPA	0
6	With 1.0 equiv. DIPA	35
7	In dark	0
8	0.1 mol% Eosin instead of PC-1	60
9	0.1 mol% Rose Bengal instead of PC-1	53
10	Run in dark at 80 °C	trace

All the yields are isolated yields

Having the optimized reaction conditions in hand, we were interested in exploring the generality of this simple, efficient and greener methodology. A series of quinoline and isoquinoline *N*-oxides with different substituents such as alkyl, alkenyl, alkoxy, halogens, amide and aryl at different positions were examined, which resulted deoxygenated quinolines and isoquinolines with excellent yield (up to 90%) without any difficulty (Fig. 3.1). A variety of electron donating mono- and di- substituted quinoline *N*-oxides such as

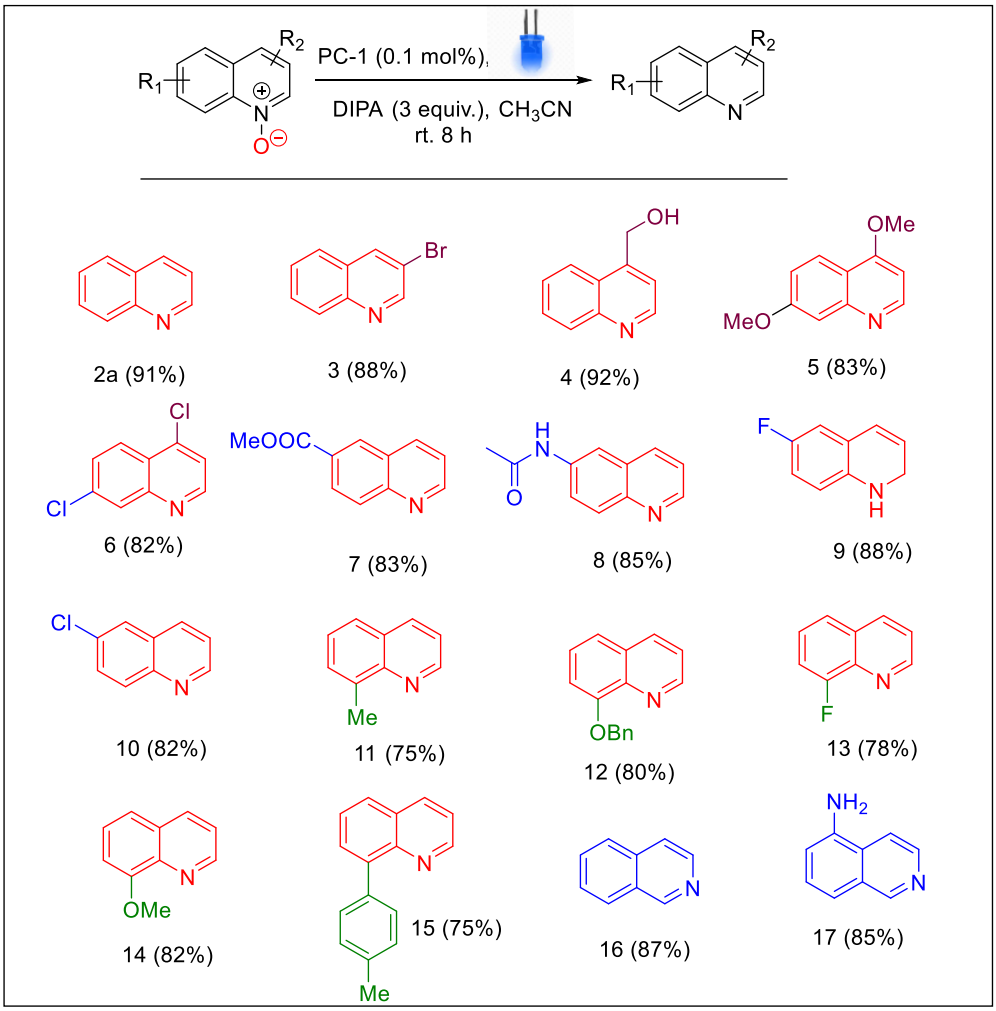

Fig. 3.1 Substrate scope for the deoxygenation of aza-aromatic N-oxides.

4,7-dimethoxy **5,** 8-methyl **11**, 8-benzyloxy **12** and 8-methoxy **14** groups and mono-substituted electron-withdrawing groups such as 6-methylcarboxylate **7,** 6-fluoro **9,** 6-chloro **10**, and 8-fluoro **13** were well compatible with this methodology. Successful deoxygenation without affecting the functional/protecting groups in the substrates **8** and **12** proves the mild nature of the developed methodology. This facile deoxygenation method also enabled us to reduce the nitro group to amine **17** along with the *N*-oxide.

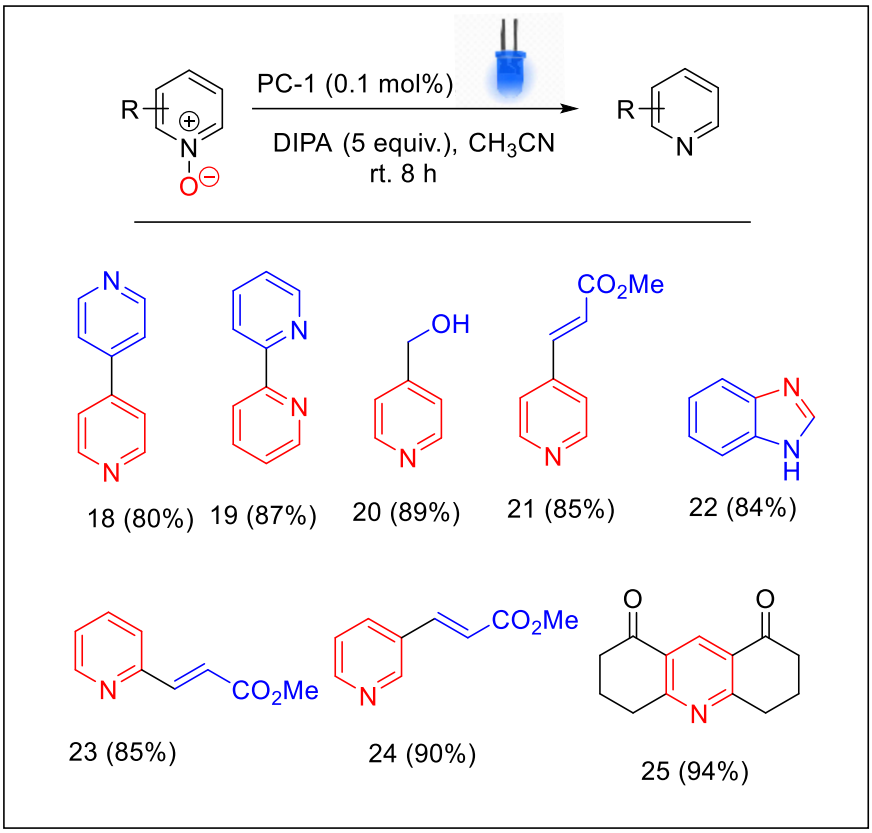

Fig. 3.2 Deoxygenation of substituted pyridine N-oxides.

We also explored the versatility of this photocatalytic deoxygenation methodology in pyridine *N*-oxide derivatives (Fig. 3.2). The deoxygenation of pyridine *N*-oxides required little more amount of di-isopropyl amine (5 equiv.) and this is probably due to the higher bond dissociation energy of the N-O bond of pyridine *N*-oxides compared to the quinoline *N*-oxides.[21,25–28] No significant impact of the electronic nature and position of the substituent has been observed on the reaction yield.

We have also demonstrated the synthetic application of this organo-photocatalyzed deoxygenation methodology, with the help of *N*-oxide as a directing group for selective C-H functionalization of quinoline at 8th position. The preparation of aryl substituted quinoline at 8th position is not possible directly from the parent molecule quinoline with the help of Pd-catalyzed coupling reaction. Because of that, we first converted it into

quinoline *N*-oxide with the help of *m*-CPBA in DCM and then did the coupling reaction with 4-iodotoluene for the formation of compound **2c** in presence of $Pd(OAc)_2$ using water as the solvent. Later on, chemoselective deoxygenation of *N*-oxide through the standard reaction conditions using acridinium based photocatalyst **PC-1** was carried out, which resulted in the final aryl substituted quinoline product **15** with excellent yield (85%).

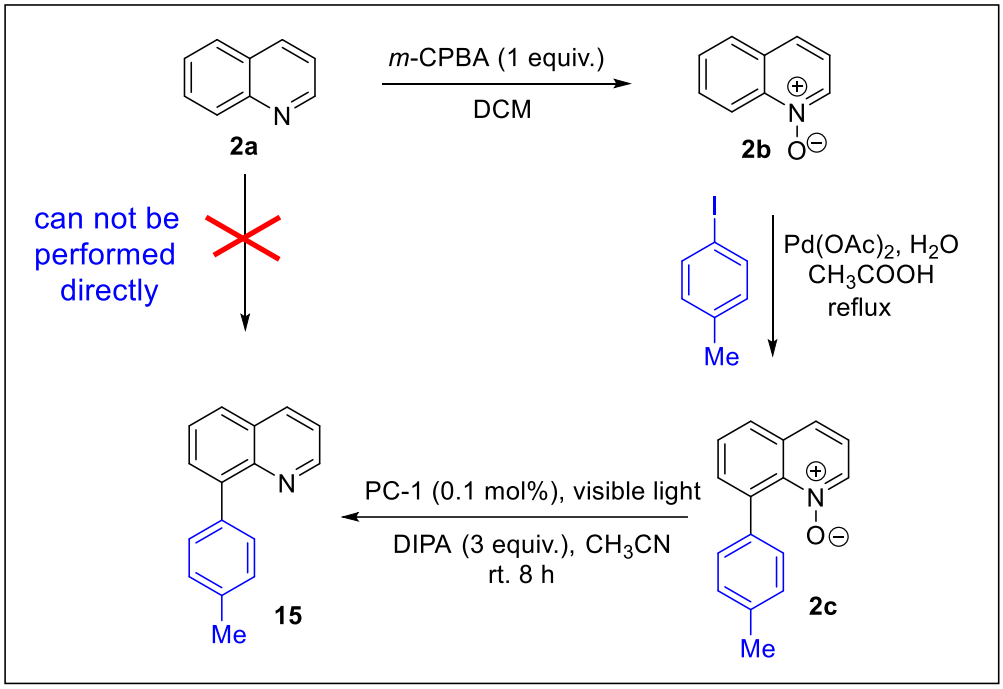

Scheme 3.11 Stepwise synthesis of 8-tolyl substituted quinoline.

A proposed mechanism for the deoxygenation process has been outlined in the Fig. 3.3. Upon irradiation of blue light, the photo catalyst (**PC**) goes to its exited state (**PC***) and then the **PC*** grabs an electron from electron rich DIPA **A** through a photocatalytic single-electron transfer (SET) process to make nitrogen-centered positive radical cation species **B**. After that, proton transfer occurs from electron deficient system **B** to an oxygenated quinoline *N*-oxide **1a**, resulting in the protonated cationic *N*-hydroxyl quinoline **1b**. Again, through another SET process, the *N*-hydroxyl quinoline **1b**

undergoes dehydroxylation with the available **PC***- *via* a reductive cleavage of N-O bond to form the radical species **1c**, with the regeneration of ground state organo-photocatalyst **PC**. The nitrogen-centered quinoline radical **1c** then undergoes a protonation reaction with di-isopropyl amine (DIPA) through a hydrogen atom transfer (HAT) process to generate protonated quinoline intermediate **1d**. Finally, the removal

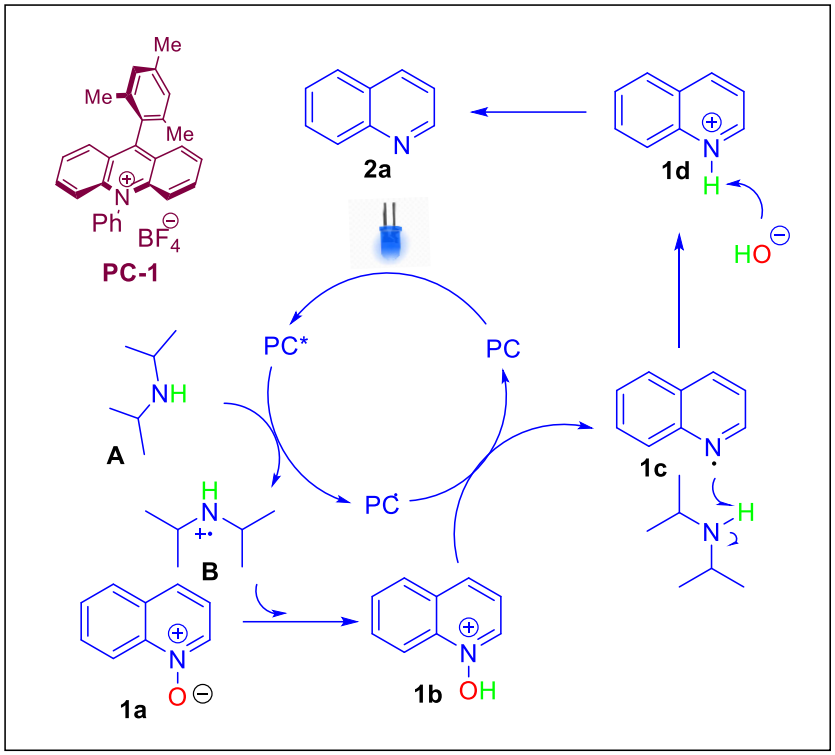

Fig. 3.3 Proposed mechanism for the organo-photocatalytic deoxygenation of N-heterocyclic N-oxides.

of proton by hydroxide ion from cation **1d** gives the deoxygenated product quinoline **2a** and H_2O as the byproduct.

3.5 Conclusions

In summary, an environmental-friendly and metal-free methodology has been developed for the deoxygenation of aza-aryl *N*-oxides using organo-photocatalyst under blue light irradiation at room temperature. Deoxygenation of a variety of quinoline and isoquinoline *N*-oxides having different functional groups like- alkyl, alkoxy or hydroxyl have been carried out to demonstrate the substrate scope and generality of this methodology. The milder conditions of this methodology were also well tolerated by different kind of protecting groups. This methodology also works smoothly in case of pyridine *N*-oxides without any difficulty. Finally, synthesis of 8-tolyl substituted quinoline through the application of *N*-oxide and subsequent oxide removal has been demonstrated to highlight the utility and versatility of this mild visible-light catalytic deoxygenation method.

3.6 Experimental Section:

3.6.1. General procedure for the synthesis of substituted quinoline *N*-oxides.

A 4 mL screw cap vial with a small magnetic bar was charged with quinoline *N*-oxide (0.4 mmol, 1 equiv.), di-isopropyl amine (DIPA) (1.2 mmol, 3 equiv.), 9-mesityl-10-phenyl-acridinium tetrafluoroborate (**PC-1)**, (0.0004 mmol, 0.1 mol%) and CH_3CN (3 mL). The vial was then sealed with plastic screw cap and placed on stirring plate and irradiated for 8 h with a 40 W blue LED at room temperature. Upon completion of the reaction as monitored by TLC, the reaction mixture was concentrated under reduced pressure on rotary evaporator. The reduced residue was purified by column chromatography (gradient eluent of EtOAc/petroleum ether: 1/3 to 1/2) on silica gel to afford quinoline as a liquid.

3.6.2 Procedure for the synthesis of 8-tolyl quinoline *N*-oxide.

A 100 mL RB was charged with quinoline *N*-oxide (1 mmol, 1 equiv.), 4-iodotoluene (2 mmol, 2 equiv.), $Pd(OAc)_2$ ((0.1 mmol, 0.1 equiv.)) and CH_3COOAg (3.5 mmol, 3.5 equiv.) in acetic acid and the whole solution mixture were stirred at 120 ^oC for 8h. Upon completion of the reaction as monitored by TLC, the reaction mixture was concentrated under reduced pressure on rotary evaporator. After that, the reaction mixture was extracted with $CHCl_3$ (20mL x 3) and dried over anhydrous Na_2SO_4. Next, the extracted residue was purified by column chromatography (gradient eluent of EtOAc/petroleum ether: 1/2 to 1) on silica gel to afford 8-tolyl quinoline *N*-oxide (73%) as a solid.

3.7 Spectral data of deoxygenated compounds

quinoline (2a):

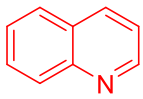

2a

^{1}H NMR (400 MHz, Chloroform-*d*) δ 8.94 (d, *J* = 4.2 Hz, 1H), 8.17 (dd, *J* = 15.0, 8.4 Hz, 2H), 7.84 (d, *J* = 8.1 Hz, 1H), 7.74 (t, *J* = 7.7 Hz, 1H), 7.57 (t, *J* = 7.5 Hz, 1H), 7.42 (dd, *J* = 8.2, 4.2 Hz, 1H). ^{13}C NMR (100 MHz, $CDCl_3$) δ 150.29, 148.17, 136.19, 129.52, 129.33, 128.32, 127.79, 126.59, 121.08. HRMS: m/z (ESI) calculated for (C_9H_7N) $[M+H]^+$: 130.0651, measured: 130.0656.

3-bromoquinoline (3):

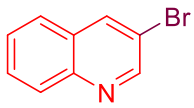

3

^{1}H NMR (400 MHz, Chloroform-*d*) δ 8.81 (d, *J* = 5.1 Hz, 1H), 8.18 (d, *J* = 8.3 Hz, 1H), 7.55 – 7.43 (m, 2H), 7.36 (d, *J* = 8.1 Hz, 1H), 7.22 (d, *J* = 7.6 Hz, 1H). ^{13}C NMR (100 MHz, $CDCl_3$) δ 152.28, 147.90, 138.36, 136.11, 128.55, 127.75, 121.82, 117.88, 110.05. HRMS: m/z (ESI) calculated for (C_9H_9BrN) $[M+H]^+$: 207.9756 and 209.9736, measured: 207.9761 and 209.9739.

quinolin-4-ylmethanol (4):

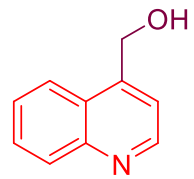

4

^{1}H NMR (400 MHz, DMSO-d_6) δ 8.88 (d, *J* = 4.3 Hz, 1H), 8.09 – 8.01 (m, 2H), 7.76 (t, *J* = 7.9 Hz, 1H), 7.63 (d, *J* = 7.9 Hz, 1H), 7.59 (d, *J* = 4.3 Hz, 1H), 5.60 (t, *J* = 5.5 Hz, 1H), 5.05 (d, *J* = 5.4 Hz, 2H). ^{13}C NMR (100 MHz, DMSO) δ 150.91, 148.14, 147.78, 129.96, 129.55, 126.84, 125.91, 123.99, 118.50, 60.11, 39.36. HRMS: m/z (ESI) calculated for ($C_{10}H_9NO$) $[M+H]^+$: 160.0757, measured: 160.0759.

7-chloro-4-methoxyquinoline (5):

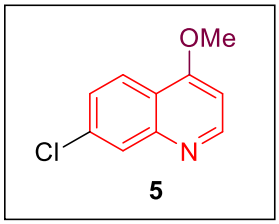

^{1}H NMR (400 MHz, Chloroform-*d*) δ 8.77 (d, *J* = 5.2 Hz, 1H), 8.15 (d, *J* = 8.9 Hz, 1H), 8.04 (s, 1H), 7.47 (d, *J* = 10.9 Hz, 1H), 6.76 (d, *J* = 5.2 Hz, 1H), 4.07 (s, 3H). ^{13}C NMR (100 MHz, $CDCl_3$) δ 162.37, 152.53, 149.66, 135.78, 127.86, 126.58, 123.41, 119.82, 100.35, 55.81. HRMS: m/z (ESI) calculated for ($C_{10}H_8ClNO$) $[M+H]^+$: 194.0367, measured: 194.0370

4,7-dichloroquinoline (6):

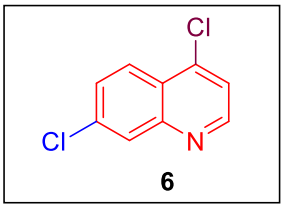

^{1}H NMR (400 MHz, Chloroform-*d*) δ 8.72 (d, *J* = 4.7 Hz, 1H), 8.06 (dd, *J* = 5.5, 3.4 Hz, 2H), 7.51 (d, *J* = 11.0 Hz, 1H), 7.41 (d, *J* = 4.7 Hz, 1H). ^{13}C NMR (100 MHz, $CDCl_3$) δ 150.88, 149.32, 142.57, 136.43, 128.67, 128.53, 125.46, 124.87, 121.33. HRMS: m/z (ESI) calculated for ($C_9H_5Cl_2N$) $[M+Na]^+$: 219.9691, measured: 219.9695.

methyl quinoline-6-carboxylate (7):

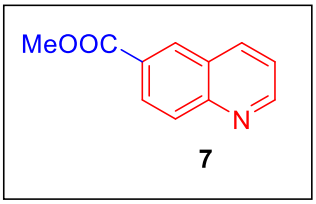

^{1}H NMR (400 MHz, Chloroform-*d*) δ 9.09 (d, *J* = 3.0 Hz, 1H), 8.62 (s, 1H), 8.32 (d, *J* = 10.2 Hz, 2H), 8.21 (d, *J* = 8.9 Hz, 1H), 7.53 (dd, *J* = 8.3, 4.3 Hz, 1H), 4.02 (s, 3H). ^{13}C NMR (100 MHz, $CDCl_3$) δ 166.52, 152.63, 149.77, 137.84, 131.05, 129.53, 129.21, 128.28, 127.53, 121.92, 52.50. HRMS: m/z (ESI) calculated for ($C_{11}H_9NO_2$) $[M+H]^+$: 188.0706, measured: 188.0702.

N-(quinolin-6-yl)acetamide (8):

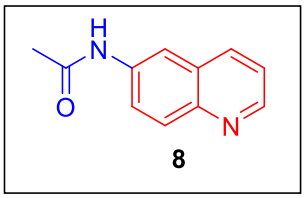

^{1}H NMR (400 MHz, DMSO-d_6) δ 10.30 (s, 1H), 8.79 (d, *J* = 5.4 Hz, 1H), 8.38 (s, 1H), 8.31 (d, *J* = 8.1 Hz, 1H), 7.97 (d, *J* = 9.0 Hz, 1H), 7.81 (d, *J* = 9.1 Hz, 1H), 7.49 (dd, *J* = 8.3, 4.2 Hz, 1H), 2.13 (s, 3H). ^{13}C NMR (100 MHz, DMSO-d_6) δ 169.28, 149.02,

144.57, 137.82, 136.38, 129.49, 128.87, 123.95, 122.18, 115.11, 24.55. HRMS: m/z (ESI) calculated for ($C_{11}H_{10}N_2O$) $[M+H]^+$: 187.0866, measured: 187.0869.

6-fluoroquinoline (9):

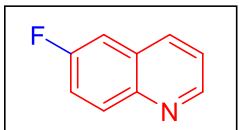

9

^{1}H NMR (400 MHz, Chloroform-*d*) δ 8.91 (d, *J* = 3.9 Hz, 1H), 8.14 (dd, *J* = 9.0, 5.3 Hz, 2H), 7.51 (td, *J* = 8.8, 2.8 Hz, 1H), 7.44 (dt, *J* = 8.2, 4.3 Hz, 2H). ^{13}C NMR (100 MHz, $CDCl_3$) δ 161.65, 159.18, 149.72, 145.36, 135.52, 131.91, 128.86, 121.79, 119.93, 119.67, 110.81. HRMS: m/z (ESI) calculated for (C_9H_6FN) $[M+H]^+$: 148.0557, measured: 148.0556.

6-chloroquinoline (10):

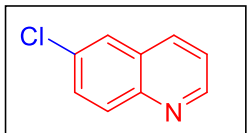

10

^{1}H NMR (400 MHz, Chloroform-*d*) δ 8.88 (dd, *J* = 4.1, 1.5 Hz, 1H), 8.03 (d, *J* = 8.9 Hz, 2H), 7.76 (d, *J* = 2.3 Hz, 1H), 7.63 (dd, *J* = 9.0, 2.2 Hz, 1H), 7.39 (dd, *J* = 8.3, 4.2 Hz, 1H). ^{13}C NMR (100 MHz, $CDCl_3$) δ 150.53, 146.57, 135.12, 132.29, 131.05, 130.40, 128.81, 126.39, 121.88. HRMS: m/z (ESI) calculated for (C_9H_6ClN) $[M+H]^+$: 164.0262, measured: 164.0269.

8-methylquinoline (11):

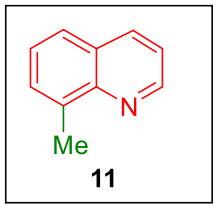

11

^{1}H NMR (400 MHz, Chloroform-*d*) δ 8.98 (dd, *J* = 4.1, 1.6 Hz, 1H), 8.16 (dd, *J* = 8.2, 1.6 Hz, 1H), 7.69 (d, *J* = 8.1 Hz, 1H), 7.59 (d, *J* = 6.9 Hz, 1H), 7.47 (d, *J* = 7.6 Hz, 1H), 7.45 – 7.39 (m, 1H), 2.86 (s, 3H). ^{13}C NMR (100 MHz, $CDCl_3$) δ 149.22, 147.31, 137.07, 136.39, 129.67, 128.31, 126.33, 125.86, 120.83, 18.10. HRMS: m/z (ESI) calculated for ($C_{10}H_9N$) $[M+H]^+$: 144.0808, measured: 144.0803.

8-(benzyloxy)quinoline (12):

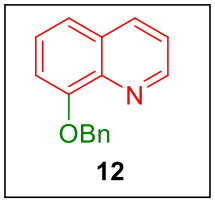

^{1}H NMR (400 MHz, Chloroform-*d*) δ 8.99 (dd, *J* = 4.2, 1.5 Hz, 1H), 8.13 (d, *J* = 9.7 Hz, 1H), 7.54 (d, *J* = 7.4 Hz, 2H), 7.44 (dd, *J* = 8.3, 4.2 Hz, 1H), 7.41 – 7.35 (m, 4H), 7.32 (d, *J* = 7.3 Hz, 1H), 7.07 – 7.02 (m, 1H), 5.46 (s, 2H). ^{13}C NMR (100 MHz, $CDCl_3$) δ 154.29, 149.40, 140.45, 136.93, 135.96, 129.51, 128.67, 127.86, 127.16, 126.61, 121.65, 119.86, 109.82, 70.70. HRMS: m/z (ESI) calculated for ($C_{16}H_{13}NO$) $[M+H]^+$: 236.1070, measured: 236.1074.

8-fluoroquinoline (13):

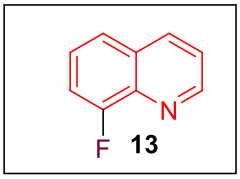

^{1}H NMR (400 MHz, Chloroform-*d*) δ 8.99 (d, *J* = 5.1 Hz, 1H), 8.21 (d, *J* = 8.4 Hz, 1H), 7.64 (d, *J* = 8.1 Hz, 1H), 7.51 (td, *J* = 8.5, 4.5 Hz, 2H), 7.46 – 7.39 (m, 1H). ^{13}C NMR (100 MHz, $CDCl_3$) δ 159.34, 156.79, 150.53, 138.61, 138.49, 135.76, 129.87, 126.43, 126.34, 123.43, 122.05, 113.62, 113.44. HRMS: m/z (ESI) calculated for (C_9H_6FN) $[M+H]^+$: 148.0557, measured: 148.0559.

8-methoxyquinoline (14):

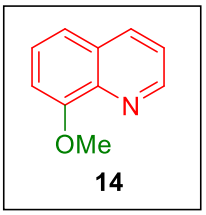

^{1}H NMR (400 MHz, Chloroform-*d*) δ 8.93 (dd, *J* = 4.1, 1.6 Hz, 1H), 8.13 (d, *J* = 9.7 Hz, 1H), 7.54 – 7.35 (m, 3H), 7.06 (d, *J* = 7.6 Hz, 1H), 4.10 (s, 3H). ^{13}C NMR (100 MHz, $CDCl_3$) δ 155.43, 149.22, 140.24, 135.86, 129.37, 126.70, 121.67, 119.55, 107.56, 55.95. HRMS: m/z (ESI) calculated for ($C_{10}H_9NO$) $[M+Na]^+$: 182.0576, measured: 182.0579.

8-(p-tolyl)quinoline (15):

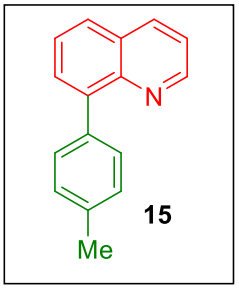

^{1}H NMR (400 MHz, Chloroform-*d*) δ 8.58 (d, *J* = 5.3 Hz, 1H), 8.07 (d, *J* = 8.4 Hz, 1H), 7.92 (d, *J* = 8.0 Hz, 1H), 7.67 (t, *J* = 7.6 Hz, 1H), 7.61 (d, *J* = 7.2 Hz, 1H), 7.41 – 7.32 (m, 1H), 7.23 (d, *J* = 7.7 Hz, 2H), 7.08 (d, *J* = 7.6 Hz, 2H), 2.20 (s, 3H). ^{13}C NMR (100 MHz, $CDCl_3$) δ 139.61, 139.14, 137.75, 136.23, 136.17, 135.99, 132.05, 131.73, 128.43, 128.31, 128.22, 127.86, 120.84, 21.13. HRMS: m/z (ESI) calculated for (C_9H_7N) $[M+H]^+$: 130.0651, measured: 130.0656.

isoquinoline (16):

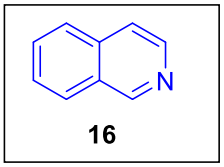

^{1}H NMR (400 MHz, Chloroform-*d*) δ 9.28 (s, 1H), 8.55 (d, *J* = 5.7 Hz, 1H), 7.99 (d, *J* = 8.2 Hz, 1H), 7.84 (d, *J* = 8.2 Hz, 1H), 7.72 (t, *J* = 7.5 Hz, 1H), 7.67 (d, *J* = 5.8 Hz, 1H), 7.63 (t, *J* = 7.4 Hz, 1H). ^{13}C NMR (100 MHz, $CDCl_3$) δ 152.53, 142.98, 135.80, 130.37, 128.70, 127.65, 127.26, 126.48, 120.48. HRMS: m/z (ESI) calculated for (C_9H_7N) $[M+H]^+$: 130.0651, measured: 130.0656.

isoquinolin-5-amine (17):

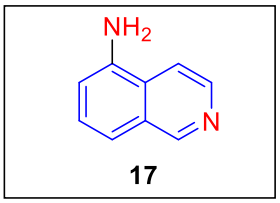

^{1}H NMR (400 MHz, Chloroform-*d*) δ 9.20 (s, 1H), 8.51 (d, *J* = 6.0 Hz, 1H), 7.60 (d, *J* = 6.0 Hz, 1H), 7.43 (d, *J* = 4.4 Hz, 2H), 6.98 (t, *J* = 4.2 Hz, 1H), 4.09 (s, 2H). ^{13}C NMR (100 MHz, $CDCl_3$) δ 152.95, 142.00, 141.30, 129.42, 127.79, 126.01, 118.01, 114.08, 113.10. HRMS: m/z (ESI) calculated for ($C_9H_8N_2$) $[M+H]^+$: 145.0760, measured: 145.0765.

4,4'-bipyridine (18):

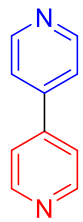

18

^{1}H NMR (400 MHz, Chloroform-*d*) δ 8.77 (d, *J* = 6.1 Hz, 1H), 7.57 (d, *J* = 6.1 Hz, 1H). ^{13}C NMR (100 MHz, $CDCl_3$) δ 150.69, 145.58, 121.46. HRMS: m/z (ESI) calculated for ($C_{10}H_8N_2$) $[M+H]^+$: 157.0760, measured: 157.0763.

2,2'-bipyridine (19):

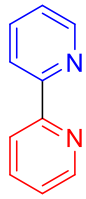

19

^{1}H NMR (400 MHz, Chloroform-*d*) δ 9.24 (d, *J* = 4.6 Hz, 1H), 8.95 (d, *J* = 8.8 Hz, 1H), 8.38 (t, *J* = 7.6 Hz, 1H), 7.87 (t, *J* = 6.9 Hz, 1H). ^{13}C NMR (100 MHz, $CDCl_3$) δ 156.15, 149.19, 136.98, 123.75, 121.14, HRMS: m/z (ESI) calculated for (C_9H_7NO) $[M+H]^+$: 157.0760, measured: 157.0758.

pyridin-4-ylmethanol (20):

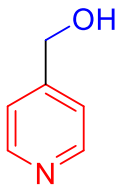

20

^{1}H NMR (400 MHz, Chloroform-*d*) δ 8.43 (d, *J* = 6.0 Hz, 2H), 7.30 (d, *J* = 5.7 Hz, 2H), 5.09 (s, 1H), 4.73 (s, 2H). ^{13}C NMR (100 MHz, $CDCl_3$) δ 151.53, 149.06, 121.31, 62.84. HRMS: m/z (ESI) calculated for (C_6H_7NO) $[M+H]^+$: 110.0600, measured: 110.0604.

methyl (E)-3-(pyridin-4-yl)acrylate (21):

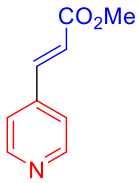

21

^{1}H NMR (400 MHz, Chloroform-*d*) δ 8.65 (d, *J* = 5.9 Hz, 2H), 7.61 (d, *J* = 16.1 Hz, 1H), 7.37 (d, *J* = 6.0 Hz, 2H), 6.60 (d, *J* = 16.1 Hz, 1H), 3.83 (s, 3H). ^{13}C NMR (100 MHz, $CDCl_3$) δ 166.45, 150.46, 141.90, 141.66, 122.49, 121.85, 52.06. HRMS:

m/z (ESI) calculated for ($C_9H_9NO_2$) $[M+Na]^+$: 186.0525, measured: 186.0529.

1H-benzo[d]imidazole (22):

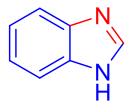

22

^{1}H NMR (400 MHz, DMSO-d_6) δ 8.25 (s, 1H), 7.61 (dd, J = 6.0, 3.2 Hz, 2H), 7.20 (dd, J = 6.0, 3.1 Hz, 2H). ^{13}C NMR (100 MHz, DMSO-d_6) δ 142.38, 138.47, 122.23, 115.77. HRMS: m/z (ESI) calculated for ($C_7H_6N_2$) $[M+H]^+$: 119.0604, measured: 119.0600.

methyl (E)-3-(pyridin-2-yl)acrylate (23):

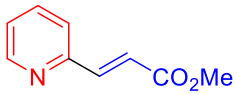

23

^{1}H NMR (400 MHz, Chloroform-d) δ 8.64 (d, J = 4.4 Hz, 1H), 7.74 – 7.65 (m, 2H), 7.42 (d, J = 7.8 Hz, 1H), 7.26 (dd, J = 6.9, 5.0 Hz, 1H), 6.93 (d, J = 15.7 Hz, 1H), 3.81 (s, 3H). ^{13}C NMR (100 MHz, $CDCl_3$) δ 167.23, 152.83, 150.14, 143.56, 136.80, 124.28, 121.92, 51.87. HRMS: m/z (ESI) calculated for ($C_9H_9NO_2$) $[M+H]^+$: 164.0706, measured: 164.00703.

methyl (E)-3-(pyridin-3-yl)acrylate (24):

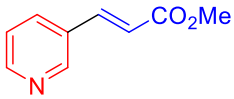

24

^{1}H NMR (400 MHz, Chloroform-d) δ 8.75 (s, 1H), 8.61 (d, J = 6.3 Hz, 1H), 7.84 (d, J = 7.9 Hz, 1H), 7.69 (d, J = 16.1 Hz, 1H), 7.34 (dd, J = 7.9, 4.9 Hz, 1H), 6.52 (d, J = 16.1 Hz, 1H), 3.83 (s, 3H). ^{13}C NMR (100 MHz, $CDCl_3$) δ 166.77, 151.04, 149.73, 141.16, 134.23, 130.14, 123.77, 119.98, 51.94. HRMS: m/z (ESI) calculated for ($C_9H_9NO_2$) $[M+H]^+$: 164.0706, measured: 164.0700.

3,4,6,7-tetrahydroacridine-1,8(2H,5H)-dione (25):

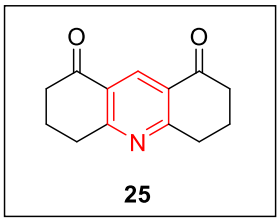

^{1}H NMR (400 MHz, Chloroform-*d*) δ 8.78 (s, 1H), 3.14 (t, *J* = 6.2 Hz, 4H), 2.68 (t, *J* = 6.8 Hz, 4H), 2.19 (p, *J* = 6.4 Hz, 4H). ^{13}C NMR (100 MHz, $CDCl_3$) δ 196.76, 167.29, 134.55, 127.23, 77.43, 77.12, 76.80, 38.40, 32.94, 21.41. HRMS: m/z (ESI) calculated for ($C_{13}H_{13}NO_2$) $[M+H]^+$: 216.1019, measured: 216.1023.

References

(1) Albratty, M.; Alhazmi, H. A. Novel Pyridine and Pyrimidine Derivatives as Promising Anticancer Agents: A Review. *Arab. J. Chem.* **2022**, *15* (6), 103846.

(2) Tahir, T.; Ashfaq, M.; Saleem, M.; Rafiq, M.; Shahzad, M. I.; Kotwica-Mojzych, K.; Mojzych, M. Pyridine Scaffolds, Phenols and Derivatives of Azo Moiety: Current Therapeutic Perspectives. *Molecules* **2021**, *26* (16), 4872.

(3) Ling, Y.; Hao, Z.-Y.; Liang, D.; Zhang, C.-L.; Liu, Y.-F.; Wang, Y. The Expanding Role of Pyridine and Dihydropyridine Scaffolds in Drug Design. *Drug Des. Devel. Ther.* **2021**, *15*, 4289–4338.

(4) Dorababu, A. Quinoline: A Promising Scaffold in Recent Antiprotozoal Drug Discovery. *ChemistrySelect* **2021**, *6* (9), 2164–2177.

(5) Herraiz, T.; Guillén, H.; González-Peña, D.; Arán, V. J. Antimalarial Quinoline Drugs Inhibit β-Hematin and Increase Free Hemin Catalyzing Peroxidative Reactions and Inhibition of Cysteine Proteases. *Sci. Rep.* **2019**, *9* (1), 15398.

(6) A. Mohamed, M. F.; A. Abuo-Rahma, G. E.-D. Molecular Targets and Anticancer Activity of Quinoline–Chalcone Hybrids: Literature Review. *RSC Adv.* **2020**, *10* (52), 31139–31155.

(7) Reiersølmoen, A. C.; Fiksdahl, A. Pyridine- and Quinoline-Based Gold(III) Complexes: Synthesis, Characterization, and Application. *Eur. J. Org. Chem.* **2020**, *2020* (19), 2867–2877.

(8) Dai, Z. Steric and Stereochemical Modulation in Pyridyl- and Quinolyl-Containing Ligands. *Molecules* **2016**, *21* (12), 1647.

(9) Chakraborty, G.; Das, P.; K. Mandal, S. Quinoline-Tagged Fluorescent Organic Probes for Sensing of Nitro-Phenolic Compounds and Zn 2+ Ions at the Ppb Level. *Mater. Adv.* **2021**, *2* (7), 2334–2346.

(10) Wrzeszcz, Z.; Siedlecka, R. Heteroaromatic N-Oxides in Asymmetric Catalysis: A Review. *Molecules* **2020**, *25* (2), 330.

(11) Wang, D.; Désaubry, L.; Li, G.; Huang, M.; Zheng, S. Recent Advances in the Synthesis of C2-Functionalized Pyridines and Quinolines Using N-Oxide Chemistry. *Adv. Synth. Catal.* **2021**, *363* (1), 2–39.

(12) Wang, Y.; Espenson, J. H. Efficient Catalytic Conversion of Pyridine N-Oxides to Pyridine with an Oxorhenium(V) Catalyst. *Org. Lett.* **2000**, *2* (22), 3525–3526.

(13) Yadav, J. S.; Subba Reddy, B. V.; Reddy, M. M. Indium-Mediated Deoxygenation of Amine-N-Oxides in Aqueous Media†IICT Communication No. 4394†. *Tetrahedron Lett.* **2000**, *41* (15), 2663–2665.

(14) Kokatla, H. P.; Thomson, P. F.; Bae, S.; Doddi, V. R.; Lakshman, M. K. Reduction of Amine N-Oxides by Diboron Reagents. *J. Org. Chem.* **2011**, *76* (19), 7842–7848.

(15) Jeong, J.; Lee, D.; Chang, S. Copper-Catalyzed Oxygen Atom Transfer of N-Oxides Leading to a Facile Deoxygenation Procedure Applicable to Both Heterocyclic and Amine N-Oxides. *Chem. Commun.* **2015**, *51* (32), 7035–7038.

(16) Romero, N. A.; Nicewicz, D. A. Organic Photoredox Catalysis. *Chem. Rev.* **2016**, *116* (17), 10075–10166.

(17) Bjørsvik, H.-R.; Gambarotti, C.; Jensen, V. R.; González, R. R. A Novel Efficient Deoxygenation Process for N-Heteroarene N-Oxides. *J. Org. Chem.* **2005**, *70* (8), 3218–3224.

(18) Rubio-Presa, R.; Fernández-Rodríguez, M. A.; Pedrosa, M. R.; Arnaiz, F. J.; Sanz, R. Molybdenum-Catalyzed Deoxygenation of Heteroaromatic N-Oxides and Hydroxides Using Pinacol as Reducing Agent. *Adv. Synth. Catal.* **2017**, *359* (10), 1752–1757.

(19) Donck, S.; Gravel, E.; Shah, N.; Jawale, D. V.; Doris, E.; Namboothiri, I. N. N. Deoxygenation of Amine N-Oxides Using Gold Nanoparticles Supported on Carbon Nanotubes. *RSC Adv.* **2015**, *5* (63), 50865–50868.

(20) Tinnermann, H.; Sung, S.; Cala, B. A.; Gill, H. J.; Young, R. D. Catalytic Deoxygenation of Amine and Pyridine N-Oxides Using Rhodium PCcarbeneP Pincer Complexes. *Organometallics* **2020**, *39* (6), 797–803.

(21) Kim, K. D.; Lee, J. H. Visible-Light Photocatalyzed Deoxygenation of N-Heterocyclic N-Oxides. *Org. Lett.* **2018**, *20* (23), 7712–7716.

(22) Gupta, S.; Sureshbabu, P.; Singh, A. K.; Sabiah, S.; Kandasamy, J. Deoxygenation of Tertiary Amine N-Oxides under Metal Free Condition Using Phenylboronic Acid. *Tetrahedron Lett.* **2017**, *58* (10), 909–913.

(23) Konev, M. O.; Cardinale, L.; Jacobi von Wangelin, A. Catalyst-Free *N* -Deoxygenation by Photoexcitation of Hantzsch Ester. *Org. Lett.* **2020**, *22* (4), 1316–1320.

(24) An, J. H.; Kim, K. D.; Lee, J. H. Highly Chemoselective Deoxygenation of N-Heterocyclic N-Oxides Using Hantzsch Esters as Mild Reducing Agents. *J. Org. Chem.* **2021**, *86* (3), 2876–2894.

(25) Łukomska, M.; Rybarczyk-Pirek, A. J.; Jabłoński, M.; Palusiak, M. The Nature of NO-Bonding in N-Oxide Group. *Phys. Chem. Chem. Phys.* **2015**, *17* (25), 16375–16387.

(26) Ribeiro da Silva, M. D. M. C.; Santos, L. M. N. B. F.; Silva, A. L. R.; Fernandes, Ó.; Acree, W. E. Energetics of 6-Methoxyquinoline and 6-Methoxyquinoline N-Oxide: The Dissociation Enthalpy of the (N–O) Bond. *J. Chem. Thermodyn.* **2003**, *35* (7), 1093–1100.

(27) Bach, R. D.; Schlegel, H. B. The Bond Dissociation Energy of the N–O Bond. *J. Phys. Chem. A* **2021**, *125* (23), 5014–5021.

(28) Miyazaki, H.; Kubota, T.; Yamakawa, M. The Characterization of the Electronic Spectra of Heterocyclic Amine <I>N</I>-Oxides by Means of the Non-Aqueous Oxidation and Reduction Potentials and the Substituent Effects on Them. *Bull. Chem. Soc. Jpn.* **1972**, *45* (3), 780–785.

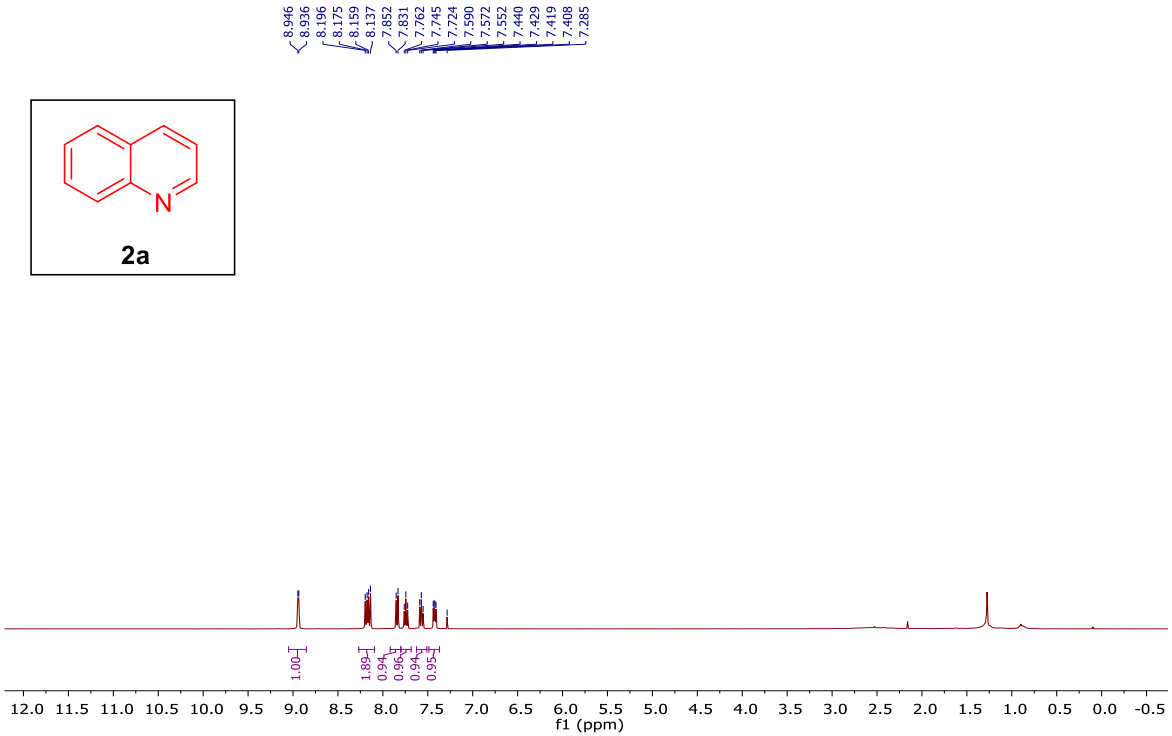

^{1}H NMR ($CDCl_3$, 400 MHz) spectrum of ***quinoline (2a).***

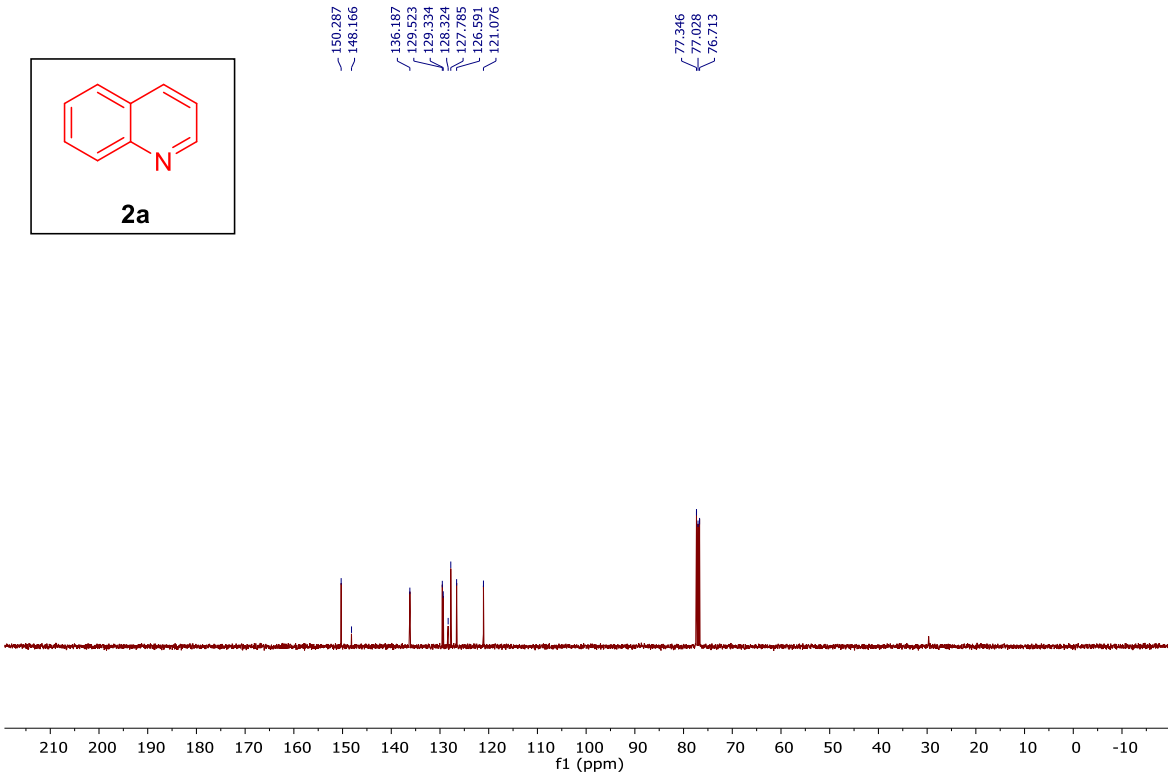

^{13}C NMR ($CDCl_3$, 100 MHz) spectrum of ***quinoline (2a).***

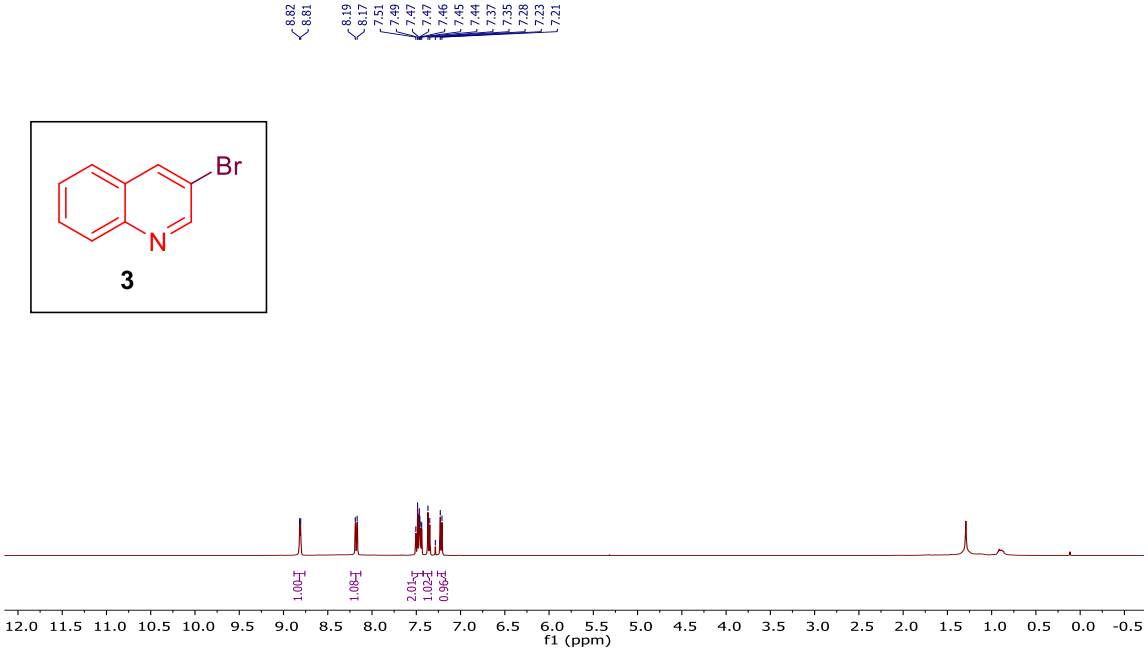

^{1}H NMR ($CDCl_3$, 400 MHz) spectrum of ***3-bromoquinoline (3).***

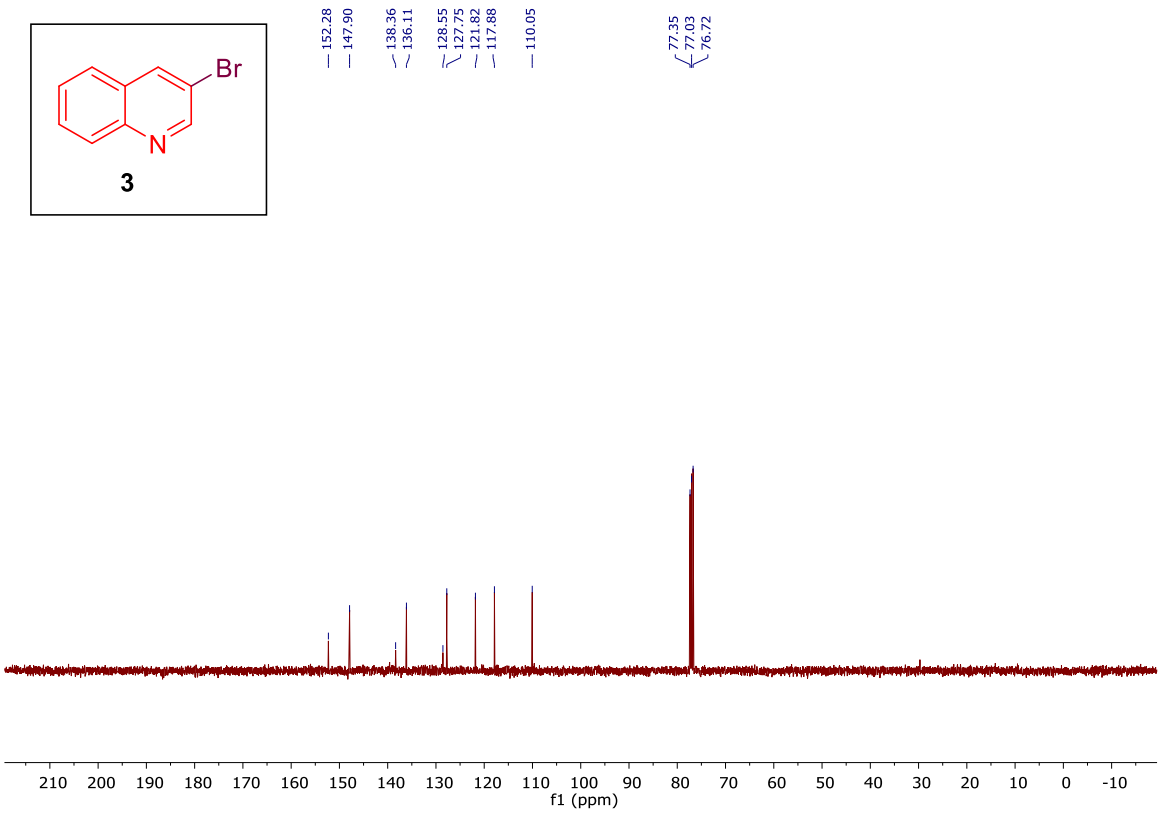

^{13}C NMR ($CDCl_3$, 100 MHz) spectrum of ***3-bromoquinoline (3).***

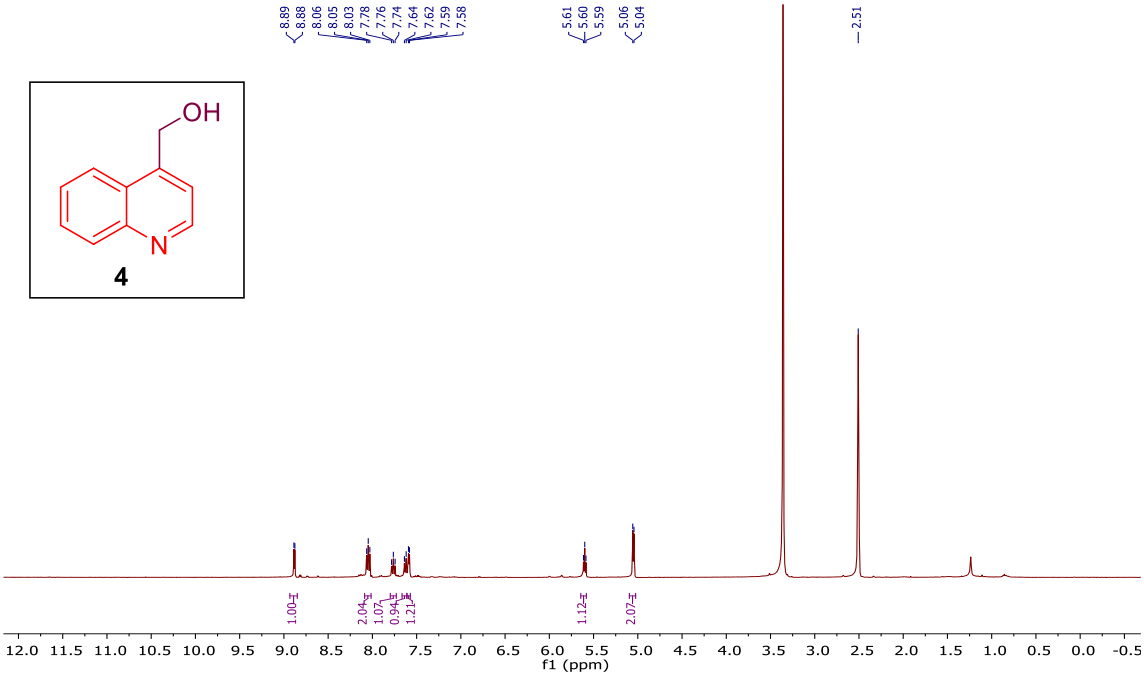

^{1}H NMR (DMSO-d_6, 400 MHz) spectrum of ***quinolin-4-ylmethanol (4).***

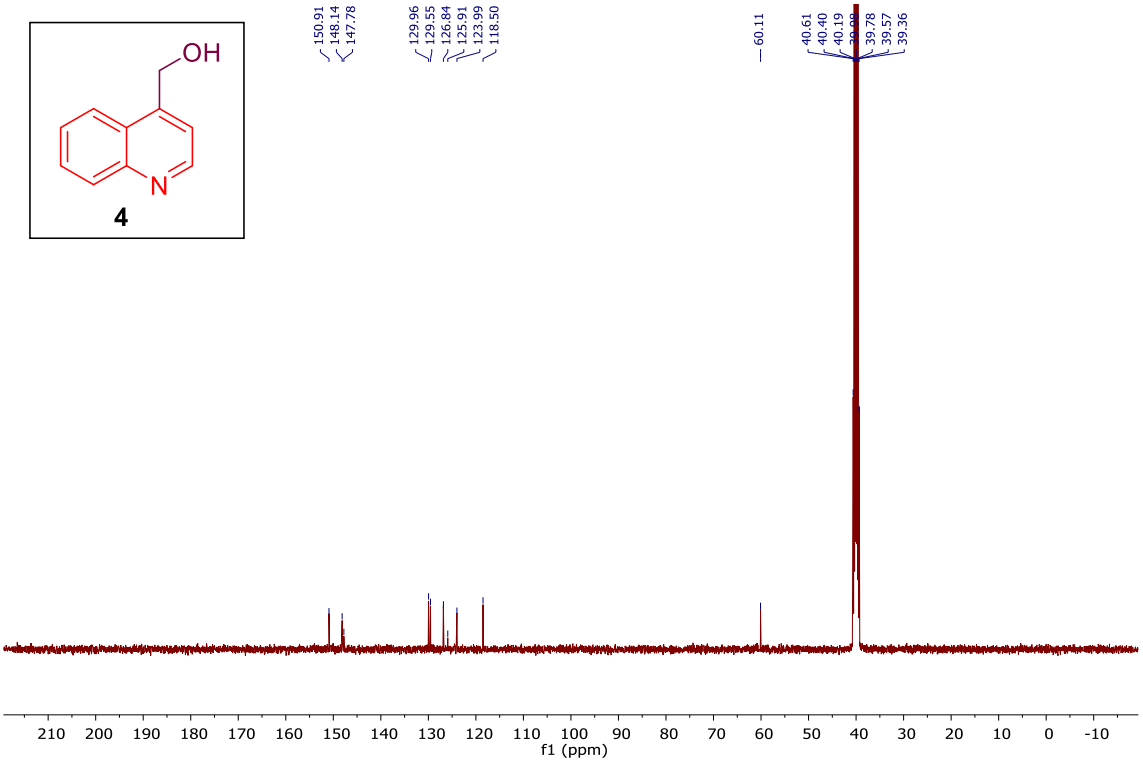

^{13}C NMR (DMSO-d_6, 100 MHz) spectrum of ***quinolin-4-ylmethanol (4).***

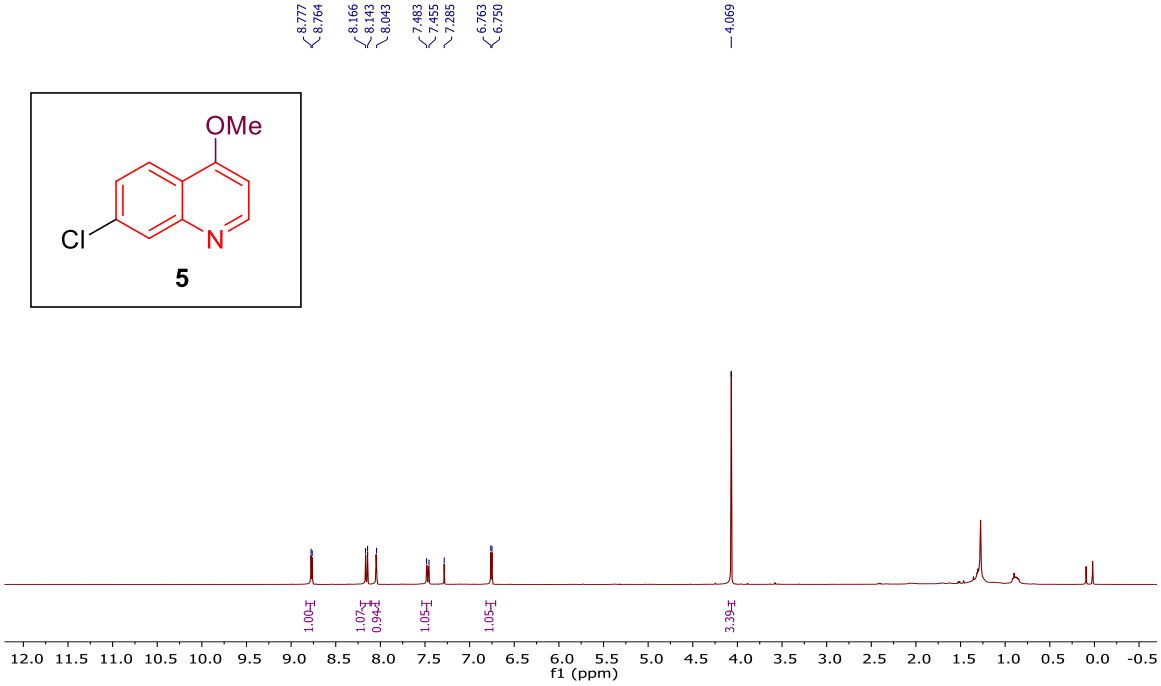

^{1}H NMR ($CDCl_3$, 400 MHz) spectrum of ***7-chloro-4-methoxyquinoline (5).***

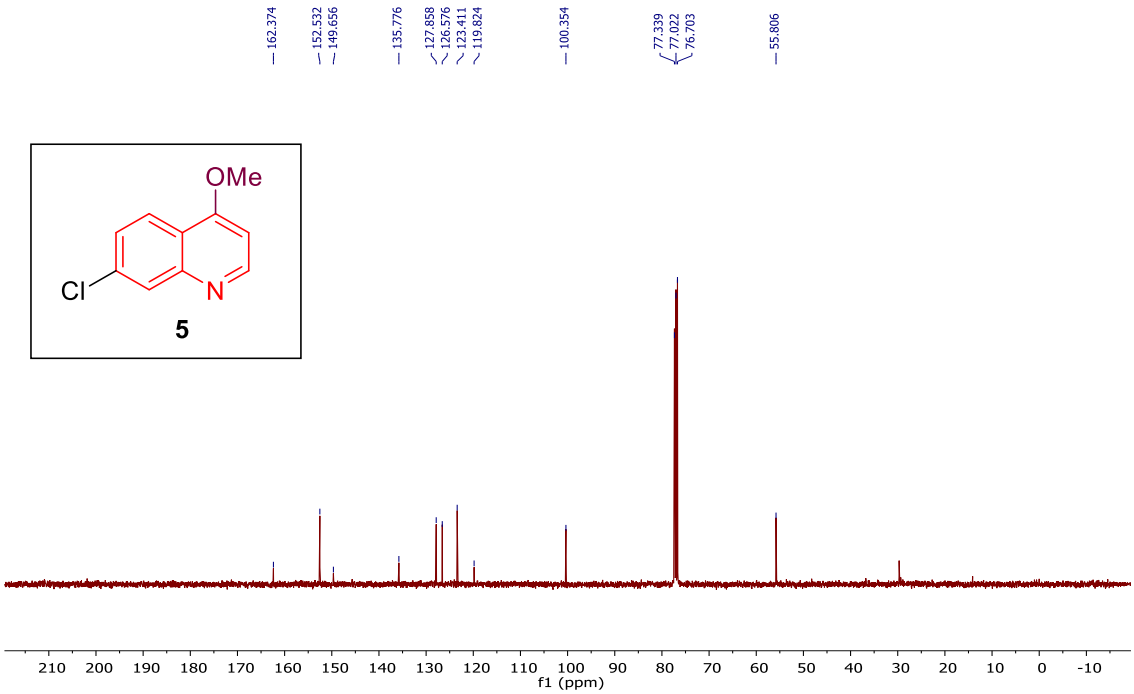

^{13}C NMR ($CDCl_3$, 100 MHz) spectrum of ***7-chloro-4-methoxyquinoline (5).***

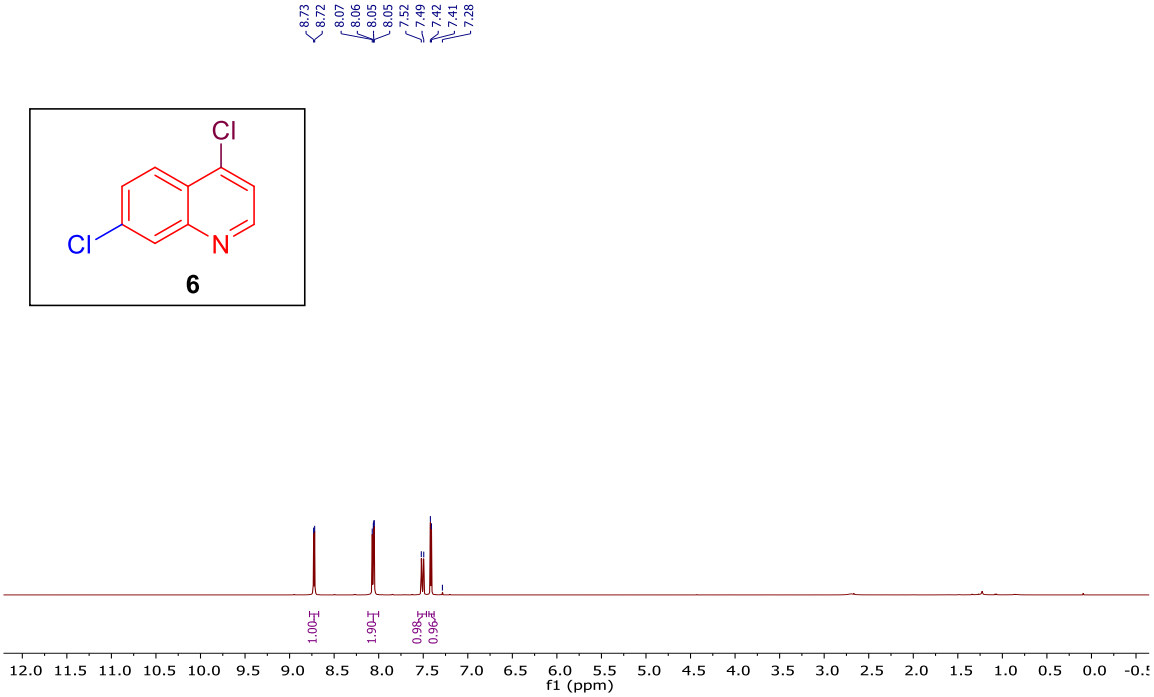

^{1}H NMR ($CDCl_3$, 400 MHz) spectrum of ***4,7-dichloroquinoline (6).***

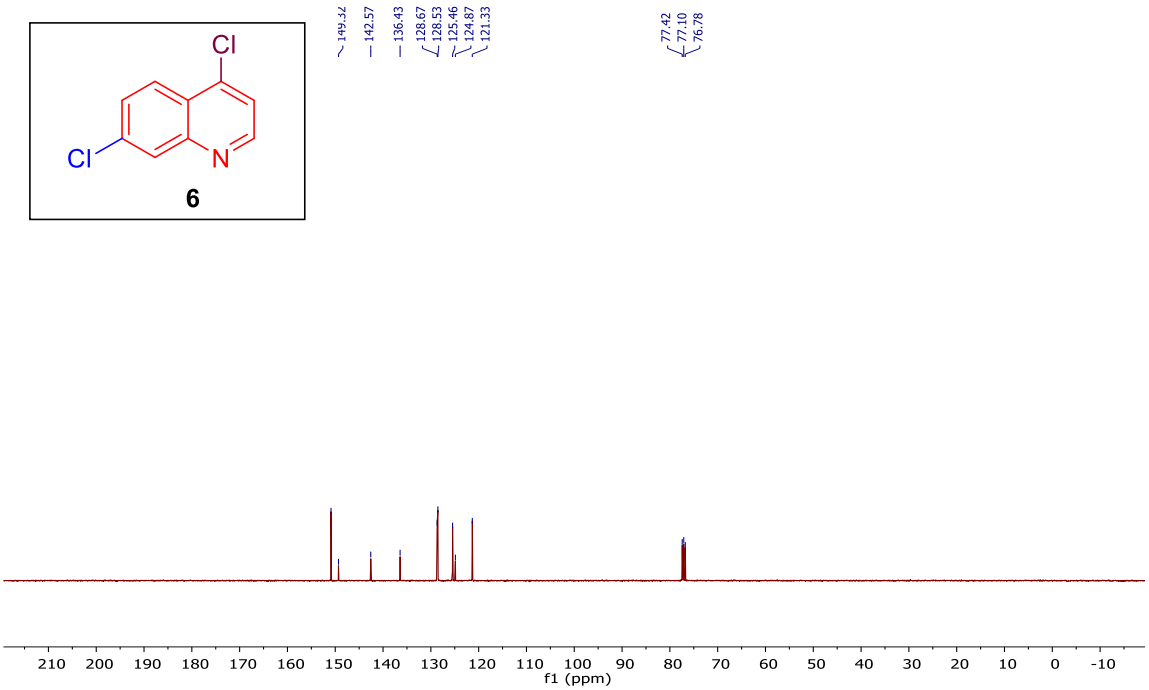

^{13}C NMR ($CDCl_3$, 100 MHz) spectrum of ***4,7-dichloroquinoline (6).***

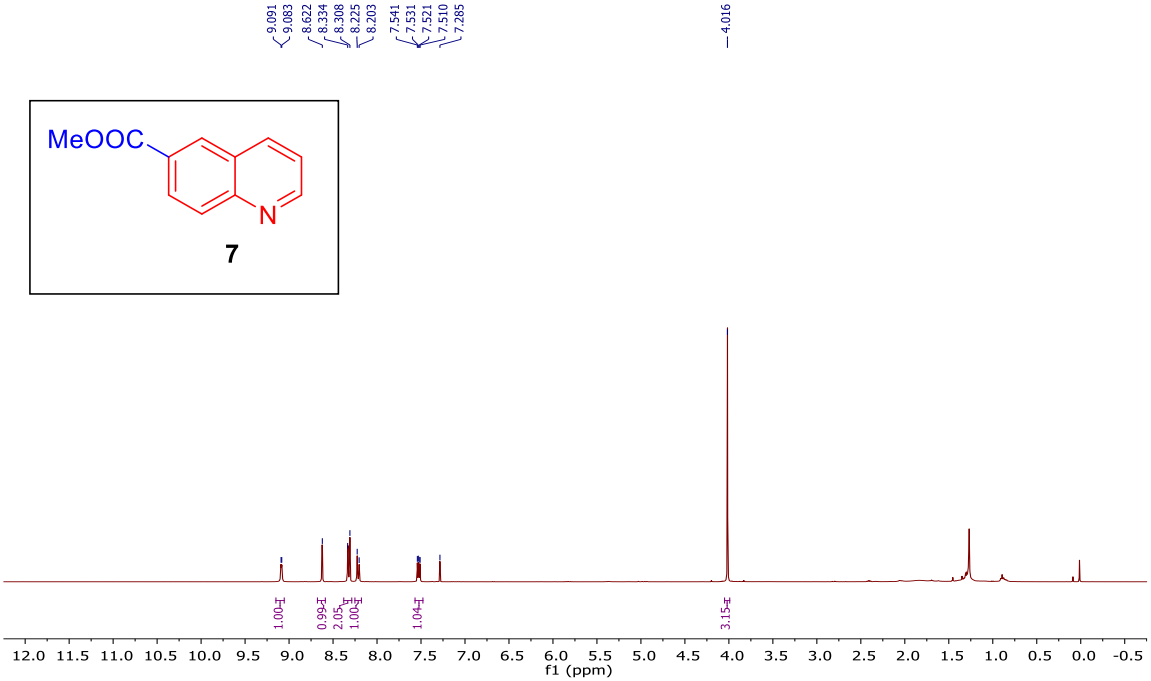

^{1}H NMR ($CDCl_3$, 400 MHz) spectrum of ***methyl quinoline-6-carboxylate (7).***

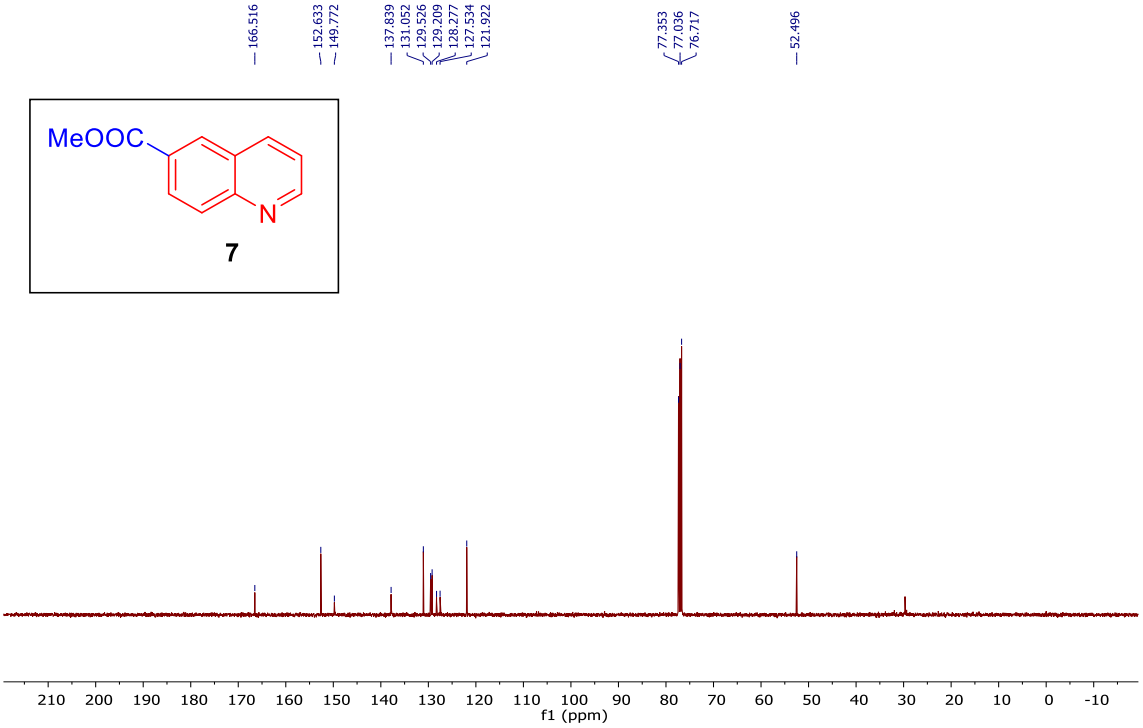

^{13}C NMR ($CDCl_3$, 100 MHz) spectrum of ***methyl quinoline-6-carboxylate (7).***

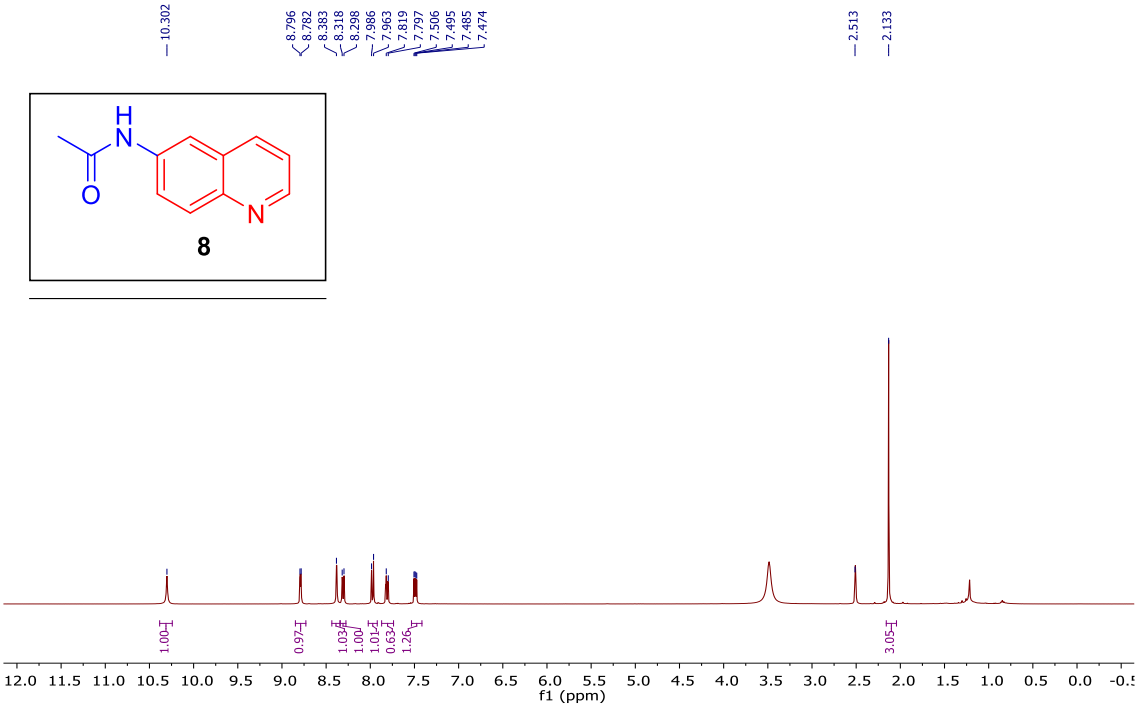

^{1}H NMR (DMSO-d_6, 400 MHz) spectrum of ***N-(quinolin-6-yl)acetamide (8).***

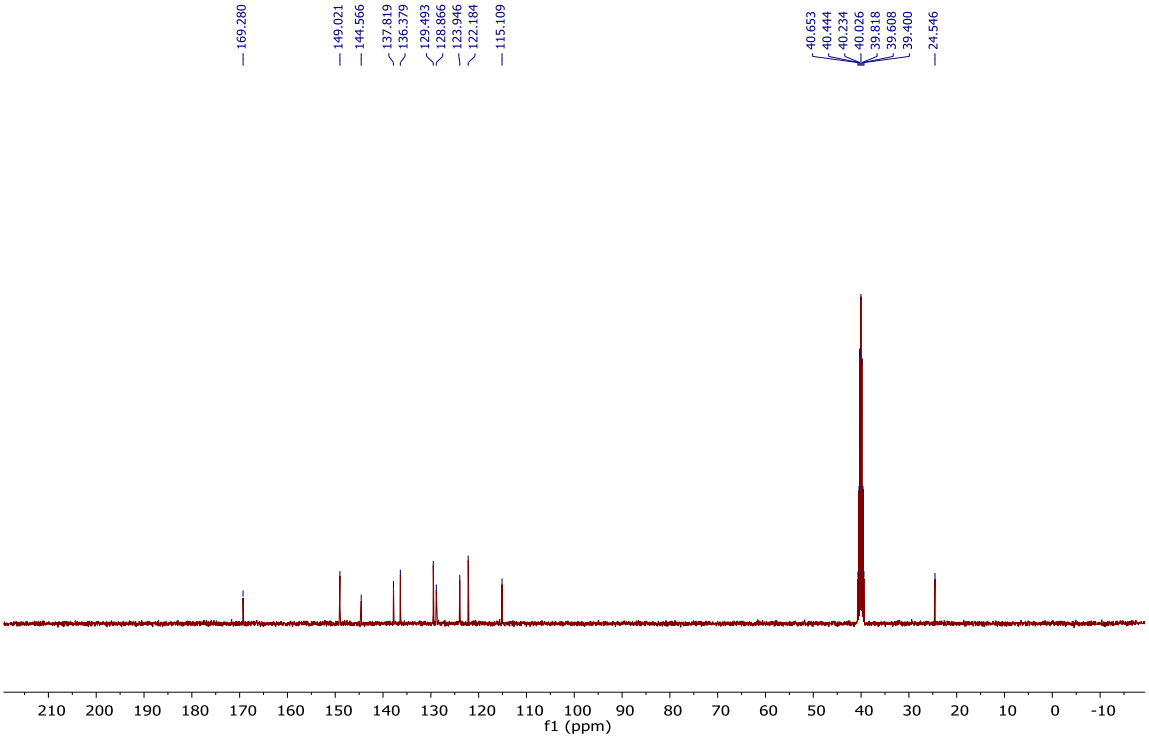

^{13}C NMR (DMSO-d_6, 100 MHz) spectrum of ***N-(quinolin-6-yl)acetamide (8).***

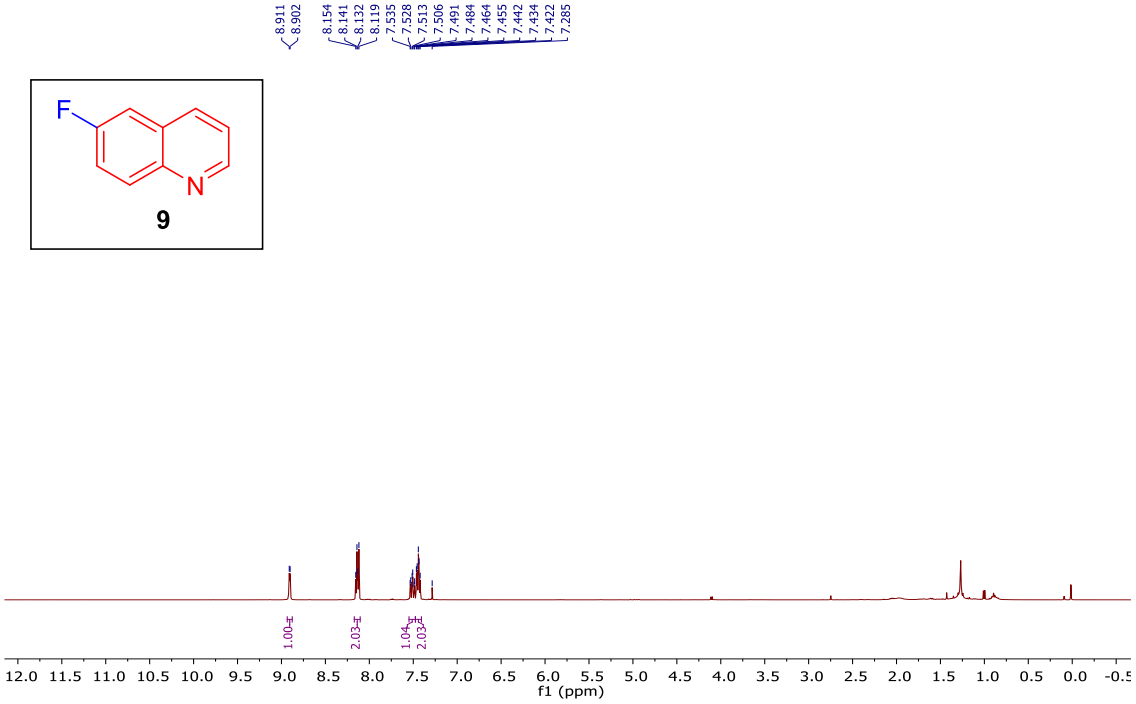

^{1}H NMR ($CDCl_3$, 400 MHz) spectrum of ***6-fluoroquinoline (9).***

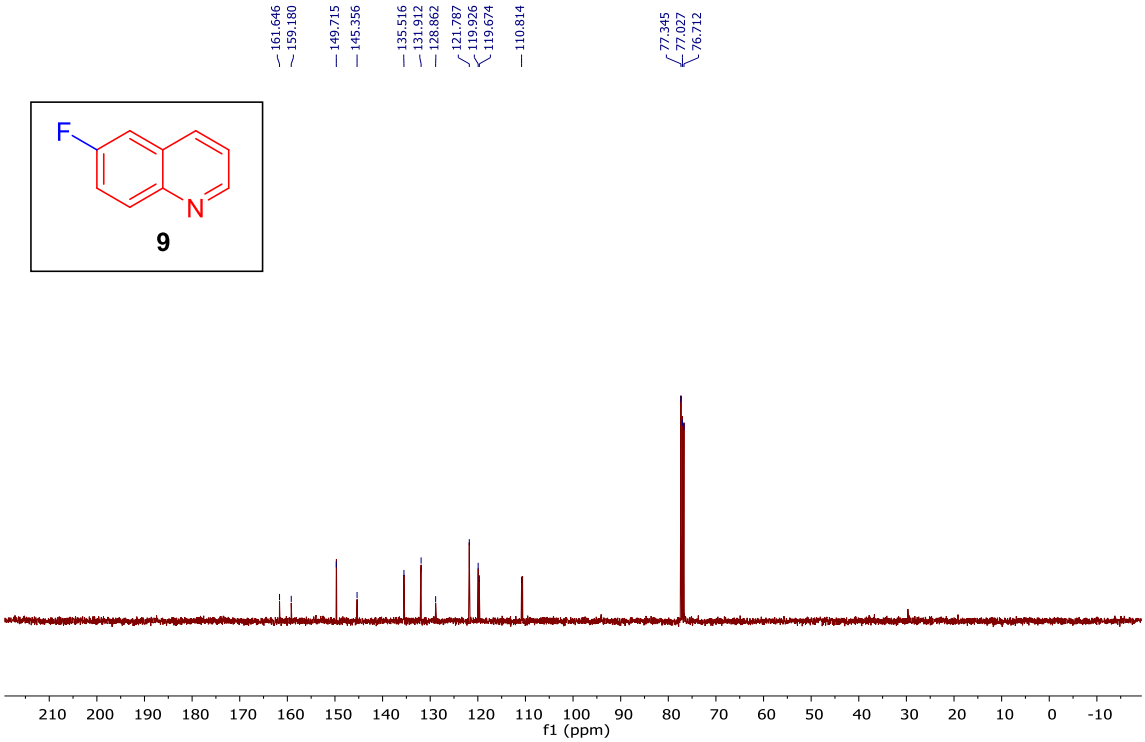

^{13}C NMR ($CDCl_3$, 100 MHz) spectrum of ***6-fluoroquinoline (9).***

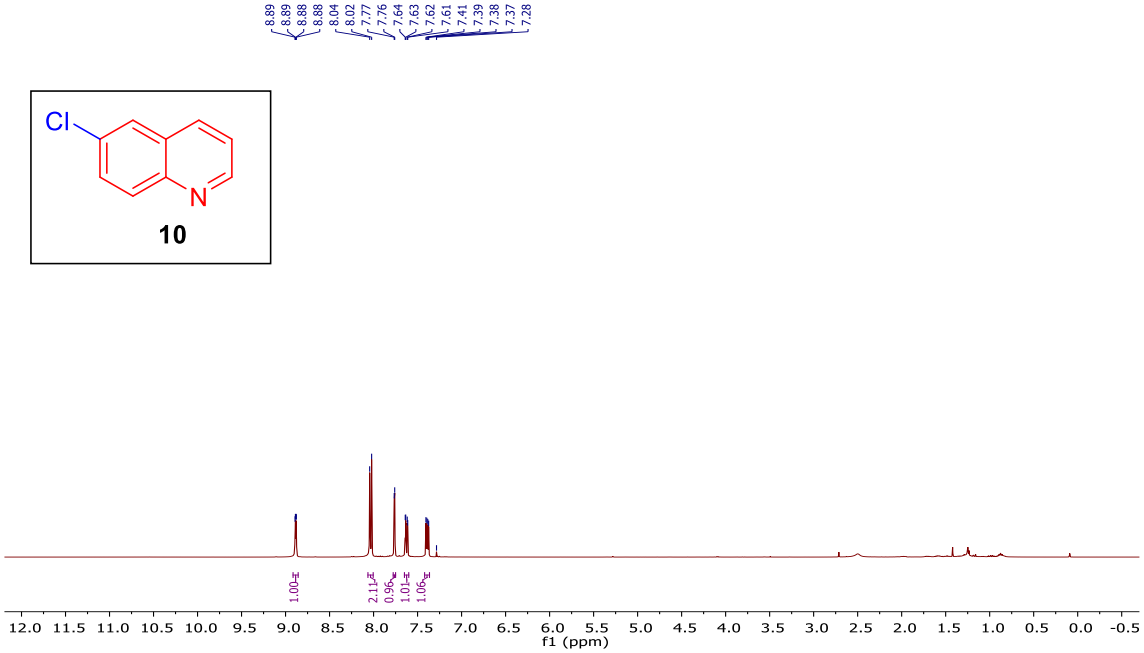

^{1}H NMR ($CDCl_3$, 400 MHz) spectrum of ***6-chloroquinoline (10).***

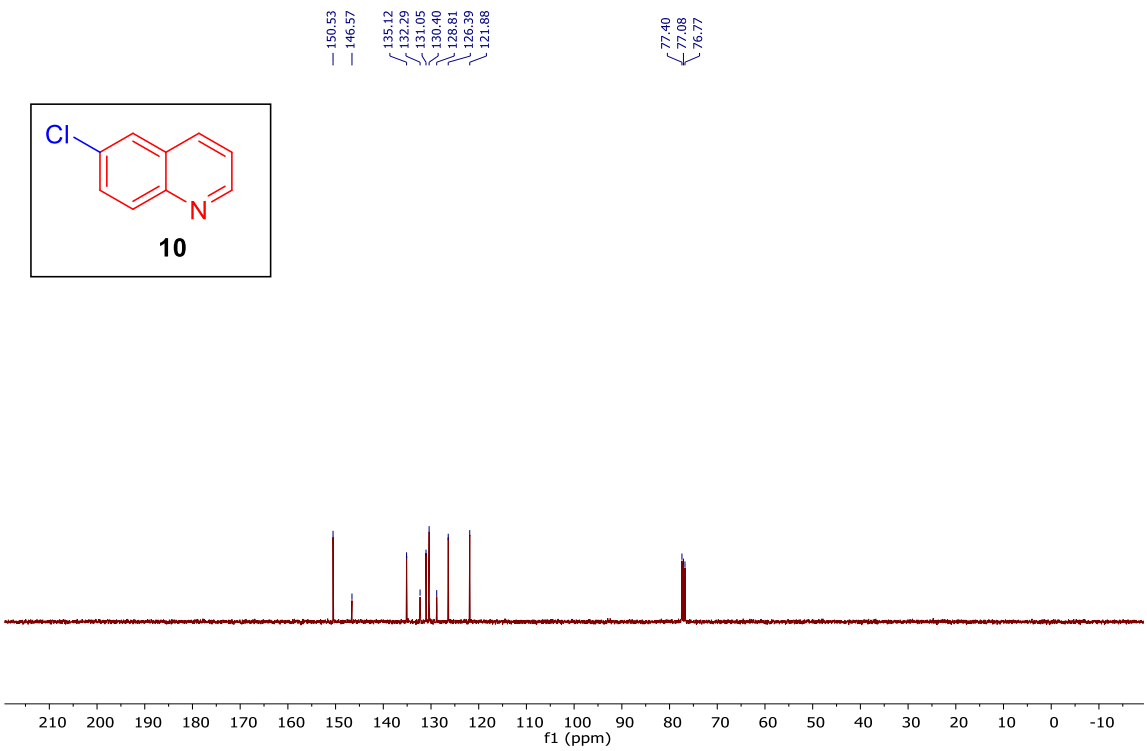

^{13}C NMR ($CDCl_3$, 100 MHz) spectrum of ***6-chloroquinoline (10).***

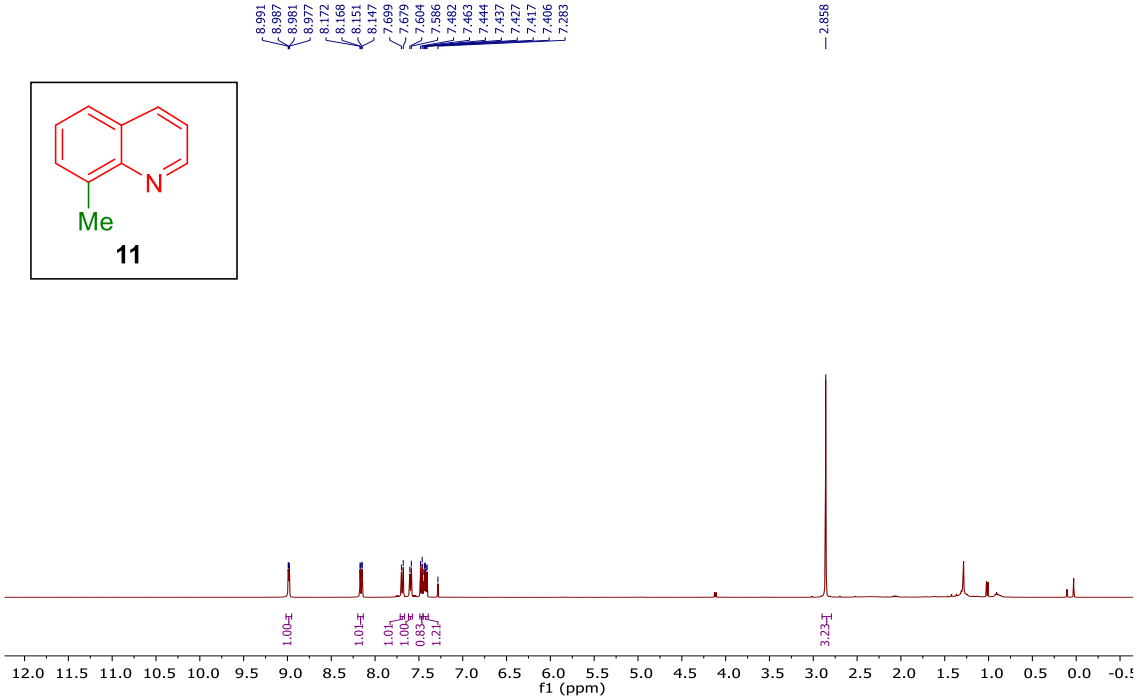

^{1}H NMR ($CDCl_3$, 400 MHz) spectrum of ***8-methylquinoline (11).***

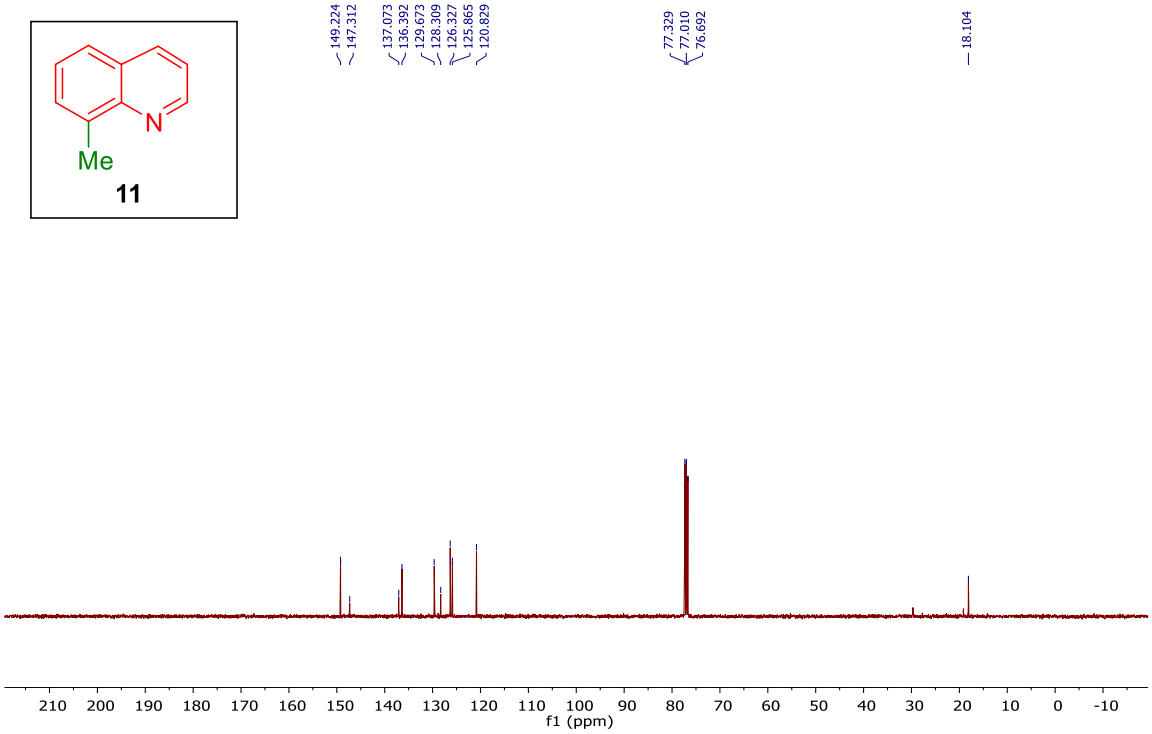

^{13}C NMR ($CDCl_3$, 100 MHz) spectrum of ***8-methylquinoline (11).***

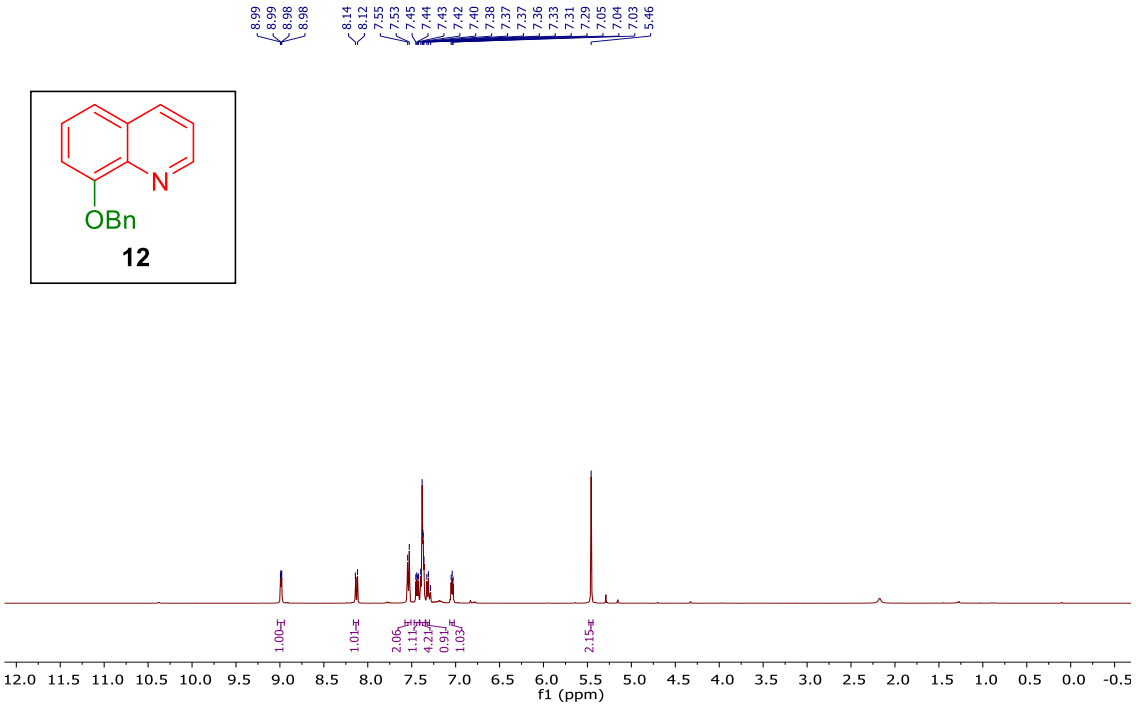

^{1}H NMR ($CDCl_3$, 400 MHz) spectrum of ***8-(benzyloxy)quinoline (12).***

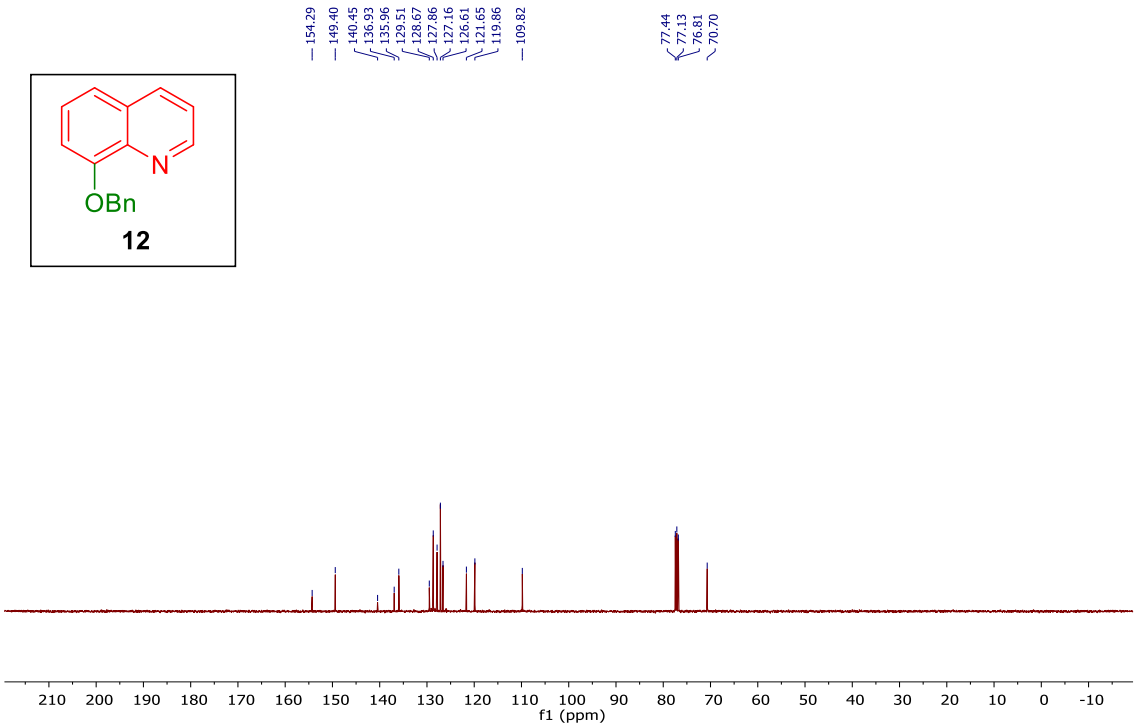

^{13}C NMR ($CDCl_3$, 100 MHz) spectrum of ***8-(benzyloxy)quinoline (12).***

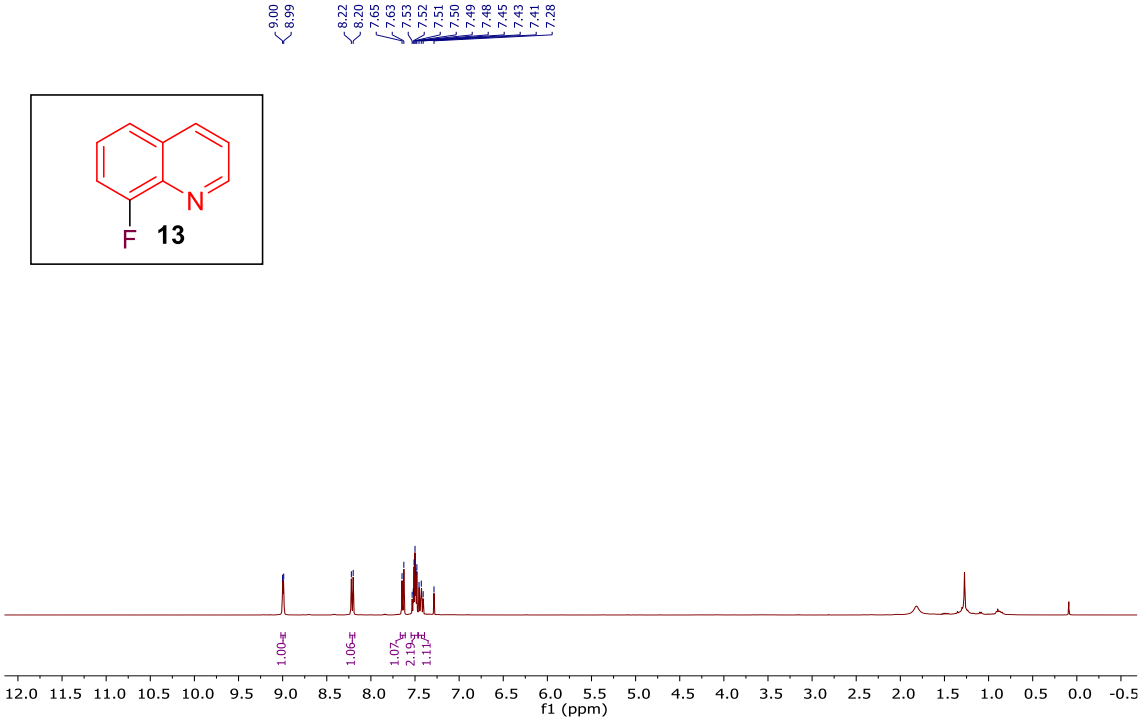

^{1}H NMR ($CDCl_3$, 400 MHz) spectrum of ***8-fluoroquinoline (13).***

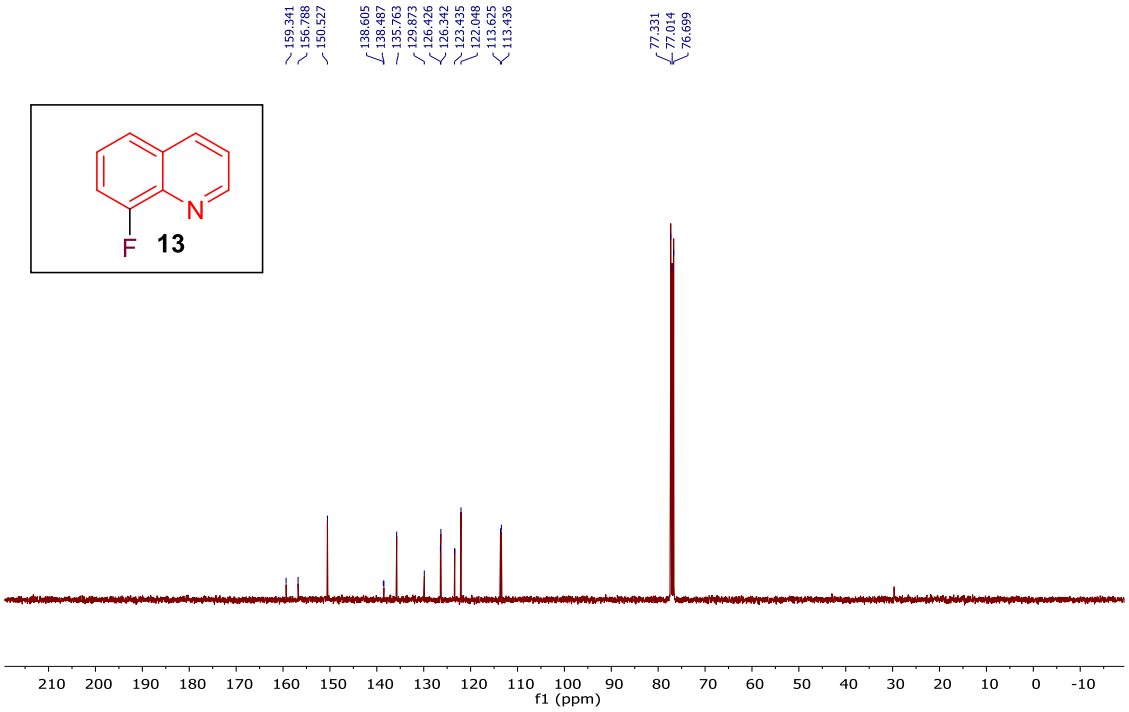

^{13}C NMR ($CDCl_3$, 100 MHz) spectrum of ***8-fluoroquinoline (13).***

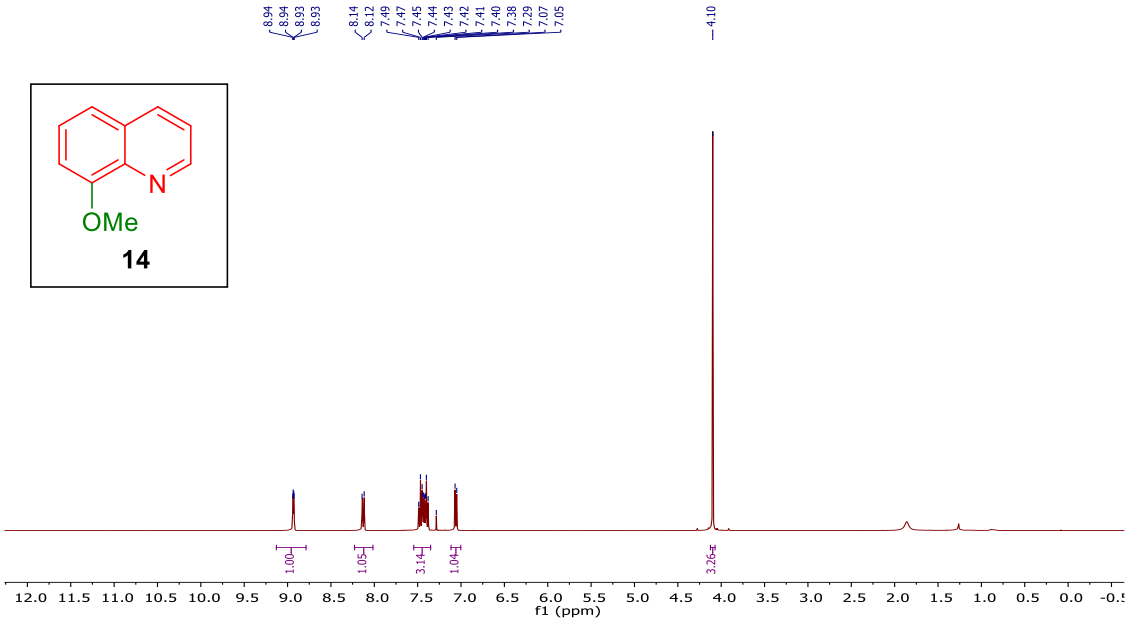

^{1}H NMR ($CDCl_3$, 400 MHz) spectrum of ***8-methoxyquinoline (14).***

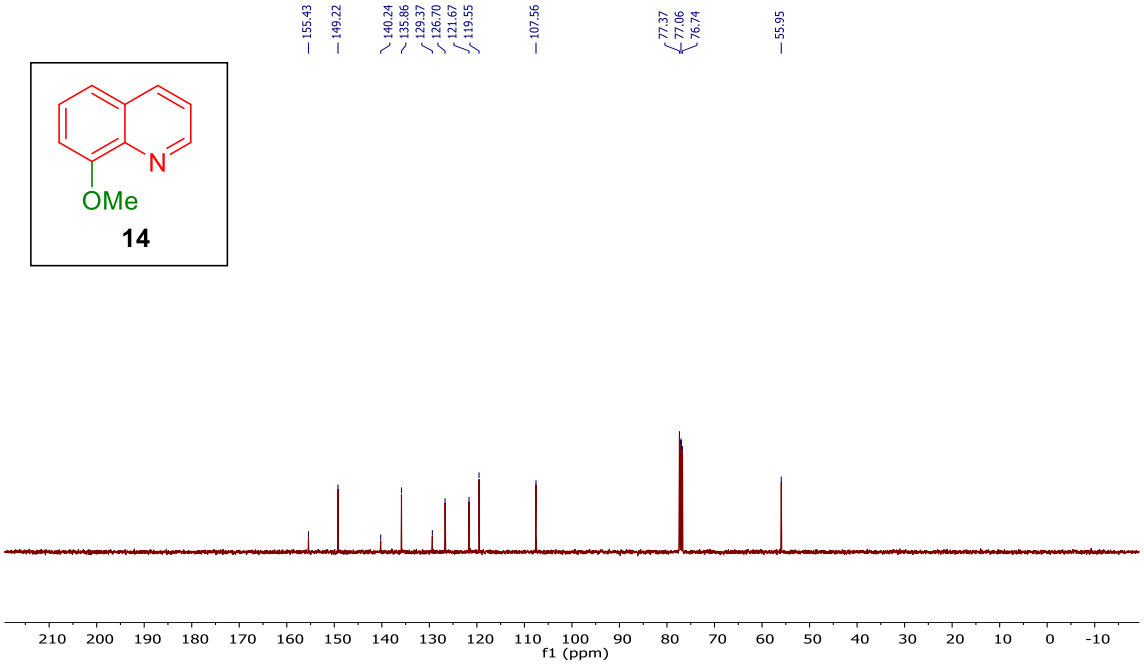

^{13}C NMR ($CDCl_3$, 100 MHz) spectrum of ***8-methoxyquinoline (14).***

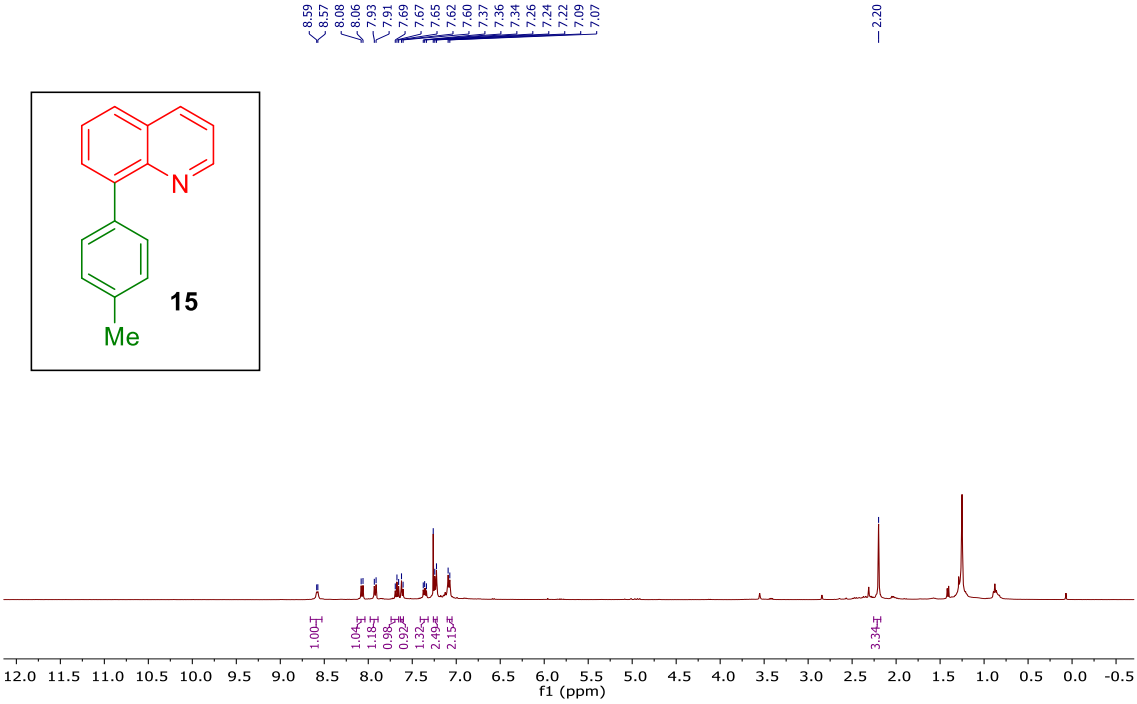

^{1}H NMR ($CDCl_3$, 400 MHz) spectrum of ***8-(p-tolyl)quinoline (15).***

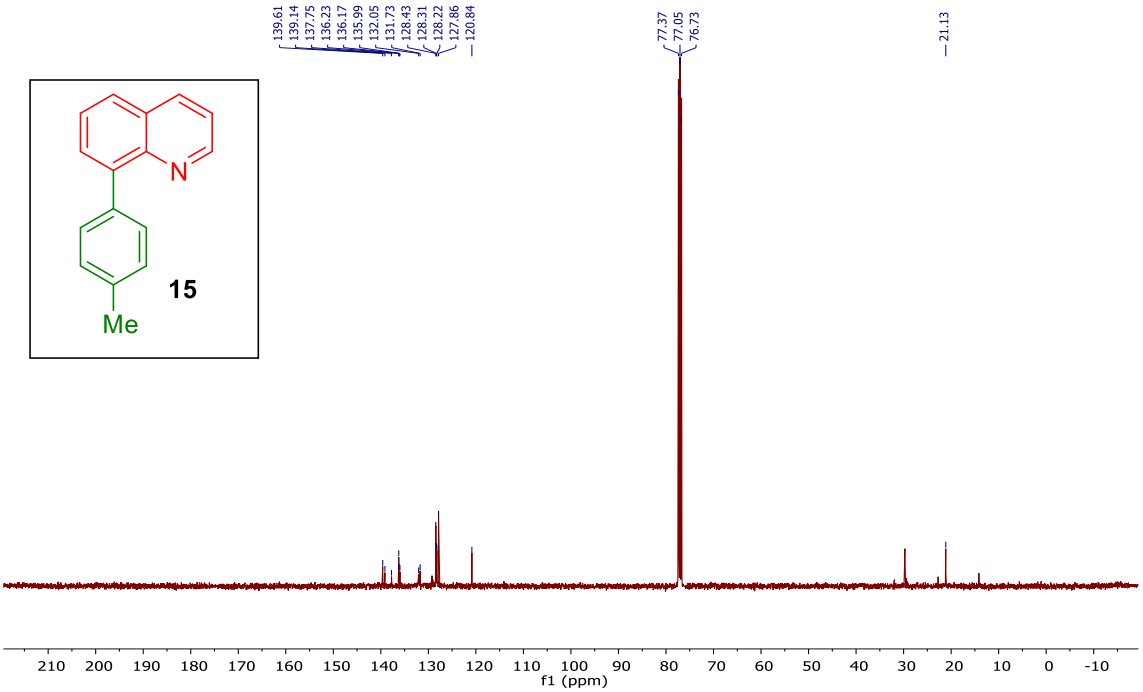

^{13}C NMR ($CDCl_3$, 100 MHz) spectrum of ***8-(p-tolyl)quinoline (15).***

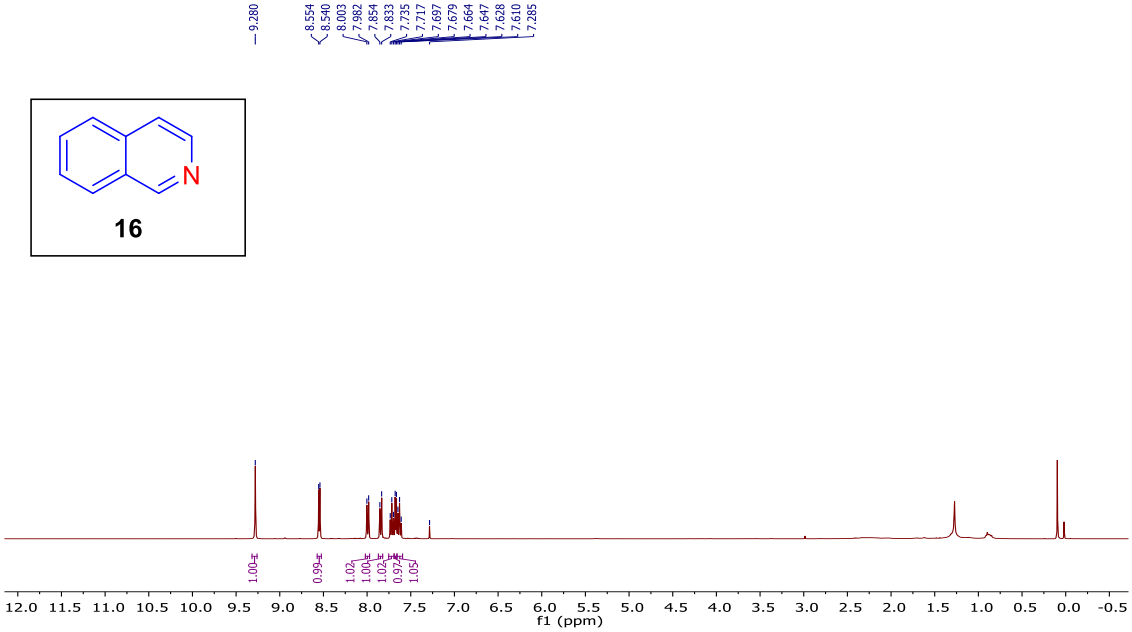

^{1}H NMR ($CDCl_3$, 400 MHz) spectrum of ***isoquinoline (16).***

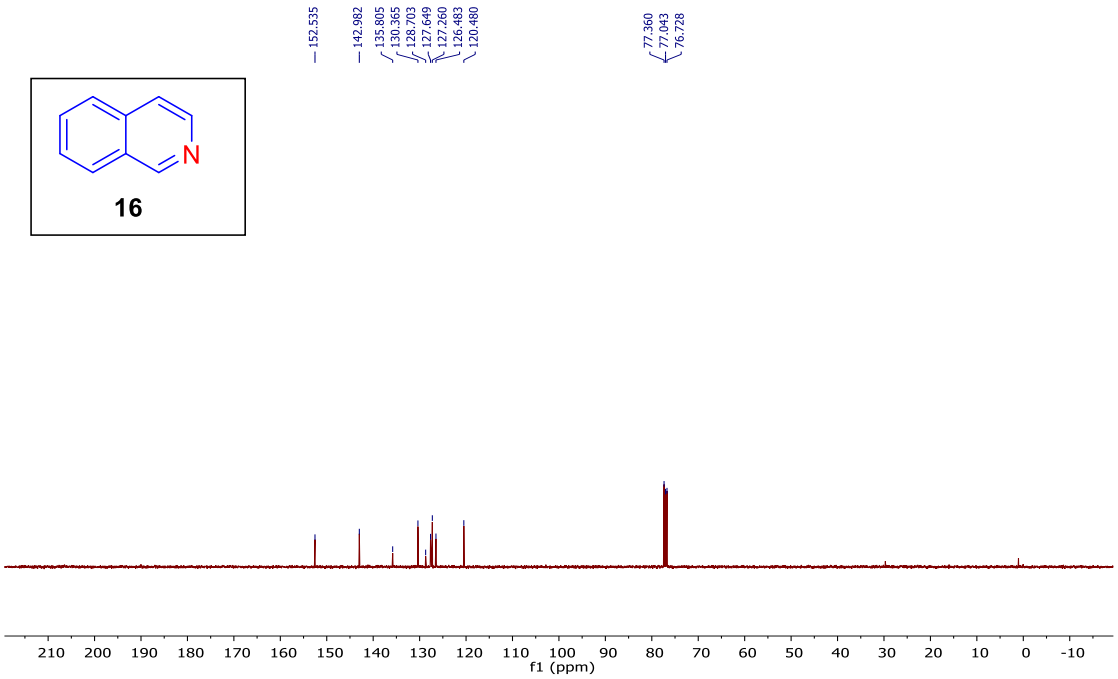

^{13}C NMR ($CDCl_3$, 100 MHz) spectrum of ***isoquinoline (16).***

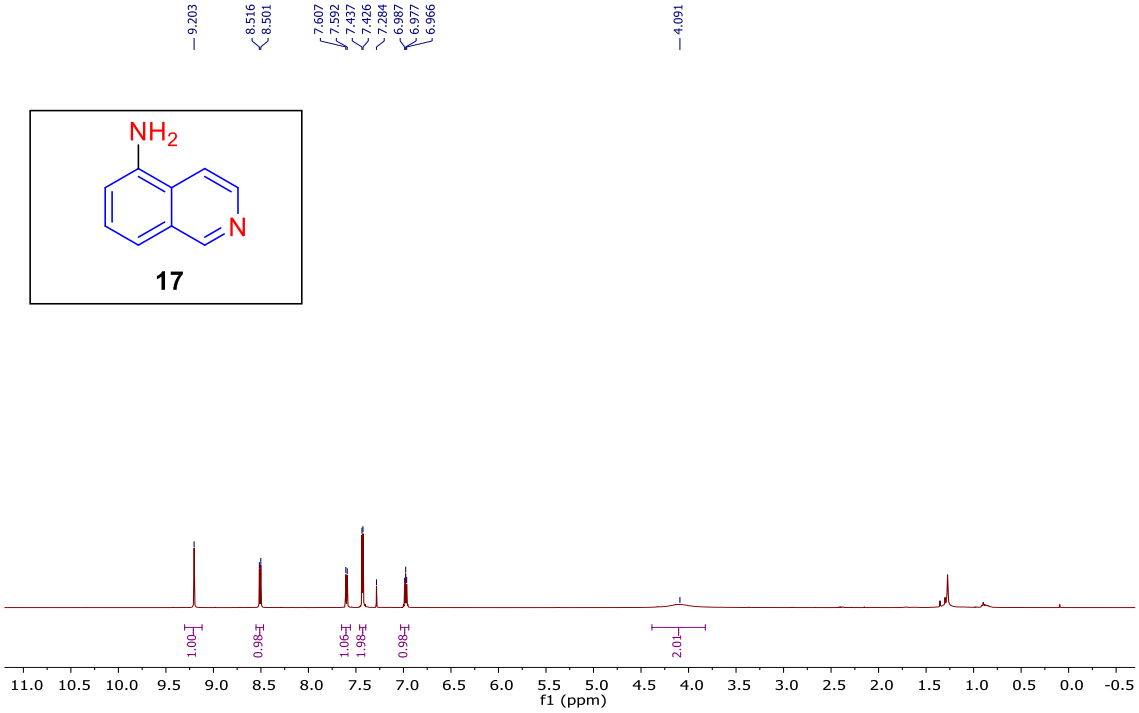

^{1}H NMR ($CDCl_3$, 400 MHz) spectrum of ***isoquinolin-5-amine (17).***

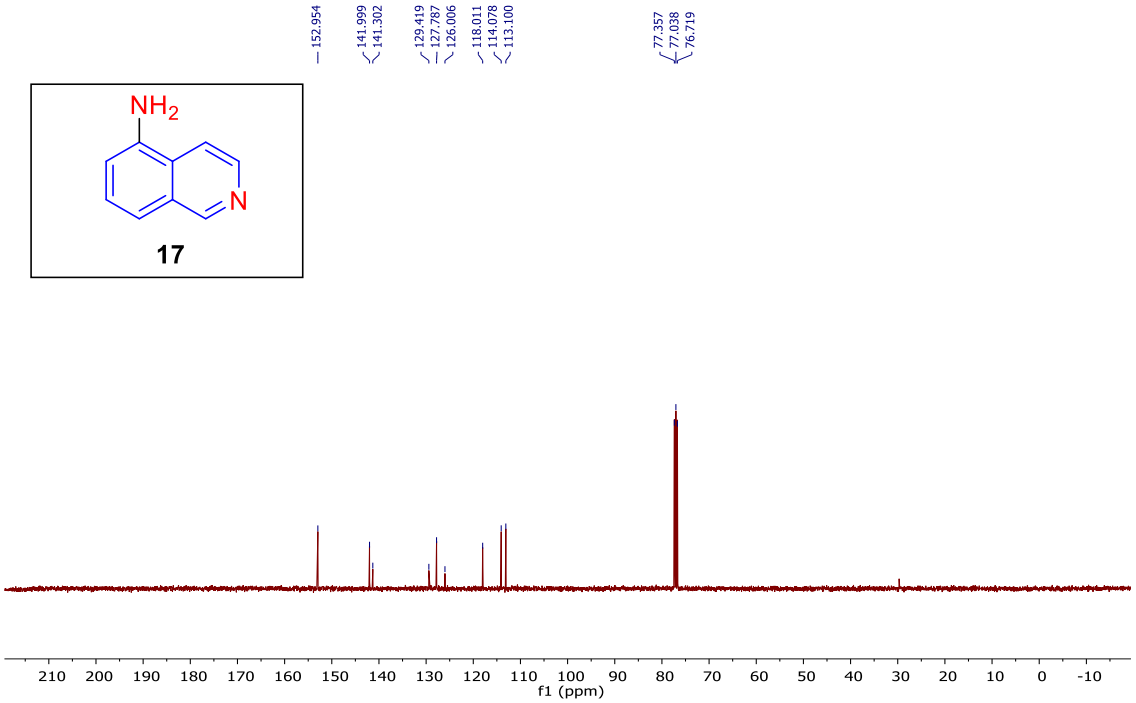

^{13}C NMR ($CDCl_3$, 100 MHz) spectrum of ***isoquinolin-5-amine (17).***

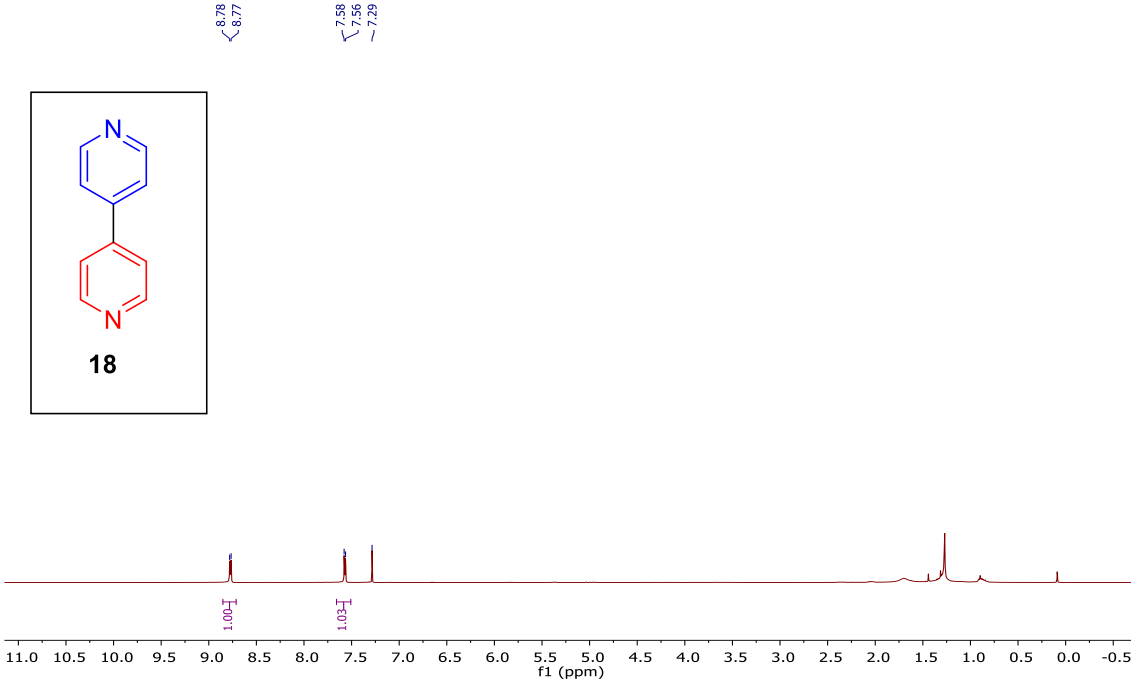

^{1}H NMR ($CDCl_3$, 400 MHz) spectrum of ***4,4'-bipyridine (18).***

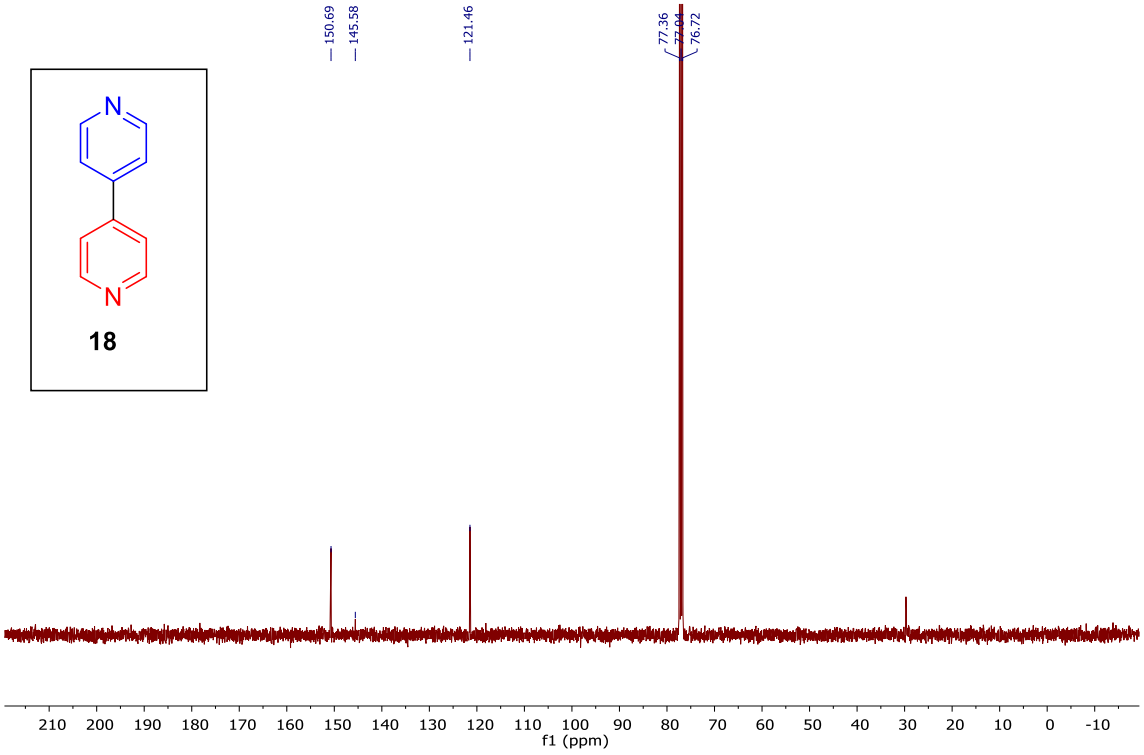

^{13}C NMR ($CDCl_3$, 100 MHz) spectrum of ***4,4'-bipyridine (18).***

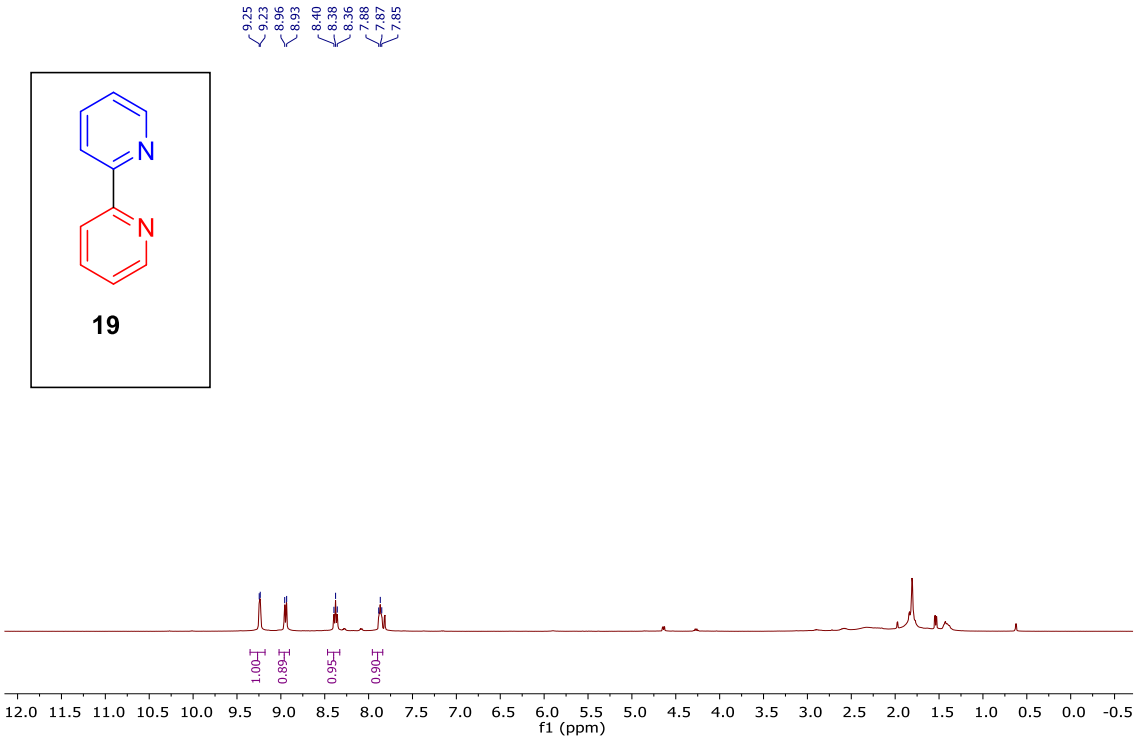

^{1}H NMR ($CDCl_3$, 400 MHz) spectrum of ***2,2'-bipyridine (19).***

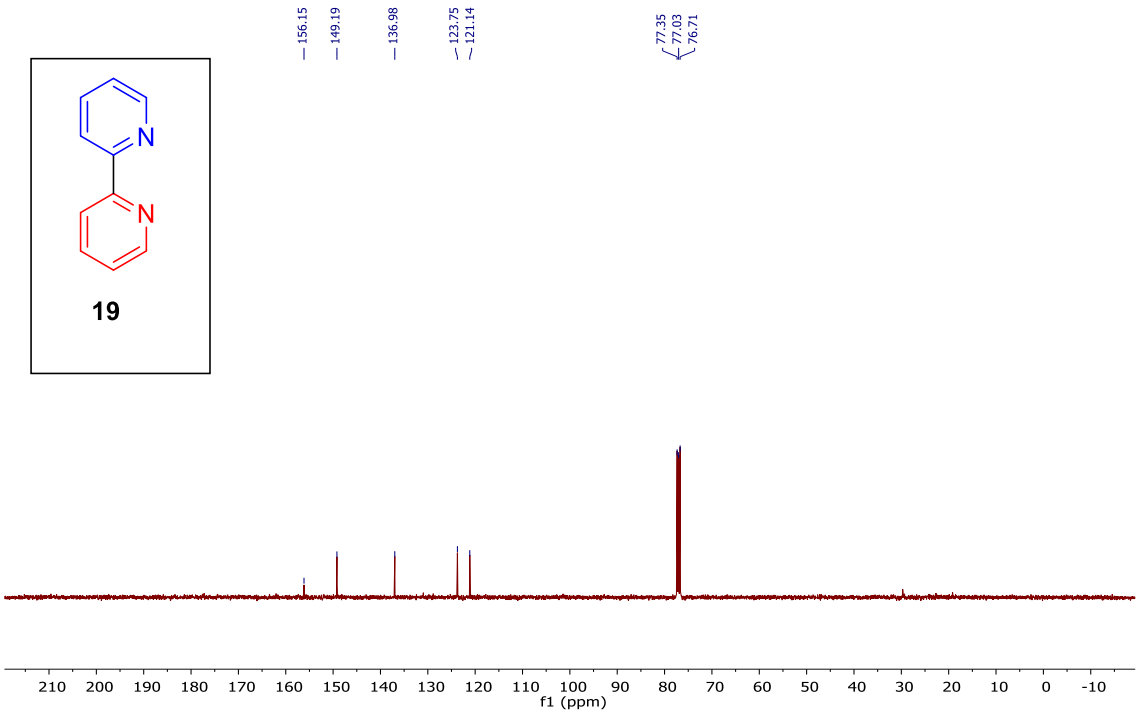

^{13}C NMR ($CDCl_3$, 100 MHz) spectrum of ***2,2'-bipyridine (19).***

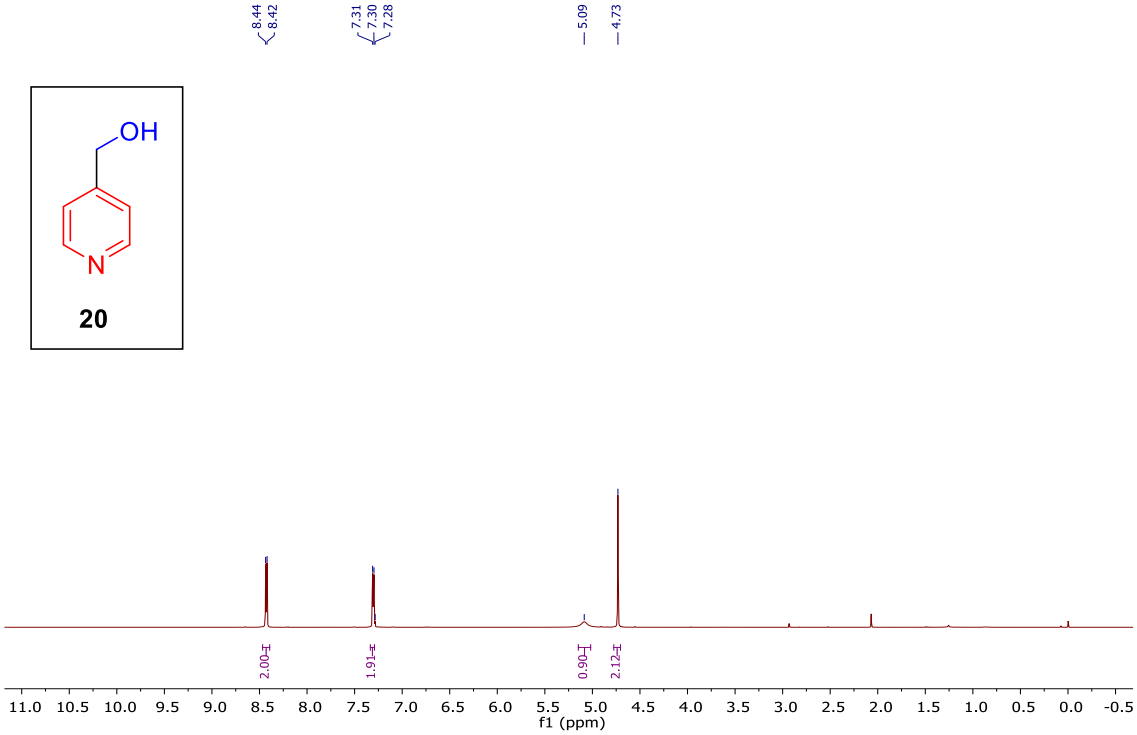

^{1}H NMR ($CDCl_3$, 400 MHz) spectrum of ***pyridin-4-ylmethanol (20).***

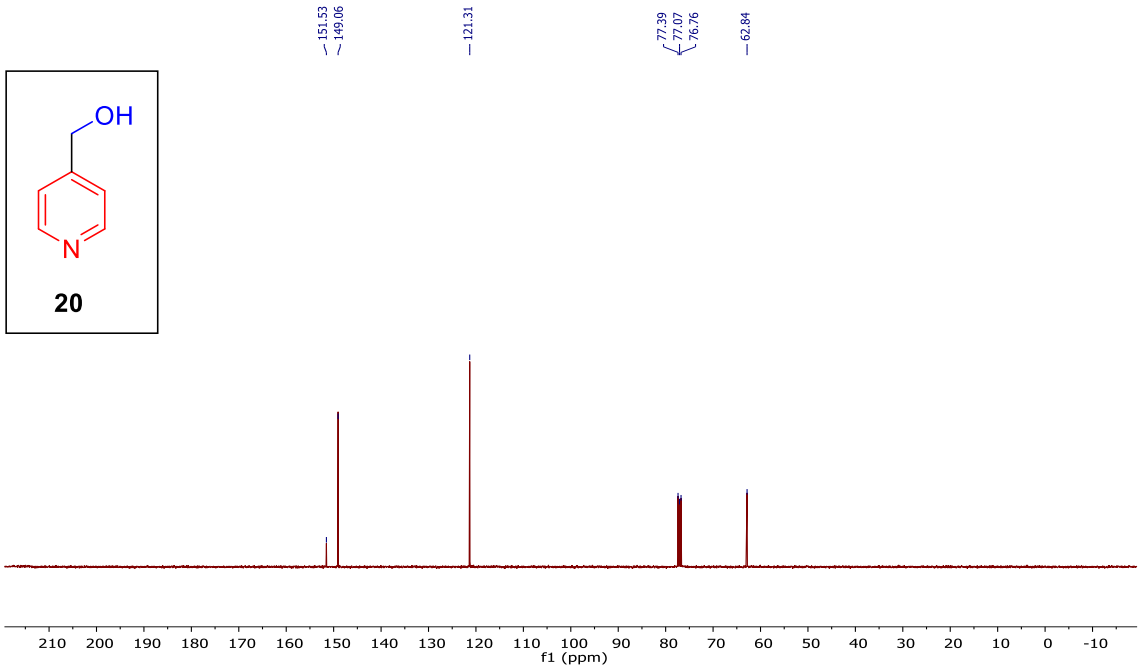

^{13}C NMR ($CDCl_3$, 100 MHz) spectrum of ***pyridin-4-ylmethanol (20).***

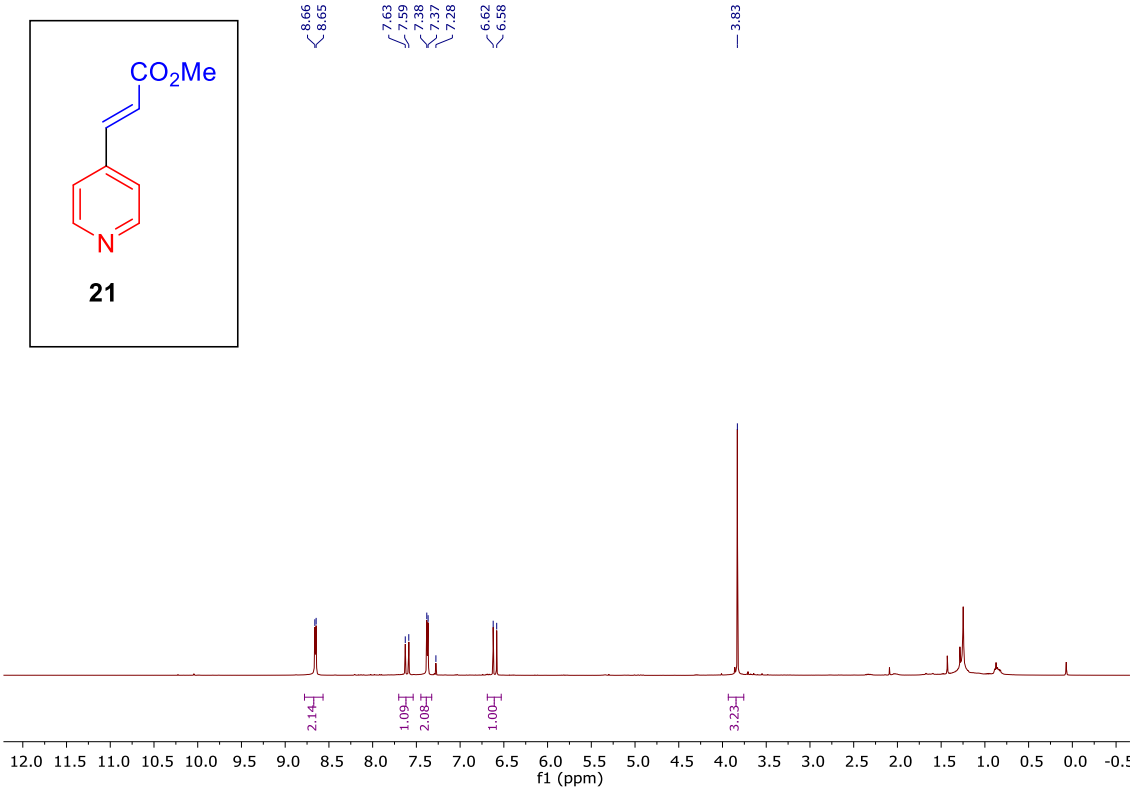

^{1}H NMR ($CDCl_3$, 400 MHz) spectrum of ***methyl (E)-3-(pyridin-4-yl)acrylate (21).***

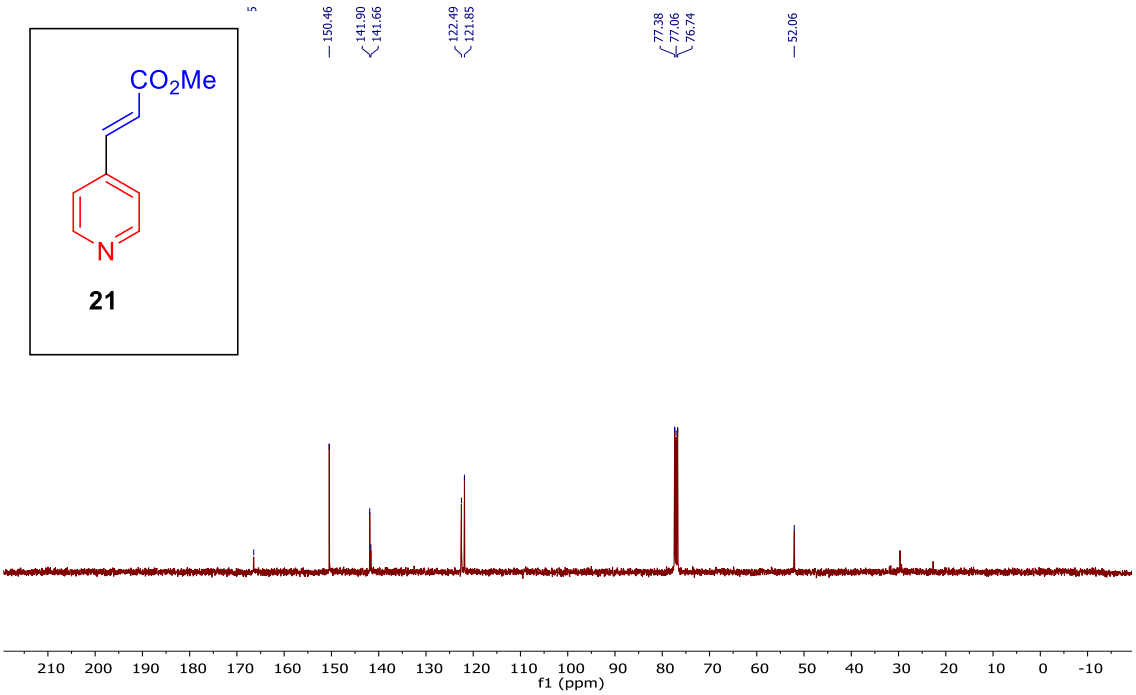

^{13}C NMR ($CDCl_3$, 100 MHz) spectrum of ***methyl (E)-3-(pyridin-4-yl)acrylate (21)***.

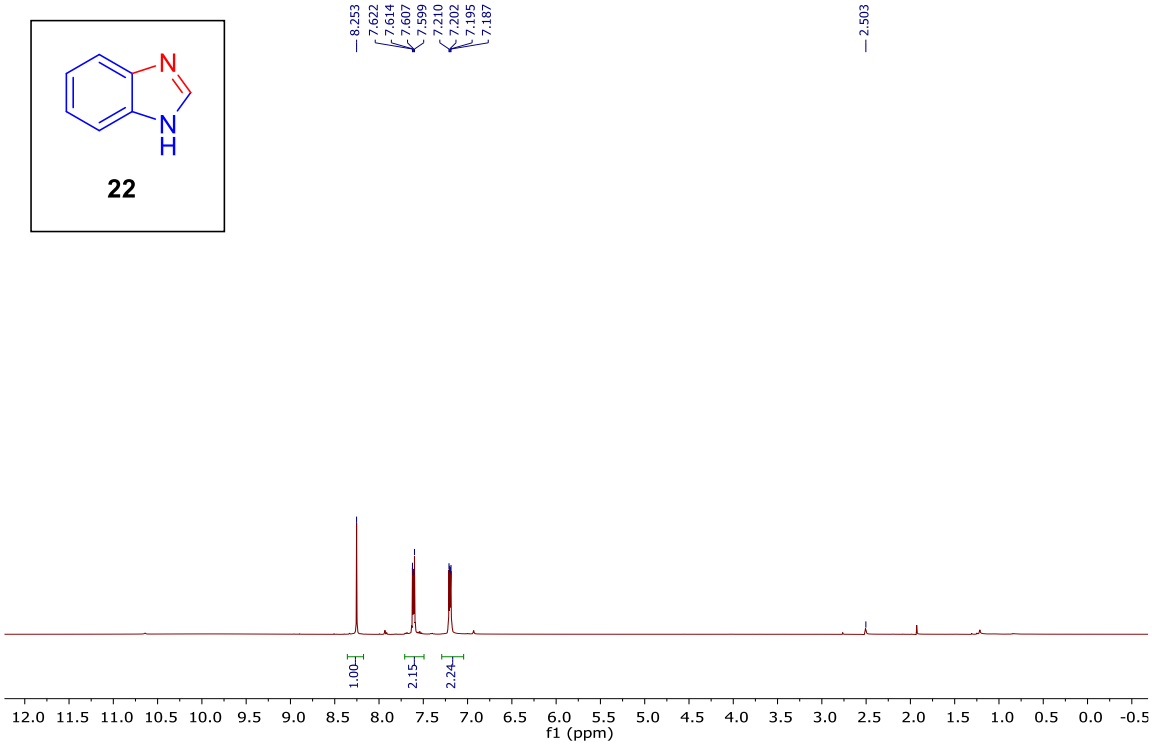

^{1}H NMR (DMSO-d_6, 400 MHz) spectrum of ***1H-benzo[d]imidazole (22).***

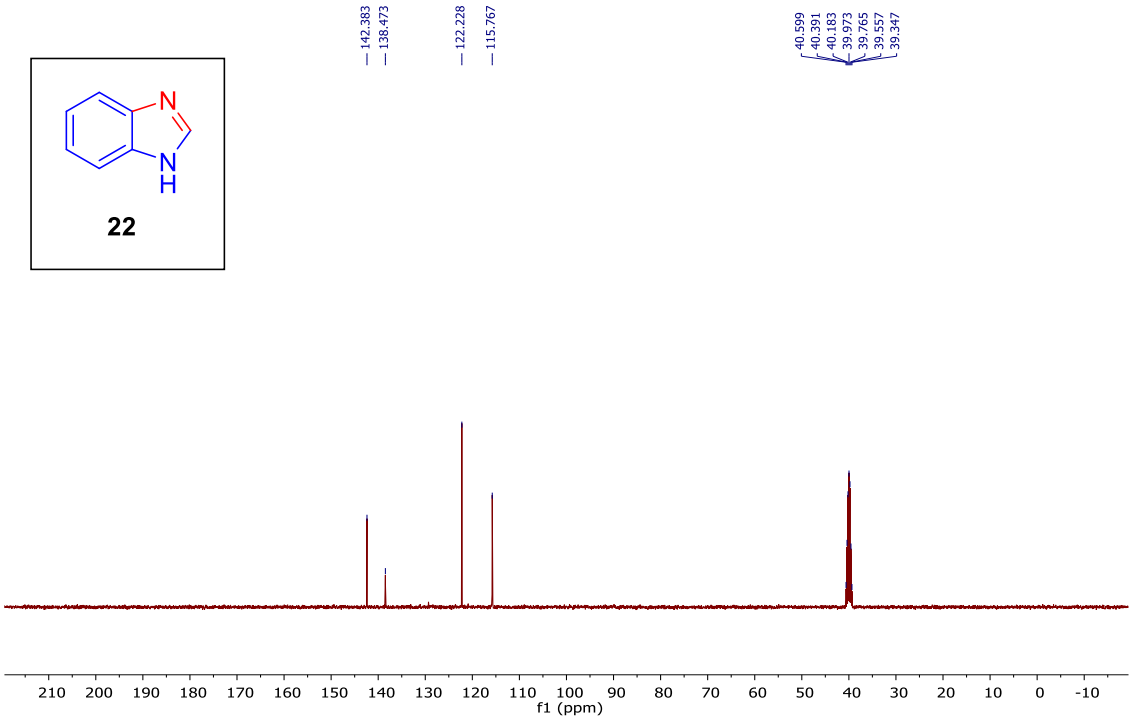

^{13}C NMR (DMSO-d_6, 100 MHz) spectrum of ***1H-benzo[d]imidazole (22).***

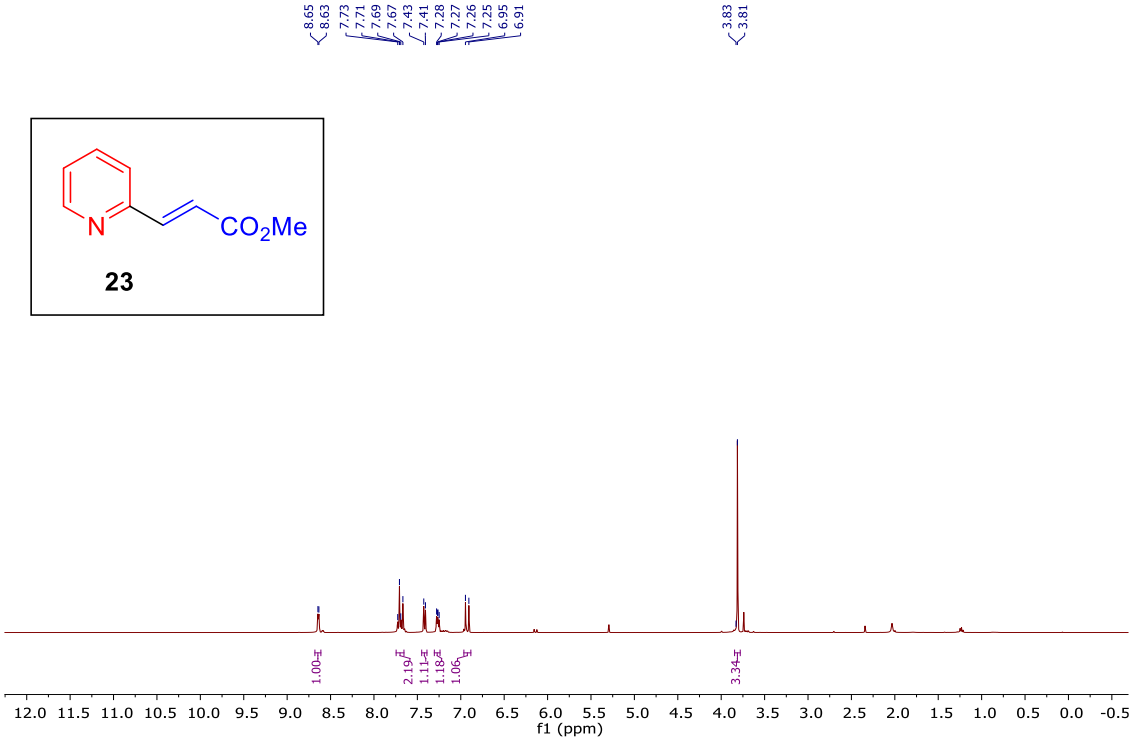

^{1}H NMR ($CDCl_3$, 400 MHz) spectrum of ***methyl (E)-3-(pyridin-2-yl)acrylate (23).***

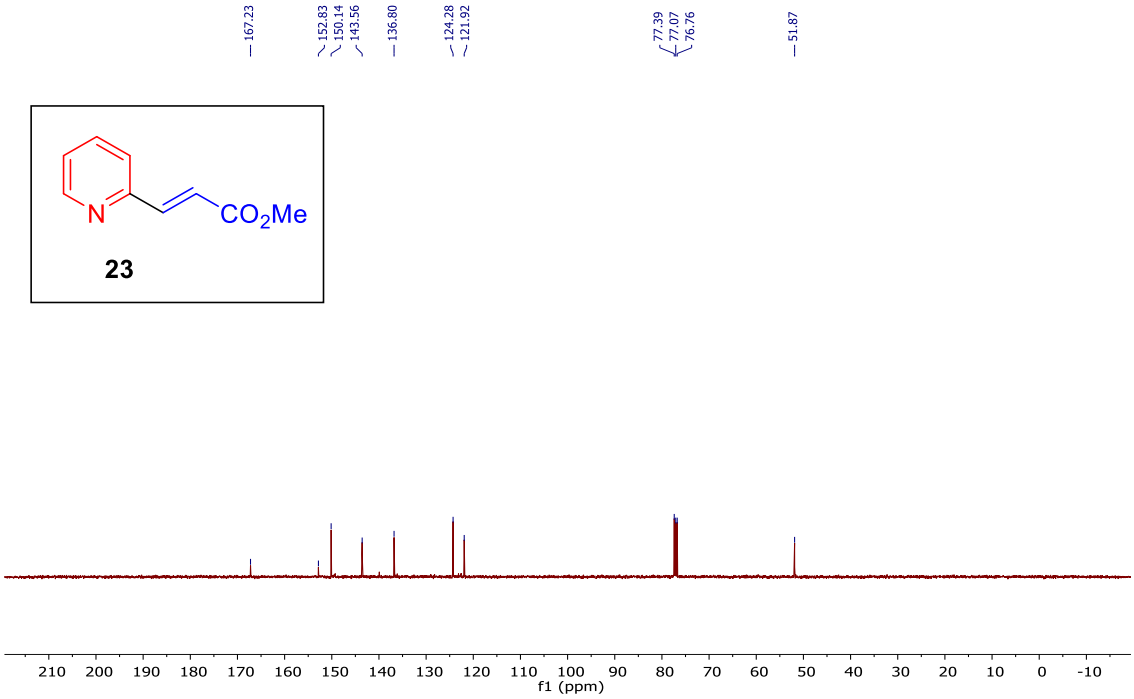

^{13}C NMR ($CDCl_3$, 100 MHz) spectrum of ***methyl (E)-3-(pyridin-2-yl)acrylate (23).***

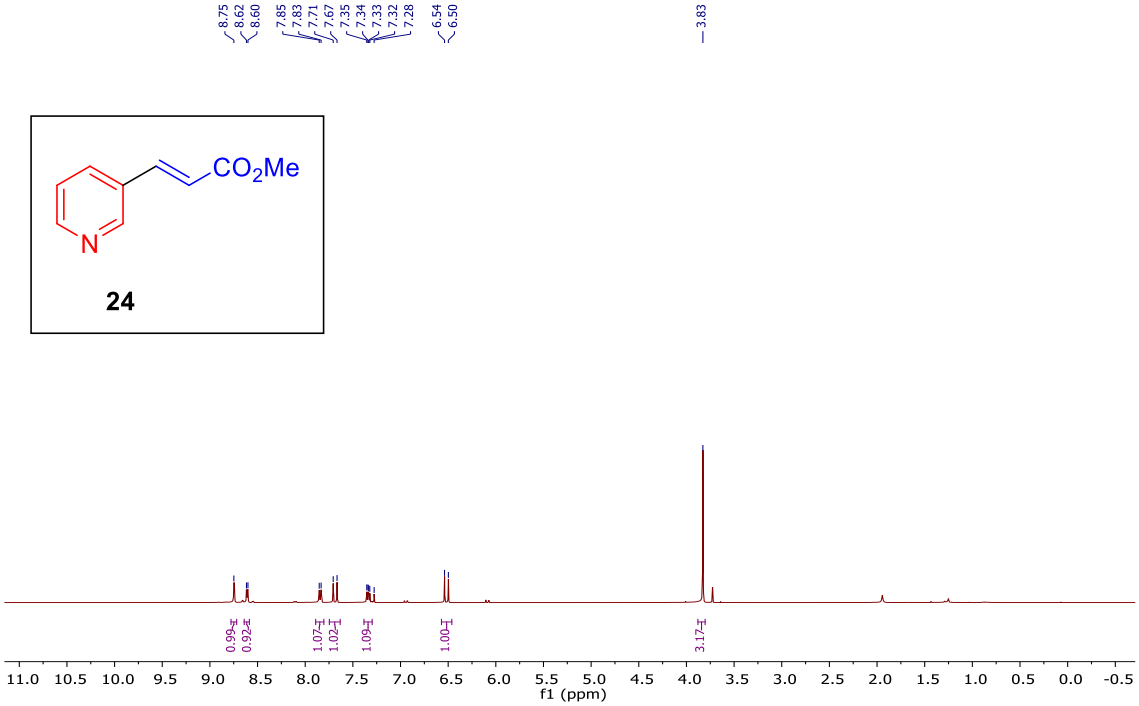

^{1}H NMR ($CDCl_3$, 400 MHz) spectrum of ***methyl (E)-3-(pyridin-3-yl)acrylate (24).***

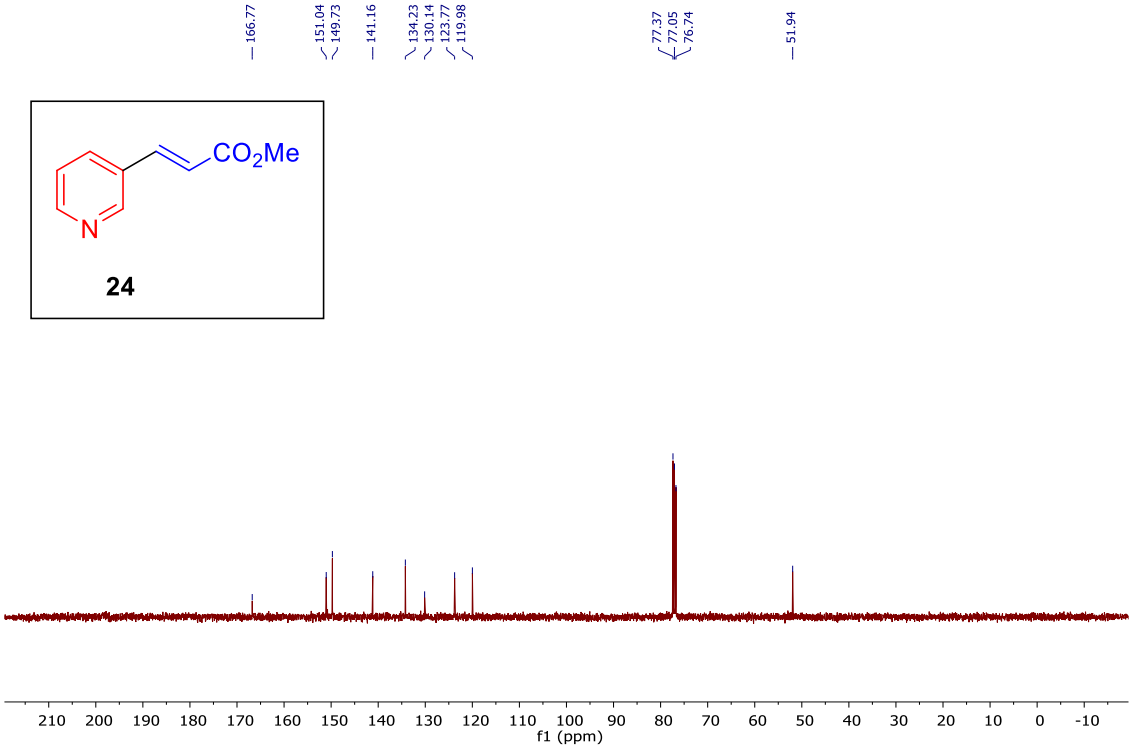

^{13}C NMR ($CDCl_3$, 100 MHz) spectrum of ***methyl (E)-3-(pyridin-3-yl)acrylate (24).***

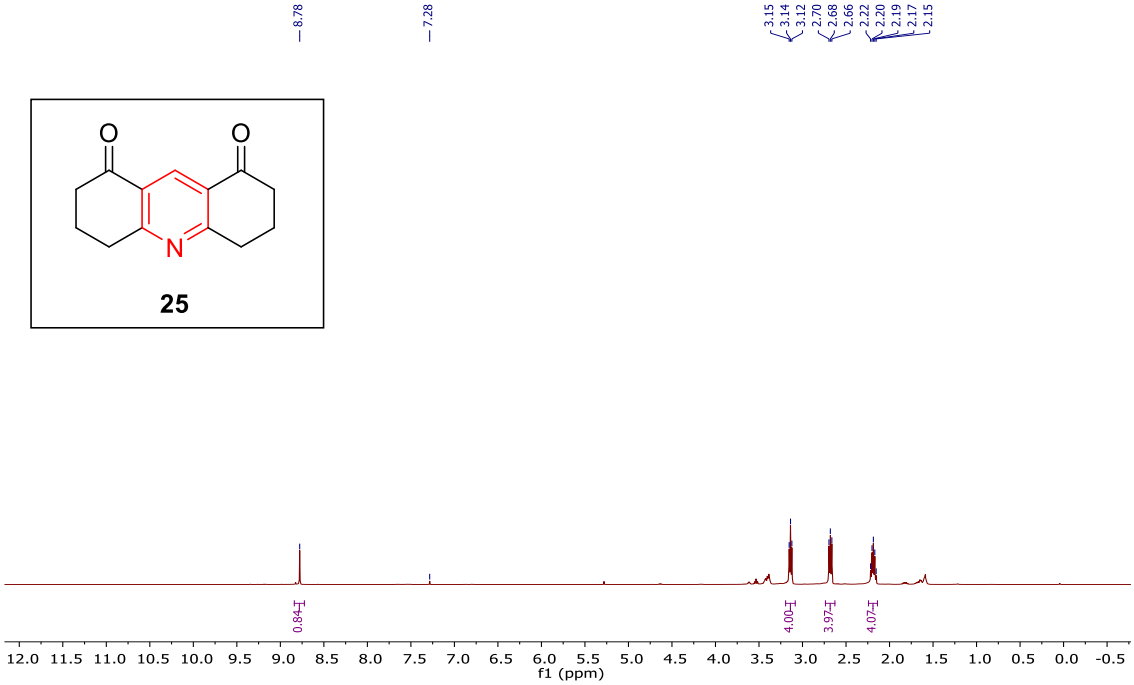

^{1}H NMR ($CDCl_3$, 400 MHz) spectrum of ***3,4,6,7-tetrahydroacridine-1,8(2H,5H)-dione (25)***

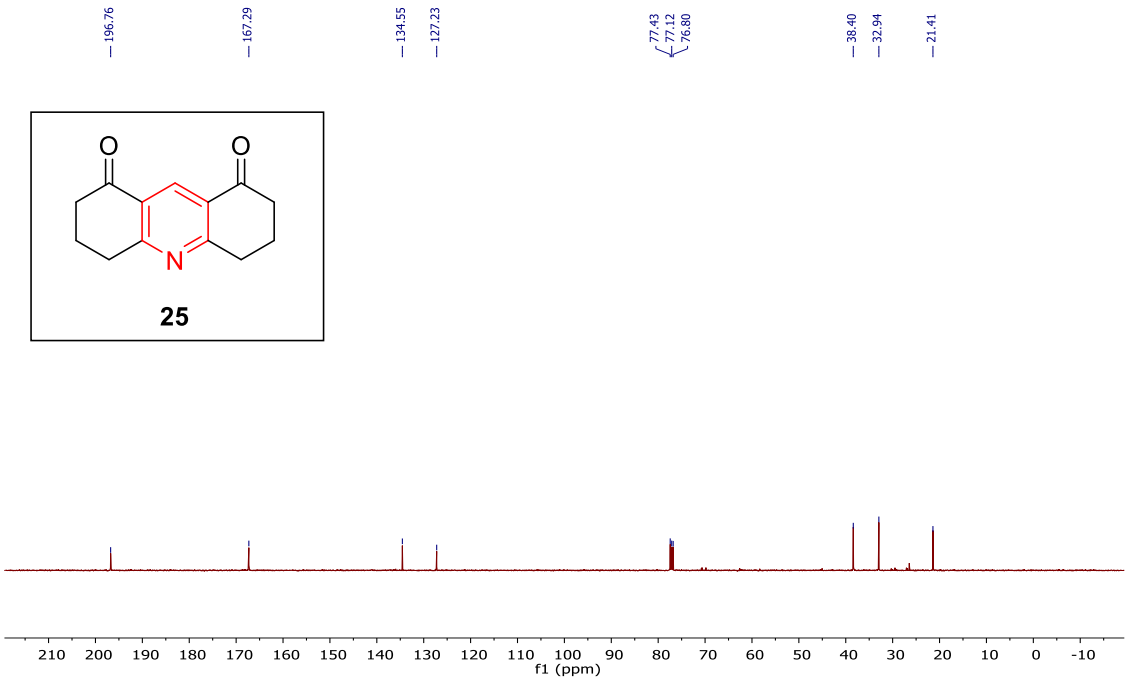

^{13}C NMR ($CDCl_3$, 100 MHz) spectrum of ***3,4,6,7-tetrahydroacridine-1,8(2H,5H)-dione (25)*.**

Instrumentation Details:

Sl. No.	Name of Instrument	Make	Model	Serial No
1	Nuclear Magnetic Resonance Spectroscopy	Bruker, Germany	AVANCE III 400	H03128MB/0509
2	Accurate Mass Q-Tof Lc/Ms	Agilent Technologies, Singapore	G6520B	SG11432202
3	FTIR Spectrometer	Bruker, Germany	ALPHA FTIR	200396
4	UV-Vis Spectrometer	Perkin Elmer, USA	LAMBDA-25	501511030903
5	Low Temperature Reaction Bath	Eyela, Japan	PSL-1810	61713730
6	Microwave Reactor	Cem Corpn, USA	DISCOVER 90801	DU9307
7	Photoreactor	Inkarp, Canada	LZC-DEV	1806
8	Milipore Water Purification System	Milipore, Bangalore	ELIX-3	F1AA24325
9	Combi Flash	Teledyne, USA	EZ PREP UV	218C02973
10	HPLC System	Agilent Technologies, Singapore	1200 INFINITY SERIES	DEACT 00698
11	Freeze Dryer	Biobase, China	BK-FD18PT	F1712-1286
12	Rotary Evaporator	Heidolph, Germany	HEI-VAP	1B12A0540

SUSANTA MANDAL
Mandal Keshra, Bankura, West Bengal, India-722139
E-mail: susantakeshra@gmail.com
Contact: +91-7076242499, +91-9564970415 **Curriculum Vitae**

PhD Thesis: Synthesis of Aromatic Aza-heterocycles and Exploration of their Chemical Characteristics.

Qualifications:

Degree	College and Affiliated University	Year of Joining	Year of Completion	Division with % of marks
B.Sc.	Burdwan University	2009	2012	53.5%
M.Sc.	Sikkim University	2012	2014	First (75.4%)

Research Interests:

- Development of New methodology.
- Photoredox Catalysis.
- Green Chemistry.

Research Publications:

1. **Mandal, S**.; Chhetri, K.; Bhuyan, S.; Roy, B. G. Efficient Iron Catalyzed Ligand-Free Access to Acridines and Acridinium Ions. *Green Chem.* **2020**.
2. **Mandal, S.**; Bhuyan, S.; Jana, S.; Hossain, J.; Chhetri, K.; Roy, B. G. Efficient Visible Light Mediated Synthesis of Quinolin-2(1H)-Ones from Quinoline N-Oxides. *Green Chem.*, **2021**, *23*, 5049–5055.
3. Chhetri, K.; Bhuyan, S.; **Mandal, S.;** Chhetri, S.; Lepcha, P. T.; Lepcha, S. W.; Basumatary, J.; Roy, B. G. Efficient Metal-Free Visible Light Photocatalytic Aromatization of Azaheterocyles. *Current Research in Green and Sustainable Chemistry* **2021**, *4*, 100135.
4. Subba, S.; Saha, S.; **Mandal, S**. A Diastereoselective Synthetic Approach towards the Synthesis of Berkeleylactone F and Its 4-Epi-Derivative. *SynOpen* **2020**, *04* (04), 66–70.
5. Bhuyan, S.; Das, D.; Chakraborty, A.; **Mandal, S.;** Dhanabal, K.; Roy, B. G. A Carbohydrate-Based Synthetic Approach to Diverse Structurally and Stereochemically Complex Chiral Polyheterocycles. *Chem. – Asian J.* **2021**, *16* (24), 4108–4121.

6. Bhuyan, S.; **Mandal, S.;** Jana, S.; Chhetri, K.; Roy, B. G. Efficient Greener Visible Light Catalyzed Debenzylation of Benzyl Ethers and Esters: A Gateway to Wider Exploitation of Stable Benzyl Protecting Group. *Asian J. Org. Chem.* **2022**.
7. Pradhan, A.; **Bhuyan, S**.; Chhetri, K.; Mandal, S.; Bhattacharyya, A. Saponins from Albizia Procera Extract: Surfactant Activity and Preliminary Analysis. *Colloids Surf. Physicochem. Eng. Asp.* **2022**, *643*, 128778.

Conferences:

Oral Presentations:

1. International Conference on Synthetic Potent Molecule and its Application (ICSPMIA-2018), October 30-31, 2018, organized by Sikkim Manipal Institute of Technology, Majitar, Rangpo, Sikkim.

Poster Presentation:

1. National seminal on Interdisciplinary Science, 10th October, 2018, on "An easy access to alkyl pyridines through simultaneous dehydroaromatization of dihydropyridine and reduction of ketone" organized by Sikkim University Science Forum.

Published on 23 March 2020. Downloaded by Indian Institute of Science Education & Research Kolkata on 4/8/2020 4:20:11 PM.

Green Chemistry

ROYAL SOCIETY OF CHEMISTRY

PAPER

View Article Online
View Journal

Check for updates

Cite this: DOI: 10.1039/d0gc00617c

Efficient iron catalyzed ligand-free access to acridines and acridinium ions†

Susanta Mandal, Karan Chhetri, Samuzal Bhuyan and Biswajit G. Roy *

Received 19th February 2020,
Accepted 23rd March 2020

DOI: 10.1039/d0gc00617c

rsc.li/greenchem

Acridines and acridinium ions are one of the important classes of compounds in terms of their usefulness in pharmaceuticals, materials, dyes and photo-catalysis. Here we present an unconventional $FeCl_3$-alcohol catalysed one-pot method for their synthesis directly from aldehydes, 1,3-cyclohexanedione and amines. This method efficiently merged high atom-economy and diversity of multicomponent reaction with novel iron catalyzed dehydrogenation, using aerobic oxygen as the terminal oxidant, in alcoholic solvent to produce water as the only by-product. Easy scaling up of the method has been successfully demonstrated.

Introduction

Acridines are an important class of hetero-aromatic compounds having a broad range of research and industrial applications[1–5] in the field of medicinal chemistry,[6–14] fluorescent organic dyes,[15–21] chemosensors,[22–24] and photocatalysis,[25] and as hole transport materials in solar cell and photovoltaic applications.[26–28]Due to their long excited state lifetime and tunable redox potential, acridinium ions are now frequently being used as an efficient visible light single electron transfer (SET) organic photocatalyst for many organic transformations.[29–36] Acridines, being one of the earliest known highly useful classes of compounds, have received considerable scientific attention, which consequently resulted in the development of many synthetic procedures.[37–46] All these synthetic procedures mainly deal with the construction of a new 6-membered ring through the formation of any one or two bonds on appropriately substituted functional groups in the pre-existing aromatic system followed by their aromatization to acridines.[4] In most cases, the suitably substituted aromatic precursors used in these methods are not commercially available. Their synthetic procedures are often difficult, require multiple steps and hence demand extra resources and create more environmental hazards. Moreover, many of these synthesis methods require high temperature and strong acidic and basic conditions, which limits their functional group tolerance and consequently reduces the generality and versatility of the reaction. Although some recent syntheses (Fig. 1A) by Buchwald,[47] Larock,[48] Ellman,[49] and others,[50–52] have evaded some of these problems by employing comparatively milder reaction conditions, they still require toxic and expensive heavy metal complexes as catalysts or highly reactive precursors[48] for the generation of acridines. Very recently, the Wang[53] group has reported an $FeCl_3$-promoted ligand/additive free one-pot method for the synthesis of benzoylacridines in good yields through aerobic aromatization from *o*-alkynylanilines and tetralones. However, suitably substituted *o*-alkenylamines are not commercially available and require multiple steps for their preparation. Furthermore, none of these previous methods have been explored for their ability to synthesize acridinium ions, which are proved to be useful as a visible light photoredox catalyst. Although 9-mesityl-10-methylacridinium ions, prepared by the addition of an organometallic nucleophile to an acridone, were initially introduced as photocatalysts by Fukuzumi in 2004[33] and efficiently used later for many photocatalytic transformations,[29–36] comparatively little effort has been expended for enhancing their effectiveness through further structural modifications. Visible light induced fast charge separation between perpendicularly situated two aromatic planes in the Fukuzumi catalyst[33] (9-mesityl HOMO and acridinium ion LUMO) followed by extremely slow recombination due to the high rotational barrier is the reason behind their long excited state life time and photoredox capability. Modulation of the photophysical properties, stability, redox potentials and excited state lifetimes of these photocatalysts through structural modification is now being actively pursued. Recently, the Nicewicz[36,54] and Sparr[55] group, in pursuit of the development of more effective photocatalysts, have developed new synthetic methods for diversely substituted *N*-arylated acridinium ions. They observed[36,54] that acridinium ions with *N*-10-aryl, 3,6-alkyl and hindered 9-*ortho*-aryl substitution

Department of Chemistry, Sikkim University, 6th Mile, Tadong, Gangtok, Sikkim – 737102, India. E-mail: bgroy@cus.ac.in

† Electronic supplementary information (ESI) available: General information, characterization data, X-ray crystallographic data and copies of ^{1}H and ^{13}C NMR spectra of products. CCDC 1949010 1947863. For ESI and crystallographic data in CIF or other electronic format see DOI: 10.1039/d0gc00617c

Green Chemistry

COMMUNICATION

Check for updates

Cite this: *Green Chem.*, 2021, **23**, 5049

Received 26th April 2021,
Accepted 17th June 2021

DOI: 10.1039/d1gc01460a

rsc.li/greenchem

Efficient visible light mediated synthesis of quinolin-2(1*H*)-ones from quinoline *N*-oxides†

Susanta Mandal,[a] Samuzal Bhuyan,[a] Saibal Jana,[b] Jagir Hossain,[a] Karan Chhetri[a] and Biswajit Gopal Roy *[a]

Quinolin-2(1*H*)-ones are one of the important classes of compounds due to their prevalence in natural products and in pharmacologically useful compounds. Here we present an unconventional and hitherto unknown photocatalytic approach to their synthesis from easily available quinoline-*N*-oxides. This reagent free highly atom economical photocatalytic method, with low catalyst loading, high yield and no undesirable by-product, provides an efficient greener alternative to all conventional synthesis reported to date. The robustness of the methodology has been successfully demonstrated with easy scaling up to the gram scale.

Quinolin-2(1*H*)-ones and their analogues represent an important class of organic compounds due to their high prevalence in natural products[1–4] and pharmacologically beneficial compounds[5–10] and as useful intermediates in organic synthesis.[11] Numerous compounds having this core skeleton are found to exhibit intriguing broad range bioactivity as antitumor agents,[12–19] endothelin receptor antagoists,[20] CDK5 inhibitor,[5] p38aMAP kinase inhibitors,[21] angiotensin II receptor antagonists,[22] and antibiotics (Fig. 1).[23–25] Many quinolin-2(1*H*)-ones are also found to be useful as efficient fluorescent markers[26,27] for amino acids, peptides, amino carbohydrates, and amino polysaccharides. Their usefulness has attracted considerable attention from synthetic chemists, which has consequently resulted in the development of multiple, efficient synthetic methods. These synthetic approaches can be divided into two main categories: (i) through the construction of quinolones/isoquinolone rings starting from a suitably pre-functionalized benzene precursor[28–41] (Fig. 2A) and (ii) through efficient *ortho*-functionalization of *N*-oxides of naturally abundant quinolines (Fig. 2B).[42–47] The inherent difficulty and associated expense in obtaining suitably pre-functionalized aromatic systems, requirement of other co-precursors, use of harmful heavy metal complexes or strong acidic or basic conditions and lower yields make the first approach fundamentally less attractive in terms of efficiency and cost effectiveness. The exploitation of easily accessible *N*-oxides of naturally abundant/easily synthesizable quinolines makes the second approach (Fig. 2B) comparatively more efficient and cost effective in most cases and therefore more suitable for bulk scale synthesis. These Reissert–Henze type approaches exploit the high oxide nucleophilicity and weak N–O bonds of quinoline *N*-oxides to generate good leaving groups at N-1, which ultimately makes C-2 highly susceptible to nucleophilic attack. However, these methodologies require stoichiometric (or excess) electrophilic reagents for successful functionalization at C-2. Thus, these methods produce significant amounts of hazardous polar aqueous soluble waste, which in turn jeopardizes the prospect of their use in bulk/industrial scale synthesis. Moreover, the use of stoichiometric electrophilic reagents makes these methods unsuitable for quinoline *N*-oxide substrates containing free nucleophilic substituents like hydroxyl or amine groups. Several early endeavors have used UV light irradiation on easily available quinoline *N*-oxides to obtain the desired 2-quinolones under stoichiometric reagent free conditions in a polar protic solvent (Fig. 2C).[48–51] However, the high energy UV light generates multiple unstable undesirable byproducts as the major components in the product mixture with a very low yield of 2-quinolones.[52,53] Furthermore, the use of high energy UV light makes these methods unsuitable for substrates containing UV labile substituents (like, nitro, carbonyls, alkenes *etc.*). Generation of a complex mixture of products, with a low yield of the desired quinolone, harsh reaction conditions and limited substrate scope, makes this method synthetically unattractive. Therefore, there remains a genuine need for the development of an easy, mild, environment friendly general method for the synthesis of quinolin-2(1*H*)-ones with a wide substrate scope.

[a]*Department of Chemistry, Sikkim University, 6th Mile, Tadong, Gangtok, Sikkim – 737102, India. E-mail: bgroy@cus.ac.in*

[b]*Department of Chemistry, University of Liverpool, Crown Street, Liverpool, L69 7ZD, UK*

† Electronic supplementary information (ESI) available: General information, characterization data, and copies of ^{1}H and ^{13}C NMR spectra of products. See DOI: 10.1039/d1gc01460a

This journal is © The Royal Society of Chemistry 2021

SMIT SIKKIM MANIPAL UNIVERSITY
SIKKIM MANIPAL INSTITUTE OF TECHNOLOGY

ROYAL SOCIETY OF CHEMISTRY

SERB INDIA
Govt. of India

PLATINUM JUBILEE 1944-2018
CSIR - IICT
Touching Lives

INTERNATIONAL CONFERENCE ON SYNTHETIC POTENT MOLECULE AND ITS APPLICATION (ICSPMIA-2018)

OCTOBER 30-31, 2018

DEPARTMENT OF CHEMISTRY
SIKKIM MANIPAL INSTITUTE OF TECHNOLOGY (SMIT)

Certificate

This is to certify that Prof./Dr./Mr./Ms. .....Susanta Mandal..... *of* .....Sikkim University..... *has actively participated in the "International Conference on Synthetic Potent Molecule and Its Application" (ICSPMIA-2018) held at SMIT, Majitar, Rangpo, Sikkim from 30 to 31 October 2018, as Delegate / Invited Speaker / Chairperson / Co-Chairperson / Paper Presenter / Poster Presenter.*

Dr. Satadru Jha Convener, ICSPMIA-2018 Department of Chemistry, SMIT	**Prof. (Dr.) Sangeeta Jha** Head of the Department Department of Chemistry, SMIT	**Prof. (Dr.) Ashis Sharma** Patron, ICSPMIA-2018 Director, SMIT

Certificate of Presentation

This is to certify that

Suanta Mandal

presented a paper in

SEMINAR ON
"INTERDISCIPLINARY SCIENCE"

organized by

Sikkim University Science Forum

held on 10th October, 2018

Dr. Dhani Raj Chhetri
Chairperson
Sikkim University Science Forum

Prof. Jyoti Prakash Tamang
Vice Chancellor
Sikkim University, Gangtok